

On the Mechanics of the Bow and Arrow ¹

B.W. Kooi
Groningen, The Netherlands

1983

¹B.W. Kooi, *On the Mechanics of the Bow and Arrow* PhD-thesis, Mathematisch Instituut, Rijksuniversiteit Groningen, The Netherlands (1983), Supported by "Netherlands organization for the advancement of pure research" (Z.W.O.), project (63-57)

Contents

1	Introduction	5
1.1	Preface and summary	5
1.2	Definitions and classifications	7
1.3	Construction of bows and arrows	11
1.4	Mathematical modelling	14
1.5	Former mathematical models	17
1.6	Our mathematical model	20
1.7	Units of measurement	22
1.8	Variety in archery	23
1.9	Quality coefficients	25
1.10	Comparison of different mathematical models	26
1.11	Comparison of the mechanical performance	28
2	Static deformation of the bow	33
2.1	Summary	33
2.2	Introduction	33
2.3	Formulation of the problem	34
2.4	Numerical solution of the equation of equilibrium	37
2.5	Some numerical results	40
2.6	A model of a bow with 100% shooting efficiency	50
2.7	Acknowledgement	52
3	Mechanics of the bow and arrow	55
3.1	Summary	55
3.2	Introduction	55
3.3	Equations of motion	57
3.4	Finite difference equations	62
3.5	Some numerical results	68
3.6	On the behaviour of the normal force T at $t = 0$	80
3.7	Acknowledgements	82

4	The static recurve bow	83
4.1	Summary	83
4.2	Introduction	83
4.3	The equations of motion	87
4.4	Finite-difference equations	93
4.5	The quality coefficients	98
4.6	Three models	100
4.7	Influence mass and stiffness of string	106
4.8	Fibratory motion	109
4.9	Sensitivity analysis for a straight-end bow	117
4.10	Model for static-recurve bow	130
4.11	Static-recurve bow	136
4.12	Influence of draw, weight and mass of limb	156
4.13	Another check on our numerical method	165

Chapter 1

Introduction

1.1 Preface and summary

The invention of the bow and arrow may rank in social impact with the invention of the art of kindling fire and that of the wheel. It must have been in prehistoric times that the first missile was projected by means of a bow. Where and when we do not know, perhaps even in different parts of the world at about the same time. Then man was able to hunt game and to engage his enemies at a distance.

In the 15th century the bow in the "civilized" world was superseded on battle fields by the fire-arm and became an instrument for pastime. Today, archery is a modern, competitive sport.

The mechanics of the bow and arrow became a subject of scientific research after the bow had lost its importance as a hunting and war weapon. In the 1930's C.N. Hickman, P.E. Klopsteg [6] and others performed experiments and made mathematical models. Their work both improved the understanding of the action of the bow and influenced the design of the bow strongly.

In this thesis a mathematical simulation is made of the mechanical performance during the projection of the arrow by means of a bow. Because nowadays fast computers are available, we are able to cope with more advanced models, which are supposed to supply more detailed results. The flight of the arrow through the air and the way it penetrates the target is beyond the scope of this thesis.

Characteristic for the bow are the slender elastic limbs. The bow is braced by putting a string shorter than the bow between the tips of the limbs. We distinguish between three different types of bows on the ground of the interplay between string and limbs. For bows of the first type, the "non-recurve" bows, the limbs have contact with the string only at their tips. The Angular bow used in Egypt and Assyria and the famous English wooden longbow are non-recurve bows. In almost all Asia a bow made of wood, horn and sinew was used. In braced situation the string lies along a part of the limbs near the tips. Along this length and often further these limbs are stiff; they do not deform during the drawing of the bow. These bows are called "static-recurve" bows. More recently bows are designed

made of wood and man-made materials such as glass or carbon fibres imbedded in resin. For these bows the string also lies along the limbs in the braced situation for a short length. However, the limbs are now elastic along their whole length. These bows are called "working-recurve" bows. In this thesis we restrict to bows of the mentioned three types which are symmetric, so we do not discuss the interesting asymmetric bow of Japan.

In Chapter 2 we deal with bracing and drawing bows of all three types. The limbs are considered as beams for which the Bernoulli-Euler equation holds. In each situation, the equations form a system of coupled ordinary differential equations with two-point boundary conditions. A shooting method is described by which this system is solved. As a result of this, the problem is reduced to the solution of two non-linear equations with two unknowns. Attention is paid to the problem of finding starting points for the secant-Newton method which is used for solving these two equations.

After loosing, part of the energy accumulated in the limbs is transferred to the arrow. In Chapter 3 we deal with the dynamics of the non-recurve bow. The bow is assumed to be clamped in the middle. The string is assumed to be without mass and to be inextensible. The governing equations are the equations of motion for the limbs. These equations are derived using Hamilton's principle, the internal as well as the external damping having been neglected. There are two independent variables, the length coordinate along the bow and the time coordinate and there are six unknown functions. The boundary conditions at the tips contain the equation of motion for the arrow. A numerical solution is obtained by means of a finite-difference method. A Crank-Nicolson scheme is used, then for each time step a system of non-linear equations has to be solved. This has been done by a modified Newtonian method. The solutions of previous times are used to obtain starting points. At the moment of release the solution of the shooting method as described in Chapter 2 is used as starting point.

In Chapter 4 the string is elastic and possesses mass. A part of this chapter deals also with the non-recurve bow, of which we consider now also the vibratory motion of bow and string after arrow exit. Then the governing equations form two coupled systems of partial differential equations. Besides time, for one system the length coordinate along the limbs and for the other one the length coordinate along the string is the independent variable. At the tips these systems are linked by the boundary conditions.

The main object of Chapter 4 is the dynamics of the static-recurve bow. For this type it is necessary to take into account that the string has contact with the tips during the first part of the shooting and after a beforehand unknown time with the part of the ears between tips and string-bridges. In this case but also when the arrow leaves the string, the boundary conditions change abruptly at a moment which has to be calculated. Because of lack of time we have to leave the dynamics of the working-recurve bow out of consideration.

In this thesis we do not deal with proofs of existence and convergence of the numerical methods. We did try, however, to obtain an insight into the accuracy of the developed methods. For example, the analytic solution of a linearized problem is compared with the obtained numerical solution. This is done in Section 4.13.

The mathematical simulation is used for theoretical experiments. The aim of these experiments is to get insight into the influence of different quantities which determine the

action of the bow and arrow. This supplies the possibility to compare several types of bows which have been developed in different human societies. This is also done in Chapter 4. It appears that the static-recurve bow is not inherently better than the long straight bow. The meaning of the word *inherent* in this context is given in Sections 1.7 and 1.9 of this introduction. When the different properties of the materials, wood, horn and sinew, are deliberately used, more energy per unit of mass can be stored in the limbs of the Asiatic bow than in those of the wooden bow. Further, the static-recurve bow can be made shorter without the loss of much quality. Their shortness makes them handier and suitable for the use on horseback.

Chapter 2 and 3 are reprints of published papers and Chapter 4 that of an unpublished one. As a result of this each chapter begins with an introductory section in which we give a short outline of archery and each chapter has a separate list of references; sometimes a reference is a chapter of this thesis.

In this introduction we quote from various books and papers given in Lake and Wright [11]. This is an indexed catalogue of 5,000 articles, books, films, manuscripts, periodicals and theses on the use of the bow, from the earliest times up to the year 1973.

1.2 Definitions and classifications

In this section we give the nomenclature of the different parts of the bow and arrow and the classification of bows we have used.

Characteristic features of the bow are the slender elastic "stave" and the light string, shorter than the stave, see Figure 1.1. Mostly there is a stiff part in the middle of the bow, called the "grip", "handle" or "riser section". The parts on both sides of this grip are called the "limbs". Because the bow is usually held vertical or nearly vertical, we can speak of the "upper limb" and of the "lower limb". The "back" of a limb is the side facing away from the archer, the "belly" the opposite side.

The string is fastened between both ends of the stave. For that purpose often grooves are notched in these ends, the "tips" or "nocks". The string is generally provided with "loops", which fit in the grooves, and sometimes it is tied to one or to both ends.

The bow is "braced" or "strung" when the string is set on the bow. The distance between the grip on the belly side and the string in that situation is called the "brace height" or "fistmele". This distance is adjusted by changing the length of the string, for example by twisting it. In general the bow is braced only when in use, because most materials of which limbs are made get a "permanent set" when loaded for a long time; the bow "follows the string". As an old proverb says: "a bow long bent at last waxed weak".

Now the bow is ready for use, that is to propel a projectile to its "target". This projectile is mostly an arrow. An arrow consists of a shaft with at one end the "head", "point" or "pile", often a separate piece attached to the shaft in one way or another and at the other end the "nock", see Figure 1.2. To stabilize the flight of the arrow often "vanes", together known as "fletching", are bound, slightly spiral wise or not, to the shaft near the nock.

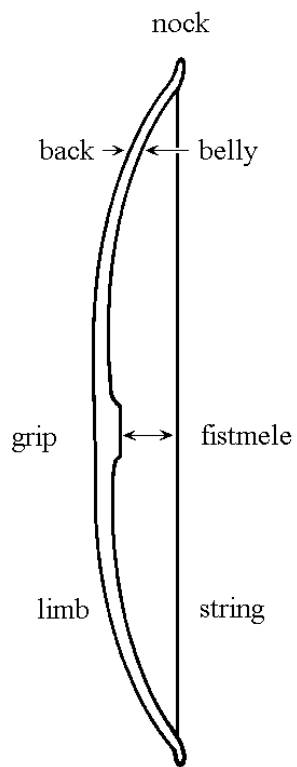


Figure 1.1: The parts of the bow.

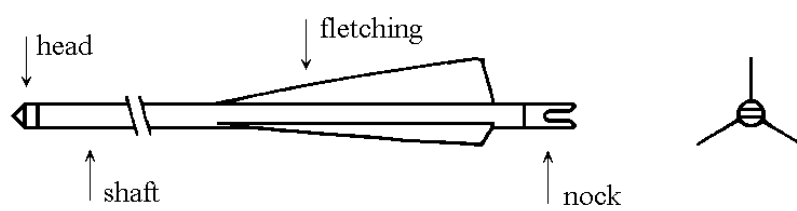


Figure 1.2: The parts of the arrow.

The nock is provided with a groove in which the string slightly sticks when the arrow is set on the string, called "nocking". The place at the string where the arrow nock meets the string is called the "nocking point".

After the arrow is set on the string, the archer pulls the bow from braced situation into "fully drawn" situation, this action is called "drawing". To that end he hooks for instance two or three fingers or the thumb of the "shaft hand" on the string. With the other hand, the "bow hand", the archer holds the bow at the grip. During drawing a force is exerted upon the grip by the bow hand applying at the so-called "pivot point" on the belly side of the grip, and by the shaft hand upon the string at the nocking point. Both forces are opposite to each other and are approximately aligned with the "line of aim". The line of aim is by definition the line through the centre line of the pointed arrow in fully drawn situation. The Static-Force-Draw (SFD) curve shows the force exerted by the shaft hand as function of the distance of the nocking point from the grip on the back side. This distance in the fully drawn situation is called the "draw". The drawing force in that situation is called the "weight" of the bow. Note that bow weight does not pertain to the actual weight caused by gravity.

After "aiming", the arrow is loosed or released by stretching the fingers or the thumb of the shaft hand, called "loosing". The bow is held in its place with the bow hand. The force acting upon the arrow as function of the position of the nocking point arrow is given by the Dynamic-Force-Draw (DFD) curve. The arrow is guided at the grip by the knuckle of the index finger or over the thumb of the bow hand or by an "arrow rest". The velocity of the arrow when leaving the string is called the "muzzle velocity" or "initial velocity". The functioning of a bow and arrow is divided into two parts. The "interior" ballistics deals with the phenomena until arrow exit. The "exterior" ballistics deals with the flight of the arrow through the air. The arrow, in its flight, is slowed down by the "drag" or resistance of the air.

The bow we described thus far actually is a "bow hand". Besides the hand bow there are the "cross bow", for instance the "foot bow", and the "compound bow". The rather short bow stave of the cross bow, the "prod", is fixed to a cross stave, the "stock". The relatively short arrow is now called the "bolt", which is guided through a straight groove in the stock. To span a cross bow, loading mechanics were developed such as the windlass or the cranequin, by which very powerful bows could be handled. In fully drawn situation the string sticks behind a lock, so the archer aims without effort. The bow is released by uncoupling the catch mechanism, the prod always held horizontally.

In North America, the first compound bow was reportedly built in 1938 by a physicist called Claude Lapp. This bow has pulleys with eccentric bearings at the end of the rather stiff elastic limbs.

We now return to the hand bow and when in the following the word bow is mentioned always the hand bow is meant. Already in the braced situation energy is stored in the limbs and to a small extent also in the string. By drawing "additional energy" is accumulated. After release part of this latter amount of energy is converted into kinetic energy of the arrow.

The classification we use is based on the geometrical shape and the elastic properties of

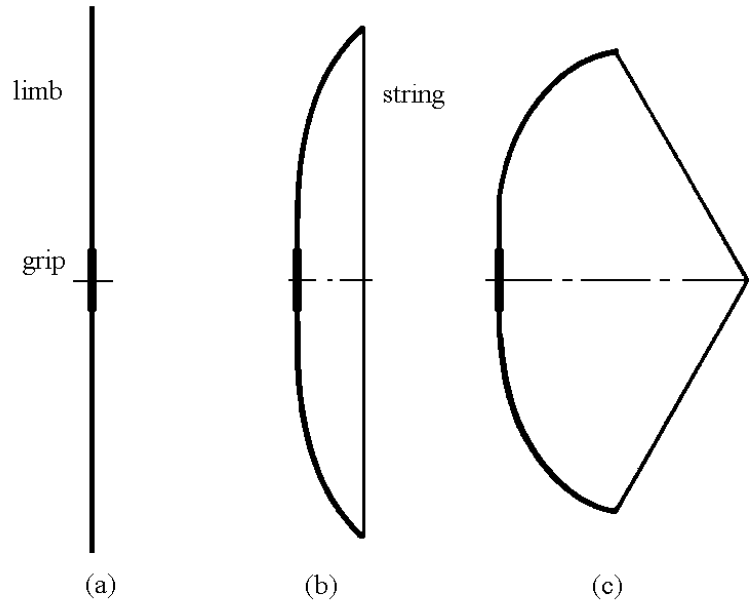


Figure 1.3: Non-recurve bow in three situations: (a) unbraced, (b) braced and (c) fully drawn.

the limbs of the bow. In Figure 1.3 we show a "non-recurve" bow in unbraced, braced and fully drawn situation. These bows have contact with the string only at their tips. When the string has contact with the limbs also at other points, we call the bow "recurved" or "reflexed" because in that case the limbs of the unbraced bow are curved backwards, this is by definition away from the archer. We distinguish between two types of recurved bows, namely the "static-recurve" bow and the "working-recurve" bow which we discuss now separately.

In the case of the static-recurve bow, see Figure 1.4, the outermost parts of the limbs are stiff. These parts are called "ears" or "rigid-end pieces". The elastic part of a limb between grip and ear is called the "working part of the limb". In the braced situation the string rests on the "string-bridges", situated at the bend of the ears. These string-bridges are hollowed out sometimes, to receive the string and retain it in its place. This prevents the string from slipping beside the limb and giving it a fatal twist. When these bows are about half drawn, the string leaves the string-bridges and has contact with the limbs only at the tips. After release, at a certain moment before arrow exit. the string touches the string-bridges again.

In the case of a working-recurve bow the parts near the tips are elastic and bend during the final part of the draw. Figure 1.5 shows a working-recurve bow in unbraced, braced and fully drawn situation. When drawing the bow the length of contact between string and limb gradually decreases until the point where the string leaves the bow coincides with the tip of the limb and remains there during the final part of the draw. After release the

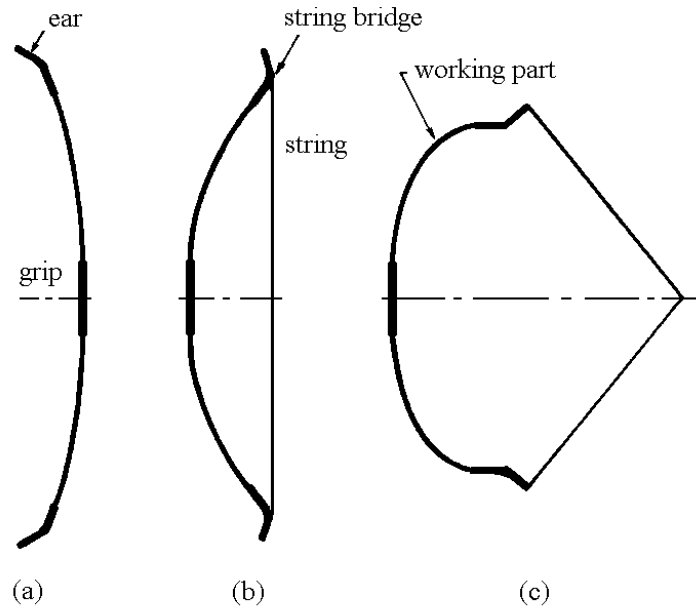


Figure 1.4: Static-recurve bow in three situations: (a) unbraced. (b) braced and (c) fully drawn.

phenomena happen in reversed order to prevent the possibility of a twist of the limbs in the case of a working-recurve bow, grooves are present on the belly side of the limbs starting at the notch and extending sufficiently far in the direction of the grip.

We note that bows belonging to each of the three types may be symmetric or more or less asymmetric. Here symmetry with respect to the horizontal plane through the pivot point and the nocking point is meant.

1.3 Construction of bows and arrows

In this section we briefly discuss the structure of bows. We introduce some classifications, but contrary to those given in the former section these are dispensable with respect to our mathematical modelling dealt with in a following section. The materials employed in making strings and arrows are touched upon at the end of this section.

In principle bows of all three types, non-recurve, static-recurve and working-recurve, symmetric or asymmetric, may be "self" bows or "composite" bows. When only one kind of material is used a bow is called a self bow. Mostly the material used is wood. Then the bow is a processed branch or part of the stem of a tree. This type of bow was very widely distributed over the world. In most parts of Africa, South America and Melanesia it has never been superseded by another kind of bow. These bows are straight bows, hence "non-recurve" bows. Also self bows solely made of horn or of bronze or steel have been

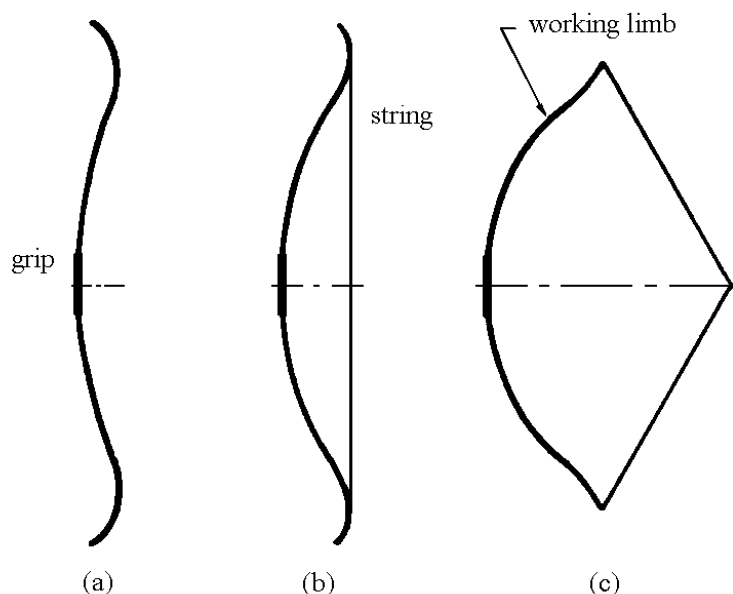


Figure 1.5: Working-recurve bow in three situations: (a) unbraced, (b) braced and (c) fully drawn.

found. In Sweden bows of steel were first produced in 1935 and later also in England. These self bows were non-recurve or working-recurve bows.

The famous English longbow, also an example of a self bow, is generally made of Yew (*Taxus Baccata*). In this case, the relatively soft "sapwood" constitutes about one-quarter of the thickness of the limb and it is situated at the back side. The remaining part of the limb is formed by stiff "heart wood".

A composite bow is a bow of which the limbs consist of more than one material. Commonly there is a skeleton or core which after completion forms the middle part of the limbs in a cross section. Application of materials on the back side of the core is called "backing", just as the material itself. When materials are applied to the belly side of the core it is called "facing". The backing of some bows is formed by cords plaited of animal sinews and lashed to the wooden core at various points along the limbs. This is called a "free backing" and these bows, non-recurve or static-recurve bows, were almost exclusively used by Eskimos. In the case of "close backing" the layer on the back side is glued to the core. The Indians in North America sometimes used close backing. At the tips the limbs were bent a little backwards, away from the archer, to counteract the effects of a permanent set, but they still are non-recurve bows by definition. Another kind of composite bow which is also a non-recurve bow is the "Angular bow", found in Egypt and Assyria. In braced situation the limbs of these bows fall straight back forming the equal sides of an isosceles triangle of which the string is the basis. Often wood sinew and horn were employed in

making these bows.

In Asia the core of a composite bow was made of wood, its belly side was faced with horn and its backing consisted of sinew. Its construction is sometimes said to parallel the make-up of living things:

‘Just as man is made of four component parts (bone, flesh, arteries and blood) so is the bow made of four component parts. The wood in the bow corresponds to the skeleton in man, the horn to the flesh, the sinew to the arteries, and the glue to the blood.’

These bows, generally static-recurve bows, were used by the Mongolian races of Eastern Asia. They reached their highest development in India, in Persia and in Turkey.

In the 1960's bows with a wooden core of maple and a backing and facing of glass fibres (more recently carbon fibres) imbedded in strong synthetic resin were designed. Hence, these bows, called "laminated bows" are composite bows and are often of the working-recurve type. They possess a long rigid middle section, the handle. These handles are generally cut-out, so that the arrow can pass it in the vertical "median plane" of the bow, see Figure 1.6 in which we show a part of a so called "centre shot" bow in braced configuration. Observe that the arrow does not make an exact angle of 90 degrees with the string in braced situation. The "nocking height" is the distance above the 90 degrees line from the arrow rest. Further, the pivot point lies below the point where the arrow passes the bow over the arrow rest.

"Stabilizers", a pair of extending metal arms, are often attached to the handle section. When the limbs can be separated from the handle the bows are called "take-down" bows/indexbow!take-down. In that case the handle often is made of magnesium alloy, and is provided with a "pistol-grip".

Many kinds of bows are slightly asymmetric. In the case of some Asiatic bows the upper limb, which is somewhat longer than the lower, is called the "shooting" limb because it is said to account for most of the shooting. A striking example of an asymmetric bow is the typical Japanese bow of which the upper limb is almost twice the length of the lower one. It is constructed of bamboo strips which are glued together by means of fish-glue. The sides are finished off with strips of hazewood. Today also glassfibre Japanese bows are available.

Many kinds of fibres have been used in making strings. In former times natural fibres were used, animal fibres (silk and sinew) and vegetable fibres (hemp, linen, cotton and strips of bamboo or rattan). For a long time the Belgian strings made of long-fibered Flemish flax were famous. Recently, man-made fibres such as dacron and kevlar are developed.

There are many different ways of fastening a string to a bow, for example by knots or loops. Because woody materials do not lend themselves easily to tying by knots, such strings are fastened to the limbs by means of different, more flexible fibres. The string of the static-recurve bow in Asia often had separate end-loops knotted to each end of its centre part. Actually, the knots rest on the string-bridges when the bow is braced.

We conclude with a short discussion of the materials used for the arrow. The construction of the arrow changed gradually to adapt it to special purposes. The arrow head

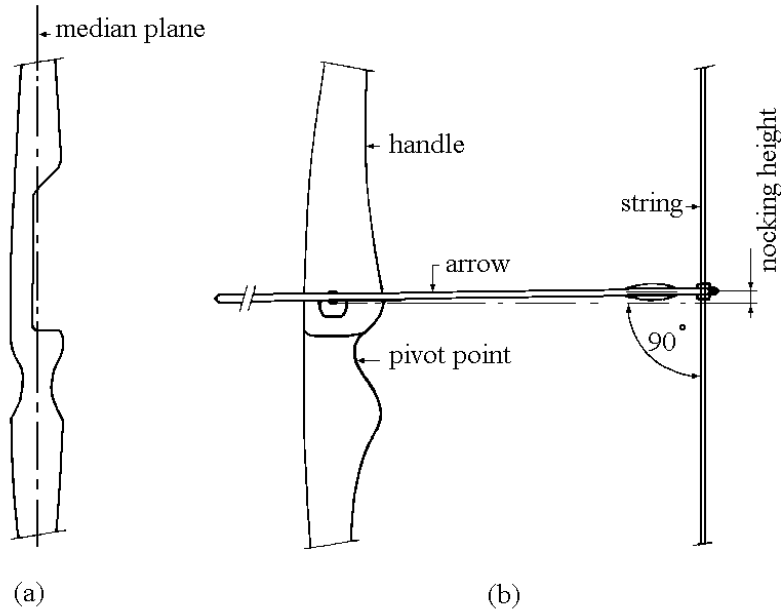


Figure 1.6: Middle part of modern bow of right-handed archer in braced situation (a) front view and (b) side view.

is often a separate piece of material such as stone, bone, wood, bronze or steel. Many different forms of heads, barbed or not, are known. In former days the shafts were made of reed, cane or wood, later on of glassfibre and today often of aluminum. Sometimes the shafts were made of two kinds of wood, "footed arrows". the part near the head being the footing. For fletching feathers of such birds as eagles, crows, geese and turkeys, have been used. Today plastic vanes are available.

1.4 Mathematical modelling

In this section we discuss some general aspects of making a mathematical simulation of the mechanical performance of the bow and arrow. In the next two sections we give a more detailed account. A number of former mathematical models developed up to now are considered in Section 1.5, while in Section 1.6 the model given in this thesis is discussed.

Making a model of the bow and arrow starts with a description of the process of propelling the arrow using principles of mechanics. Doing this, assumptions are made in order to obtain equations which can be solved. Models based on fewer simplifications are supposed to yield more accurate and detailed results, but on the other hand they certainly are more difficult to handle. To which extent the mathematical approach is useful depends largely on the grade of validity of the assumptions. A comparison with experimentally

obtained results gives insight into this matter.

Up to now all models, our model included, presume the existence of two planes with respect to which the bow is symmetric. The (vertical) median plane intersects the limbs and string of the braced bow lengthwise, see Figure 1.6. The other (horizontal) plane is perpendicular to the first one and intersects it along the line through the pivot point on the grip and the nocking point on the string. This implies, apart from equality of upper and lower limb, that the bow is centre shot, that the pivot point is on the line of aim, that the nocking height is zero and that the nocking point coincides with the middle of the string. Further, the limbs, the string and the arrow are assumed to move in the median plane. This presupposes that the grip is fixed in its position and the arrow is released without lateral movement. During the process of acceleration it is assumed that gravitation forces are negligible.

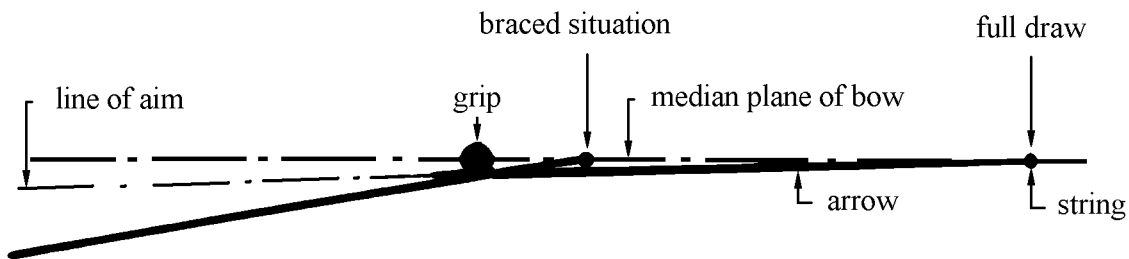


Figure 1.7: Illustration of archer's paradox (after Klopsteg [6, page 187]).

In [8] and in articles in [6], Klopsteg gives an explanation of the so-called "archers paradox" which is related to a classic non-centre shot bow. In Figure 1.7 we show the position of the arrow in two situations, the braced and the fully drawn situation. The angle between the arrow and the median plane of the bow differs in these two positions. For the fully drawn bow this angle is about 1.5 degrees and in the braced situation 6 degrees. Hence, if the arrow would be a stave, rigid with respect to bending and if it slips along the grip then it deviates about 4.5 degrees from the line of aim at the moment it leaves the string. Rendtorff suggested in 1913 that the ability of bending of the arrow could be an important property with respect to this. In 1932 Klopsteg photographed a bow discharging an arrow and found that the arrow "snakes" its way around the grip Figure 1.8 is after Klopsteg and shows the shape of the arrow at a number of consecutive times. The shaded circle indicates the position of the cross section of the grip. The arrow performs about one and a quarter vibrations before it departs from the bow. The oscillations take place approximately about the line of aim and there is no departure of the arrow as a whole from this line. The oscillations persists for a considerable time after arrow exit.

These findings show that the dynamic properties of the arrow must be correctly matched to those of the bow. The eigenfrequency of the arrow, depending on its mass and bending stiffness distributions, must be adjusted to avoid the hitting of the bow by the rear end of the arrow. As measure of stiffness of an arrow the concept "spine" is introduced. This

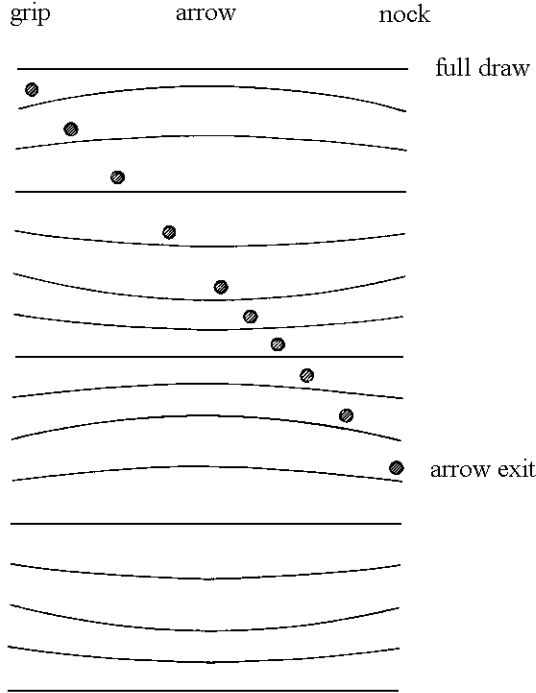


Figure 1.8: Schematic representation of the phases of the arrow in its passage by the bow, based on the evidence from speed-flash photography (after Klopsteg [6, page 182]).

is the deflection of the centre of the shaft, measured in some unit, when a weight is hung at that point while the arrow is supported at the base of the nock and at the shoulder of the head. In [6, page 231] Nagler and Rheingans derive mathematically that for any given bow and archer, the spine of all arrows should be constant, regardless of arrow mass.

Photographs revealed that in reality the bow hand has not a fixed position but moves after loosing and that the motion of the string is not exactly in the median plane. Reasons for this can be found. First, the release of the string over the finger tips or thumb and second, the angular acceleration of the arrow out of the median plane mentioned above cause some lateral deflections of the system.

The introduction of lateral movements makes the problem much more difficult. Then the arrow has to be treated like a flexible beam, pushed at the rear end and hampered with respect to its sideways movement at the grip. Further, one has to know the response of the body of the archer to the force of the bow exerted on the bow hand.

In Section 4.8, we investigate the influence of the freedom of the grip to move away from the bow hand of the archer in the direction of shooting, a situation which may occur when the bow is shot "open-handed". In all other cases the bow is assumed to be clamped at the grip.

Up to now no mathematical model takes internal nor external damping of limbs and string into account. In practice the vibrations of the limbs and string after arrow exit tend to zero rather soon, indicating the existence of damping. Other possibly less serious assumption are that the arrow passes the grip without friction and that the arrow is set

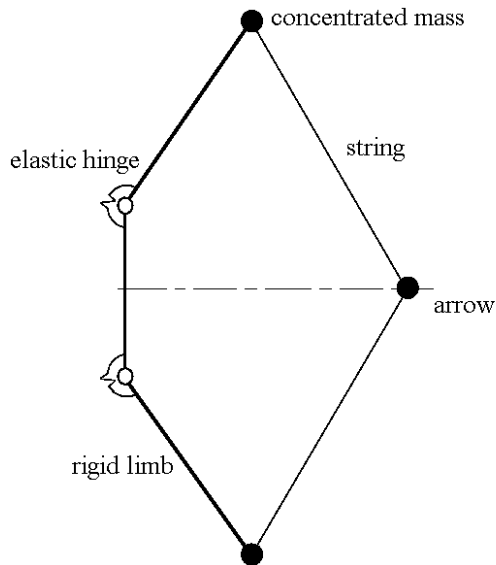


Figure 1.9: Bow with two linear elastic hinges and rigid limbs, Hickman's model and Marlow's model.

loosely on the string, so without "nocking tension".

1.5 Former mathematical models

Starting in 1929 Hickman published on archery from a physical point of view. In [5] he develops an analytical method to determine the dynamic forces, the accelerations and velocities of the arrow, string and bow limbs. His model, though very simple, reveals already some of the characteristics of the bow and arrow. He replaces the flexible limbs by rigid ones, which are connected to the grip by linear elastic hinges, see Figure 1.9. The mass of the rigid limbs is concentrated at the tips where the string is connected to the limbs. The place and strength of the elastic hinges and the masses at the tips are determined using measured quantities of the real bow, so that the essence of the mechanical behavior of the limbs of the model and of the limbs of the real bow treated as slender elastic beams, for small deflections be alike. The string is assumed to be inextensible and its mass is accounted for by adding one third of it (we call this the added mass) to the mass of the arrow. After this manipulation the string can be considered not only inextensible but also as massless.

Under general conditions all the additional energy stored in the elastic hinges by drawing this bow from braced situation into fully drawn situation is transferred to the arrow and the added mass which possess both the same speed at arrow exit, see also Appendix of Chapter 3.

After departure of the arrow, in Hickman's model the limbs and string with the concentrated added mass in the middle oscillate around the braced situation. At this stage the total energy in hinges, limbs and string equals the potential energy in the hinges in braced situation plus the kinetic energy of the added mass of arrow exit.

This simple model shows a characteristic feature of the bow. During the first part of the period the arrow is accelerated, the limbs absorb energy as kinetic energy. In the final part,

however, this energy is transferred by the string to the arrow and added mass. Further, we observe the importance of the lightness of the string, for a smaller added mass means more kinetic energy in the arrow. If the mass of the string were zero, even all additional energy accumulated in the bow during the draw would be imparted to the arrow.

In his explanatory article on the physics of the bow and arrow [8], Klopsteg introduces the concept of so-called "virtual mass"; "the mass which, if it were moving with the speed of the arrow at the instant the latter leaves the string, would have precisely the kinetic energy of the limbs and the string at that moment". He measured experimentally that the virtual mass is in fact a constant for some bow shooting arrows with different masses. We discuss this concept in Section 3.5 and Section 4.9. Klopsteg introduces also a "figure of merit" of a bow, "representing the limiting velocity that the bow could impart to an arrow with mass approaching to zero". He uses his concepts for the explanation of several facts well-known to archers.

Schuster in [16] deals with the ballistics of the working-recurve bow. He made a mathematical model assuming the recurved limbs to be a part of a circle which unroll along the initial tangent, see Figure 1.10 where we show such a bow in various situations. The string is assumed to be inextensible and it possesses a constant mass per unit of length and the half parts free from the limbs are straight.

Schuster uses the Lagrangian formalism to obtain the equations of motion. He considers a limb having a flexible core of uniform thickness which is sandwiched between two sheets of longitudinal fibres of an elastic material. As the limb rolls out the fibres on the inside of the limb (the back side of the limb) are elongated and those on the outside (the belly side) are compressed. In this way he obtains an expression for the potential energy in the limbs. For normalization a point on an experimental SFD curve of a commercially available working-recurve bow was used.

The equations of motion are integrated numerically by means of a computer. Schuster shows plots of the SFD curve and displacement, velocity and acceleration of the arrow as function of time before arrow exit. During these calculations the string was taken to be without mass. He also gives an approximation of the amount of energy which is transferred to the arrow when the string possesses mass and finds that the action of the string is almost equal to that of an added mass, i.e. one third of the mass of the part of the string being not in contact with the limbs and connected to the arrow, at the moment the arrow leaves the string. He assumes that arrow exit occurs when the string is stretched.

In [13] Marlow comments on Schuster's paper. With respect to the distribution of the energy on the different parts of the bow, he shows that the action of the string equals exactly that of the added mass mentioned above, if the arrow leaves the string when the latter is stretched. However, Marlow argues that arrow exit does not occur at that moment but somewhat later.

In [14] Marlow obtains results using a model for a non-recurve bow which resembles Hickman's. The limbs are replaced by rigid ones, connected by linear elastic hinges to the grip as in Figure 1.9. However, the place and strength of the elastic hinges and the amount of mass at the tips, are determined differently. The place of the hinges is at the end of the grip where it meets the limbs. The strength is determined using the measured SFD curve

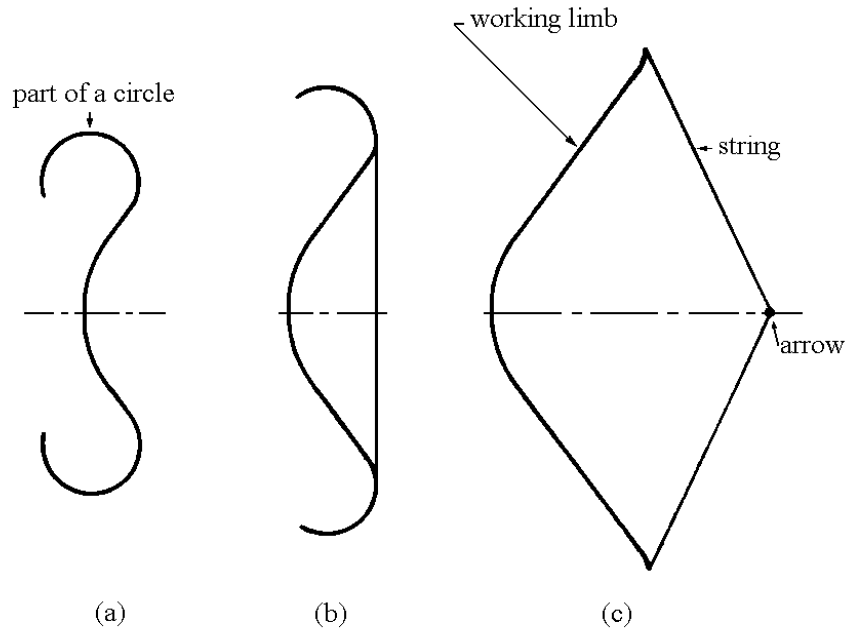


Figure 1.10: Working-recurve bow, Schuster's model.

of the real bow. The mass at the tips are chosen so that the moment of inertia of it with respect to the place of the hinge equals that of the "frozen" limbs with respect to the same point.

Marlow replaces the string by two equal rods connected to each other at the place of the arrow and to the tips of the limbs by hinges. Both rods are rigid with respect to bending but elastic in longitudinal direction with a constant mass per unit of length. His refinement of Hickman's model is this introduction of the elasticity of the string. In this case it is no longer possible to find a solution of the equations of motion in closed form. These equations are obtained by using the Lagrangian formalism and their solution is approximated numerically.

Finally, we mention a mathematical model for the interior ballistics given by Beckhoff in [2] and [1]. In [2] Beckhoff deals with statics. He determines the weight of a bow found in the neighbourhood of Vrees. He uses a linearized beam theory and introduces parameters for adoptions. His results agree well with experiments; the calculated weight and amount of additional energy differ slightly from those of a replica. In a footnote in his paper on a bow found in Nijdam [1] Beckhoff suggests a simple method to calculate the part of the additional energy which is transferred to the arrow when it leaves the string. The considerations given in this thesis show that it is not that easy.

At the end of this section we discuss for the sake of completeness also mathematical models for the exterior ballistics of the arrow. Exterior ballistics describes the flight of the arrow through the air. In all these models the arrow is treated as a point mass. A very

simple model is obtained by neglecting the resistance of the arrow in air. The path of the arrow is a parabola, depending on the initial velocity and the angle of elevation, but not on the mass of the arrow.

Earlier mathematical models of the exterior ballistics were given by English [3], Higgins [7] and Rheingans in [6], page 236. Rheingans assumes that the drag varies as velocity squared. The constant of proportionality, the so-called "drag constant", is the sum of three terms. The first term is proportional to a coefficient depending on the form of the head and the diameter of the shaft squared. It accounts for the head-on resistance. The second term accounts for the skin friction of the shaft. This term is proportional to length and diameter of the shaft. The third term reflects the skin friction of the fletching and is proportional to the area of both sides of feathers. The three constants of proportionality and the coefficient depending on the form of the head can be determined by wind tunnel tests.

Further, Rheingans gives a definition of the ballistic coefficient which is proportional to the mass of the arrow and inversely proportional to the drag constant. Having determined the ballistic coefficient, the path of the arrow is found by solving numerically an initial value problem for a system of two coupled ordinary differential equations the equations of motion for the arrow.

1.6 Our mathematical model

The main subject of this thesis is the development of a mathematical model for the interior ballistics of the bow and arrow. In our model the limb is considered a slender inextensible elastic beam subjected to large deformations. The string is able to withstand tensile forces only in the longitudinal direction. As for the models described in Section 1.5, it is, because of the symmetry, sufficient to deal with one half, the upper half, of the bow.

In Chapter 2 we deal with the static deformation of all three types of bows, non-recurve, static-recurve and working-recurve. The main objective is to find the SFD curve. The string is assumed to be inextensible. The adoptions of the theory to an elastic string, however, is easy.

From the braced situation to fully drawn situation in each position of the middle of the string the limb is deflected by a force in the string, while the middle of the bow is clamped. The deflection curve of an elastic beam, especially when large elastic deformations may occur, is called the "elastica". In each position we have to find the elastica as well as the force in the string. The drawing force can be determined afterwards.

In the case of the non-recurve bow, the governing equations for each position form a system of coupled ordinary differential equations with two-point boundary conditions. This system consists of two geometric equations and the Bernoulli-Euler equation, which states that the change of the curvature with respect to the unloaded situation, at any point is proportional to the bending moment at that point in the limb. The constant of proportionality is called the "bending stiffness" or flexural rigidity. The limb is assumed to be perfectly rigid in shear.

Basically the same holds for the static-recurve bow. In the case of the working-recurve bow the part of the limb in contact with the string remains undeformed. The boundary conditions are now prescribed at the point where the string leaves the limb, while this point is unknown a priori and has to be calculated as part of the solution. Then we have a so-called free boundary value problem.

Many articles have been written on related subjects, see Gorski [4], who gives a review of literature and a bibliography on large deformation of beams. In [18] Wang and Watson solve a problem very similar to ours. Characteristic for problems related to beams subjected to large displacements is the existence of more than one solution.

Our numerical approach is the same for the three types of bows. A simple shooting method is used, by which the problem is transformed into the problem of the solution of two non-linear equations for two unknowns. Attention is paid to the problem of finding starting points for the secant-Newton method which we used for solving these two equations. If the solution is not unique the developed method seems to yield all the possible relevant solutions (we do not have proof).

In Chapter 3 we deal with the dynamics of the non-recurve bow between release of arrow and its departure from the string. Part of the solution is the DFD curve. In Chapter 3 the string is also assumed to be inextensible and without mass. In that case the governing equations are the equations describing the motion of the limb, which is considered a slender inextensible beam. The boundary conditions are fixed by the fact that the bow is clamped in the middle and that the arrow assumed to be a mass point, is connected to the tip by a string without mass. Woodall in [19] considers a differential element of the beam in order to obtain the governing equations. We use Hamilton's principle. The rotatory inertia of the cross section of the limb is neglected and also in the dynamic case the Bernoulli-Euler equation is assumed. The equations form a system of coupled non-linear partial differential equations with two independent variables, one space and one time coordinate, and with initial and boundary conditions.

A finite-difference method is developed to solve the equations numerically. The values of the unknown functions in points of a grid covering the part of interest in the plane of the two independent variables is dealt with. At consecutive times a system of non-linear equations has to be solved. To that end we use a Newtonian method. As starting point the solutions at former times are extrapolated. At the instant of release the solution obtained by the method described in Chapter 2 is used.

No proof of stability and convergence of the finite-difference scheme is given. Instead, we check the accuracy of the results by means of computer experiments, for instance by bisecting the mesh width of the grid. Also mechanically inspired reasoning indicates that the equations are solved correctly. Further we compare our solution with one obtained by means of a commercially available finite-element method. The velocities of the arrow predicted by the two methods agree well; the difference for one bow and arrow combination is less than 2%. The dynamic force draw (DFD) curve produced by the finite-element method agrees roughly with ours but it does show some non-physical oscillations.

In the Section 3.6 we calculate the behaviour of the normal forces in the limb at the instant of release for the case of concentrated masses at the tip of the limb. We show that

in our model a discontinuity of this force occurs. The finite-difference scheme is adapted, so that this phenomenon cannot generate unrealistic oscillations of the solution.

The dynamics of the static-recurve bow is the main subject of Chapter 4.

Another subject is again the non-recurve bow, but now with a string which is elastic, obeying Hooke's law, and which possesses mass per unit of length. Hooke's law states that the longitudinal force in the string is proportional to the relative elongation. The constant of proportionality is called the "strain stiffness". The equations of motion for the string were given by Roos, Schweigman and Timman in [15]. In this case the governing equations form two systems of partial differential equations, one convective space coordinate along the limb and another one along the string. These systems are linked by boundary conditions at the tip of the bow. Further we consider in Chapter 4 the vibratory motion of bow and string after the arrow has left the string. Also the influence of the grasp of the grip by the bow hand is dealt with, as we mentioned in Section 1.4. Besides clamping the grip by the bow hand, the bow hand is allowed to be open in which case the hand can exert only a force on the bow in the direction of the shooting and the bow is able to move in that direction.

In all these cases, so for the static-recurve bow as well, the boundary conditions change abruptly when some condition is fulfilled. In the case of the static-recurve bow this happens at the moment the string touches the string-bridges again before arrow exit. For both types of bows, non-recurve and static-recurve, the boundary conditions change at the moment the arrow leaves the string or when the bow departs from the bow hand if the bow is shot open-handed.

The equations are solved numerically using the finite-difference method described in Chapter 3, adapted to the more general problem of Chapter 4. In Section 4.13 we check the finite-difference method again. To that end a vibrating cantilever with a rigid body fixed to the free end is considered. The deflections remain small, so that the elementary linearized beam theory applies. The Laplace transform technique is used to obtain an analytical solution. This solution is compared with the one produced by our finite-difference method.

Unfortunately lack of time prevents us from dealing in a sufficiently accurate way with the interesting problem of the dynamics of a working-recurve bow and the essentially asymmetric Japanese bow.

1.7 Units of measurement

We now discuss the units of measurement we use in this thesis. We start with some remarks on dimensional analysis.

As far as we know no paper on the mechanics of bow and arrow deals with the technique of dimensional analysis, although in [12] Langhaar gives an application of it to an archery bow. Some simple results obtained by applying dimensional analysis are the following. First, the weight of a bow is approximately (because the string is in reality slightly extensible) proportional to the bending stiffness of the limbs. Second, the part of the additional energy stored in the fully drawn bow which is transferred to the arrow, remains the same

when all the masses mass of limbs, string and arrow are multiplied by the same constant.

Because we have the equations of equilibrium and equations of motion at our disposal, dimensional analysis boils down to making these equations dimensionless. We choose in the case of statics two (draw and weight) and in the case of dynamics three (draw, weight and mass of one limb) "fundamental parameters". The other parameters which determine the action of the bow and arrow combination together with the fundamental parameters, appear in the dimensionless equations multiplied or divided by an appropriate combination of the fundamental parameters. The resulting quantities are called the "dimensionless parameters". We define the "inherent properties" of a bow and arrow combination to be those which depend only on these parameters.

The selection of the fundamental parameters is not unique. The motivation to take draw, weight and mass of one limb is the following. The maximum draw and weight depend on the stature of the archer. His "span" determines the maximum draw and his strength the maximum weight, so both have physical limitations. In practice the minimum mass of one limb has technical limitations. By taking these three parameters as fundamental, we compare automatically bows with the same draw, weight and mass of one limb with each other when we deal with the dimensionless equations of motion.

As units of measurement for the length, force and mass we use cm, kg force and kg mass, respectively. From this it follows that the unit of time the second is used, thus the velocity in cm/sec, acceleration in cm/sec², and so on. We apologize for this complication.

In literature forces, for example the weight, are usually given in pounds (1 pound=0.14536 kg force); lengths, for example the draw, in inches (1 inch=2.54 cm); masses, for example the mass of the bow, in pounds avoirdupois (1 pound=0.14536 kg mass) but mass of the arrow often in grains (1 grain=0.000648 kg mass).

1.8 Variety in archery

In this section we give a short enumeration of the varieties in archery. The purpose for which the bow is used has to be considered in the judgment of the performance of a bow. The performance will be the subject of the next section in which we define coefficients which give information about the quality of a bow.

Already old cave paintings in Spain, France and parts of Africa show hunting scenes. These make clear that the bow held an important place with the hunters in prehistoric times. In our time hunting with bow and arrow as pastime is popular in some parts of North America.

In history many world empires were founded and maintained for some time owing to the superior performance of their bows and the skilled use made of them by the archers (English yeoman) or horseman (Asiatic nomadic hordes). In the 15th century the bow disappeared from the battle fields in the "civilized" world. On the Continent of Europe the hand bow was already superseded for the most part by the cross bow (Genoese and Swiss mercenary cross bowmen). The cross bow is a powerful weapon which demands less training and skill, but is also much slower in operation. It was prohibited by Pope Innocent

II in 1139, as being: "deathly and hateful to God and unfit to be used among Christians".

For hunting and warfare good penetration capacity of the arrow is required. As mentioned in the preface we do not deal with the mechanics of the penetration of the projectile into the target. It is evident that it depends on the shape of the head of the arrow and the material of the target. A large kinetic energy of the arrow at the moment of impact and perhaps also a large linear momentum are indispensable. The velocity of the arrow has to be not too small in order to get a flat trajectory of the arrow.

Foot soldiers and hunters in open spaces can use rather long bows, for example about the height of the archer. On the other hand, a hunter in a wooded area and a mounted archer are unable to handle a long bow easily.

As has been said already nowadays archery has a certain importance as a pastime. We distinguish between three types of pastime archery, which proceed from the archery used for hunting or for military practice

In the first type of pastime archery the archer tries to hit some kind of mark. By the 17th century in England, shooting was done at "rovers" or at "clout". Roving consists of shooting at marks unknown beforehand, the winner of each flight selecting the next mark. The clout is a small white target on the ground shot at from a known, rather large distance. These two forms have now changed into field archery and target archery. There is a large variety in field archery, by which the archers proceed round a course shooting at different distances and at different marks. In the case of target shooting arrows are shot at faces divided into a number of zones and at different but known distances. In this form it became very popular at first in England and later also in North America. Target archery events were included in the Olympic Games of 1900, 1904, 1908 and 1920 and again since 1972. It is now the most popular form, practiced in many countries all over the world.

In England the famous longbow, which contributed to its victories in the Middle Ages, was used. Later, when archery became popular in America, the English example was followed with respect to equipment (use of longbow), competitive events, and so on. Nowadays, the laminated, centre-shot, take-down bow with stabilizers is almost solely seen on shooting meetings.

Popinjay is also an old form of shooting at marks. It consists of shooting down feathered "birds" from a tall mast. For instance in some parts of Europe, France, Belgium, Holland and Northern Germany, it was very popular. In Belgium it is still a public game. The cross bow has been used for Popinjay shooting, but also the same kind of bows as for target shooting.

For forms of archery belonging to this type, accuracy is most important. With respect to mathematical modelling this is a feature difficult to handle. Each shot differs from the proceeding one because the loose or the movement of the bow arm may vary, this in contrast with the use of a perfect shooting machine. However, even in that case not every shot is exactly the same. For example, when six arrows are shot the mass of these arrows may differ slightly or the weather conditions may change. Hence, first all the parameters which determine the action of a bow and arrow combination have to be as constant as possible and second the action of the bow must not exaggerate small differences in these parameters. Some of the parameters are already fixed by the bowyers (manufacturers of

bows and arrows) for instance the mechanical properties of the material of the limbs. Other parameters are determined by the archer himself, such as the weight of the arrow or the brace height.

The second type of pastime archery is flight shooting. The purpose of flight shooting is to shoot an arrow as far as possible. The Turkish bowmen became famous because of their skill in flight shooting. Turkish archery reached the zenith of its achievement in the 15th century and had a revival as a sport in the 19th century.

For flight shooting a very short, recurved composite bow (which were powerful) were used. The arrows were very light and often shorter than the draw, so that a so-called "siper" had to be used to guide the arrow along the grip. Today laminated bows are used for flight shooting.

In this case it is easy to judge the performance of a bow. For, with respect to the interior ballistics, the muzzle velocity is very important and has to be as large as possible.

Finally there is ceremonial target archery, by which hitting the target is secondary but unity of mind, body and bow is most important. For this form the Japanese use their typical asymmetric bow.

1.9 Quality coefficients

In this section we discuss some quality coefficients, which are introduced in order to compare the mechanical performance of bows more easily. These coefficients are numbers associated with quantities of which the importance depends on the fields of application of the bow. The quality coefficients will be dimensionless and are formed by means of the dimensionless parameters. They measure in this way the inherent performance of a bow.

With respect to statics we introduce the "static quality coefficient" q , being the dimensionless amount of additional energy, which equals the area below the SFD curve. In the case of real bows, the bow returns to its braced shape after each shot, as a result of internal and external damping. Then, using energy conservation, the maximum available energy which can be imparted to the arrow equals the additional energy and is accumulated in the bow while drawing it from braced situation into fully drawn situation. In Section 4.5 we show that this is also true when damping is neglected and the bow is clamped in the middle or shot open-handed. Some flight shooters loose with a trust of the bow hand against the grip. If this is accompanied with a move in the direction of the shooting then the during this action supplied energy can be transferred to the arrow together with the additional energy.

In practice only a part of the additional energy is transferred to the arrow. The kinetic energy of the arrow at arrow exit equals the area below the DFD curve. The "efficiency" η , our second quality coefficient, is defined as this kinetic energy divided by the additional energy.

The third quality coefficient is the muzzle velocity ν made dimensionless in the manner we described in Section 1.7.

The amount of kinetic energy and linear momentum of the arrow when leaving the

string can be calculated easily using the quality coefficients. The kinetic energy is the product of the static quality coefficient and the efficiency and the linear momentum is this amount of kinetic energy divided by half the muzzle velocity.

The influence of the dimensionless parameters can be determined just by changing each parameter separately. Such an investigation delivers which parameters are most significant. The smoothness of action may be important with respect to the magnification of differences in handling of the bow. The behaviour of the acceleration force acting upon the arrow and the so-called "recoil force", as function of time are salient factors which determine whether the bow is a so-called sweet bow or not. The recoil force, which is felt by the archer, is the force exerted by the bow on the bow hand. Sometimes the word "kick" is used when a jerk is felt after release of the arrow.

Finally the three fundamental parameters, discussed in Section 1.7, namely draw, weight and mass of one limb are of course important. Men strong enough to pull heavy bows, or tall men with long arms, or those who have materials with excellent mechanical properties at their disposal and know how to use them in making a bow, are always favoured.

Note that when the strength of materials of limbs and string is taken into account, the maximum occurring bending moments in the limbs and maximum tensile force in the string have to be kept within certain bounds. In Section 4.8 we briefly deal with these quantities.

In our theoretical approach the performance (static quality coefficient, efficiency, muzzle velocity, smoothness of action) is considered as a function defined on the space spanned by the parameters of the bow. We divided the set of parameters into two groups, the fundamental parameters and the dimensionless parameters. The dimensionless quality coefficients depend only on the dimensionless parameters. Representations of different existing types of bows form clusters in the dimensionless parameter space. This space is infinitely dimensional, because some of these parameters are functions of the length coordinate along the limb, for example the mass distribution. If these functions are approximated by polynomials or splines of some finite degree, which has to be large enough in order to get reasonable approximations, the dimensionless parameter space becomes finite dimensional.

1.10 Comparison of different mathematical models

In this section we compare the different mathematical models mentioned in Sections 1.5 and 1.6. To that end we use results of our calculations on basis of these different models, about the mechanical action of a specific bow given by Hickman in [8], referred to as H bow.

In Section 2.5 we determine the static performance of the H bow by means of Hickman's model and by means of our model. The SFD curves look very similar, the difference in the calculated weights is less than 3%, the static quality coefficients differ less than 2%. In Section 3.5 we deal with the dynamic performance of the H bow provided with an inextensible string without mass. The efficiency of this bow calculated with Hickman's

model is 100%, our model yields 89%.

In Section 1.5 the same bow but now with an elastic string with mass, referred to as \tilde{H} bow, is considered. Marlow's model predicts a weight of this bow about 25% smaller than our model. His static quality coefficient is almost 5% larger. The efficiency of the H bow using Marlow's model equals 74% and using our model 81%. This results in a small difference in the calculated dimensionless muzzle velocities. The DFD curve, calculated using Marlow's model shows heavy oscillations of the acceleration force acting upon the arrow.

These results show that Hickman's model, being very simple, gives rather good predictions for the static performance of the H bow. Observe that for other bows it may be not this good, because he adapted his model to some of the characteristics of the H bow. Marlow's model does not seem to be an improvement of Hickman's, although his model for the string is more realistic. For, the combination of rigid limbs rotating about elastic hinges and an elastic string gives unreliable results and unrealistic heavy oscillations in the DFD curve.

Observe that we do not discuss the results of Schuster's model [16], because we are not able to deal accurately enough with the dynamic performance of the working-recurve bow.

As mentioned in Section 1.4, in all models, including our model, the lateral movements of bow, string and arrow are neglected. Unfortunately, these motions seem to be an important factor with respect to the utility of the bow for shooting at marks, where accuracy is indispensable. Hence, one cannot expect to get an overall picture of the performance of a bow used for target shooting. For instance, the influence of the mass of the grip and of the stabilizers on the lateral movements and the twisting of the bow round the vertical axis, called "torque", is beyond our scope. The same holds for the influence of the nocking height (Figure 1.6).

For flight shooting these small random movements have almost no influence on the range of the arrow. For hunting and in the old times warfare, these lateral movements are of some importance.

Finally a remark on the validity of the use of the Bernoulli-Euler equation. Many text books on strength of materials, e.g. Timoshenko [17], show how the bending stiffness depends on the shape and the dimensions of the cross section and the physical properties of the materials and discuss the presumptions which are made. We note that, especially in the case of the ancient composite bow, the assumption that the Bernoulli-Euler equation holds, may lead to inaccuracies. With respect to a simple bow made of wood the difficulty arises that wood is a rather incalculable material, see Kollmann et al. [9, 10]. Also for the physical properties of the material of the string, the application of Hooke's law can be said to be questionable.

1.11 Comparison of the mechanical performance of different types of bows

In this final section of the introduction we discuss the performance of different types of bows. We use the quality coefficients given in Section 1.9, keeping in mind the remarks given in the last paragraphs of Section 1.10.

In order to gain insight into the influence of a change of the parameters on the action of the bow, we change these parameters separately one by one, starting with one bow of each type. In what follows we mention only those influences of parameters which are striking.

In Sections 2.5 and 3.5 we start with a non-recurve bow, described by Hickman in [8] which we called the H bow. The static performance depends strongly on the brace height and length of the bow. As expected, it becomes less good for a larger brace height and a shorter bow. Short straight bows have a tendency to "stack". This is the property of a bow to be drawn easily for a large part of the draw length and to build up to full weight rapidly as the string comes to full draw. Stacking goes hand in hand with a small static quality coefficient. On the other hand a short bow possesses a larger efficiency but when the bow becomes too short, the arrow leaves the string before the string is stretched. A longer bow has a more smooth action by which the string keeps a good contact with the arrow.

With respect to dynamics, the mass of the arrow is most important. A light arrow yields a small efficiency but also a larger muzzle velocity. If the arrow is too light, however, the arrow leaves the string before the string becomes taut. So, in practice there is a lower bound for the mass of the arrow.

The effect of concentrated masses at the tips appeared to be negligible with respect to the mentioned two dynamic quality coefficients, namely efficiency and muzzle velocity. Obviously, as in Hickman's model, the absorbed energy in these masses is recovered before the arrow leaves the string.

In Section 4.7 we deal with the influence of the strain stiffness and mass of the string. From the point of view of statics the influence of the elasticity of the string is small. As to dynamics if the number of strands changes (mass is about directly and strain stiffness about inversely proportional to number of strands), there are two effects which counteract each other. More strands mean a heavier string and therefore a smaller efficiency, but it also means a stiffer string and hence a larger efficiency.

We repeat in Section 4.9 the above mentioned changes of parameters, but now for a bow called the KL bow, which resembles a bow described by Klopsteg in [6]. It differs from the H bow because its limbs possess more mass per unit of length near the tip and the string is extensible and possesses mass. So this bow is more realistic. Further we deal in that section with the vibratory motion of limbs and string after arrow exit.

Roughly speaking the influence of the change of parameters for the KL bow is the same as in the case of the H bow. In Figure 1.11 we show the static quality coefficient q of the KL bow as function of the dimensionless half length L of the bow and in Figure 1.12 the efficiency η and muzzle velocity ν as function of the dimensionless half mass m_a of the

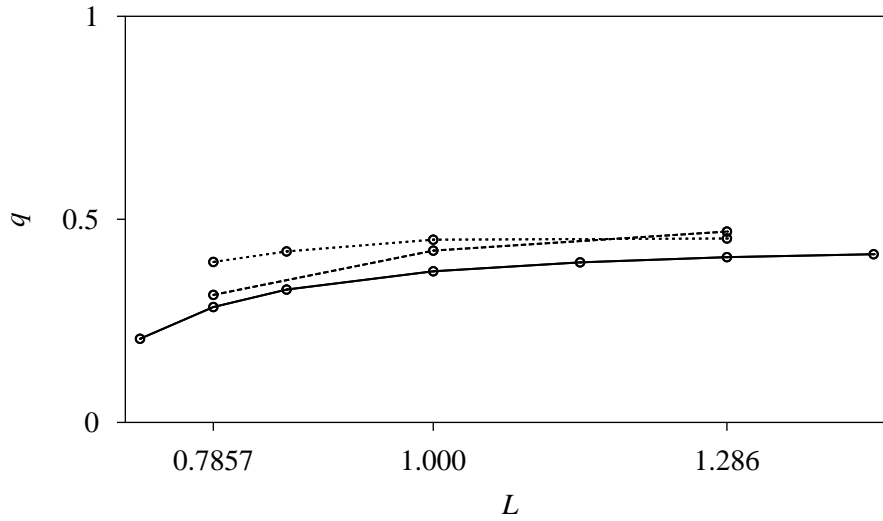


Figure 1.11: Static quality coefficient q as function of the dimensionless half bow length L for different types of bows. Solid line: straight bow KL, dashed line: static-recurve bow PE and dotted line: angular bow AN.

arrow. Concentrated masses at the tips or heavier limbs near the tips in combination with an elastic string, appear to be disadvantageous now. Further, for small brace heights the string slaps against the grip after arrow exit. This means that a minimum brace height has to be used. Archers often wear a "bracer" on the bow arm to protect this arm from the blow of the string. In many cases, for instance when the bow has no grip, the force in the string becomes negative after arrow exit. At that moment the string becomes slack. When the string suddenly is stretched again, it is possible that a kick is felt by the archer. At the end of Section 4.9 we discuss the angular bow denoted by AN bow. The static quality coefficient of this bow, especially when it is short, is much better than that of the straight KL bow of the same length, see Figure 1.11. Unfortunately the efficiency of the angular bow is worse, still the muzzle velocity is better than that of the corresponding straight KL bow when both are not too long.

The static-recurve bow is the subject of Section 4.11. Starting with a bow, referred to as PE bow which resembles the old Asiatic bow depicted in many books and articles, we change the parameters as we did for the KL bow. The introduction of rigid ears produces a larger static quality coefficient, see Figure 1.11. The efficiency, however, is worse than that of the straight KL bow, having the same length, see Figure 1.12. This is largely due to heavy ears. We stated already that concentrated masses at the tip in combination with an elastic string are disadvantageous. The DFD curve of the PE bow oscillates severely, so it seems to be an unpleasant bow to shoot with.

The influence of the change of all parameters look the same as those in the case of the KL bow. For instance; a light arrow implies a large muzzle velocity.

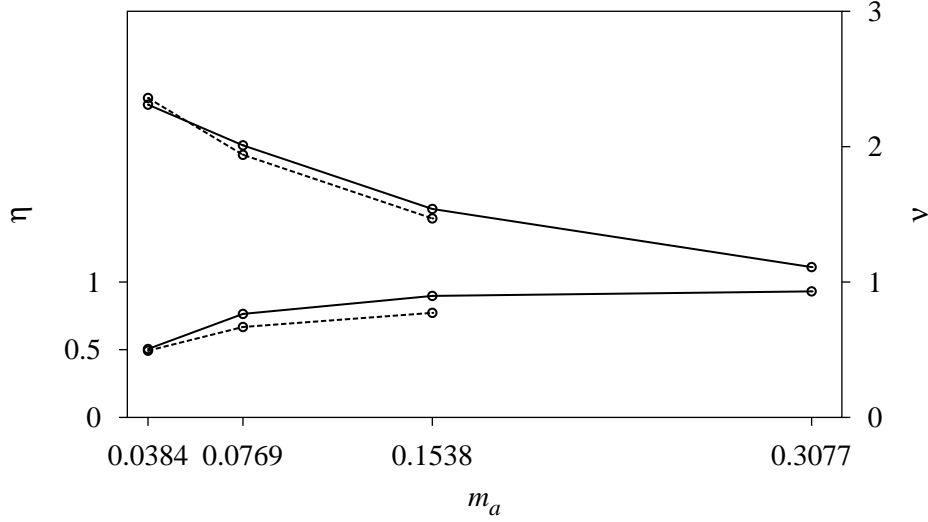


Figure 1.12: Efficiency η and muzzle velocity ν as function of dimensionless half mass m_a of arrow. Solid line: straight bow KL, dashed line: static-recurve bow PE.

To sum up the results, we notice that the dimensionless muzzle velocities of all the bows we have considered, keeping the mass of the arrow constant, differ relatively little. The values lie between 1.72 and 2.06. The influence of a change of the mass of the arrow is almost the same for the different types. The short angular bow and static-recurve bow do not have a better inherent performance than the long straight KL bow.

So far the dimensionless parameters. The discussion of the change of the fundamental parameters is the same for both types of bows, non-recurve and static-recurve ones. In Section 4.12 we deal with this subject. As already mentioned (Section 1.7 of this introduction) the draw and weight have physical limitations and the mass of one limb has a technical limitation. This means that at this place the mechanical properties appear on the stage. These properties determine the maximum amount of energy that can be stored in the limbs and string of the bow.

In order to get an insight into this we consider in Section 4.12 a number of bows described in literature, of which the draw, weight, mass of the arrow and sometimes mass of the bow are given. These data indicate that more energy per unit of mass of the limb can be stored in the ancient Asiatic composite bow than in simple wooden bow. However, much of this energy is already stored in the bow in the braced situation, and this energy is not available for the shooting. Nevertheless, the main reason for the fact that the short Asiatic static-recurve bow had a good performance, is that excellent materials have deliberately been put to use. As we mentioned already, the dimensionless muzzle velocity and therefore also the kinetic energy, of the short static-recurve bow is reasonable in contrast with this quantity for a short straight bow. The shortness of these bows made them suitable for the use on horseback.

Concerning the performance of the working-recurve bow, we deal in Section 4.5 with the statics of a modern recurve bow and of a bow with an excessive recurve. The static quality coefficient of the first mentioned bow, used for target shooting is rather small. Obviously, for shooting at marks less importance is attached to the static performance. Data of mechanical properties of the materials used for modern bows indicate that a large amount of energy per unit of mass can be stored in these bows.

The other bow dealt with in Section 4.5 resembles a bow developed by Hickman [6, page 50]. The limbs are semicircles, curving away from the archer when at rest, resembling a figure 3. The SFD curve of this bow even decreases over some interval, just as in the case of the compound bow. In 1948 Hickman shot at a flight shooting meeting further than many who were using bows twice as strong! This information shows that the dynamics of a working-recurve bow is an interesting subject for future research.

Bibliography

- [1] Beckhoff K. (1963). Die eisenzeitlichen Kriegsbogen von Nydam. *OFFA* 20:39–48.
- [2] Beckhoff K. (1964). Der Eibenbogen von Vrees. *Die Kunde N.F.* 15:113–125.
- [3] English F. (1930). The exterior ballistics of the arrow. *Journal of the Franklin Institute* 210:805–819.
- [4] Gorski W. (1976). A review of literature and a bibliography of finite elastic deflections of bars. *The Institute of Engineers, Australia, Civil Engineering Transacts* pp. 74–85.
- [5] Hickman CN. (1937). The dynamics of a bow and arrow. *J. of Applied Physics* 8:404–409.
- [6] Hickman CN, Nagler F, Klopsteg PE. (1947). *Archery: the technical side*. National Field Archery Association, Redlands (Ca).
- [7] Higgins GJ. (1933). The aerodynamics of an arrow. *Journal of the Franklin Institute* 216:91–101.
- [8] Klopsteg PE. (1943). Physics of bows and arrows. *Am. J. Phys.* 11:175–192.
- [9] Kollmann FFP, Côté WA. (1968). *Principle of wood science and technology, I Solid Wood*. Springer Verlag, Berlin.
- [10] Kollmann FFP, Kuenzi EW, Stamm AJ. (1968). *Principle of wood science and technology, II Wood based materials*. Springer Verlag, New York.
- [11] Lake F, Wright H. (1971). *Bibliography of archery*. The Simon Archery Foundation, Manchester.

- [12] Langhaar HL. (1951). *Dimensional analysis and theory of models*. Wiley, New York, London.
- [13] Marlow WC. (1980). Comment on: Ballistics of the modern working recurve bow and arrow. *Am. J. Phys.* 48:983–984.
- [14] Marlow WC. (1981). Bow and arrow dynamics. *Am. J. Phys.* 49:320–333.
- [15] Roos JP, Schweigman C, Timman R. (1973). Mathematical formulation of the laws of conservation of mass and energy and the equation of motion for a moving thread. *Journal of Engineering Mathematics* 7:139–146.
- [16] Schuster BG. (1969). Ballistics of the modern-working recurve bow and arrow. *Am. J. Phys.* 37:364–373.
- [17] Timoshenko S. (1955). *Strength of materials*. Van Nostrand Reinhold, New York.
- [18] Wang CY, Watson LT. (1980). On the large deformation of c-shaped springs. *International Journal of Mechanical Science* 22:395–400.
- [19] Woodall SR. (1966). On the large amplitude oscillations of a thin elastic beam. *Int. J. Non Linear Mechanics* 1:217–238.

Chapter 2

On the static deformation of the bow¹

2.1 Summary

The storage of deformation energy in a bow with or without recurve is considered. Some numerical examples are discussed. For a simple bow it is shown that theoretically a shooting efficiency of hundred percent is possible.

2.2 Introduction

The bow and arrow have been invented by mankind already in prehistoric times. During many millineries it was its most effective long range weapon and hunting device. Nowadays it is used in archery, a sport practiced by many people all over the world.

A bow can store energy as deformation energy in its elastic arms or limbs. Its special feature is that this energy, delivered by the relatively slow human body, can be quickly released to a light arrow in a very effective way. Probably essential for the effectiveness of the transformation of the deformation energy into kinetic energy of the arrow is the string, as light and inextensible as possible, which couples bow and arrow.

The main object of this paper is to discuss the statics of the bow. It will be represented by an infinitely thin elastic line endowed with bending stiffness, which is a function of a length parameter along this line. In the unbraced situation, which is the situation of the bow without string, the elastic line can be curved in the "opposite" direction. It turns out that this curvature called recurve is important with respect to the way in which the deformation energy can be stored. When drawing a bow, in general the force exerted by the archer on the string, will increase. So in order to keep a bow in fully drawn position, the maximum force, called the weight of the bow must be exerted by the archer while he aims at the target. Hence one of the objectives for more relaxed shooting is that this force is not too large while still a sufficient amount of deformation energy is stored in the bow. A properly chosen recurve is one of the possibilities to achieve this. It will be shown that by

¹B.W. Kooi and J.A. Sparenberg, On the static deformation of a bow *Journal of Engineering Mathematics* **14**(1):27-45 (1980)

such a recurve it even is possible that the drawing force can decrease in the neighbourhood of maximum draw. Such a phenomenon is well known in the nonlinear theory of elasticity.

We will not discuss here the "compound" bow, invented about fifty years ago by a physicist named Claude Lapp [2]. This bow uses, in order to cause the just mentioned effect of the decreasing drawing force, pulley's with eccentric bearings at the end of the elastic limbs.

Much research has been carried out already on the bow and arrow. For a general background we refer to the article of Klopsteg [6], where many aspects of bow and arrow are thoroughly discussed from a physical point of view. Other papers are for instance [5] and [8] where by making simplifying assumptions, calculations of the stored energy have been carried out. In this paper we use the theory of elastica with large deformations as discussed for instance by Frisch-Fay [4]. Because nowadays computers are available the non linear deformation of our model can be calculated without further simplification. It turns out that it can happen, al be it for not too realistic bows, that there is more than one solution to the problem.

In calculating properties of bows it is the intention to obtain an insight in what makes a bow a good bow, in this paper from the static point of view only. Besides by a number of parameters, length of the bow, ultimate drawing force and some others, the static behaviour of a bow is determined by two functions namely its shape without string, and its distribution of bending stiffness. These functions have to be chosen in one way or another. This means that there is a large measure of freedom which is not so easy to catalogue. It is not the aim of this paper to give a full account of possibilities however in the section on numerical results some trends are shown. In a following paper we hope to return to this subject in a more exhaustive way. We remark that when the dynamics of a bow is considered even a third function, the mass distribution, comes into play.

We have also applied our theory to two ancient bows. One is an Asiatic bow of the 14th century and is described in [7]. The other one is much older and is possibly constructed ± 3500 years ago [3].

It must be remarked that in general it is not possible that all the deformation energy stored statically in the bow can be transferred, during the dynamic process of shooting, as kinetic energy to the arrow. This depends on the way in which the kinetic energy of the arms or limbs can be recovered. It is shown in the Appendix 2.6, for a simple model of a bow, when the mass of the string can be neglected and when it is inextensible, that all the deformation energy stored in this bow can be transformed into kinetic energy of the arrow. Hence, no kinetic energy is left behind in the arms.

2.3 Formulation of the problem

We will consider bows which are symmetric or nearly symmetric with respect to some line, in the latter case we treat them approximately as being symmetric. The bow is placed in a Cartesian coordinate system (\bar{x}, \bar{y}) , the line of symmetry coincides with the \bar{x} axis. Its midpoint coincides with the origin O . The upper half is drawn in Figure 2.1. We assume

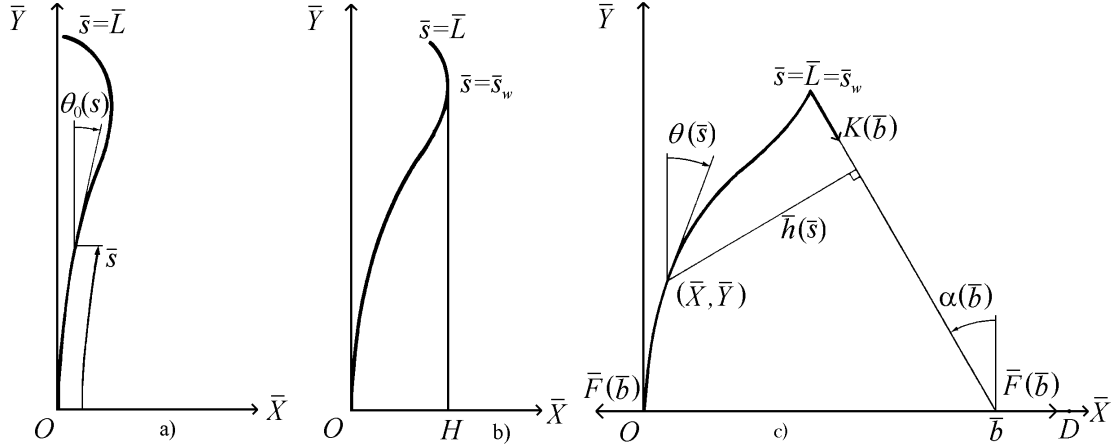


Figure 2.1: Three situations of the working-recurve bow: a) unbraced, b) braced, c) partly drawn.

the bow to be inextensible and of total length $2\bar{L}$. In our theory it will be represented by an elastic line of zero thickness, along which we have a length coordinate \bar{s} , measured from O hence $0 \leq \bar{s} \leq \bar{L}$. This elastic line is endowed with bending stiffness $\bar{W}(\bar{s})$.

In Figure 2.1.a the unbraced situation (without string) is drawn. The geometry of the bow is described by the local angle $\theta_0(\bar{s})$ between the elastic line and the y axis, where $\theta_0(\bar{s})$ is a given function of \bar{s} . Because the bow possesses recurve it is predominantly curved to the left.

In Figure 2.1.b the bow is braced by applying a string of total length $2\bar{l} (\bar{l} < \bar{L})$, which also is assumed to be inextensible. In the braced position no force in the \bar{x} direction is exerted on the string which intersects the \bar{x} axis under an angle of 90° . It is possible for a bow with recurve as is drawn in Figure 2.1 that a value $\bar{s} = \bar{s}_w < \bar{L}$ exists such that for values of \bar{s} with $\bar{s}_w \leq \bar{s} \leq \bar{L}$ the string lies along the bow. We assume that in that case there is no friction between bow and string. The string at $\bar{s} = \bar{s}_w$ has to be tangent to the bow of which the curvature for $\bar{s}_w \leq \bar{s} \leq \bar{L}$ is the same as the curvature in the unbraced situation. However, it is also possible that for a bow with less or without recurve, the string starts from the tip, then $\bar{s}_w = \bar{L}$ and the string can make a non zero angle with the tangent to the bow at the tip (Figure 2.4). Instead of the length of the string the brace height or "fistmele" $|\overline{OH}|$ can be used as a basic quantity of the braced position.

In Figure 2.1.c the bow is pulled by force $\bar{F}(\bar{b})$ into a partly drawn position where the middle of the string has the \bar{x} -coordinate \bar{b} . Also in this situation the string can still lie partly along the bow for values of \bar{s} with $\bar{s}_w(\bar{b}) \leq \bar{s} \leq \bar{L}$ and the same considerations hold as were given for the region of contact in the braced situation. To each bow belongs a value $\bar{b} = |\overline{OD}|$ for which it is called fully drawn. The force $\bar{F}(|\overline{OD}|)$ is called the "weight" of the bow and the distance $|\overline{OD}|$ is its "draw".

In our theory we have to consider only the upper half of the bow, clamped at O . The

Bernoulli-Euler equation, which we assume to be valid for the elastic line, reads

$$\overline{M}(\overline{s}) = \overline{W}(\overline{s}) \left(\frac{d\theta}{d\overline{s}} - \frac{d\theta_0}{d\overline{s}} \right), \quad 0 \leq \overline{s} \leq \overline{L}. \quad (2.1)$$

Besides (2.1x) we have two geometric equations

$$\frac{d\overline{y}}{d\overline{s}} = \cos \theta, \quad \frac{d\overline{x}}{d\overline{s}} = \sin \theta, \quad 0 \leq \overline{s} \leq \overline{L}. \quad (2.2)$$

The moment $\overline{M}(\overline{s})$ is caused by the tension force $\overline{K}(\overline{b})$ in the string, we find

$$\overline{M}(\overline{s}) = \overline{K}(\overline{b}) \overline{h}(\overline{s}) = \overline{K}(\overline{b}) (\overline{b} \cos \alpha - \overline{x}(\overline{s}) \cos \alpha - \overline{y}(\overline{s}) \sin \alpha), \quad 0 \leq \overline{s} \leq \overline{s}_w, \quad (2.3)$$

where $\overline{h}(\overline{s})$ (Figure 2.1.c) is the length of the perpendicular from the point $(\overline{x}, \overline{y})$ to the string and $\alpha(\overline{b})$ is the angle between the string and the \overline{y} axis, reckoned positive in the indicated direction. There are three boundary conditions at $\overline{s} = 0$, namely

$$\theta(0) = \theta_0(0), \quad \overline{x}(0) = \overline{y}(0) = 0. \quad (2.4)$$

Besides we have a geometrical condition with respect to the length of the string. In our model the thickness of the elastic line is assumed to be zero hence the length of the parts of bow and string which are in contact with each other are equal and we find

$$(\overline{b} - \overline{x}(\overline{s}_w))^2 + (\overline{y}(\overline{s}_w))^2 = (\overline{l} - (\overline{L} - \overline{s}_w))^2. \quad (2.5)$$

When \overline{b} is prescribed the equations (2.1), (2.2) and (2.3) together with the conditions (2.4) and (2.5) are sufficient to determine the situation of the bow hence also the unknown functions $\theta(\overline{s})$, $\overline{x}(\overline{s})$, $\overline{y}(\overline{s})$ and $\overline{M}(\overline{s})$ and the unknown constants $\overline{s}_w(\overline{b})$, $\overline{K}(\overline{b})$ and $\alpha(\overline{b})$.

It is clear that

$$\overline{M}(\overline{s}) = 0, \quad \overline{s}_w \leq \overline{s} \leq \overline{L}, \quad (2.6)$$

hence it follows from (2.1) that for the region of contact of string and bow, the bow has kept its curvature of the unbraced situation as has been mentioned previously. Thus

$$\theta(\overline{s}) = \theta_0(\overline{s}) + (\theta(\overline{s}_w) - \theta_0(\overline{s}_w)), \quad \overline{s}_w \leq \overline{s} \leq \overline{L}. \quad (2.7)$$

We want to calculate the force $\overline{F}(\overline{b})$ (Figure 2.1.c) from which follows the energy \overline{A} stored in the bow when it is brought from the braced position $\overline{b} = |\overline{OH}|$ into the fully drawn position $\overline{b} = |\overline{OD}|$. We have

$$\overline{A} = \int_{|\overline{OH}|}^{|\overline{OD}|} \overline{F}(\overline{b}) d\overline{b}. \quad (2.8)$$

This amount of energy must be equal to the difference between the deformation energy of the bow in the fully drawn position and the deformation energy in the braced position. Hence we have another representation of \overline{A}

$$\overline{A} = \left[\int_0^{\overline{L}} \overline{W}(\overline{s}) (\theta'(\overline{s} - \theta_0 \overline{s}))^2 d\overline{s} \right]_{\overline{s}=\frac{|\overline{OD}|}{|\overline{OH}|}}^{\overline{s}=\frac{|\overline{OD}|}{|\overline{OH}|}}, \quad (2.9)$$

which can be used to check the computations.

We now introduce dimensionless quantities by

$$\begin{aligned} (\overline{x}, \overline{y}, \overline{s}, \overline{L}, \overline{l}) &= (x, y, s, L, l) \frac{|\overline{OD}|}{|\overline{OH}|}, \quad \overline{M} = M \frac{|\overline{OD}|}{|\overline{OH}|} \overline{F}(|\overline{OD}|), \quad \overline{K} = K \frac{|\overline{OD}|}{|\overline{OH}|} \overline{F}(|\overline{OD}|), \\ \overline{W} &= W \frac{|\overline{OD}|^2}{|\overline{OH}|^2} \overline{F}(|\overline{OD}|), \quad \overline{A} = A \frac{|\overline{OD}|}{|\overline{OH}|} \overline{F}(|\overline{OD}|). \end{aligned} \quad (2.10)$$

In (2.10) we have used the still unknown force $\overline{F}(|\overline{OD}|)$ to obtain dimensionless quantities, however, this sometimes makes it more simple to compare numerical results for several types of bows.

Also we introduce the angle

$$\varphi = \theta - \theta_0, \quad (2.11)$$

then after combining (2.1) and (2.3) the relevant equations become

$$W \frac{d\varphi}{ds} = K ((b-x)\cos\alpha - y\sin\alpha), \quad 0 \leq s \leq s_w, \quad (2.12)$$

$$\varphi(s) = \varphi(s_w), \quad s_w \leq s \leq L, \quad (2.13)$$

$$\frac{dx}{ds} = \sin(\varphi + \theta_0), \quad \frac{dy}{ds} = \cos(\varphi + \theta_0), \quad 0 \leq s \leq L, \quad (2.14)$$

$$(b - x(s_w))^2 + (y(s_w))^2 = (l - L + s_w)^2, \quad (2.15)$$

$$\varphi(0) = x(0) = y(0) = 0. \quad (2.16)$$

In the next section a method to solve these equations is discussed.

2.4 Numerical solution of the equation of equilibrium

In this section we consider some aspects of the numerical method used to solve the equations (2.12)–(2.16). We take for b a fixed value

$$\frac{|\overline{OH}|}{|\overline{OD}|} \leq b \leq 1. \quad (2.17)$$

When b passes through this range the bow changes from its braced position to its fully drawn position. First we assume the bow to be partly or fully drawn hence not to be in the braced position. The length $2l$ of the string is prescribed.

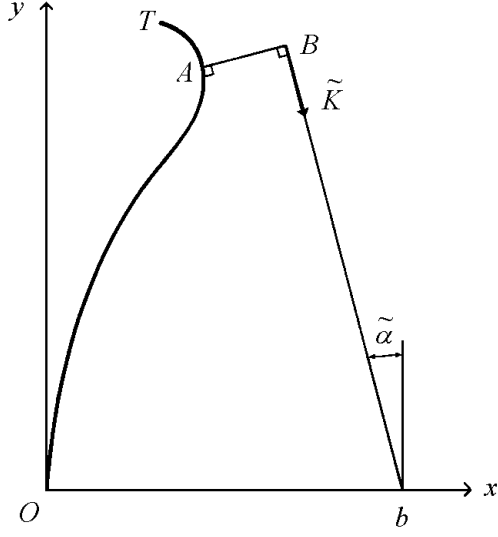


Figure 2.2: The bow deflected by a force \tilde{K} , making an angle $\tilde{\alpha}$ with the y axis, at the arm AB .

The unknown force K exerted on the bow by the string passes through the point $(b, 0)$ and makes an unknown angle α with the y -axis. We make some choice \tilde{K} and $\tilde{\alpha}$ for the values of K and α , and solve the equations (2.12) and (2.14) starting at $s = 0$ where we satisfy the initial conditions (2.16). We assume the functions $W(s)$ and $\theta_0(s)$ to be continuous and $W(s) \geq \epsilon > 0$. Then it is not difficult to show that the solution exists and is unique. A Runge-Kutta method is used to obtain this solution.

There are two possibilities which can occur. First, when continuing the solution of (2.12) and (2.14) for a suitable choice of \tilde{K} and $\tilde{\alpha}$, we reach a point A with a value of $s = \tilde{s}_w < L$ for which

$$\varphi(\tilde{s}_w) = -\tilde{\alpha} - \theta_0(\tilde{s}_w), \quad (2.18)$$

in words, a value of s for which the tangent at the bow is parallel with the chosen direction $\tilde{\alpha}$ of the force \tilde{K} . After this the undeformed part AT (Figure 2.2), is added to complete the "bow" hence

$$\varphi(s) = -\tilde{\alpha} - \theta_0(\tilde{s}_w), \quad \tilde{s}_w \leq s \leq L. \quad (2.19)$$

Second, there is no $\tilde{s}_w < L$ that satisfies (2.18), the solution is continued until $s = L$, then the point A coincides with the tip T of the bow.

So, we have found a deflected position OAT of the bow which in fact is caused by connecting to the bow, at $s = \tilde{s}_w$ in the first case or at $s = L$ in the second one, a rigid bar AB perpendicular to the direction $\tilde{\alpha}$, at the end of which acts the force \tilde{K} . This is illustrated in Figure 2.2 for the first case.

The force \tilde{K} and the angle $\tilde{\alpha}$ have to be determined such that $|A - B| = 0$ and the "distance" between the point $(b, 0)$ and the tip T , measured from A to T along the bow

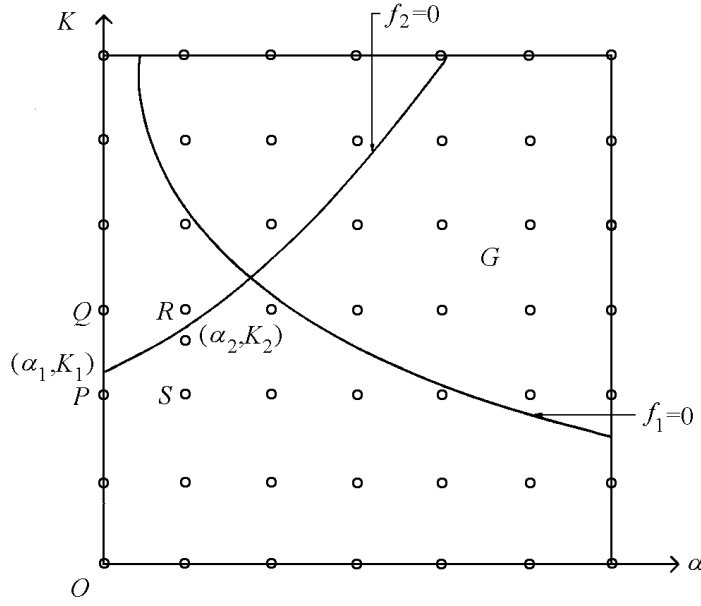


Figure 2.3: Determination of the zero's of $f_1 = 0$ and $f_2 = 0$.

equals l . These two conditions are written as

$$f_1(\tilde{K}, \tilde{\alpha}) \stackrel{\text{def}}{=} (x(\tilde{s}_w) - b) \cos \tilde{\alpha} + y(\tilde{s}_w) \sin(\tilde{\alpha}) = 0, \quad (2.20)$$

and

$$f_2(\tilde{K}, \tilde{\alpha}) \stackrel{\text{def}}{=} y(\tilde{s}_w) - (l - L + \tilde{s}_w) \cos \tilde{\alpha} = 0, \quad (2.21)$$

respectively. The problem is now to solve numerically these two non-linear equations with respect to \tilde{K} and $\tilde{\alpha}$.

For the solution of (2.20) and (2.21) a Newtonian method is chosen. Starting points in the α, K plane for this method have to be close enough to a zero point of both f_1 and f_2 to ensure convergence. To obtain starting points we could compute the values of f_1 and f_2 in all nodal points of a grid placed over a suitable chosen region G of the (α, K) plane, where the zero's are expected. This, however, would be rather time consuming.

Another method is developed, in which we move step by step for instance along the line $f_2(\alpha, K) = 0$. After each step we check for a change of sign of $f_1(\alpha, K)$. Such a change of sign gives an approximation of a zero of both f_1 and f_2 . This procedure has been realized as follows.

For a given value b we take α "too small" for instance $\alpha = 0$ and using a properly chosen step size we increase K , starting at $K = 0$ and keep $a = 0$. Hence we move along the boundary of the region G , which is a rectangle as drawn in Figure 2.3. Calculating the values of f_2 along this boundary a zero of f_2 can be located approximately by its change of sign in between two succeeding grid points. In Figure 2.3 this point is in between P and Q . By linear interpolation a better approximation $(\alpha_1 = 0, K_1)$ for the zero of f_2 is found and $f_1(\alpha_1, K_1)$ is calculated. Now the values of f_2 at R and S are calculated. When there is a change of sign between Q and R , R and S or S and P we know through which

side the line $f_2=0$ leaves the rectangle $PQRS$. A linear interpolation again gives a better approximation (α_2, K_2) for a zero of f_2 and $f_1(\alpha_2, K_2)$ is calculated. When $f_1(\alpha_1, K_1)$ and $f_1(\alpha_2, K_2)$ have different signs these points are chosen as starting points for the Newtonian method. When there is no change in sign of f_1 we have to start with the adjacent rectangle, of which one side contains the last found approximation for a zero of f_2 . This procedure is repeated until we reach the boundary of region G again.

It is assumed that the functions f_1 and f_2 behave sufficiently smooth with respect to the size of the grid placed at the region G . This causes no trouble in practice.

In this way possibly a number of zero's of the equations (2.20) and (2.21) can be found. Each of these correspond to an equilibrium situation of the bow, while the midpoint of the string has the coordinates $(b, 0)$. Not all of these equilibrium situations need to be stable.

We now discuss the braced position which corresponds to $b = |\overline{OH}||\overline{OD}|^{-1}$ in (2.17). This value of b called the brace height or fistmele, is a basic quantity for the adjustment of a bow. We know that $\alpha = 0$ hence we use only equation (2.20) in order to determine the unknown force K . This is done by increasing K stepwise from zero and checking for a change in sign of f_1 . By iteration K can be determined sufficiently accurate. Then equation (2.21) gives us the half length l of the string.

The braced position of the bow can also be determined by prescribing the half length l of the string. Then equations (2.20) and (2.21) can be considered as equations for the two unknowns b and K , again $\alpha = 0$. A procedure analogous to the one prescribed in the first part of this section can be used to satisfy both (2.20) and (2.21). Small changes however in the length $2l$ of the string can cause rather large variations of the fistmele b . Because this is in general the more important quantity, the first method to calculate the braced position of the bow is recommended.

To check our program we have compared solutions obtained by it with solutions obtained by other methods. We can take the bending stiffness W constant and the bow straight in unbraced situation, $\theta_0(\bar{s}) \equiv 0$. For given values of l and b our program yields the values of K and α . Now we can use the theory of the largely deflected cantilever described in [4] to compute the strain energy, due to bending caused by the force defined by K and α . The elliptic integrals needed for this computation are obtained by linear interpolation of values in the tables given in [1]. The results agreed very well and differed only by an amount of 0.1%.

Another check has been made by using, in the case of a bow without recurve the finite element program MARC of the MARC Analysis Research Corporation. Also these results agreed with ours, a comparison of the drawing force $F(b)$ showed discrepancies of only 0.5%.

2.5 Some numerical results

As we mentioned already, it is important for a bow to possess a sufficient amount of deformation energy at full draw, kept in check by a not too large ultimate force or weight. The measure in which the bow meets this demand can be described to a certain extent by

a dimensionless number q , called the static quality coefficient. Suppose we have an amount of deformation energy A in the bow in the situation of full draw $b = |OD|$ and the force is F , then

$$q = \frac{\overline{A}}{\overline{F(|\overline{OD}|)}|\overline{OD}|} = A, \quad (2.22)$$

where the second equality follows from (2.10). The dimensionless deformation energy A depends on a number of parameters and functions,

$$q = A(L, W(s), \theta_0(s), |OH| \text{ or } l), \quad 0 \leq s \leq L. \quad (2.23)$$

This number q is also a measure for the concavity of the function $F = F(b)$. When we compare two bows with the same value of $|\overline{OD}|$, one with a larger q then the other, the first bow is from the static point of view the best because it can store more deformation energy "per unit of weight". Sometimes another definition of q is given by replacing $|\overline{OD}|$ in (2.22) by $|\overline{OH}|$. Then however when $|\overline{OH}|$ is changed the just mentioned property is no longer valid. It is clear that q can not give a decisive answer to questions about shooting efficiency. In the case of a real bow the length's $|\overline{OH}|$ and $|\overline{OD}|$ have to be measured from a reasonably chosen elastic line representing the bow, to the midpoint of the string.

One of our objectives is to get insight into the dependency of q on the quantities denoted in (2.23). To this end we start with the bow described in [5] and change in a more or less systematic way its parameters and functions.

Some bows possess a nearly rigid central section of which the grip forms part of, its length is denoted by $2\overline{L}_0$. From the ends of this section start the elastic limbs each of length \overline{L}_1 the half length of the bow is $\overline{L} = \overline{L}_0 + \overline{L}_1$. For the grip, hence for $0 \leq \overline{s} \leq \overline{L}_0$, we put $\overline{W}(\overline{s}) = \infty$.

The units we use are the cm (=0.3937 inch) and the kg force (=2.205 lbs). Because in the literature characteristic lengths are often given in inches by "simple" numbers, for instance $\overline{L}_0 = 4$ inch, $|\overline{OD}| = 28$ inch, these lengths expressed in cm sometimes suggest an accuracy, which is not intended. The same holds for lbs and kg. In the following we do not mention anymore the dimensions of a quantity, it is tacitly understood that a length is expressed in cm, a force in kg, a bending stiffness in kg cm^2 , an energy in kg cm and an angle in radians.

The bow (H bow) discussed in [5] by Hickman has the following characteristics

$$\overline{L} = 91.4, \quad \overline{L}_0 = 10.2, \quad \theta_0(\overline{s}) \equiv 0, \quad |\overline{OH}| = 15.2. \quad (2.24)$$

The bending stiffness distribution for $\overline{s} > \overline{L}_0$ is a linear function

$$\overline{W}(\overline{s}) = 1.30 \cdot 10^5 \frac{\overline{L} - \overline{s}}{\overline{L}}, \quad \overline{L}_0 \leq \overline{s} \leq \overline{L}. \quad (2.25)$$

For future reference we mention $\overline{W}(\overline{L}_0) = 1.15 \cdot 10^5$. For the draw of the bow we have chosen $|\overline{OD}| = 71.1$ which is slightly different from the value used in [5]. However when we compare Hickman's theory with this one, his results are corrected for this difference.

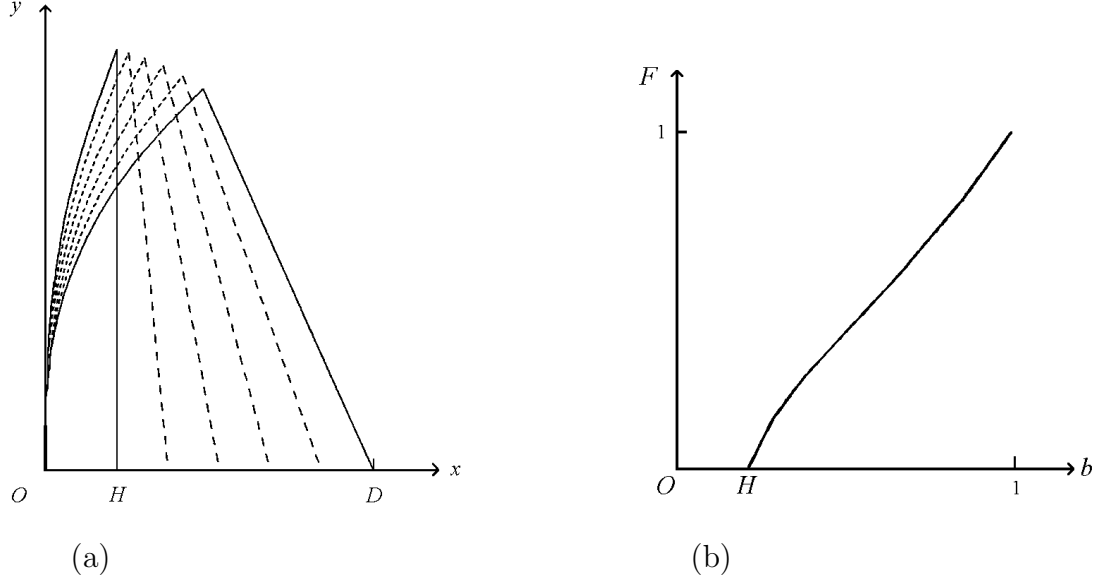


Figure 2.4: (a) Some shapes of the dimensionless deformations of the H bow. (b) Dimensionless force-draw curve of the H bow.

It follows from (2.25) that $\overline{W}(\overline{L}) = 0$. Because we use the Euler-Bernoulli equations this is not a difficulty from the theoretical point of view, because the limit of the curvature of the elastic line for $\overline{s} \rightarrow \overline{L}$ remains finite. However, in order to avoid computational complications we put

$$\overline{W}(\overline{s}) = 7.69, \quad (2.26)$$

whenever in (2.25) the values of $\overline{W}(\overline{s})$ become smaller than 7.69. This interpretation has to be given also to other bending stiffness distributions which occur later on.

A number of times we consider the consequences of a change of one or more characteristic quantities of the H bow. This means that only these quantities are varied while the other ones are the same as those given above. We remark that our results for the weight of a bow $\overline{F}(|\overline{OD}|)$ and for the deformation energy \overline{A} , are linearly dependent on λ when we replace $\overline{W}(\overline{s})$ by $\lambda W(s)$. Hence, it is easy to adjust the weight of a described bow to a desired value by multiplying $\overline{W}(\overline{s})$ by a suitable λ . The quality factor q is independent of λ .

In Figure 2.4.a we have drawn a number of dimensionless deformations of this bow up to its fully drawn position and in Figure 2.4.b its dimensionless force-draw curve both calculated by this theory. When curves given by Hickman are made dimensionless there is an excellent agreement with figure the numbers with dimension show some difference. Numerical results theory and of this one are given in Table 2.1.

In Table 2.2 we show the influence of a change of the length of the grip \overline{L}_0 and the brace height $|\overline{OD}|$ of a H bow. It is seen that the largest value of q occurs for the smallest

Table 2.1: Comparison between Hickman's theory and this theory.

	Hickman	this theory
$\overline{F}(\overline{OD})$	15.1	15.5
\overline{A}	444	450
q	0.414	0.407

Table 2.2: Influence of length of grip \overline{L}_0 and of brace height $|\overline{OH}|$ on the H bow.

\overline{L}_0	5.08			10.2			15.2		
$ \overline{OH} $	12.7	15.2	17.8	12.7	15.2	17.8	12.7	15.2	17.8
$\overline{F}(\overline{OD})$	13.9	14.0	14.1	15.4	15.5	15.7	17.3	17.4	17.6
\overline{A}	417	408	398	460	450	439	510	500	488
q	0.423	0.411	0.397	0.420	0.407	0.393	0.415	0.403	0.389

grip and smallest brace height and the smallest value of q for the largest grip and largest brace height, however this difference is not very spectacular.

In Table 2.3 we give the influence of a change of the length \overline{L} of a H bow. It follows that the weight of the bow increases strongly when the bow becomes shorter while there is, as in Table 2.2, only a weak influence on the quality factor q .

We next discuss the influence of a change of the bending stiffness on the H bow. We choose

$$\overline{W}_n(\overline{s}) = 1.15 \cdot 10^5 \left(\frac{\overline{L} - \overline{s}}{\overline{L} - \overline{L}_0} \right)^{\beta_n}, \quad \overline{L}_0 \leq \overline{s} \leq \overline{L}, \quad n = 1, 2, 3, 4. \quad (2.27)$$

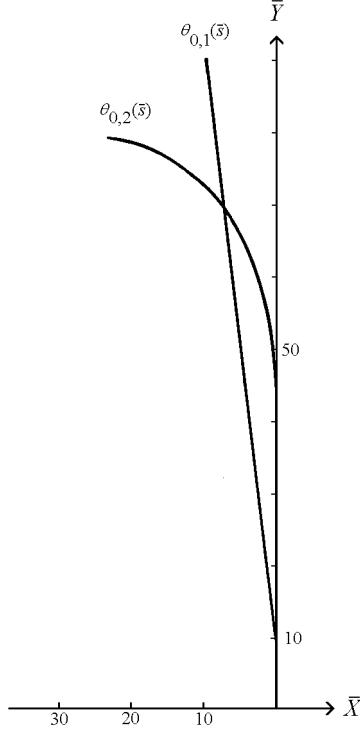
with $\beta_1 = 0$, $\beta_2 = 1/2$, $\beta_3 = 1$, $\beta_4 = 2$. We refer with respect to $\overline{W}(\overline{L}) = 0$, to (2.26) and the remark belonging to it. The bending stiffness $\overline{W}_3(\overline{s})$ is equal to $\overline{W}(\overline{s})$ from (2.25). With increasing values of n the relative flexibility of the tip becomes larger. The results are given in Table 2.4. We find that an increase of the stiffness of the tip causes some increase of q , and that the bending stiffness distribution has only a modest favourable influence on q for n changing from 3 to 1.

Table 2.3: Influence of the length \overline{L} on the H bow.

\overline{L}	81.3	86.4	91.4	96.5	102
$\overline{F}(\overline{OD})$	24.6	19.3	15.5	12.7	10.5
\overline{A}	687	551	450	373	312
q	0.393	0.400	0.407	0.413	0.417

Table 2.4: Influence of the bending stiffness $\overline{W}(\overline{s})$ on the H bow.

	$\overline{W}_1(\overline{s})$	$\overline{W}_2(\overline{s})$	$\overline{W}_3(\overline{s})$	$\overline{W}_4(\overline{s})$
$\overline{F}(\overline{OD})$	23.6	19.6	15.5	9.02
\overline{A}	701	576	450	229
q	0.417	0.414	0.407	0.356

Figure 2.5: The two types of recurve $\theta_{0,1}(\overline{s})$ and $\theta_{0,2}(\overline{s})$ considered in Table 2.5.

We now consider the influence of two recurve shapes denoted by $\theta_{0,1}(\overline{s})$ and $\theta_{0,2}(\overline{s})$ on the H bow. The first one is very simple, $\theta_{0,1}(\overline{s}) = -0.12$, the second one $\theta_{0,2}(\overline{s})$, is given by the unbraced shape of the bow in the (x, y) plane in Figure 2.5, where for reference also $\theta_{0,1}(\overline{s})$ is drawn. For each of these bows we have used $\overline{W}_2(\overline{s})$ as well as $\overline{W}_3(\overline{s})$ as bending stiffness distribution. The results are given in Table 2.5. For reference we also give in this table the straight bow $\theta_0(\overline{s}) = 0$, which already is given in Table 2.4 under the headings $\overline{W}_2(\overline{s})$ and $\overline{W}_3(\overline{s})$. It is seen that both recurves have statically a favourable influence on the bow because the coefficient q is in both cases larger than q belonging to $\theta_0(\overline{s}) \equiv 0$. The recurve $\theta_{0,2}(\overline{s})$ has the highest values of q . The best one of these $q = 0.575$ (which is a rather large value) occurs for $\overline{W}_3(\overline{s})$ which has a more flexible tip than $\overline{W}_2(\overline{s})$. It is remarkable that this is opposite to that of recurves $\theta_0(\overline{s})$ and $\theta_{0,1}(\overline{s})$ where the highest q occurs for $\overline{W}_2(\overline{s})$.

Next we consider two bows B_1 and B_2 also with recurve of which the unbraced situation however, differs from those of the bows we considered up to now. The bow B_1 drawn in Figure 2.6.a is a normal modern recurve bow for target shooting.

Table 2.5: Influence of recurve on the H bow for two bending stiffness distributions.

		$\theta_0(\bar{s}) \equiv 0$	$\theta_{0,1}(\bar{s})$	$\theta_{0,2}(\bar{s})$
$\bar{W}_2(\bar{s})$	$\overline{F}(\overline{OD})$	19.6	25.0	38.4
	\bar{A}	576	776	1510
	q	0.414	0.437	0.554
$\bar{W}_3(\bar{s})$	$\overline{F}(\overline{OD})$	15.5	20.1	29.2
	\bar{A}	450	607	1200
	q	0.407	0.424	0.575

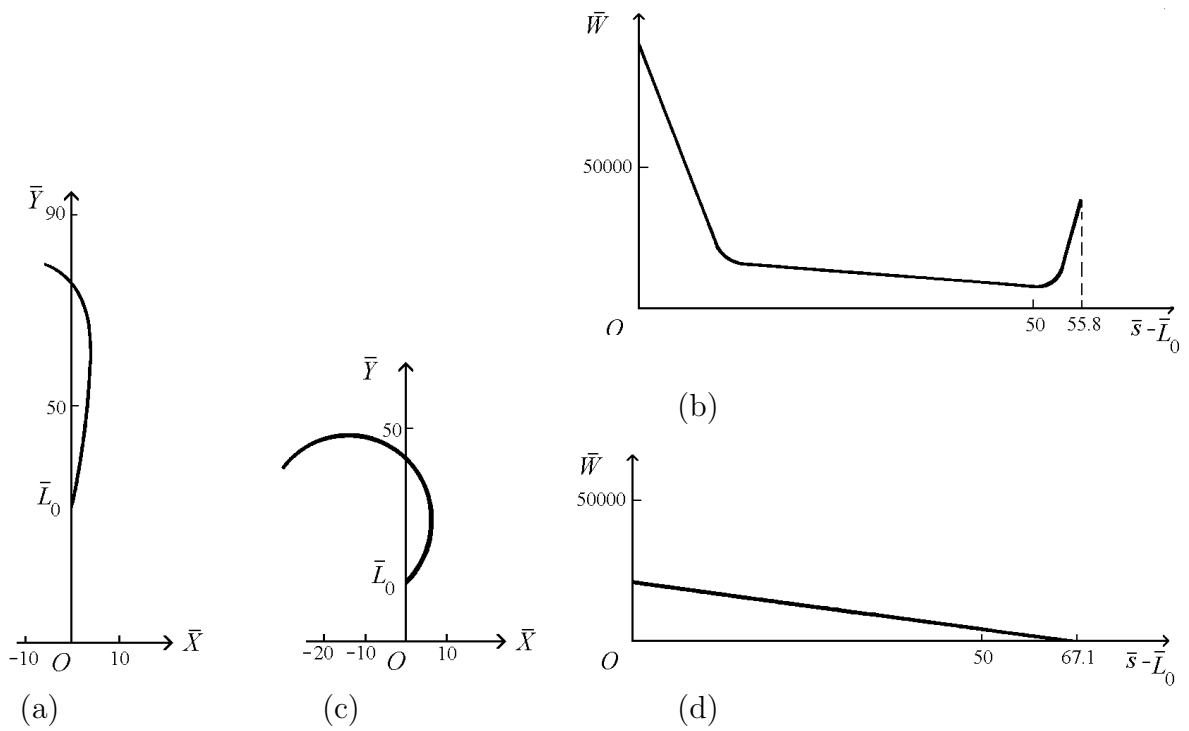
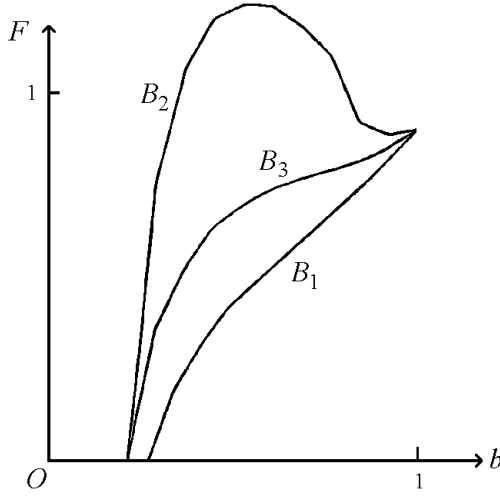
Figure 2.6: (a), (b) a modern recurve bow B_1 , $\theta_0(\bar{s})$ and $\bar{W}(\bar{s})$, (c), (d) a bow with strong recurve B_2 , $\theta_0(\bar{s})$ and $\bar{W}(\bar{s})$.

Table 2.6: Two recurve bows B_1 and B_2 .

	\bar{L}	\bar{L}_0	$ \overline{OH} $	$ \overline{OD} $	$\overline{F}(\overline{OD})$	\bar{A}	q
B_1	84.2	28.4	17.4	62.5	13.6	362	0.426
B_2	81.9	14.8	15.2	71.1	13.6	854	0.883

Figure 2.7: The dimensionless force draw curves of B_1 , B_2 and the bow B_3 of Table 2.4 $(\theta_{0,2}(\bar{s}), \bar{s}_3(\bar{s}))$.

The difference with bows considered before is that the elastic limb starts at the end $\bar{s} = \bar{L}_0$ of the rigid section in the direction of the archer. Its measured bending stiffness distribution is given in Figure 2.6.b. The bow B_2 has an excessive recurve (Figure 2.6.c). Its bending stiffness varies linearly from the rigid section to the tip (Figure 2.6.d). In Table 2.6 we give the parameters of these bows and the calculated quantities $\overline{F}(|\overline{OD}|)$, \bar{A} and q .

It is remarkable that the static quality coefficient q of B_2 is very high with respect to all the bows we have considered. The reason is that the main part of its force draw curve is strongly convex as can be seen from the dimensionless force draw curve of Figure 2.7, where also the curves of bow B_1 and of the bow B_3 denoted by $(\theta_{0,2}(\bar{s}), \bar{s}_3(\bar{s}))$ in Table 2.5 are given. This shape of force draw curve (bow B_2) resembles the force draw curve of the compound bow mentioned in the introduction, here however no pulley's are needed. In Figure 2.8 we have drawn the dimensionless deformation curves of B_1 and B_2 .

We emphasize that it is not clear that B_2 will be a good bow for shooting because our considerations are only based on statics. However, it seems worthwhile to investigate the dynamic behaviour of this bow, which will depend also on the choice of the mass distribution of the elastic limbs.

The following bow resembles an Asiatic bow ([7, plate 18]). It has a rather strong

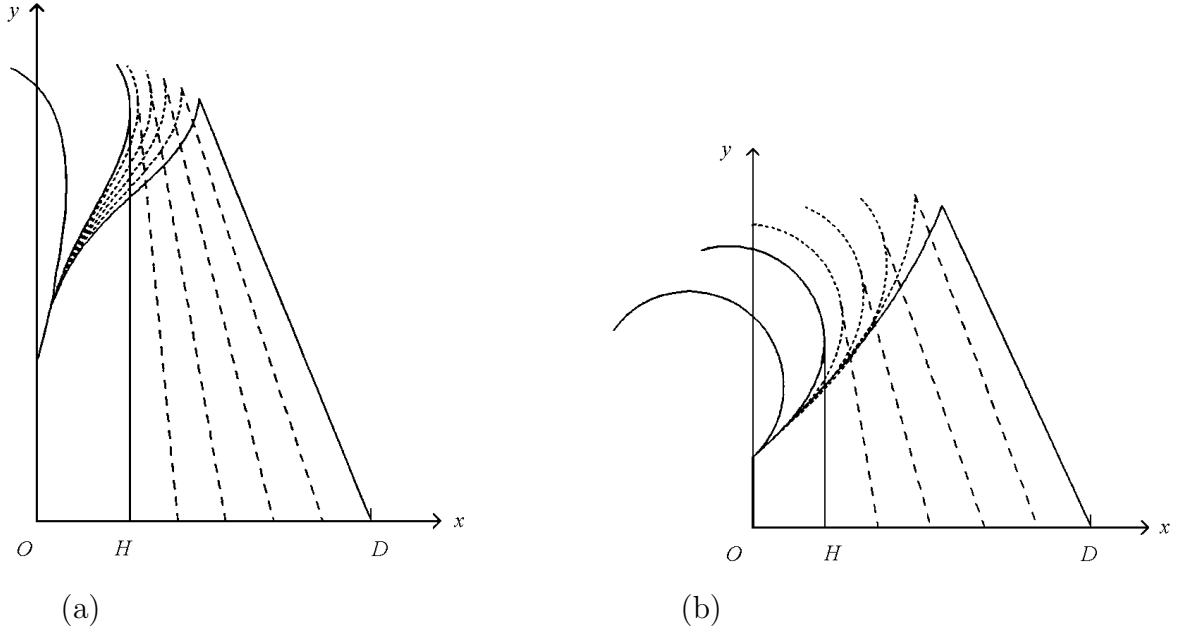


Figure 2.8: (a) Dimensionless deformations of the B_1 bow. (b) Dimensionless force-draw curve of the B_2 bow.

Table 2.7: Bending stiffness of the bow of Vrees.

\bar{s}	0	15.2	27.5	35.8	44	64.5	69.8	83.8
$\bar{W}(\bar{s}) \cdot 10^{-4}$	35.4	27.0	23.8	21.7	16.6	5.31	3.24	1.26

recurve. We have tried to guess a bending stiffness so that its calculated braced and fully drawn position resemble the photographs given in [7]. Opposite to the bows discussed up to now this bow has a rigid tip which is strengthened by a ridge. A difficulty is that this bow does not show too clearly a line of symmetry, it even is said that the upper limb is the shooting limb which "accounts for most of the shooting". In Figure 2.9 we give its chosen bending stiffness distribution. For $0 \leq \bar{s} \leq \bar{L}_0 = 6.24$ and for $46.8 = \bar{L}_2 \leq \bar{s} \leq \bar{L} = 63.5$ we take $\bar{W} = \infty$. The brace height $|\overline{OH}| = 18.4$ and the draw $|\overline{OD}| = 76.2$. Figure 2.10 gives the dimensionless deformation curves and force draw curve. From Figure 2.10.a we have also an impression of its unbraced shape. Calculated quantities are $\bar{F}(|\overline{OD}|) = 22.7$, $\bar{A} = 586$ and $q = 0.339$. Hence its static quality factor q is rather low.

We also consider a bow found in the neighbourhood of Vrees which is described by Beckhoff [3]. The quantities measured or guessed, given in that paper are $\bar{L} = 83.8$, $\bar{L}_0 = 0$, $|\overline{OH}| = 17$, $|\overline{OD}| = 70$, $\theta_0(\bar{s}) = 0$ and $\bar{W}(\bar{s})$ is given in Table 2.7. The weight and deformation energy calculated in [3] and by this theory are given in Table 2.8. The reason for the discrepancies between the two calculations is possibly that Beckhoff used a linearized theory and other approximations. It is remarkable that q is the same in both

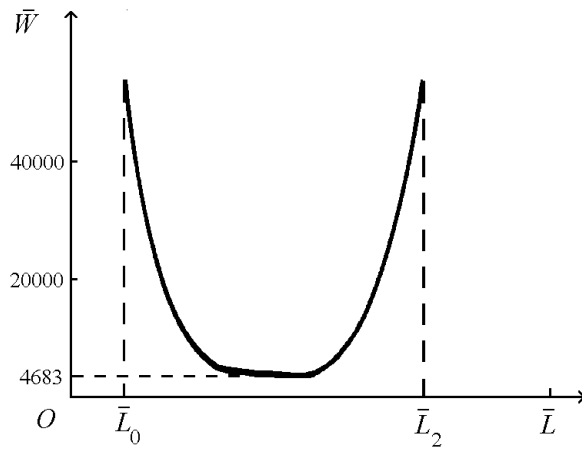


Figure 2.9: Chosen bending stiffness of "Asiatic bow".

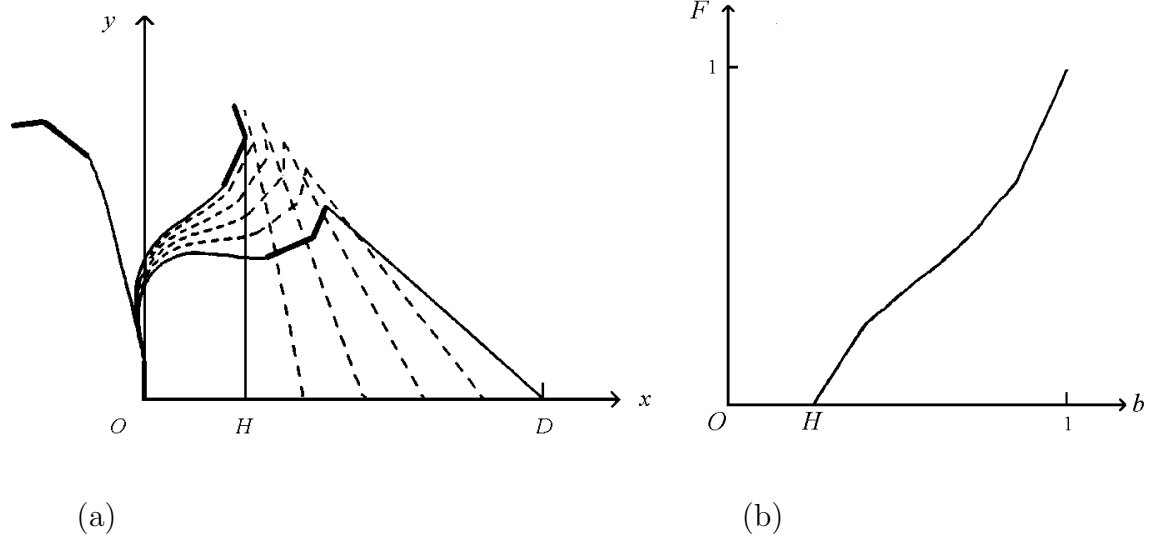


Figure 2.10: (a) Dimensionless deformation curves of the "Asiatic bow". (b) Dimensionless force-draw curve of the "Asiatic bow".

Table 2.8: Comparison of results of [3] and this theory.

	Beckhoff	this theory
$\overline{F}(\overline{OD})$	27.2	45.1
$\overline{A}(\overline{OD})$	748	1240
q	0.393	0.393

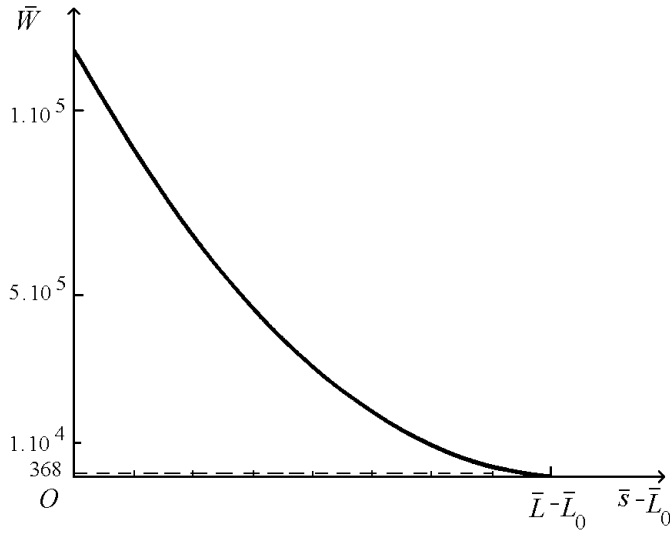


Figure 2.11: Bending stiffness of bow with three braced positions shown in Figure 2.12.

theories.

At last we give an example of the possibility of more than one braced situation of a bow. This phenomenon is liable to happen because our theory is non linear and it can be expected to occur when the tip of the bow is rather flexible with respect to its central parts. In order to find several situations we prescribe the length 1 of the string instead of the brace height or fistmele. We have chosen $\overline{L} = 90.4$, $\overline{L}_0 = 10.2$, $\overline{l} = 82.9$. Its bending stiffness $\overline{W}(\overline{s})$ is given in Figure 2.11 and $\theta_0(\overline{s})$ follows from Figure 2.12. The three braced positions are drawn in Figure 2.12 and denoted by 1, 2 and 3. When we perturb these shapes in a number of ways, it was numerically found that 1 and 3 possibly belong to a local minimum of the deformation energy and 2 belongs to a maximum. In other words it seems that the shapes 1 and 3 are stable and 2 unstable although this has not been proved analytically.

	1	2	3
$\overline{A}(\overline{OH})$	1090	1120	1080

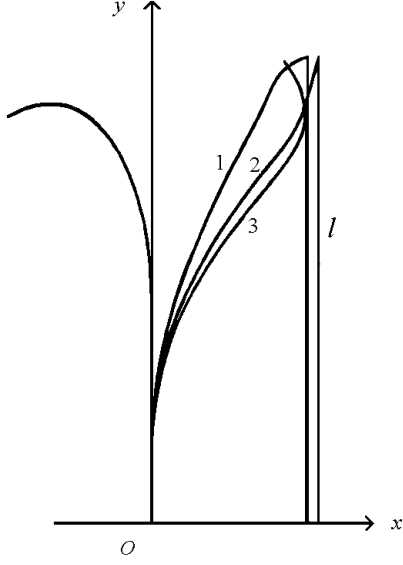


Figure 2.12: Three possible equilibrium positions.

2.6 A model of a bow with 100% shooting efficiency

Although the main subject of this paper is the static deformation of a bow we will show, as is already announced in the introduction, the essential importance of the string for a good shooting efficiency.

A shooting efficiency of 100% can easily be obtained if the model of the bow is unrealistic simple. Consider a bow of which the elastic limbs and the string are without mass, then it is clear that all the deformation energy is transformed into kinetic energy of the arrow which is assumed to have a non-zero finite mass. The assumption of a string without mass seems acceptable, however, the assumption of limbs without mass is not at all in correspondence with reality. Therefore we now discuss a more realistic model.

The bow consists of a rigid grip of length $2L_0$ and two rigid limbs of length L_1 (Figure 2.13.a) which are connected each to the grip by means of an elastic hinge (S for the upper limb) of strength $k > 0$. The moment of inertia of the limb with respect to S is J . The string of length $2l$ is inextensible and without mass, the mass of the arrow is $m > 0$. The assertion is that this bow (Figure 2.13.a) converts all the deformation energy of the elastic hinge into kinetic energy of the arrow. From Figure 2.13.a it follows that

$$L_1 \cos \varphi \leq l - L_0 < L_1, \quad \varphi_0 \stackrel{\text{def}}{=} \arccos\left(\frac{l - L_0}{L_1}\right) \leq \varphi < \varphi_e \stackrel{\text{def}}{=} \pi - \arccos\left(\frac{L_0}{L_1 + l}\right). \quad (2.28)$$

Also from that figure we find for the x coordinate ξ of the end of the arrow

$$\xi = L_1 \sin \varphi + \left(l^2 - (L_1 \cos \varphi + L_0)^2\right)^{1/2}. \quad (2.29)$$

Writing down the equations of motion of limbs and arrow we find after a straight forward analysis,

$$\ddot{\xi} \left(J + \frac{m}{2} Q^2(\varphi)\right) = J Q'(\varphi) \dot{\varphi}^2 - k(\varphi - \tilde{\varphi}) Q(\varphi). \quad (2.30)$$

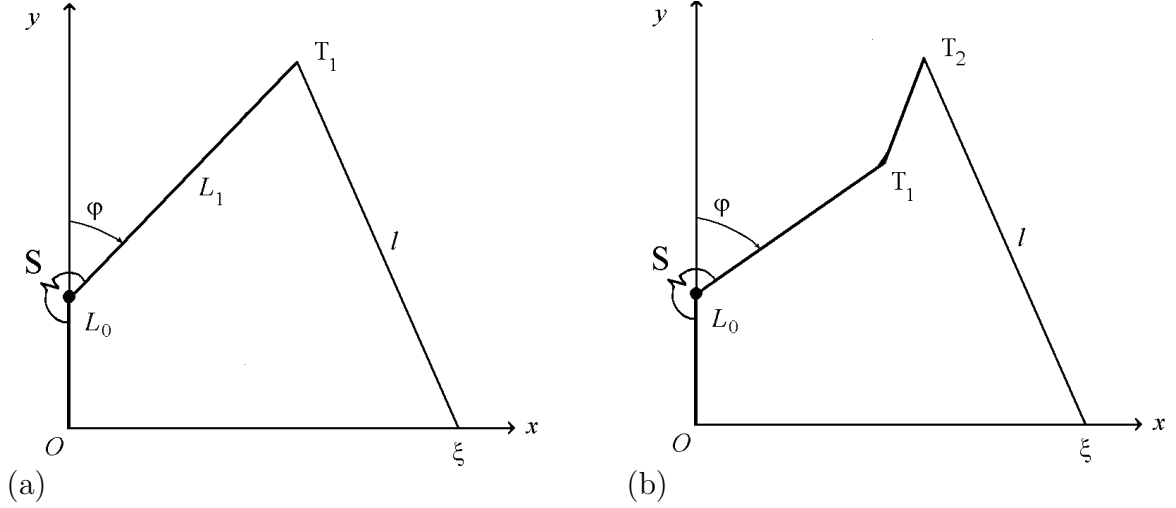


Figure 2.13: Two bows each with two elastic hinges and rigid limbs.

where

$$Q(\varphi) = \left[L_1 \cos \varphi + L_1 \frac{(L_1 \cos \varphi + L_0) \sin \varphi}{(l^2 - (L_1 \cos \varphi + L_0)^2)^{1/2}} \right] \geq 0, \quad \varphi_0 \leq \varphi < \varphi_e, \quad (2.31)$$

and $\tilde{\varphi} < \varphi_0$ is the angle of zero moment of the elastic hinge. Because it can be shown that $Q'(\varphi) \leq 0$ it follows from (2.30) that

$$\ddot{\xi} \leq 0, \quad \varphi_0 \leq \varphi < \varphi_e. \quad (2.32)$$

An important conclusion results from this equation. During the stretching of the bow (Figure 2.13.a) the arrow keeps its contact with the string which, along straight lines, connects the arrow end to the tips of the limbs.

Next we consider the bow of Figure 2.13.b. The only difference between this bow and the previous one is that now the rigid limb ST_2 has an infinitely sharp bend at T_1 . During positions as drawn this bow behaves exactly as the one of Figure 2.13.a, hence $\ddot{\xi} \leq 0$. When, however, $T_2 - T_1$ coincides partly with the string we can describe the process of shooting after that situation, by a bow of which the limb is ST_1 and of which the half length of the string is $(l - |T_1 - T_2|)$. It is easily proved that $\dot{\xi}$ is continuous during this transition and hence also for this bow we have $\ddot{\xi} \leq 0$ for all possible values of φ . This means that *mutates mutandis*, for this bow the same conclusion (below (2.32)) holds.

Now consider the situation that the string is nearly stretched

$$\varphi_0 \leq \varphi \leq \varphi_0 + \epsilon, \quad (2.33)$$

for a small number $\epsilon > 0$. From (2.32) it follows that the arrow is still in contact with the string. Suppose that for these values of φ the angular velocity of the limb is non-zero, hence that a positive number δ exists with

$$0 < \delta \leq -\dot{\varphi}(\varphi) . \quad (2.34)$$

Then it follows from (2.29)

$$\lim_{\varphi \rightarrow \varphi_0} \dot{\xi}(\varphi) = \lim_{\varphi \rightarrow \varphi_0} Q(\varphi) \dot{\varphi} = -\infty . \quad (2.35)$$

However, this is impossible because then the kinetic energy of the arrow becomes infinite while the deformation energy of the bow is finite. Hence we have

$$\lim_{\varphi \rightarrow \varphi_0} \dot{\varphi}(\varphi) = 0 . \quad (2.36)$$

This means that theoretically by the action of the inextensible string without mass all the kinetic energy of the rigid limbs is conveyed to the arrow, how large J and how small m may be. This holds for both bows of Figure 2.13, it holds analogously for bows with rigid limbs with more sharp bends

That these models are not too unrealistic follows for the type of Figure 2.13.a from [9] where on analogous device, a catapult, is described. The elastic hinges are made of strongly twisted cables to which rigid limbs are connected. The bow of Figure 2.13.b resembles a Turkish flight bow [7, page 105]. There it is remarked that the ancient bowyers tried to keep the elastic parts of the limbs as short as possible in order to obtain a good shooting efficiency. With other words they tried to realize an elastic hinge in each of the limbs. The purpose of the bend at T_1 in the rigid limb in Figure 2.13.b is to increase the value of q .

By choosing nonlinear elastic hinges, which are not difficult to design, it is of course possible to obtain force-draw curves of the type of B_2 of Figure 2.7, hence to obtain a high static quality factor q . When contact between string and arrow remains during the shooting, with other words when the acceleration of the arrow is non positive, also 100% shooting efficiency can be obtained.

It seems likely that suitably designed bows with more elastic hinges or even continuously distributed elasticity, can also have theoretically an efficiency of 100%. An analytic proof however will be more complicated in that case.

2.7 Acknowledgement

Our thanks are due to Dr. Ir. J.C. Nagtegaal and Ir. J.E. de Jong for their willingness to check some of our calculations by means of the MARC program. Also we thank the "Netherlands organization for the advancement of pure research" (Z.W.O.), for its support (63-57).

Bibliography

- [1] Abramowitz M, Stegun A. (1972). *Handbook of mathematical functions*. Dover Publications, Inc, New York.
- [2] Arinson RB. (1977). The compound bow: Ugly but effective. *Machine Design* pp. 38–40.
- [3] Beckhoff K. (1964). Der Eibenbogen von Vrees. *Die Kunde N.F.* 15:113–125.
- [4] Frisch-Fay R. (1962). *Flexible bars*. Butterworth, London.
- [5] Hickman CN. (1937). The dynamics of a bow and arrow. *J. of Applied Physics* 8:404–409.
- [6] Klopsteg PE. (1943). Physics of bows and arrows. *Am. J. Phys.* 11:175–192.
- [7] Latham JD, Paterson WF. (1970). *Saracen Archery*. The Holland Press, London.
- [8] Schuster BG. (1969). Ballistics of the modern-working recurve bow and arrow. *Am. J. Phys.* 37:364–373.
- [9] Soedel W, Foley V. (1979). Ancient catapults. *Scientific American* 240:120–128.

Chapter 3

On the mechanics of the bow and arrow¹

3.1 Summary

Some aspects of the dynamics of the bow and arrow have been considered. The governing equations are derived by means of Hamilton's principle. The resulting nonlinear initial-boundary-value problem is solved numerically by use of a finite-difference method. The influence of the characteristic quantities on the performance of a bow is discussed.

3.2 Introduction

This paper deals with the interior ballistics of the bow and arrow, hence with the phenomena which happen between the moment of release of the arrow and the moment that the arrow leaves the string. This subject is amply investigated experimentally by Hickman and Klopsteg [1]. Hickman used also a mathematical model. In order to be able to get numerical results without the help of a computer his model had rather severe simplifications. Because of these simplifications only bows with specific features could be dealt with. We hope that this article will add to the understanding of the action of rather general types of bows, by giving more accurate and detailed numerical results.

We are concerned with bows of which the flexible parts (limbs) move in a flat plane, and which are symmetric with respect to the line of aim. The arrow will pass through the midpoint of the bow, as in the case of a "centre-shot bow". We assume that the bow is clamped at its midpoint by the bow hand. The bows are allowed to possess a mild "recurve" of "reflex". This means that the limbs of the bow in unstrung situation are allowed to be curved away from the archer, however, not too strongly.

We will consider the bow as a slender inextensible beam. The dynamic boundary conditions at the tips of the elastic limbs follow from the connection of the tips, by means

¹B.W. Kooi, On the mechanics of the bow and arrow *Journal of Engineering Mathematics* **15**(2):119-145 (1981)

of a string, to the end of the arrow. The initial deformation of the bow is given by its shape in the fully drawn position, the initial velocities are zero. Also in our theory some assumptions have been made. Most of these result from the use of the Euler-Bernoulli equation for the elastic line which represents the bow. Further, the mass of the string is taken to be zero, the string is assumed to be inextensible and the arrow is taken to be rigid. Neither internal or external damping nor hysteresis are taken into account.

Nonlinear vibrations of beams have been studied by many authors. Most of them are concerned with periodic motions. Woodall [7] obtains the governing equations of motion by considering a differential element of a beam. Wagner [6] and later Verma and Krishna Murthy [5] applied Hamilton's principle. However, in [6] and [5] the constraint which follows from the fact that the beam is assumed to be inextensible is not taken into account in the variational problem itself, but is used afterwards. This makes their equations differ from ours in Section 3.3 Hamilton's principle is used and a physical meaning of the Lagrange multiplier connected to the inextensibility of the bow is given. This has been done by comparing our equations with those obtained by Woodall. In the static case such a method was already applied by Schmidt and Da Deppo [4].

In Section 3.4 a finite-difference method to solve the equations of motion numerically is described. The results are compared with the results of a finite-element method.

The performance of a bow and arrow depends on a number of parameters, the length of the bow, the brace height or the length of the string, the draw, the mass of the arrow and the mass of concentrated masses at the tips (if any). It depends also on three functions, namely the distributions of bending stiffness and mass along the bow and the shape of the bow in its unstrung situation. In order to get insight into the influence of the afore mentioned quantities, in Section 3.5 these quantities are changed systematically, starting from a bow described by Hickman [1, page 69]. Besides the static quality coefficient, already introduced in [2], two dynamic quality coefficients are introduced. One is the efficiency and the other is related to the velocity of the arrow when it leaves the string, sometimes called the muzzle velocity. These three numbers cannot give by themselves a complete insight into what makes a bow a good one, for instance, with respect to target shooting, flight shooting or hunting. Also other subjects become important, such as smoothness of the recoil of the bow, its manageability, and so on. Whenever it is possible our results are compared with experimental and theoretical results given in [1].

Although it belongs clearly to the interior ballistics of a bow and arrow, we will not discuss in this paper the interesting "archers paradox". This is the phenomenon that the elastic arrow, during the shooting period of a conventional non-centre-shot bow, carries out a vibrational motion. Because we only consider centre-shot bows, the assumption that the arrow be rigid with respect to bending is without loss of generality.

In Section 3.6 some attention is paid to the behaviour of the normal or longitudinal force in our model of the bow, at the moment the arrow is released. When concentrated masses at the tips are present, the normal force seems to have a jump at that moment. This jump disappears when in an approximate way extensibility of the bow is simulated.

3.3 Equations of motion

In this section the equations of motion of the bow and the dynamic boundary conditions are derived by means of Hamilton's principle. The equations of motion can also be obtained by applying the linear momentum and angular momentum balance of a differential element of the bow, as is done for instance by Woodall [7].

First we introduce the quantities which fix, with respect to our problem, the features of bow and arrow. The total length of the inextensible bow is denoted by $2\bar{L}$. The bow will be represented by an elastic line, along which we have a length coordinate \bar{s} , measured from the midpoint, hence $0 \leq \bar{s} \leq \bar{L}$. This elastic line is endowed with bending stiffness $\bar{W}(\bar{s})$ and mass per unit of length $\bar{V}(\bar{s})$. The rigid arrow has a mass $2\bar{m}_a$, where the factor 2 is inserted for convenience later on. In addition, there may be concentrated masses \bar{m}_t at each of the tips, representing the mass of the horns used to fasten the string or artificially added masses. The bow is placed in a Cartesian coordinate system (\bar{x}, \bar{y}) , the \bar{x} -axis coinciding with the line of aim and the origin O with the centre of the bow. Because the bow is symmetric with respect to the line of aim, only the upper half of the bow is dealt with in what follows. The unbraced situation (Figure 3.1.a) is given by the functions $\bar{x} = \bar{x}_0(\bar{s})$ and $\bar{y} = \bar{y}_0(\bar{s})$ or by the angle $\theta(\bar{s})$ between the \bar{y} -axis and the tangent to the bow, reckoned positive in clockwise direction. Because \bar{s} is the length parameter the functions $\bar{x}_0(\bar{s})$ and $\bar{y}_0(\bar{s})$ have to satisfy $\bar{x}_0'^2(\bar{s}) + \bar{y}_0'^2(\bar{s}) = 1$, where the prime indicates differentiation with respect to \bar{s} . \bar{L}_0 is the half length of the rigid part in the middle of the bow, called the "grip", thus for $0 \leq \bar{s} \leq \bar{L}_0$ we have $\bar{W}(\bar{s}) = \infty$.

In Figure 3.1.b the braced situation is depicted. The distance $|\overline{OH}|$ is the "brace height" or "fistmele". The length of the inextensible string, used to brace the bow, is denoted by $2\bar{l}$ ($\bar{l} < \bar{L}$). It is possible that, when recurve is present, the string lies along part of the bow in the braced situation. However, in this paper we assume the string to have contact with the bow only at the tips in all situations, static or dynamic. Hence, only bows without recurve or with moderate recurve will be considered. In Figure 3.1.c the bow is in fully drawn position. The geometry in this position is described by the functions $\bar{x} = \bar{x}_1(\bar{s})$ and $\bar{y} = \bar{y}_1(\bar{s})$ ($\bar{x}_1'^2 + \bar{y}_1'^2 = 1$), or by the angle $\theta_1(\bar{s})$. The distance $|\overline{OD}|$ is called the "draw" and the force $\bar{F}(|\overline{OD}|)$ is the "weight".

The following short notation of a specific bow and arrow combination will be used:

$$B(\bar{L}, \bar{L}_0, \bar{W}(\bar{s}), \bar{V}(\bar{s}), \theta_0(\bar{s}), \bar{m}_a, \bar{m}_t, |\overline{OH}| \text{ or } l; |\overline{OD}|, \bar{F}(|\overline{OD}|), \bar{m}_b), \quad (3.1)$$

where the brace height $|\overline{OH}|$ or half of the length l of the string can be given. Further \bar{m}_b is half of the mass of the limbs, the flexible parts of the bow, so

$$\bar{m}_b = \int_{\bar{L}_0}^{\bar{L}} \bar{V}(\bar{s}) d\bar{s}. \quad (3.2)$$

The variables before the semicolon in (3.1) together with the draw $|\overline{OD}|$ determine completely the features of the bow, while the quantities behind the semicolon are used when we introduce dimensionless variables.

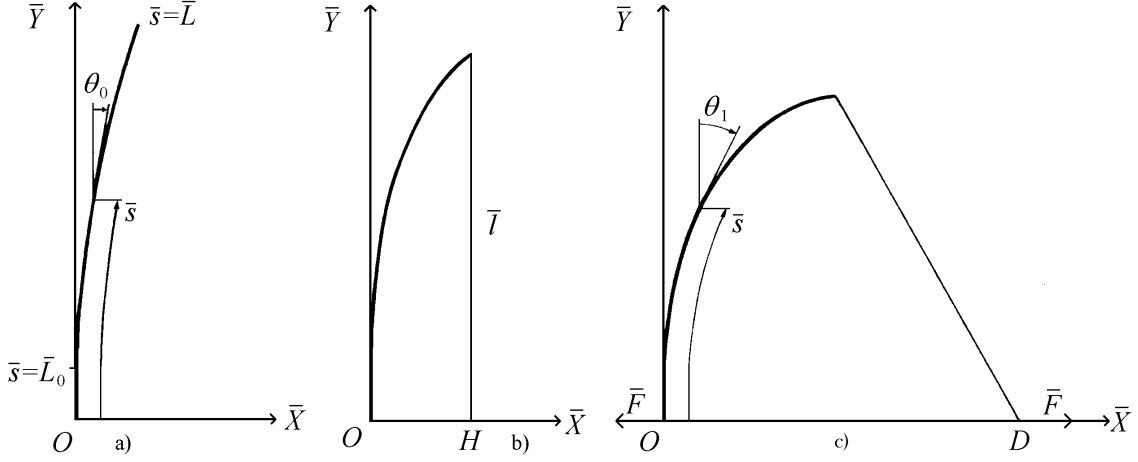


Figure 3.1: Three situations of the non-recurve bow: a) unbraced, b) braced, c) fully drawn.

We now derive the equations of motion of bow and arrow. For simplicity we take $\bar{L}_0 = 0$; if this is not the case the obtained equations have to be changed in an obvious way. The Bernoulli-Euler equation (which is assumed to be valid) reads

$$\bar{M}(\bar{s}, \bar{t}) = \bar{W}(\bar{s})(\bar{x}'\bar{y}'' - \bar{y}'\bar{x}'' + \theta'_0), \quad 0 \leq \bar{s} \leq \bar{L}, \quad (3.3)$$

where $\bar{M}(\bar{s}, \bar{t})$ is the resultant bending moment at a cross section (see Figure 3.2 for sign). We recall that because the bow is symmetric with respect to the line of aim, we confine ourselves to its upper half, clamped at the origin O . The potential energy \bar{A}_p of the deformed upper half is its bending energy

$$\bar{A}_p = 1/2 \int_0^{\bar{L}} \frac{\bar{M}^2(\bar{s}, \bar{t})}{\bar{W}(\bar{s})} d\bar{s}. \quad (3.4)$$

The kinetic energy \bar{A}_k is the sum of the kinetic energy of the upper half of the bow, half the kinetic energy of the arrow and the kinetic energy of the concentrated mass at the tip. Then when a dot indicates differentiation with respect to time \bar{t} ,

$$\bar{A}_k = 1/2 \int_0^{\bar{L}} \bar{V}(\bar{s})(\dot{\bar{x}}^2 + \dot{\bar{y}}^2) d\bar{s} + 1/2\bar{m}_a\dot{\bar{b}}^2 + 1/2\bar{m}_t(\dot{\bar{x}}^2(\bar{L}, \bar{t}) + \dot{\bar{y}}^2(\bar{L}, \bar{t})), \quad (3.5)$$

where \bar{b} is the \bar{x} -coordinate of the end of the arrow or the middle of the string, which can be expressed in the coordinates of the tip of the bow by

$$\bar{b}(\bar{t}) = \bar{x}(\bar{L}, \bar{t}) + (\bar{t}^2 - \bar{y}^2(\bar{L}, \bar{t}))^{1/2}, \quad (3.6)$$

because the string is assumed to be inextensible.

The string is also assumed to be without mass, hence it contributes neither to the potential nor to the kinetic energy. Because the bow is inextensional we have the constraint

$$\bar{x}_1'^2 + \bar{y}_1'^2 = 1, \quad 0 \leq \bar{s} \leq \bar{L}. \quad (3.7)$$

We introduce

$$\bar{\Lambda} = \bar{A}_k - \bar{A}_p + \int_0^{\bar{L}} \bar{\lambda}(\bar{s}, \bar{t}) (\bar{x}_1'^2 + \bar{y}_1'^2 - 1) d\bar{s}, \quad 0 \leq \bar{s} \leq \bar{L}, \quad (3.8)$$

where $\bar{\lambda}(\bar{s}, \bar{t})$ is an unknown Lagrangian multiplier to meet the constraint (3.7). Then by Hamilton's principle we have to find an extremum of

$$\int_{\bar{t}_0}^{\bar{t}_1} \bar{\Lambda} d\bar{t}, \quad (3.9)$$

hence

$$\delta \int_{\bar{t}_0}^{\bar{t}_1} \bar{\Lambda} d\bar{t} = 0, \quad (3.10)$$

for fixed initial time $\bar{t} = \bar{t}_0$ and fixed final time $\bar{t} = \bar{t}_1$.

Because the bow is clamped at the origin O , we have for $\bar{s} = 0$ the geometric boundary conditions

$$\bar{x}(0, \bar{t}) = \bar{y}(0, \bar{t}) = 0, \quad \bar{y}'(0, \bar{t}) = \bar{y}_0(0). \quad (3.11)$$

By standard methods of calculus of variations and using (3.11) we find the Euler equations as necessary conditions for the extremum of (3.9)

$$\bar{V}\ddot{\bar{x}} = (\bar{y}''\bar{M})' - 2(\bar{\lambda}\bar{x}')' + (\bar{y}'\bar{M})'', \quad (3.12)$$

and

$$\bar{V}\ddot{\bar{y}} = -(\bar{x}'\bar{M})' - 2(\bar{\lambda}\bar{y}')' - (\bar{x}'\bar{M})''. \quad (3.13)$$

Also the dynamic boundary conditions at $\bar{s} = \bar{L}$ follow from the variational procedure, they become

$$\bar{M}(\bar{L}, \bar{t}) = 0, \quad (3.14)$$

$$\bar{m}_a \ddot{\bar{b}} + \bar{m}_t \ddot{\bar{x}}(\bar{L}, \bar{t}) = 2\bar{\lambda}(\bar{L}, \bar{t})\bar{x}'(\bar{L}, \bar{t}) - \bar{y}'(\bar{L}, \bar{t})\bar{M}'(\bar{L}, \bar{t}) \quad (3.15)$$

$$\bar{m}_a \frac{\bar{y}(\bar{L}, \bar{t})\ddot{\bar{b}}}{\bar{b} - \bar{x}(\bar{L}, \bar{t})} + \bar{m}_t \ddot{\bar{y}}(\bar{L}, \bar{t}) = -2\bar{\lambda}(\bar{L}, \bar{t})\bar{y}'(\bar{L}, \bar{t}) - \bar{x}'(\bar{L}, \bar{t})\bar{M}'(\bar{L}, \bar{t}) \quad (3.16)$$

The initial conditions which complete the formulation of the problem are

$$\bar{x}(\bar{s}, 0) = \bar{x}_1(\bar{s}), \quad \bar{y}(\bar{s}, 0) = \bar{y}_1(\bar{s}), \quad \dot{\bar{x}}(\bar{s}, 0) = \dot{\bar{y}}(\bar{s}, 0) = 0, \quad 0 \leq \bar{s} \leq \bar{L}. \quad (3.17)$$

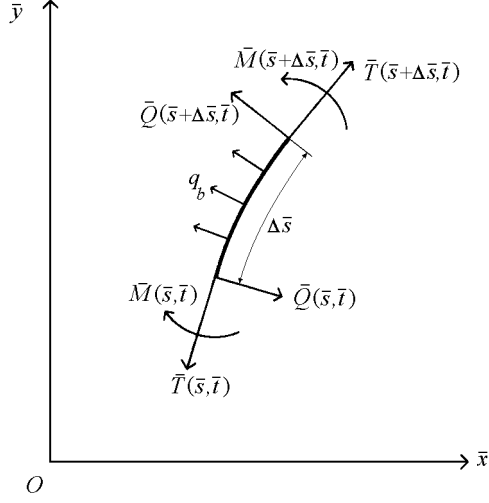


Figure 3.2: Forces and moments on a differential element of the bow.

Although it is not necessary for the computations, we look for a physical meaning of the function $\bar{\lambda}(\bar{s}, \bar{t})$. In Figure 3.2 the resultant forces and moments acting on a differential element of the bow are shown. The momentum balance in the \bar{x} - and \bar{y} -direction gives

$$\bar{V}\ddot{\bar{x}} = (\bar{T}\bar{x}') - (\bar{Q}\bar{y}') , \quad (3.18)$$

and

$$\bar{V}\ddot{\bar{y}} = (\bar{T}\bar{y}') + (\bar{Q}\bar{x}') , \quad (3.19)$$

respectively, where $\bar{T}(\bar{s}, \bar{t})$ is the normal force and $\bar{Q}(\bar{s}, \bar{t})$ the shear force on a cross-section (see Figure 3.2). If the rotatory inertia of the cross-section of the bow is neglected, the moment balance of the element gives

$$\bar{M}'(\bar{s}, \bar{t}) = -\bar{Q}(\bar{s}, \bar{t}) . \quad (3.20)$$

Comparing equations (3.18) and (3.19), using (3.20) to replace \bar{Q} by \bar{M}' , with (3.12) and (3.13), we find the physical meaning of

$$\bar{\lambda}(\bar{s}, \bar{t}) = -1/2\bar{T} + \frac{\bar{M}}{\bar{W}}(\bar{M} - \bar{W}\theta'_0) , \quad 0 \leq \bar{s} \leq \bar{L} . \quad (3.21)$$

Substitution of (3.21) in the boundary conditions (3.15) and (3.16) yields

$$\bar{m}_a\ddot{\bar{b}} + \bar{m}_t\ddot{\bar{x}}(\bar{L}, \bar{t}) = -\bar{T}(\bar{L}, \bar{t})\bar{x}'(\bar{L}, \bar{t}) - \bar{y}'(\bar{L}, \bar{t})\bar{M}'(\bar{L}, \bar{t}) , \quad (3.22)$$

and

$$\bar{m}_a\frac{\bar{y}(\bar{L}, \bar{t})\ddot{\bar{b}}}{\bar{b} - \bar{x}(\bar{L}, \bar{t})} + \bar{m}_t\ddot{\bar{y}}(\bar{L}, \bar{t}) = \bar{T}(\bar{L}, \bar{t})\bar{y}'(\bar{L}, \bar{t}) - \bar{x}'(\bar{L}, \bar{t})\bar{M}'(\bar{L}, \bar{t}) . \quad (3.23)$$

Equations (3.22) and (3.23) connect the deformation of the bow at $\bar{s} = \bar{L}$ to the force components in the \bar{x} - and \bar{y} -direction, exerted by the string and by the mass \bar{m}_t the tip.

The functions $\bar{x}_1(\bar{s})$ and $\bar{y}_1(\bar{s})$ occurring in the initial conditions (3.17) satisfy the equations of static equilibrium, with $\bar{b} = |\overline{OD}|$, obtained from (3.18), (3.19) and (3.20) by putting the left-hand sides of the first two mentioned equations equal to zero. The two relations (3.3) and (3.7) remain unchanged. Besides we have the boundary conditions (3.11), (3.14), (3.22) and (3.23), where in the latter two we have to replace the first term on the left-hand sides by $-1/2\bar{F}(|\overline{OD}|)$ and $-1/2\bar{y}_1(\bar{L})\bar{F}(|\overline{OD}|)/(\bar{b} - \bar{x}_1(\bar{L}))$, respectively. The weight of the bow $\bar{F}(|\overline{OD}|)$ is unknown and has to be determined in the course of the solution of these equations. In Equation (3.6) \bar{b} has to be replaced by its known value $|\overline{OD}|$, the draw of the bow. The static deformations are discussed in [2].

The acceleration (or dynamic) force on the arrow, denoted by \bar{E} , is given by

$$\bar{E}(\bar{t}) = -2\bar{m}_a\ddot{\bar{b}}(\bar{t}) . \quad (3.24)$$

and the recoil force \bar{P} , which is the force of the bow exerted on the bow hand (reckoned positive in the positive \bar{x} -direction) by

$$\bar{P}(\bar{t}) = 2(\bar{M}'(0, \bar{t})\bar{y}'_0(0) + \bar{T}(0, \bar{t})\bar{x}'_0(0)) . \quad (3.25)$$

We introduce dimensionless quantities in the following way

$$\begin{aligned} (\bar{x}, \bar{y}, \bar{s}, \bar{L}, \bar{L}_0, \bar{l}) &= (x, y, s, L, L_0, l) |\overline{OD}| , \\ (\bar{T}, \bar{F}, \bar{E}, \bar{P}) &= (T, F, E, P) \bar{F}(|\overline{OD}|) , \\ \bar{M} &= M |\overline{OD}| \bar{F}(|\overline{OD}|) , \quad \bar{W} = W |\overline{OD}|^2 \bar{F}(|\overline{OD}|) , \quad \bar{V} = V \bar{m}_b / |\overline{OD}| , \\ (\bar{m}_a, \bar{m}_t) &= (m_a, m_t) \bar{m}_b , \quad \bar{t} = t (\bar{m}_b |\overline{OD}| / \bar{F}(|\overline{OD}|))^{1/2} . \end{aligned} \quad (3.26)$$

where we used the a priori unknown weight $\bar{F}(|\overline{OD}|)$ of the bow to make the quantities dimensionless. In the following we will systematically label quantities with dimension by means of a bar "—" quantities without bar are dimensionless. Quantities, when they have dimensions, will be expressed *unless stated otherwise*, by means of the following units: length in cm, force in kg force, mass in kg mass and time in 0.03193 sec.

If the velocities $u(s, t) = \dot{x}(s, t)$ and $v(s, t) = \dot{y}(s, t)$ are introduced the system of six nonlinear partial differential equations for the six functions x, y, u, v, M, T of two independent variables $s \in [L_0, L]$ and $t > 0$ assumes the form

$$V\dot{u} = (Tx')' + (M'y')' , \quad (3.27)$$

$$V\dot{v} = (Ty')' - (M'x')' , \quad (3.28)$$

$$\dot{x} = u , \quad (3.29)$$

$$\dot{y} = v , \quad (3.30)$$

$$x'^2 + y'^2 = 1 , \quad (3.31)$$

$$M = W(x'y'' - y'x'' + \theta'_0) . \quad (3.32)$$

The boundary conditions at $s = L_0$ become

$$x(L_0, t) = x_0(L_0) , \ y(L_0, t) = y_0(L_0) , \ x'(L_0, t) = x'_0(L_0) , \quad (3.33)$$

and at $s = L(t > 0)$,

$$M(L, t) = 0 , \quad (3.34)$$

$$m_a \ddot{b} + m_t \ddot{x}(L, t) = -T(L, t)x'(L, t) - M'(L, t)y'(L, t) , \quad (3.35)$$

$$m_a y(L, t) \ddot{b} - m_t \ddot{y}(L, t)(b(t) - x(L, t)) = \\ (T(L, t)y'(L, t) - M'(L, t)x'(L, t))(b(t) - x(L, t)) , \quad (3.36)$$

with

$$b(t) = x(L, t) + (l^2 - y^2(L, t))^{1/2} , \quad (3.37)$$

The initial conditions (3.17) become

$$x(s, 0) = x_1(s) , \quad (3.38)$$

$$y(s, 0) = y_1(s) , \quad (3.39)$$

$$u(s, 0) = v(s, 0) = 0, L_0 \leq s \leq L . \quad (3.40)$$

The dimensionless dynamic force E and recoil force P are given by

$$E(t) = -2m_a \ddot{b} , \quad (3.41)$$

and

$$P(t) = 2(M'(L_0, t)y'_0(L_0) + T(L_0, t)x'_0(L_0)) . \quad (3.42)$$

The finite-difference method discussed in the next section can be used for the solution of both the static and the dynamic equations. In [2] the static problem, which is a two-point boundary-value problem for a system of ordinary differential equations, is solved by means of a shooting method.

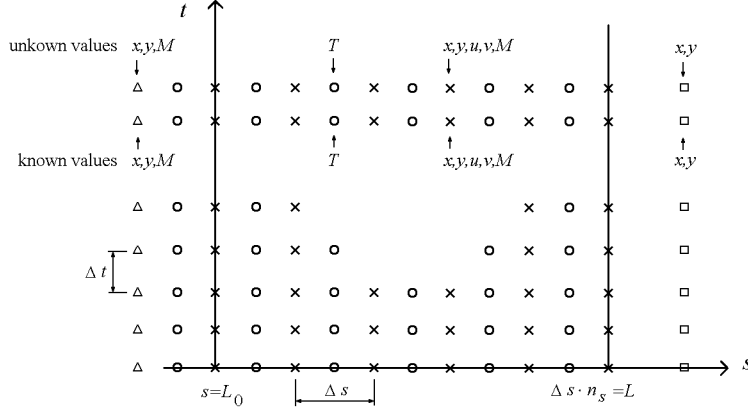
3.4 Finite difference equations

In order to obtain approximations for the solution of the partial differential equations (3.27)···(3.32) with boundary conditions (3.33)···(3.36) and initial conditions (3.38)···(3.40) we use a finite-difference method. We consider the grid

$$s = j\Delta s , \ j = 0(1)n_s , \ n_s\Delta s = L - L_0 , \quad (3.43)$$

and

$$t = k\Delta t , \ k = 0(1)n_t , \quad (3.44)$$

Figure 3.3: Grid placed over the s, t -plane.

n_t being an integer large enough to cover the time interval of interest grid points are indicated by "x" in Figure 3.3. To satisfy the boundary conditions external mesh points are introduced, $(L_0 - \Delta s, k\Delta t)$ and $(L + \Delta s, k\Delta t)$, with $k = 0(1)n_t$, indicated by "Δ" and "□", respectively. The value of a function $f(s, t)$ at the grid point $(j\Delta s, k\Delta t)$ is denoted by $f_{j,k}$ and of $h(s)$ and $g(t)$ by h_t and g_k , respectively.

There are many difference schemes possible to approximate the differential equations. For instance the term $(Tx')'(j\Delta s, k\Delta t)$ can be approximated by

$$T_{j,k} \frac{x_{j+1,k} - 2x_{j,k} + x_{j-1,k}}{\Delta s^2} + \frac{T_{j+1/2,k} - T_{j-1/2,k}}{2\Delta s} \frac{x_{j+1,k} - x_{j-1,k}}{2\Delta s}, \quad (3.45)$$

but also by

$$(T_{j+1/2,k} \frac{x_{j+1,k} - x_{j,k}}{\Delta s} + T_{j-1/2,k} \frac{x_{j,k} - x_{j-1,k}}{\Delta s}) / \Delta s. \quad (3.46)$$

In the last case the normal force T is defined at each time level only at points just in between the grid points (3.43), indicated by "o" in the boundary conditions (3.35) and (3.36), can at time $t = k\Delta t$ for instance be approximated by

$$3/2 T_{n_s-1/2,k} - 1/2 T_{n_s-3/2,k}. \quad (3.47)$$

The same kind of approximation (3.45) and (3.46) can be used for the other terms on the right-hand sides of (3.27) and (3.28). The constraint (3.31) can be approximated at the grid points, yielding for point $(j\Delta s, k\Delta t)$

$$\left(\frac{x_{j+1,k} - x_{j-1,k}}{2\Delta s}\right)^2 + \left(\frac{y_{j+1,k} - y_{j-1,k}}{2\Delta s}\right)^2 = 1. \quad (3.48)$$

When we approximate this constraint at points in the middle of the grid points we obtain

$$\left(\frac{x_{j,k} - x_{j-1,k}}{\Delta s}\right)^2 + \left(\frac{y_{j,k} - y_{j-1,k}}{\Delta s}\right)^2 = 1. \quad (3.49)$$

The type of approximation (3.46) in combination with (3.49) turned out to be satisfactory because it is well matched to the boundary conditions.

Two difference operators are defined

$$\delta f_{j,k} = \frac{f_{j+1/2,k} - f_{j-1/2,k}}{\Delta s}, \quad \Delta f_{j,k} = 0.5 (\delta f_{j+1/2,k} - \delta f_{j-1/2,k}). \quad (3.50)$$

If we use (3.46), and take a weighted average by means of the factor μ of forward and backward approximations of each of the four equations (3.27) \cdots (3.30) we find

$$V_j(u_{j,k+1} - u_{j,k})/\Delta t = \mu(\delta(T\delta x)_{j,k+1} + \delta(\delta M\delta y)_{j,k+1}) + (1 - \mu)(\delta(T\delta x)_{j,k} + \delta(\delta M\delta y)_{j,k}) \\ , \quad j = 0(1)n_s, \quad (3.51)$$

$$V_j(v_{j,k+1} - v_{j,k})/\Delta t = \mu(\delta(T\delta y)_{j,k+1} + \delta(\delta M\delta x)_{j,k+1}) + (1 - \mu)(\delta(T\delta y)_{j,k} + \delta(\delta M\delta x)_{j,k}) \\ , \quad j = 0(1)n_s, \quad (3.52)$$

$$(x_{j,k+1} - x_{j,k})/\Delta t = \mu u_{j,k+1} + (1 - \mu)u_{j,k}, \quad j = 0(1)n_s, \quad (3.53)$$

$$(y_{j,k+1} - y_{j,k})/\Delta t = \mu v_{j,k+1} + (1 - \mu)v_{j,k}, \quad j = 0(1)n_s, \quad (3.54)$$

Using (3.49) we approximate (3.31) and (3.32) by

$$(\delta x_{j-1/2,k+1})^2 + (\Delta y_{j-1/2,k+1})^2 = 1, \quad j = 0(1)n_s + 1, \quad (3.55)$$

and

$$M_{j,k+1} = W_j(\Delta x_{j,k+1}\delta^2 y_{j,k+1} - \Delta y_{j,k+1}\delta^2 x_{j,k+1} + \theta'_0(j\Delta s)), \quad j = 0(1)n_s, \quad (3.56)$$

For $\mu = 1/2$ these equations become the Crank-Nicolson scheme and the truncation error is $O(\Delta t^2) + O(\Delta s^2)$. For $\mu = 1$ we have the fully implicit backward time difference scheme, then the truncation error is $O(\Delta t) + O(\Delta s^2)$.

The boundary conditions (3.33) are approximated by

$$x_{0,k+1} = x_0(L_0), \quad y_{0,k+1} = y_0(L_0), \quad (3.57)$$

and

$$y'_0(L_0) \Delta x_{0,k+1} = x'_0(L_0) \Delta y_{0,k+1}, \quad (3.58)$$

Before writing down the boundary conditions at $s = L$ we mention that besides the x -coordinate b of the arrow. it appeared to be advantageous to introduce also its velocity

$$c \stackrel{\text{def}}{=} \dot{b}, \quad (3.59)$$

as another unknown function. Then the three boundary conditions (3.34) ··· (3.36) at $s = L$ are approximated by the difference relations

$$M_{n_s, k+1} = 0 , \quad (3.60)$$

$$\begin{aligned} m_a (c_{k+1} - c_k) / \Delta t + m_t (u_{n_s, k+1} - u_{n_s, k}) / \Delta t = \\ - \mu \left[(3/2 T_{n_s-1/2, k+1} - 1/2 T_{n_s-3/2, k+1}) (x_{n_s+1, k+1} - x_{n_s-1, k+1}) + \right. \\ \left. (y_{n_s+1, k+1} - y_{n_s-1, k+1}) (-4M_{n_s-1, k+1} + M_{n_s-2, k+1}) \right] \\ - (1 - \mu) \left[(3/2 T_{n_s-1/2, k} - 1/2 T_{n_s-3/2, k}) (x_{n_s+1, k} - x_{n_s-1, k}) + \right. \\ \left. (y_{n_s+1, k} - y_{n_s-1, k}) (-4M_{n_s-1, k} + M_{n_s-2, k}) \right] , \end{aligned} \quad (3.61)$$

$$\begin{aligned} (\mu y_{n_s, k+1} + (1 - \mu) y_{n_s, k}) m_a (c_{k+1} - c_k) / \Delta t - \\ (\mu (b_{k+1} - x_{n_s, k+1}) + (1 - \mu) (b_k - x_{n_s, k})) m_t (v_{n_s, k+1} - v_{n_s, k}) / \Delta t = \\ \left[\mu (b_{k+1} - x_{n_s, k+1}) + (1 - \mu) (b_k - x_{n_s, k}) \right] \\ \left[\mu \left[(3/2 T_{n_s-1/2, k+1} - 1/2 T_{n_s-3/2, k+1}) (y_{n_s+1, k+1} - y_{n_s-1, k+1}) - \right. \right. \\ \left. (x_{n_s+1, k+1} - x_{n_s-1, k+1}) (-4M_{n_s-1, k+1} + M_{n_s-2, k+1}) \right] \\ \left. + (1 - \mu) \left[(3/2 T_{n_s-1/2, k} - 1/2 T_{n_s-3/2, k}) (y_{n_s+1, k} - y_{n_s-1, k}) - \right. \right. \\ \left. (x_{n_s+1, k} - x_{n_s-1, k}) (-4M_{n_s-1, k} + M_{n_s-2, k}) \right] \right] . \end{aligned} \quad (3.62)$$

Finally we take as approximations for (3.37) and (3.59)

$$(b_{k+1} - x_{n_s, k+1})^2 + y_{n_s, k+1}^2 = l^2 , \quad (3.63)$$

and

$$(b_{k+1} - b_k) / \Delta t = \mu c_{k+1} + (1 - \mu) c_k , \quad (3.64)$$

respectively. The dynamic force E (3.41) is approximated by

$$E_{k+1} = -2m_a (c_{k+1} - c_k) / \Delta t , \quad (3.65)$$

and the recoil force P (3.42) by

$$P_{k+1} = 2 \left((M_{1, k+1} - M_{-1, k+1}) y'_0(L_0) + 1/2 (T_{1/2, k+1} + T_{-1/2, k+1}) x'_0(L_0) \right) . \quad (3.66)$$

At $t = 0$ the initial values of the unknown functions x, y, u, v are given by (3.38) ··· (3.40). The finite difference approximation for the static equations can be found in a straightforward way from equations (3.51) ··· (3.64).

At each time, hence for each $k\Delta t$ ($k = 0(1)n_t$), we have to solve a set of nonlinear equations, which is done by means of a Newtonian method. For this method it is essential to have reliable starting values or the unknowns

i) *The equations for the static case, for $t = 0$.*

Starting values for the solution of the static finite difference equations are obtained by using the values computed by means of the program described in [2]. The reason that we revise these values by means of the static finite difference scheme, is that the values obtained in this way are better matched to the finite difference scheme for the dynamic equations.

- ii) *The dynamic case, from $t = 0$ to $t = \Delta t$, ($k = 0$).*

We use as starting values of the unknowns at time level $t = 0$ the values obtained in 3.4. In order to avoid the use of the values of the accelerations at $t = 0$ we take $\mu = 1$. In Section 3.6 we return to this.

- iii) *The dynamic case, from $t = k\Delta t$ to $t = (k + 1)\Delta t$, ($k = 1(i)n_t$)*

The starting values for the time level $(k + 1)\Delta t$ of the unknowns x, y, u, v, M, b and c are obtained from the equations (3.51) \cdots (3.54), (3.56), (3.60) \cdots (3.62) and (3.64), with $\mu = 0$. This means that we explicitly calculate these values from the final results at the preceding time level $k\Delta t$. From these starting values we calculate the values at the time level $(k + 1)\Delta t$ with $\mu = 1/2$. Hence the further dynamic development for $t > \Delta t$ is determined by a Crank-Nicolson scheme.

In order to get accurate information about the way in which the arrow leaves the string, the mesh width Δt in the t -direction is chosen continuously smaller from a certain time, at which the string is nearly stretched. Because the difference scheme is a two-time-level one with approximations for only first-order derivatives with respect to time, no special provisions are needed.

For instance, in [3] numerical methods to solve related problems are analysed. In the nonlinear case only for specific problems stability and convergence of some difference schemes can be proved analytically. Here no proof is given of the stability and convergence of our difference scheme, however, we have checked our method numerically. First, in the static case, we compare automatically (see i) the results of the finite-difference method with the results obtained with the program described in [2]. The difference between the weight of the bow computed by both programs appears to be about 0.5%, if we take $n_s = 64$. Second the total energy $\bar{A}_p + \bar{A}_k$ (equations (3.4) and (3.5)) has to be constant during the motion. Third, we can investigate the convergence of the difference equations by refining the grid. We consider the special bow

$$\begin{aligned} &B(91.44, 10.16, \bar{W}(\bar{s}), \bar{V}(\bar{s}), \theta_0 \equiv 0, 0.0125, 0, |\overline{OH}| = 15.24; \\ &71.12, 15.53, 0.1625) . \end{aligned} \quad (3.67)$$

The bending stiffness $\bar{W}(\bar{s})$ and the mass distribution $\bar{V}(\bar{s})$ are given by

$$\bar{W}(\bar{s}) = 1.30 \cdot 10^5 \left(\frac{\bar{L} - \bar{s}}{\bar{L}} \right) , \quad (3.68)$$

and

$$\bar{W}(\bar{s}) = 7.69 \quad \text{if} \quad 1.30 \cdot 10^5 \left(\frac{\bar{L} - \bar{s}}{\bar{L}} \right) \leq 7.69 , \quad (3.69)$$

$$\bar{V}(\bar{s}) = 4.52 \cdot 10^{-3} \left(\frac{\bar{L} - \bar{s}}{\bar{L}} \right) . \quad (3.70)$$

The value at the tip of $\bar{W}(\bar{s})$ (3.69) is necessary in order to avoid difficulties in the calculation. This bow (H bow) is also discussed by Hickman in [1, page 69].

Table 3.1: Dependence of \bar{b} , \bar{c} , \bar{a} and $\bar{A}_p + \bar{A}_k$ on $\Delta\bar{t}$, $\Delta\bar{s} = 1.27$ cm, $\bar{t} = 0.0157$ sec.

$\Delta\bar{t}$ sec	\bar{b} cm	\bar{c} cm/sec	\bar{a} cm/sec ²	$\bar{A}_p + \bar{A}_k$
$4.9089 \cdot 10^{-4}$	16.379	-5544	-147704	560.48
$2.4544 \cdot 10^{-4}$	16.375	-5548	-139432	560.43
$1.2272 \cdot 10^{-4}$	16.373	-5549	-132578	560.41

Table 3.2: Dependence of \bar{b} , \bar{c} , \bar{a} and $\bar{A}_p + \bar{A}_k$ on $\Delta\bar{s}$, $\Delta\bar{t} = 1.2272 \cdot 10^{-4}$ sec, $\bar{t} = 0.0157$ sec.

$\Delta\bar{s}$ cm	\bar{b} cm	\bar{c} cm/sec	\bar{a} cm/sec ²	$\bar{A}_p + \bar{A}_k$
5.08	16.06	-5583	-136392	569.8
2.54	16.24	-5563	-132585	563.6
1.27	16.37	-5549	-132578	560.4

In Tables 3.1 and 3.2 we show the dependence of some calculated dynamic quantities on the mesh widths $\Delta\bar{t}$ and $\Delta\bar{s}$, respectively. The quantities are the x -coordinate \bar{b} (cm) of the end of the arrow, the velocity $\bar{c} = \dot{\bar{b}}$ (cm/sec), the acceleration $\bar{a} = \dot{\bar{c}}$ (cm/sec²) and the energy $\bar{A}_p + \bar{A}_k$ (kgfcm). The values are given for a fixed time $\bar{t} = 0.0157$ sec, which is near to the time at which the arrow leaves the string (0.01662 sec). The same can be done for other times, then the results are similar with respect to convergence. From these tables it seems reasonable that with decreasing values of $\Delta\bar{t}$ and $\Delta\bar{s}$ the solutions of the difference equations "converge". The energy for $\Delta\bar{t} = 1.2272 \cdot 10^{-4}$ sec and $\Delta\bar{s} = 1.27$ cm differs about 0.5% from its value 557.207 kgfcm at time $\bar{t} = 0$. A fourth check is to compare our results with those obtained by the use of the finite-element program MARC of the MARC Analysis Research Corporation. This has been done for the bow

$$\begin{aligned} &B(91.44, 10.16, \bar{W}, \bar{V}, \theta_0 \equiv 0, 0.01134, 0, \bar{l} = 89.34; \\ &70.98, 15.43, 0.1589), \end{aligned} \quad (3.71)$$

where the bending stiffness $\bar{W}(\bar{s})$ and the mass distribution $\bar{V}(\bar{s})$ are given by

$$\bar{W}(\bar{s}) = 1.15 \cdot 10^5 \left(\frac{\bar{L} - \bar{s}}{\bar{L} - \bar{L}_0} \right), \quad (3.72)$$

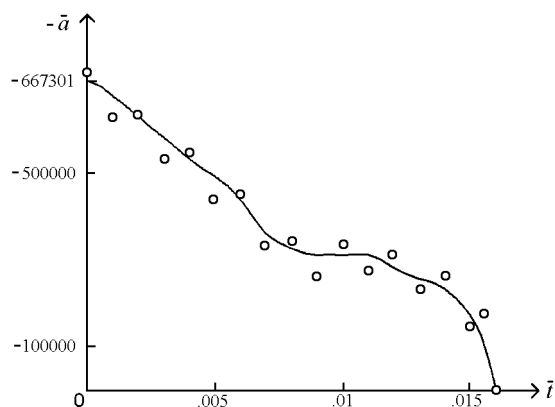
and

$$\bar{W}(\bar{s}) = 7.69 \quad \text{if} \quad 1.15 \cdot 10^5 \left(\frac{\bar{L} - \bar{s}}{\bar{L} - \bar{L}_0} \right) \leq 7.69, \quad (3.73)$$

$$\bar{V}(\bar{s}) = 3.91 \cdot 10^{-3} \left(\frac{\bar{L} - \bar{s}}{\bar{L}} \right). \quad (3.74)$$

Table 3.3: Comparison between finite-difference and finite-element solution.

\bar{t}	finite elements		finite difference	
	\bar{b} cm	\bar{c} cm/sec	\bar{b} cm	\bar{c} cm/sec
$0.501 \cdot 10^{-2}$	63.69	-2739	63.53	-2795
$0.501 \cdot 10^{-2}$	45.47	-4399	44.98	-4480
$0.501 \cdot 10^{-2}$	25.69	-5449	24.84	-5537

Figure 3.4: Acceleration of arrow. \circ : finite element and $—$: finite difference.

In the MARC program the functions \bar{W} and \bar{V} are approximated by step functions and both the bow and the string are taken slightly extensible. The number of elements used was eight, and $\delta\bar{t} = 0.001$ sec. For the finite-difference scheme we used $\Delta\bar{t} = 0.001$ sec and $\Delta\bar{s} = 1.27$ cm. The values of \bar{b} and \bar{c} are given in Table 3.3 for several values of \bar{t} . In Figure 3.4 the acceleration \bar{a} of the arrow in cm/sec² as function of the time in sec, computed by both programs is drawn. We conclude that there is a reasonable agreement between the results with respect to the x -coordinate \bar{b} and the velocity \bar{c} of the arrow. The acceleration curve obtained by using the MARC-program is, however, oscillating in a non-physical way.

3.5 Some numerical results

In [2] the so called static quality coefficient, denoted by q , was defined. This quantity is given by

$$q = \frac{\bar{A}}{|\overline{OD}| \overline{F}(|\overline{OD}|)}, \quad (3.75)$$

where \overline{A} is the energy stored in the bow by deforming it from the braced position into the fully drawn position. This energy reads

$$\overline{A} = \int_{|\overline{OH}|}^{|\overline{OD}|} \overline{F}(\overline{b}) d\overline{b} = \left[\int_0^{\overline{L}} \overline{W}(\overline{s}) (\theta'(\overline{s}) - \theta'_0(\overline{s}))^2 d\overline{s} \right]_{\overline{b}=|\overline{OH}|}^{\overline{b}=|\overline{OD}|} . \quad (3.76)$$

We now introduce two dynamic quality coefficients η and ν in order to be able to compare more easily the performance of different bows in combination with various arrows. This efficiency η of a bow is defined by

$$\eta = \frac{\overline{m}_a \overline{c}_l^2}{\overline{A}} , \quad (3.77)$$

where \overline{c}_l is the muzzle velocity. The product $q\eta$ is a measure for the energy imparted to the arrow. It is evident that in all kinds of archery we want this quantity to be as large as possible. However, it cannot be on its own an appropriate measure of the performance of the bow. If we let for instance increase the mass \overline{m}_a of the arrow indefinitely, then the efficiency (3.77) tends to its largest value, namely one, hence $q\eta$ tends to its largest value q , however, the muzzle velocity \overline{c}_l tends to zero. Klopsteg [1, page 162], mentioned the cast as another criterion of the quality of a bow. He defines the cast as the property of a bow that enables it to impart velocity to an arrow of stated mass. So, a second dynamic quality coefficient can be defined by

$$\nu = \left(\frac{q\eta}{\overline{m}_a} \right)^{1/2} = c_l , \quad (3.78)$$

where the last equality follows from (3.75), (3.77) and (3.26). Thus, if the weight, draw and mass of the limbs are stated, then ν is a measure for the muzzle velocity of a given arrow. In order to show on which dimensionless quantities ν depends, we write

$$\nu = c_l(L, L_0, W(s), V(s), \theta_0(s), m_a, m_t, |OH| \text{ or } l) , \quad 0 \leq s \leq L . \quad (3.79)$$

For flight shooting the quality coefficient ν is important because then ν is wanted to be sufficiently large. For hunting (but certainly for target shooting) it is not easy to find a criterion for the good performance of bow and arrow. What we can state is that the bow has to shoot "sweetly" and without an unpleasant recoil. By this we mean that the acceleration of the arrow should happen smoothly enough and that the recoil force P (3.42) should be not too large or fluctuating too strongly.

One of our objectives is to get insight into the influence of the quantities which determine a bow on the numbers q , η and ν , and on the behaviour of the forces $E(b)$ and $P(b)$. To this end we start with the H bow.

$$B(1.286, 0.143, W(s), V(s), \theta_0 \equiv 0, 0.0769, 0, |OH| = 0.214; 1, 1, 1), \quad (3.80)$$

and change in a more or less systematic way its parameters. The bending stiffness W and the mass distribution V in (3.80) are given by (3.68), (3.69) and (3.70) of which the values have been made dimensionless by using (3.26)

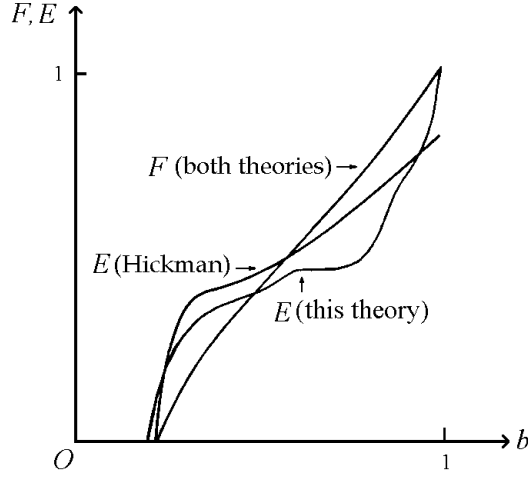


Figure 3.5: SFD and DFD curves. Hickman's theory and this theory.

If the three quantities q , η and ν are known, the muzzle velocity \bar{c}_l (cm/sec) can be computed. Using (3.78) and (3.26) we find

$$\bar{c}_l = 31.32 \nu \left(\frac{\bar{F}(|\overline{OD}|)|\overline{OD}|}{\bar{m}_b} \right)^{1/2} \text{cm/sec} , \quad (3.81)$$

where the number 31.32 is caused by the choice of our units. The kinetic energy (kgfcm) imparted to the arrow of mass $2\bar{m}_a$ follows from

$$\bar{m}_a \bar{c}_l^2 = m_a \nu^2 \bar{F}(|\overline{OD}|)|\overline{OD}| = \eta q \bar{F}(|\overline{OD}|)|\overline{OD}| . \quad (3.82)$$

These equations show the dependence of the two important quantities, the muzzle velocity (3.81) and the kinetic energy of the arrow (3.82), on the weight draw and mass of the limbs. For the H bow (3.67) we have $\bar{F}(|\overline{OD}|) = 15.53$ kgf, $|\overline{OD}| = 71.1$ cm and $\bar{m}_b = 0.1625$ kg, and the computed values of q , η and ν are 0.407, 0.89 and 2.16, respectively. Thus for this bow, $\bar{c}_l = 5578$ cm/sec and $\bar{m}_a \bar{c}_l^2 = 400$ kgfcm.

The shooting time (the time interval between the loosing of the arrow and its leaving the string) appeared to be 0.01662 sec.

In Figure 3.5 we have drawn the dimensionless static-force-draw (SFD) curve $F(b)$, and dynamic-force-draw (DFD) curve $E(b)$, calculated by our theory for the H bow. Also the curves obtained by Hickman's theory [1, page 69], are drawn. The SFD-curves coincide with each other within drawing accuracy. As can be seen from Figure 3.5 the DFD-curve obtained by using the finite-difference method is gradually decreasing. There is no jump in the force on the arrow at $t = 0$. The finite-difference method will in general give an efficiency which is smaller than one. The x -coordinate b of the arrow for which the force at the arrow is zero, hence the value of b where the arrow leaves the string, is a bit smaller than the brace height.

Hickman used a simple model (H model) which consists of two rigid limbs without mass, connected each to the grip by means of a linear elastic hinge. The strength of these hinges is determined in some way by the elastic properties of the real bow. The mass of the real limbs is accounted for by concentrated masses at the tips of the limbs. Because

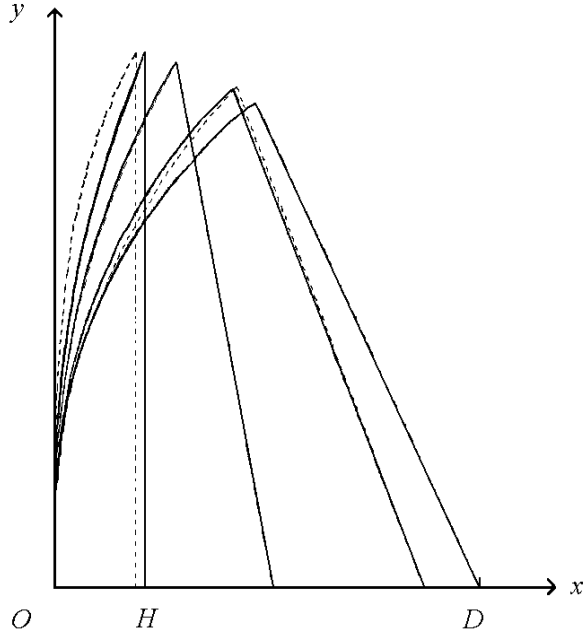


Figure 3.6: Shapes of limbs of H bow.

of these masses the force on the arrow has, when calculated by means of the H model, a jump at time $t = 0$. In [2] it is proved that the efficiency η of a H model bow is always 1. That is why in Figure 3.5 the area below the SFD curve and the area below the DFD curve, calculated by means of the H model, are equal.

We mention that in the figures given by Hickman in [1, pages 5 and 7], the acceleration of the arrow measured experimentally, and hence also the force on the arrow, is zero at time $t = 0$, which is in contradiction with his own model. The dynamic force on the arrow in our theory at that moment is, if there are no concentrated masses at the tips ($m_t = 0$), equal to the static force in fully drawn position (see Section 3.6). The shapes of the limbs of the H bow for some positions of the arrow, both static and dynamic, are shown in Figure 3.6. For $b = 1$ both shapes are the same. After loosing the arrow first the outer parts of the limbs stretch themselves. The released bending energy is used to accelerate both the arrow and the limbs. For a certain value of b the shape in the dynamic and static case are nearly the same. After that the outer parts of the limbs are decelerated and become more sharply bent than in the static case. Now the inner parts of the limbs become more stretched and loose their bending energy.

In Figure 3.7 the DFD curve and the recoil force P , as a function of the position of the end of the arrow b , are drawn. It can be seen that although the force E at the arrow decreases after release of the arrow, the recoil force P increases and becomes more than two times the weight of the bow. We note that at a certain moment it becomes negative; this means that the archer has to pull instead of to push the bow at the end of the shooting in order to keep the grip at its place. In modern archery, however, it is practice to shoot open-handed. But then it is impossible for an archer to exert a force on the bow directed

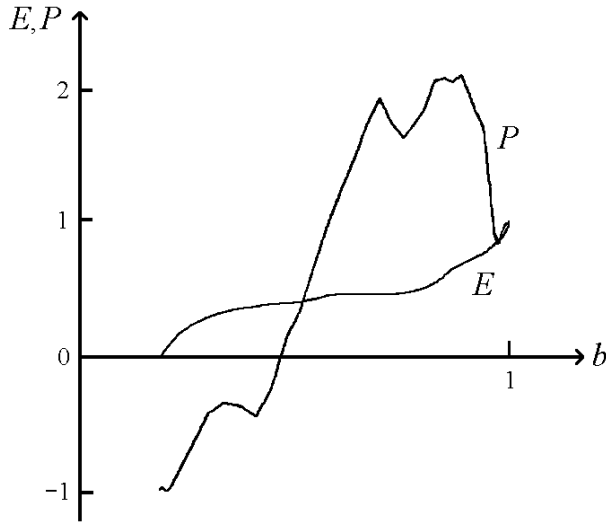


Figure 3.7: Dynamic force $E(b)$ and recoil force $P(b)$ for the H bow.

to himself and the assumption that the bow is clamped at the grip, is violated. Possibly less kinetic energy will be recovered from the bow when negative recoil forces occur if the bow is shot open-handed. In this paper we adhere to the assumption that the grip of the bow is clamped.

Klopsteg [1, page 141], carried out experiments to investigate the motion of the bow hand while the arrow is being accelerated. He finds, besides other movements, always a small excursion of this hand backwards after the loose. He states:

‘A satisfactory explanation for the slight backward motion is that during the 20 or 30 thousands of a second after the loose, a very considerable force is being exerted by the string on the arrow and consequently an equal backward force is exerted by the handle of the bow on the bow hand. During this brief impulse the instantaneous value of the force may rise to several hundred pounds, but lasting for an exceedingly few thousands of a second.’

This explanation is in contradiction with the results shown in Figure 3.7. The dynamic force E at the arrow and the force P at the bow hand are not equal at all.

In what follows we consider the consequences of a change of one characteristic quantity of the H bow at a time, the other ones being kept the same. The values of the static quality coefficient q given in the following tables are computed by means of the program described in [2]. Only if the smoothness of the DFD curve or the behaviour of the recoil force P differs clearly from the smoothness of that curve in the case of the H bow, this is explicitly mentioned.

The influence of a change of the length of the grip $2L_0$ is shown in Table 3.4. In [1, page 18], the effect of a rigid middle section, a grip, is also dealt with. This is an interesting subject because it is known that a bow which bends throughout its whole length is not a pleasant bow to shoot. It has a so-called "kick". Because Hickman did not find striking

Table 3.4: Influence of grip length $2L_0$.

L_0	0	0.0714	0.143	0.214
q	0.415	0.411	0.407	0.403
n	0.88	0.88	0.89	0.90
ν	2.18	2.18	2.16	2.16

Table 3.5: Influence of brace height $|OH|$.

$ OH $	0.0714	0.107	0.143	0.179	0.214	0.250
q	0.444	0.438	0.430	0.420	0.407	0.392
η	0.91	0.91	0.90	0.89	0.89	0.88
ν	32.29	2.28	2.25	2.21	2.16	2.12

theoretical differences with respect to the static properties of two bows, one with $L_0 = 0$ and the other with $L_0 = 0.143$, he states:

‘The greatest difference between these two types of bows is due to dynamic conditions.’

However, it is seen from Table 3.4 that the values of q , η and ν nearly do not change. From our calculations it follows that the behaviour of the dynamic force E and of the recoil force P , are almost the same for the two types. Hence also with respect to these dynamic properties no dear differences appear in our theory. In Table 3.5 the influence of the brace height is shown. In [1, page 21], Hickman makes the following statement based on experiments:

‘The arrow velocity increases with increase in bracing height up to a certain point, after which it slowly decreases with additional increases in bracing height. The bracing height for maximum arrow velocity depends principally on the length of the bow.’

This does not agree with the results of our theory. From Table 3.5 we see that there is always a small decrease of the arrow velocity when the brace height is increased. This is due to both static (q) and dynamic (ν) effects.

To investigate the influence of the length $2L$ of the bow we considered five different lengths. From Table 3.6 we find that there is almost no perceptible change in the efficiency η of the bow hence ν shows the same tendency as q .

Now we consider the influence of the distribution of the bending stiffness W and the mass V along the bow. We take

$$W_n(s) = W(L_0) \left(\frac{L-s}{L-L_0} \right)^{\beta_n}, \quad L_0 \leq s \leq L, \quad (3.83)$$

Table 3.6: Influence of length $2L$.

L	1.143	1.214	1.286	1.357	1.429
q	0.393	0.400	0.407	0.413	0.417
η	0.88	0.88	0.89	0.89	0.89
ν	2.12	2.15	2.16	2.18	2.21

Table 3.7: Influence of bending stiffness W and of mass V .

$W(s)$	W_1	W_2	W_3	W_3			
$V(s)$		V_3		V_1	V_2	V_3	V_4
q	0.417	0.414	0.407	0.407	0.407	0.407	0.407
η	0.93	0.91	0.89	0.74	0.81	0.89	0.97
ν	2.25	2.21	2.16	1.98	2.08	2.16	2.28

and

$$V_n(s) = V(L_0) \left(\frac{L-s}{L-L_0} \right)^{\beta_n}, \quad L_0 \leq s \leq L. \quad (3.84)$$

where $n = 1, 2, 3, 4$ and $\beta_1 = 0$, $\beta_2 = 1/2$, $\beta_3 = 1$, $\beta_4 = 2$. A value of β_n chosen in (3.84) needs not to be the same as the one chosen in (3.83). In order to avoid numerical difficulties we take again

$$W_n(s) = 10^{-4} \text{ if } W(L_0) \left(\frac{L-s}{L-L_0} \right)^{\beta_n} \leq 10^{-4}, \quad (3.85)$$

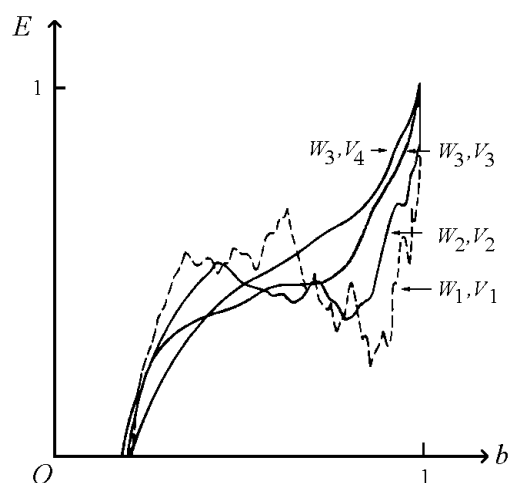
The results of changing W and V separately are given in Table 3.7. We conclude that if the mass distribution V is taken to be linear (V_3), the constant bending stiffness distribution (W_1) is the best, due to both static (q) and dynamic (η) effects. If the bending stiffness W is linear (W) then the mass distribution V_4 , which has light tips, is undoubtedly the best. We refer to Figure 3.8 for its DFD curve.

In Table 3.8 W and V are changed simultaneously. The results in this table show that the quantities q , η and ν of the bow nearly depend only on the ratio of the two functions W and V . However, as can be seen from Figure 3.8 the DFD curve of the bow with W_3 and V_3 is far more smooth than those of the other two bows. It shows that although the efficiency of a bow with uniform distributions of bending stiffness and mass is acceptable, it will shoot almost surely unpleasant.

We now consider the influence of the shape of the bow in unbraced situation. This

Table 3.8: Influence of bending stiffness W and of mass V .

W, V	W_1, V_1	W_2, V_2	W_3, V_3
q	0.417	0.414	0.407
η	0.87	0.86	0.89
ν	2.16	2.15	2.16

Figure 3.8: DFD curves for bows (W_1, V_1) , (W_2, V_2) , (W_3, V_3) and (W_3, V_4) .

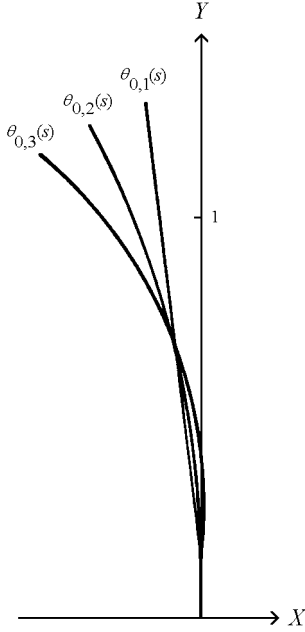


Figure 3.9: Three types of recurve $\theta_{0,1}(s)$, $\theta_{0,2}(s)$ and $\theta_{0,3}(s)$.

shape is determined by the function $\theta_0(s)$. We choose

$$\theta_{0,1} = 0, \quad 0 \leq s \leq L_0, \quad \theta_{0,1} = -0.12, \quad L_0 \leq s \leq L, \quad (3.86)$$

$$\theta_{0,2} = 0, \quad 0 \leq s \leq L_0, \quad \theta_{0,2} = -0.5 \frac{s - L_0}{L - L_0}, \quad L_0 \leq s \leq L, \quad (3.87)$$

$$\theta_{0,3} = 0, \quad 0 \leq s \leq L_0, \quad \theta_{0,3} = 0.12 - \frac{s - L_0}{L - L_0}, \quad L_0 \leq s \leq L, \quad (3.88)$$

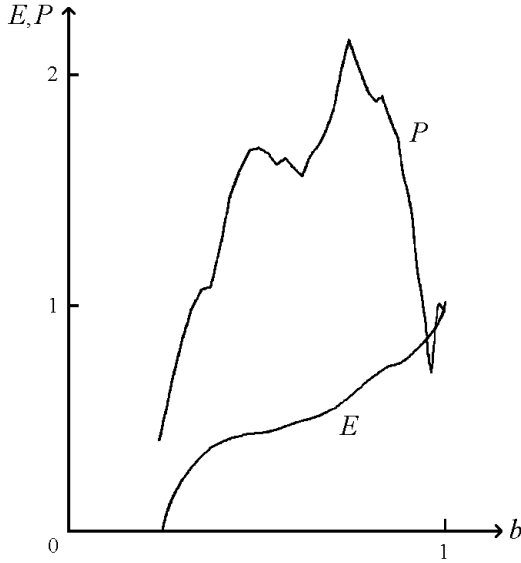
The three forms are drawn in Figure 3.9. The H bow in unbraced situation is straight, hence it is part of the y-axis, $\theta_0 \equiv 0$. The unbraced situations (3.86), (3.87) and (3.88) are called to possess recurve as we mentioned before. We have to choose a moderate recurve in order to agree with the assumption that the string has contact with the bow only at the tips of the bow. It is seen from Table 3.9 that the efficiency of the recurved bows is slightly smaller than the efficiency of the H bow ($\theta_0 \equiv 0$). In the case of $\theta_{0,3}$ however, there is a more important favourable influence of the recurve on the static quality coefficient q . This agrees with the experience of Hickman [1, pages 22, 24 and 50]. In [2] a bow with even a coefficient q equal to 0.833 is described. However, for this bow the string lies partly along the bow during some time interval. In a following paper we hope to be able to describe the dynamic performance of such a bow.

We stress that for a bow with a shape given by $\theta_{0,3}$ the recoil force P at the bow hand is positive at all times in between loosing the arrow and its leaving the string (Figure 3.10). This is in contradiction to all other bows mentioned so far.

Next the influence of the mass of the arrow is considered. In Table 3.10 the consequences of changing m_a are collected. Now also the product of q and η is given, being a measure

Table 3.9: Influence of shape of unbraced bow.

θ_0	$\theta_0 \equiv 0$	$\theta_{0,1}$	$\theta_{0,2}$	$\theta_{0,3}$
q	0.407	0.424	0.457	0.487
η	0.89	0.83	0.81	0.83
ν	2.16	2.14	2.19	2.29

Figure 3.10: Dynamic force $E(b)$ and recoil force $P(b)$ for recurve $\theta_{0,3}$.

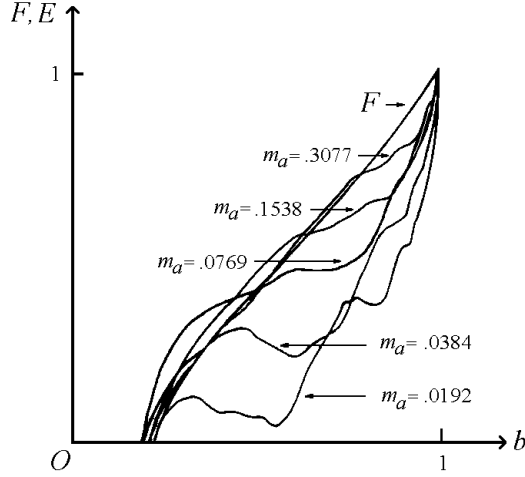
of the energy imparted to the arrow. The factor q is 0.407 in all cases. The first and last given arrow masses in Table 3.10 are of little practical importance, however, they show what happens in the case of a light or heavy arrow. When the mass of the arrow is somewhat smaller than the smallest mass mentioned in this table the force exerted on the arrow by the string becomes zero before the string is stretched and hence our theory may be no longer valid. We remark that the decrease of the efficiency with the decrease of the arrow mass, shown in Table 3.10, does not occur in the H model. Table 3.10 shows further that although the efficiency of a bow shooting a light arrow is bad, the muzzle velocity will be high, a fact already mentioned in many books about archery.

In [1, page 167], Klopsteg defines the concept of virtual mass as: mass which, if it were moving with the speed of the arrow at the instant the latter leaves the string, would have precisely the kinetic energy of the limbs and the string at that instant. If \overline{K}_h denotes the half of the virtual mass then

$$\overline{A} = (\overline{m}_a + \overline{K}_h) \overline{c}_l^2. \quad (3.89)$$

Table 3.10: Influence of mass of arrow $2m_a$, $q = 0.407$.

m_a	0.0192	0.0384	0.0769	0.1538	0.3077
η	0.48	0.69	0.89	0.98	0.98
$q\eta$	0.20	0.28	0.36	0.40	0.40
ν	3.20	2.72	2.16	1.63	1.14

Figure 3.11: SFD curve $F(b)$ and DFD curves $E(b)$ of H bow, different arrow masses $2m_a$, Table 3.10.

If we define $K_h = \overline{K}_h / \overline{m}_b$ we obtain by using (3.77)

$$K_h = m_a \left(\frac{1 - \eta}{\eta} \right). \quad (3.90)$$

Klopsteg continues:

‘That the virtual mass is in fact a constant, has been determined in many measurements with a large number of bows.’

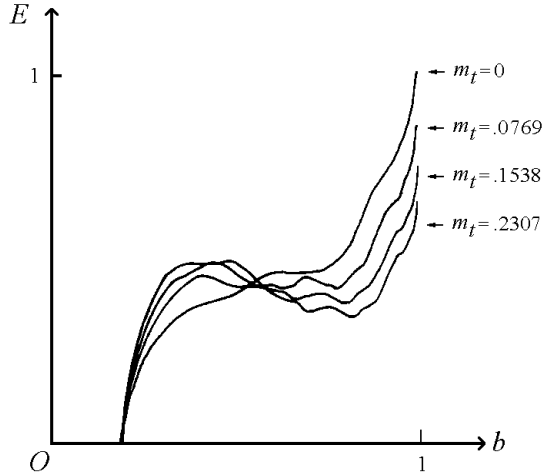
However, if we compute K_h using (3.90) for three values of $m_a = 0.0384, 0.0769, 0.1538$, we get $K_h = 0.017, 0.010, 0.003$, respectively. So, by our theory K_h is definitely not independent of the mass of the arrow in the case of the H bow.

In Figure 3.11 we depict one SFD curve and a number of DFD curves for different values of m_a . If the mass m_a becomes larger the DFD curve approaches the SFD curve. With respect to the maximum value of the recoil force P we note that, if m_a tends to infinity, we get a quasi-static situation and hence also P as a function of b will follow closely the SFD curve. It appeared that the maximum value of P increases if the mass of the arrow decreases. For $m_a = 0.0192$ we even get a maximum value of P equal to about 5 times the weight a of the bow.

Finally the influence of concentrated masses m_t at each of the tips of a bow is described. For that purpose we give the parameter m_t three different, non-zero values. In Table 3.11

Table 3.11: Influence of concentrated tip masses m_t , $q = 0.407$.

m_t	0	0.0769	0.1538	0.2307
η	0.89	0.87	0.84	0.82
ν	2.16	2.15	2.11	2.08

Figure 3.12: DFD curves for H bow with masses m_t at the tips, Table 3.11.

the value of q is 0.407 in all cases. From this table it follows that the efficiency decreases slightly if the mass m_t at the tips increases. In Figure 3.12 the DFD curves are drawn. It is seen that the force E on the arrow possesses a jump at the time $t = 0$. This jump becomes larger when m_t increases. Most of the energy used to accelerate at early instants the concentrated masses at the tips is transferred later on to the arrow. This follows from the fact that the forces on the arrow grow with increasing values of b in the region where the string becomes more stretched.

In [1, page 47], Hickman describes an experiment made to find the effect of the mass at the bow tips. We quote:

‘Measurements of velocities for different weight arrows showed that a load of 400 grain (0.02592 kg) added to the arrow weight, reduced the velocity by about 42 feet per second or 25 percent. In contrast to this, the same load added to the tips only reduced the velocity, even for a light arrow, by about 1 1/2 feet per second or approximately one percent.’

From Table 3.10, third and fourth column, it follows that if we increase the half arrow mass m_a by 0.0769, the velocity decreases by 24.8 percent. From Table 3.11, first and second column, it follows that if we add a mass $m_t = 0.0769$ to each of the tips the velocity decreases only by 0.7 percent. Although we do not know what type of bow Hickman used for his experiment, his findings agree qualitatively with these results.

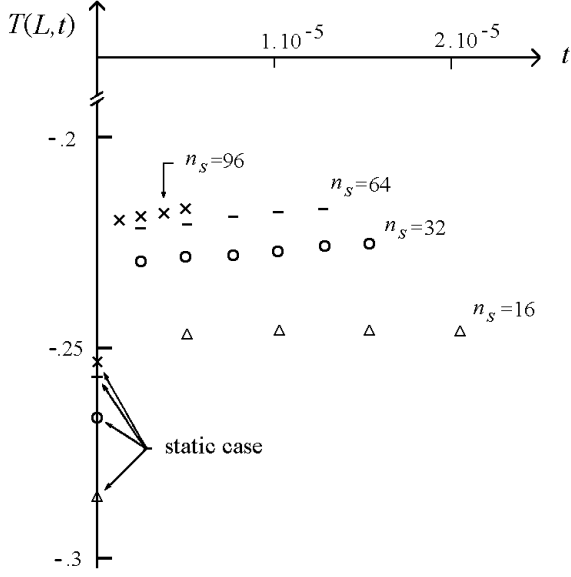


Figure 3.13: Normal force $T(L, t)$ at tip, both static and dynamic for different values of n_s .

3.6 On the behaviour of the normal force T at $t = 0$

In this section we discuss the behaviour of the normal or longitudinal force T in the bow at the time the arrow is released, $t = 0$. In an early attempt we took for the first time step, from $t = 0$ to $t = \Delta t$ in the finite-difference scheme (Section 3.4) $\mu = 1/2$. For the initial values of the unknown x, y, M and T we took their values in the static fully drawn position. When masses $m_t \neq 0$ were present at the tips we found that the resulting solution a non-physical oscillatory character, indicating that the initial values for the unknowns were not sufficiently accurate. To improve the procedure, a fully implicit backward-time difference scheme ($\mu = 1$) for the first step ($k = 0$) is chosen (Section 3.4, ii)). In this way the initial values of the normal force T are not used. We will now show that the static values of T cannot be used with respect to our method as initial values, when concentrated masses at the tips are present.

In Figure 3.13 the normal force $T(L, t)$ at the tip is drawn as a function of time, for a very small time interval after the release of the arrow. This normal force is calculated by the method described in Section 3.4, for the bow has

$$\begin{aligned} &B(91.49, 10.16, \overline{W}(\overline{s}), \overline{V}(\overline{s}), \theta_0 \equiv 0, 0.0125, 0.0125, |\overline{OH}| = 15.29; \\ &71.12, 15.53, 0.1625), \end{aligned} \quad (3.91)$$

where \overline{W} and \overline{V} are defined by (3.68), (3.69) and (3.70). From (3.91) it is seen that $\overline{m}_t = \overline{m}_a = 0.0125$. If we extrapolate the dynamic normal force $T(L, t)$ with $t > 0$ to time zero, we find a value unequal to the static normal force $T_1(L)$ at the tip. This static force is indicated at the vertical axis of Figure 3.13. The magnitude of the jump appeared to be dependent on the mass \overline{m}_t at the tip. It is zero for $\overline{m}_t = 0$. For increasing values of \overline{m}_t it first increases but then decreases, such that for $\overline{m}_t \rightarrow \infty$ the jump tends to zero again.

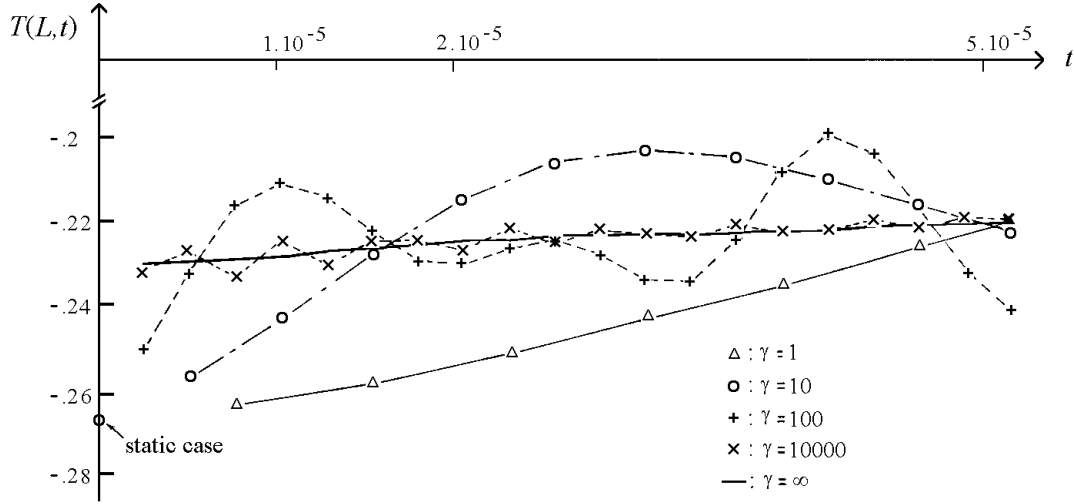


Figure 3.14: Normal force $T(L, t)$ at tip for different values of γ . Δ : $\gamma = 1$, \circ : $\gamma = 10$, $+$: $\gamma = 100$, \times : $\gamma = 10000$ and $—$: $\gamma = \infty$.

This jump phenomenon seems to be related to the inextensibility of the bow by which possibly longitudinal disturbances can be transferred instantaneously. In order to investigate this we replaced the constraint (3.31), expressing the inextensibility of the bow by the relation

$$T(s, t) = 1/2\gamma U(s)(x'^2 + y'^2 - 1), \quad (3.92)$$

where $U(s)$ is the distribution function of the strain stiffness (cross-sectional area times Young's modulus) of the bow and γ is a parameter.

Increasing values of γ correspond to less extensibility of the bow. In Figure 3.14 the normal force is shown as a function of time, again immediately after the release of the arrow. The stiffness parameter γ ranges through the values 1, 10, 100, 10000. Also the curve for an inextensible bow ($\gamma \rightarrow \infty$) is drawn. It can be seen that, if the bow is definitely extensible, $\gamma = 1, 10$ or 100 , the normal force at the tip is continuous with respect to time at $t = 0$. If the strain stiffness is increased the obtained curve "converges" to the curve in the inextensible case and a jump appears. For values of s , $L_0 \leq s \leq L$, we observed the same behaviour of the normal force.

We mention that for a consistent treatment of an extensible bow the Euler-Bernoulli equation (3.32) has to be changed also, because then the parameter s is no longer the length parameter. However, by the foregoing results it is at least reasonable that the inextensibility of the bow has a strong influence on the behaviour of T after the release of the arrow.

3.7 Acknowledgements

The author wishes to acknowledge the advice and criticism received from Prof.dr. J.A. Sparenberg and the valuable discussions with Dr. E.F.F. Botta and Prof.Ir. M. Kuipers. Further his thanks are due to Dr.Ir. J.C. Nagtegaal and Ir. J.E. de Jong for their willingness to check some of the numerical calculations by means of the MARC program. This work was sponsored by the Netherlands Organization for the Advancement of Pure Scientific Research (Z.W.O.) (Grant 63-57).

Bibliography

- [1] Hickman CN, Nagler F, Klopsteg PE. (1947). *Archery: the technical side*. National Field Archery Association, Redlands (Ca).
- [2] Kooi BW, Sparenberg JA. (1980). On the static deformation of a bow. *Journal of Engineering Mathematics* 14:27–45.
- [3] Richtmeyer R, Morton K. (1967). *Difference methods for initial-value problems*. New York.
- [4] Schmidt R, Deppo DAD. (1973). Variational formulation of non-linear equations for straight elastic beams. *J. of Industrial Mathematics Society* 23:117–136.
- [5] Verma MK, Krishna Murthy AV. (1974). Non-linear vibrations of non-uniform beams with concentrated masses. *J. of Sound and Vibrations* 33:1–12.
- [6] Wagner H. (1965). Large-amplitude free vibrations of a beam. *J. of Applied Mechanics* 32:887–892.
- [7] Woodall SR. (1966). On the large amplitude oscillations of a thin elastic beam. *Int. J. Non Linear Mechanics* 1:217–238.

Chapter 4

The static recurve bow

4.1 Summary

In a former paper we dealt with some aspects of the dynamics of the non-recurve bow, of which the string was assumed to be inextensible and without mass. One aim of this paper is to investigate the influence of the elasticity and mass of the string on the non-recurve bow. The main object is to discuss the dynamics of the static-recurve bow. The governing equations of motion lead to a system of non-linear partial differential equations with initial and boundary conditions. These boundary conditions vary abruptly in the course of the dynamic process. Numerical solutions are obtained using a finite-difference method. The vibratory motion of the bow after the arrow has left the string is described for a clamped bow as well as for a bow shot open-handed.

4.2 Introduction

The bow is a mechanical device to propel a projectile, which is generally an arrow. To that end a string, shorter than the bow, is placed between the tips of the bow. Then holding the middle of the bow in place with the "bow" hand, the string is drawn with the other hand, the "shaft" hand. During this, additional energy is stored in the elastic limbs and to a lesser extent also in the string. A part of this energy is, after release, transferred to the arrow.

One way to differentiate between types of bows is to do this on the ground of the shape of the unstrung bow. Then we distinguish between the non-recurve bow, the static-recurve and the working-recurve bow. A recurved or reflexed bow is a bow of which the limbs are in unstrung situation curved away from the archer if he/she holds the unstrung bow just like during shooting. For such a bow it is possible that in the strung conditions the string lies along part of the limbs.

In the case of a non-recurve bow the string has contact with the bow only at the tips in all situations, static or dynamic. The bow with flexible straight limbs (straight-end bow) Figure 4.1.a, but also a bow of which the flexible limbs meet at an angle (Angular bow),

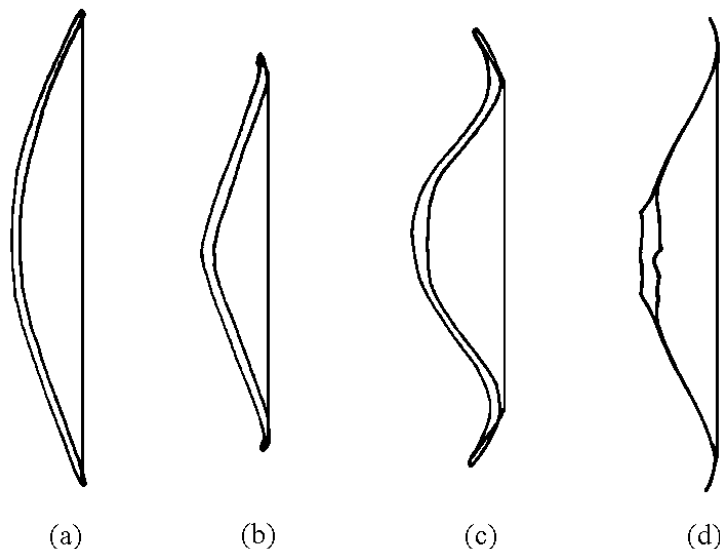


Figure 4.1: Shapes of different types of bows: (a) and (b) non-recurve, (c) static-recurve and (d) working-recurve.

see Rausing [16] and Figure 4.1.b, and even a bow with a slight reflex are non-recurve bows by definition.

The static-recurve bow is a bow which possesses rigid, strongly curved outer parts (ears) of the limbs. In the braced situation the string rests upon the string-bridges, see Figure 4.1.c. These string-bridges are fitted to prevent the string from slipping past the bow. If such a bow is drawn, at some moment the string leaves the bridges and has contact with the bow only at the tips. Because the ears are stiff, they do not deform when the bow is drawn. After release the string touches at a certain moment the string-bridges again before the arrow leaves the string. Some Tartar, Chinese, Persian, Indian and Turkish are static-recurve bows, see Rausing [16], Payne-Gallwey [14], Latham and Paterson [10], Faris and Elmer [4], or Balfour [1].

The entire limbs of a working-recurve bow are flexible. In the braced situation the string has contact with the bow along a part of the limbs near the tips, see Figure 4.1.d. The length of those parts diminishes with increasing draw-length. If the draw-length exceeds a certain value the string leaves the limbs from the tips. After release both phenomena occur in reversed order before arrow exit. Essential difference between the static-recurve and working-recurve is that for the static-recurve the points of contact of string and limbs change abruptly from tip to string-bridge or inversely. For the working-recurve the points where the string leaves the limbs change gradually. Most modern bows are working-recurve bows.

In [9] we dealt with the statics of all three types of bows. In [8] we considered the

dynamics of the non-recurve bows. We assumed the string to be inextensible and without mass and stopped the computations at the moment the arrow leaves the string. In this paper we investigate the influence of the mass and elasticity of the string on a non-recurve bow. Further we consider the behaviour of the bow and string after the arrow has left the string. This is done for two different cases, one by which the bow is clamped and the other for a bow shot open-handed. The main object of this paper is the dynamics of the static-recurve bow. The dynamics of the working-recurve bow will be the subject of a forthcoming paper.

In reality a static-recurve bow is very complicated. It nearly always is made of wood, horn and sinew, hold together with glue and protected from the weather by a thin covering of tree bark, lacquer or leather. This holds also to a certain extend for the English longbow, where the different properties of sapwood and heartwood are deliberately put to use. In spite of this, these bows are considered as an inextensible elastic line endowed with bending stiffness and mass distribution, which depend on the properties of the employed materials and structure of the bow. Other assumptions are the symmetry of the bow with respect to the line of aim, the bow is centre-shot and the rigid arrow is released without lateral deflections. Also neither internal or external damping nor hysteresis are taken into account. The absence of damping throws some measure of uncertainty into our calculations especially for what happens after the arrow has left the string.

In Section 4.3 we derive the governing equations of motion of the static-recurve bow. For such a bow a simple lumped parameter model for the string is used. The dynamic process of shooting is divided in a number of time intervals which are bounded by characteristic events. These events are: the string touches the string-bridges again, the bow leaves the bow hand and the arrow leaves the string. During each of these time intervals, of which the length is not known beforehand, we have the same system of partial differential equations, however the boundary conditions are different. The initial conditions are determined for the first time interval by the static fully drawn position and for the succeeding intervals by the end conditions of the preceding interval.

In the second part of Section 4.3 we give the equations of a string now considered as a continuum. This mathematical model for the string is used only for non-recurve bows. In this case we get at each time interval two systems of partial differential equations defined on two space intervals, one along the bow, the other along the string. These systems are connected by the boundary conditions at one end of each space interval.

In order to obtain a numerical approximation of the solution of the equations of motion we use a finite-difference method. In Section 4.4 a finite-difference scheme is given for the static-recurve bow. After that, the finite-difference equations for the motion of a string considered as a continuum, are discussed. These equations are, with the exception of the boundary conditions, the same as the equations of motion in the case of a refined lumped parameter model for the string.

In [9] and [8] we introduced quality coefficients to be able to compare the performance of different bows. One coefficient is related to the amount of energy stored in the bow in pulling it from the braced situation to full draw. Another one is the efficiency, which is the percentage of energy put into the bow that is imparted to the arrow. Finally, the muzzle

velocity, this is the velocity of the arrow when it leaves the bow. For flight shooting, a form of shooting with the object of reaching the greatest distance, it is the last mentioned quality coefficient which is important. For target shooting and hunting the efficiency is important and also the smoothness with which the bow delivers its power. In Section 4.5 we re-examine the definitions of these quality coefficients. They are used in Sections 4.6 · · · 4.12 in order to judge the performance of a bow.

Hickman [6] and recently Marlow [12] developed mathematical models for a type of a non-recurve bow. They used a model where the elasticity of the limbs is concentrated in two elastic hinges. The mass of the limbs is accounted for by concentrated masses placed at the rigid limbs. Hickman assumed the string to be inextensible. Marlow dropped this assumption and he claims that the results of his elastic string considerations are in reasonable agreement with experiment and remove the long standing discrepancy between theory and practice. However, in Section 4.6 we show that his model can yield unreliable results. It turns out that when the model for the string is replaced by a more realistic one possessing elasticity, however keeping the limbs rigid and rotating about elastic hinges, unrealistic heavy oscillations of the acceleration force acting upon the arrow may occur.

In Section 4.7 we discuss the influence of the strain stiffness and mass of the string of a non-recurve bow. Changing both parameters simultaneously gives us the opportunity to deal with the influence of the number of strands of a string. Increasing this number makes a string stiffer but also heavier. These effects have an opposite influence on the shooting performance. It appears that there exists an optimum number of strands. At the end of Section 4.7 we compare our results with those obtained experimentally by Hickman in [6].

The vibratory motion of the bow after the arrow has left the string is investigated in Section 4.8. It appears that the tensile force in the string attains its maximum after arrow exit. This maximum force determines among others the number of strands needed to make the string strong enough. In the second part of Section 4.8 we discuss the influence of the mass of the grip when the bow is shot open-hand.

In Section 4.9 we start with a straight-end bow and change some of its parameters one by one. In [8] we followed the same procedure, there we started with a bow described by Hickman in [6]. The bow we are interested in now is more realistic; the string is extensible and possesses mass while the tips of the limb have non-zero mass per unit of length and bending stiffness.

In Section 4.10 we consider again the model of a bow consisting of a grip, two elastic hinges, two rigid limbs and an inextensible string. However, in this case the limbs have a sharp bend, hence the bow resembles a static-recurve bow. It is possible to reveal with this simple model some essential favourable features of a static-recurve bow.

The static-recurve bow is also the subject of Section 4.11. We have no accurate experimental information with respect to these bows. The shape of the unstrung bow, as depicted in a number of books and papers shows a large variety. Therefore we deal in Section 4.11 with a few bows which seem to be representative for the static-recurve bow. The lack of detailed information however, makes that we have to be cautious with the interpretation of the results. Yet, it is likely that the performance of a static-recurve bow differs not much from the performance of a long straight-end bow. For a comparable performance, however,

it can be chosen shorter and this makes the static-recurve bow easier in operation.

In Section 4.12 we compare the performance of some bows, non-recurve and static-recurve, mentioned in literature. The results obtained in Section 4.9 and Section 4.11 are used to explain the differences in the performances.

In Section 4.13 we check the finite-difference procedure developed in Section 4.4. To that end we consider a vibrating beam with small deflections, hence the linearized theory applies. Numerical solutions by means of our finite-difference method are compared with the results obtained by an analytic method.

4.3 The equations of motion

In the first part of this section we give the equations of motion for a static-recurve bow. The mass of the extensible string is distributed as point masses over the two tips and the arrow. In the second part we give the equations of motion for an extensible string possessing mass per unit of length. The string is then considered as a continuum. These string equations will be used for non-recurve bow.

Figure 4.2 shows a static-recurve bow placed in a Cartesian coordinate system (\bar{x}, \bar{y}) in the unbraced, braced and fully drawn situation. Because the bow is assumed to be symmetric with respect to the line of aim coinciding with the \bar{x} -axis, we restrict attention to the upper half of the bow. The length coordinate s along the bow is measured from the midpoint, placed at O . For $0 \leq \bar{s} \leq \bar{L}_0$ we have half of the rigid part in the middle of the bow, called "grip". The mass of this grip is denoted by $2\bar{m}_g$. The flexible part $\bar{L}_0 \leq \bar{s} \leq \bar{L}_2$ or the "working part of the limb", is endowed with bending stiffness $\bar{W}(\bar{s})$ and mass per unit of length $\bar{V}(\bar{s})$. For $\bar{L}_2 \leq \bar{s} \leq \bar{L}$, where $2\bar{L}$ is the total length of the bow measured along it from tip to tip, there is a "rigid end piece" or "ear". Its mass and moment of inertia with respect to the centre of gravity $(\bar{x}_{cg}, \bar{y}_{cg})$ are denoted by \bar{m}_e and \bar{J}_e , respectively.

The time dependent variables in the unbraced situation (Figure 4.2.a) are provided with a subscript "0". The shape of the bow in this situation is given by the function $\theta_0(s)$, ($L_0 \leq s \leq L_2$), which is the angle between the \bar{y} -axis and the tangent to the bow, reckoned positive in clockwise direction.

In Figure 4.2.b the bow is braced with a string connected to the bow at the tip, where the loop fits in the nock, of which the place is denoted by (\bar{x}_t, \bar{y}_t) . We see that in this situation the string leaves the bow from the string-bridge with coordinates (\bar{x}_b, \bar{y}_b) . The length of the string without load is denoted by $2\bar{l}_0$. We assume that the material of the string obeys Hooke's law; the strain stiffness is denoted by \bar{U}_s . The string possesses in unstrung situation a mass per unit of length \bar{V}_s and its total mass is $2\bar{m}_s$. The distance $|\overline{OH}|$, see Figure 4.2.b, is as usual called the "brace height".

When the bow changes from the braced situation $\bar{b} = |\overline{OH}|$, where \bar{b} is the \bar{x} -coordinate of the middle of the string, to the fully drawn situation $\bar{b} = |\overline{OD}|$, see Figure 4.2.c, at a certain moment the string leaves the bridge. After this it has contact with the bow only at the tip. The distance $|\overline{OD}|$ is called the "draw" and the force $\bar{F}(|\overline{OD}|)$, exerted in the

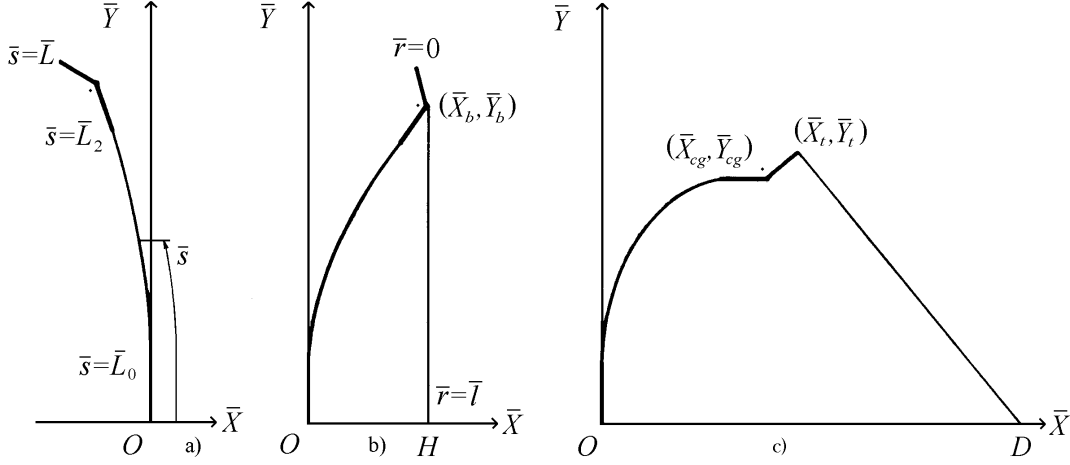


Figure 4.2: Three situations of the static-recurve bow: a) unbraced, b) braced, c) fully drawn.

middle of the string in the \bar{x} -direction, the "weight" of the bow. In the fully drawn position the time dependent variables are provided with a subscript "1".

By releasing the drawn string at time $\bar{t} = 0$ and holding the bow at its place with the bow hand, an arrow with mass $2\bar{m}_a$ is propelled. We assume that the limbs and string and arrow move in a flat plane, the (\bar{x}, \bar{y}) -plane.

The force acting upon the arrow, positive in negative \bar{x} -direction is referred to as \bar{E} . During the acceleration at some moment $\bar{t} = \bar{t}_b$, the string touches the string-bridge again. From that moment a part of the string, between the tip and the bridge, sticks to the bow. We assume that this part slips along the bow without friction.

If the acceleration of the arrow becomes negative, the arrow leaves the string. The moment is denoted by \bar{t}_l and the velocity of the arrow at that moment is called the muzzle velocity, denoted by \bar{c}_l .

If the bow is shot open-handed then it is impossible for an archer to exert a force on the bow directed to himself. This means that after the time $\bar{t} = \bar{t}_p$, the moment the force exerted on the bow hand, the recoil force \bar{P} reckoned positive in the positive \bar{x} -direction, becomes negative, the centre of the bow will move away from the archer. One of the physical constants which determine the motion of the bow for $\bar{t} > \bar{t}_p$ in this case is the mass of the grip $2\bar{m}_g$. Unless stated otherwise we assume that the bow is shot clamped; then the mass of the grip is unimportant.

As in [8] we introduce dimensionless quantities by using the draw $|\overline{OD}|$, the force $\bar{F}(|\overline{OD}|)$ and mass \bar{m}_b of one of the limbs, as units of length, force and mass, respectively. The mass \bar{m}_b is given by

$$\bar{m}_b = \int_{\bar{L}_0}^{\bar{L}_2} \bar{V}(\bar{s}) d\bar{s} + \bar{m}_e. \quad (4.1)$$

Dimensionless quantities are denoted without a bar " $\bar{}$ ", so we have, for instance, $\bar{t}_0 = t_0 |\overline{OD}|$, $\bar{E} = E \bar{F}(|\overline{OD}|)$, $\bar{m}_g = m_g \bar{m}_b$ and $\bar{t} = t |\overline{OD}| / \bar{F}(|\overline{OD}|)^{1/2}$. Quantities having

dimensions will be expressed, unless stated otherwise, in the following units: length in cm, force in kg force, mass in kg mass and time in .03193 sec

We introduce a short hand notation for a bow and arrow combination which resembles the one used in [8], however, because here the problem is more general, a larger number of parameters is needed. We define a bow B by

$$\begin{aligned} B(\bar{L}, \bar{L}_0, \bar{W}(\bar{s}), \bar{V}(\bar{s}), \theta_0(\bar{s}), \bar{m}_a, \bar{m}_t, \bar{J}_t, \bar{m}_e, \bar{J}_e, \bar{m}_g, \\ \bar{x}_{cg0}, \bar{y}_{cg0}, \bar{x}_{b0}, \bar{y}_{b0}, \bar{x}_{t0}, \bar{y}_{t0}, \bar{L}_2, \bar{U}_s, \bar{m}_s, |\overline{OH}| \text{ or } l; \\ |\overline{OD}|, \bar{F}(|\overline{OD}|), \bar{m}_b) \end{aligned} \quad (4.2)$$

For $\bar{m}_e = 0$, $\bar{J}_t = \bar{J}_e = 0$, $\bar{m}_g = 0$, $\bar{x}_{cg0} = \bar{x}_{b0} = \bar{x}_{t0} = \bar{x}_0(\bar{L})$, $\bar{y}_{cg0} = \bar{y}_{b0} = \bar{y}_{t0} = \bar{y}_0(\bar{L})$, $\bar{L}_2 = \bar{L}$, $\bar{U}_s = \infty$, $\bar{m}_s = 0$ we have a non-recurve bow dealt with in [8]. The parameters \bar{m}_t and \bar{J}_t are in the case of the static-recurve bow zero, however, in the case of the non-recurve bow they are the mass and moment of inertia respectively of rigid bodies fixed to the bow at both tips. We now turn to the equations of motion. The limb is considered as an inextensible elastic beam, by which we neglect damping, shear and rotary inertia. To avoid complications we use, as we mentioned already in the case of a static-recurve bow, a very simple mathematical model for the string. The elastic constant (tensile force divided by the relative elongation) is equal to the strain stiffness of the string \bar{U}_s . The mass of the string is accounted for by placing one third of the mass of the string $2\bar{m}_s$ at the end of the string where it fits in the nock of the limb and one sixth at the other end, where the arrow contacts the string. The equations which describe the motion of the flexible part of the limb are; $s \in [L_0, L_2]$, $t > 0$, $''' = \frac{\partial}{\partial t}''' = \frac{\partial}{\partial s}$

$$V\dot{u} = (Tx')' + (M'y')' , \quad (4.3)$$

$$V\dot{v} = (Ty')' - (M'x')' , \quad (4.4)$$

$$\dot{x} = u , \quad (4.5)$$

$$\dot{y} = v , \quad (4.6)$$

where $M(s, t)$ is the resultant bending moment and $T(s, t)$ the normal force reckoned positive when it causes tension in the limbs. Because we assume the limbs to be inextensible and the Euler-Bernoulli equation to be valid, we have

$$x_1'^2 + y_1'^2 = 1 , \quad (4.7)$$

$$M = W(x'y'' - y'x'' + \theta_0') . \quad (4.8)$$

The boundary conditions at $s = L_0$, for $0 < t \leq t_p$, read

$$\begin{aligned} x(L_0, t) = x_0(L_0) , \quad y(L_0, t) = y_0(L_0) , \quad y_0'(L_0) \\ x'(L_0, t) = x_0'(L_0)y_0'(L_0), \end{aligned} \quad (4.9)$$

In this time interval the bow is clamped and the recoil force P equals

$$P(t) = 2(M'(L_0, t)y_0'(L_0) + T(L_0, t)x_0'(L_0)) . \quad (4.10)$$

For $t > t_p$ the first equation of (4.9) has to be replaced, if the bow is shot open-handed, by the equation of motion for the grip in the x -direction

$$m_g \dot{u}(L_0, t) = M'(L_0, t) y'_0(L_0) + T(L_0, t) x'_0(L_0) . \quad (4.11)$$

The boundary conditions at $s = L$, are connected with the force K in the string by the three equations of motion for the ear. These equations read, for $0 < t \leq t_b$

$$m_e \dot{u}_{cg} = -T(L_2, t) x'(L_2, t) - M'(L_2, t) y'(L_2, t) + \frac{K(b - x_t)}{l} , \quad (4.12)$$

$$m_e \dot{v}_{cg} = T(L_2, t) y'(L_2, t) - M'(L_2, t) x'(L_2, t) + \frac{K y_t}{l} , \quad (4.13)$$

$$J_e(y'(L_2, t) \dot{u}'(L_2, t) - x'(L_2, t) \dot{v}'(L_2, t)) = \\ M(L_2, t) - T(L_2, t) h_T + M'(L_2, t) h_Q + K h_K , \quad (4.14)$$

where

$$u_{cg} = u(L_2, t) + (y_{cg0} - y_0(L_2)) u'(L_2, t) + (x_{cg0} - x_0(L_2)) v'(L_2, t) , \quad (4.15)$$

$$v_{cg} = v(L_2, t) + (y_{cg0} - y_0(L_2)) v'(L_2, t) + (x_{cg0} - x_0(L_2)) u'(L_2, t) , \quad (4.16)$$

and

$$h_T = (x_{cg0} - x_0(L_2)) y'_0(L_2) - (y_{cg0} - y_0(L_2)) x'_0(L_2) \quad (4.17)$$

$$h_Q = (x_{cg0} - x_0(L_2)) x'_0(L_2) - (y_{cg0} - y_0(L_2)) y'_0(L_2) \quad (4.18)$$

$$h_K = [(x'(L_2, t) y_t + y'(L_2, t)(b - x_t))((x_{t0} - x_{cg0}) x'_0(L_2) + (y_{t0} - y_{cg0}) y'_0(L_2)) \\ \{y'(L_2, t) y_t - x'(L_2, t)(b - x_t)\}((x_{t0} - x_{cg0}) y'_0(L_2) - (y_{t0} - y_{cg0}) x'_0(L_2))] / l(t) , \quad (4.19)$$

with

$$x_t = x(L_2, t) + (y_{t0} - y_0(L_2)) x'(L_2, t) + (x_{t0} - x_0(L_2)) y'(L_2, t) , \quad (4.20)$$

$$y_t = y(L_2, t) + (y_{t0} - y_0(L_2)) y'(L_2, t) + (x_{t0} - x_0(L_2)) x'(L_2, t) , \quad (4.21)$$

The x -coordinate of the middle of the string b is given by

$$b(t) = x_t + (l^2 - y_t^2)^{1/2} . \quad (4.22)$$

The time t_b , the moment the string touches the bridge again, is the time upon which the following equation is satisfied

$$(x'(L_2, t) y_b + y'(L_2, t)(b - x_b))((x_{t0} - x_{b0}) x'_0(L_2) + (y_{t0} - y_{b0}) y'_0(L_2)) + \\ (y'(L_2, t) y_b - x'(L_2, t)(b - x_b))((x_{t0} - x_{b0}) y'_0(L_2) - (y_{t0} - y_{b0}) x'_0(L_2)) = 0 , \quad (4.23)$$

where

$$x_b = x(L_2, t) + (y_{b0} - y_0(L_2)) x'(L_2, t) + (x_{b0} - x_0(L_2)) y'(L_2, t) , \quad (4.24)$$

$$y_b = y(L_2, t) + (y_{b0} - y_0(L_2)) y'(L_2, t) + (x_{b0} - x_0(L_2)) x'(L_2, t) . \quad (4.25)$$

For $t > t_b$ the following changes in the formulas have to be made. In (4.12) the term $K(b-x_t)/l$ has to be replaced by $K(b-x_b)/(l-h_b)$, in (4.13) the term Ky_t/l by $Ky_b/(l-h_b)$ and in (4.14) h_K is given by

$$h_K = \frac{[(x'(L_2, t)y_b + y'(L_2, t)(b - x_b))((x_{b_0} - x_{cg_0})x'_0(L_2) + (y_{b_0} - y_{cg_0})y'_0(L_2)) \\ (y'(L_2, t)y_b - x'(L_2, t)(b - x_b))((x_{b_0} - x_{cg_0})y'_0(L_2) - (y_{b_0} - y_{cg_0})x'_0(L_2))]}{(l(t) - h_b)}, \quad (4.26)$$

with

$$h_b^2 = (x_{t_0} - x_{b_0})^2 + (y_{t_0} - y_{b_0})^2. \quad (4.27)$$

Equation (4.22) has to be replaced by

$$b(t) = x_b + ((l - h_b)^2 - y_b^2)^{1/2}. \quad (4.28)$$

The relation between the force in the string and its length is

$$K = U_s(l - l_0)/l_0, \quad t \geq 0. \quad (4.29)$$

This equation is also valid for $t > t_b$ because of our assumption that the string experiences no friction force from the bridge. The mass at the end of the string which has contact with the bow is taken part of the ear. So, the mass m_e in (4.12) and (4.13) is actually the mass of the ear plus one third of the mass of the string $2m_s$. In the same way the moment of inertia of the ear J_e is adapted.

We denote the velocity of the arrow by

$$c = \dot{b}. \quad (4.30)$$

Then the equation of motion for the arrow becomes

$$-1/2 E(t) + 1/3 m_s \dot{c} = (m_a + 1/3 m_s) \dot{c} = -K(b - x_t)/l, \quad 0 < t \leq t_b, \quad (4.31)$$

and

$$-1/2 E(t) + 1/3 m_s \dot{c} = (m_a + 1/3 m_s) \dot{c} = -K(b - x_b)/(l - h_b), \quad t_b < t. \quad (4.32)$$

The arrow leaves the string when the force E becomes negative. We denoted this moment by t_l . For $t > t_l$, in the boundary conditions (4.31) or (4.32) we have to put m_a equal to one sixth of the mass $2m_s$ of the string. In addition to the equations of motion and the boundary conditions we have to give the initial values of the dependent variables. The initial values of the unknown functions x, y, M, T, b, K are the values of these functions occurring in the fully drawn position and the velocities u, v and c are zero for $t = 0$. The bow in fully drawn position is described by a boundary value problem for a system of ordinary differential equations. These equations are obtained by putting the left-hand sides of

(4.3)···(4.6), (4.12)···(4.14). equal to zero. Further the bow is clamped, b equals 1 and the left-hand side of (4.31) equals $-1/2$, while $\overline{F}(|\overline{OD}|)$ occurring in $M = \overline{M}/(|\overline{OD}|\overline{F}(|\overline{OD}|))$, $W = \overline{W}/(|\overline{OD}|^2\overline{F}(|\overline{OD}|))$, $U = \overline{U}/\overline{F}(|\overline{OD}|)$ and $K = \overline{K}/\overline{F}(|\overline{OD}|)$ is unknown.

We now derive the equations of motion for a string treated as a continuum, only able to withstand tensile forces. Longitudinal and transverse vibrations of the string are possible. We use this model in the case of non-recurve bows, then the string has contact with the bow only at the tip. We recall that the string possesses in the unstrung situation a mass per unit of length V_s , that the material of the string obeys Hooke's law, with strain stiffness U_s . Furthermore we assume that V_s and U_s are uniform distributed along the unloaded string.

We introduce a length coordinate \bar{r} along the string, measured from the point of attachment of the string to the bow, thus $0 \leq \bar{r} \leq \bar{l}(\bar{t})$, where $\bar{l}(\bar{t})$ is still an unknown function of time. Using dimensionless quantities in the way mentioned before, the equations of motion for the string become, for $0 \leq r \leq l(t)$, $t > 0$,

$$V_s \dot{u}_s = (Kx'_s)' , \quad (4.33)$$

$$V_s \dot{v}_s = (Ky'_s)' , \quad (4.34)$$

$$\dot{x}_s = u_s , \quad (4.35)$$

$$\dot{y}_s = v_s , \quad (4.36)$$

where "·" indicates the material derivative and "' = $\frac{\partial}{\partial r}$. The functions $x_s(r, t)$ and $y_s(r, t)$ are the x - and y -coordinates of the string, respectively. The velocities in x - and y -direction are denoted by $u_s(r, t)$ and $v_s(r, t)$, respectively. The tensile force $K(r, t)$ in the string is in this model a function of r as well as t . Hooke's law reads

$$K(r_0, t) = U_s \frac{\partial r(r_0, t)}{\partial r_0} , \quad 0 \leq r_0 \leq l_0 , \quad t \geq 0 , \quad (4.37)$$

and the equation which expresses that r is the length coordinate

$$(x'_s)^2 + (y'_s)^2 = 1 , \quad 0 \leq R_0 \leq l_0 , \quad t \geq 0 , \quad (4.38)$$

We note that when the string is taken to be inextensible the obtained equations agree with equations (4.3)···(4.8) for the bow with $W(s) = 0$.

The boundary conditions at $r = 0$ are linked to the boundary conditions of the bow at $s = L$, where the string contacts the limb. Although we consider for this model only non-recurve bows, it is possible that at the tip of the elastic limb we have a rigid body possessing mass m_t and moment of inertia J_t with respect to the tip. The boundary conditions, which form the equations of motion for the rigid body become, for $t > 0$

$$m_t \dot{u}(L, t) = -T(L, t)x'(L, t) - M'(L, t)y'(L, t) + K(0, t)x'_s(0, t) , \quad (4.39)$$

$$-m_t \dot{v}(L, t) = (T(L, t)y'(L, t) - M'(L, t)x'(L, t))(b(t) - x(L, t)) + K(0, t)y'_s(0, t) , \quad (4.40)$$

$$J_t(y'(L, t)\dot{u}'(L, t) - x'(L, t)\dot{v}'(L, t)) = M(L, t) . \quad (4.41)$$

The boundary conditions at $r = l$ become in this case

$$-1/2 E(t) = m_a \dot{u}(l, t) = -K(l, t) x'_s(l, t) , \quad (4.42)$$

and

$$y_s(l, t) = 0 , \quad (4.43)$$

where $l = l(t)$ and (4.43) takes into account the assumed symmetry with respect to the line of aim, the x -axis. The time the arrow leaves the string is determined by the condition $E(t) = 0$. For $t > t_l$, m_a is zero in (4.42). The x -coordinate of the middle of the string $x_s(l, t)$ is as in the case of the static-recurve bow denoted by $b(t)$ and the velocity $u_s(l, t)$ again by $c(t)$.

The equations of motion of the limb and the boundary conditions at $s = L_0$ are the same as those for the static-recurve bow. The initial conditions are obtained from the equations of motion in the same way as we did for the static-recurve bow.

In order to get numerical approximations for the solution of the problem discussed in this section, we develop in the next section a finite-difference procedure.

4.4 Finite-difference equations

In this section we give the finite-difference scheme used to get numerical approximations for the solution of the equations of motion given in the previous section. We deal first with the static-recurve bow and after that with the non-recurve bow in which case we use the continuum model for the string.

We consider a grid, with respect to the elastic part of the limb in the s, t -plane; $L_0 \leq L_2$, $t \geq 0$. The gridpoints are denoted by $(j\Delta s, k\Delta t)$, where $j = -1(1)n_s + 1$, $n_s\Delta s = L_2 - L_0$ and $k = 0(1)n_t$, n_t an integer large enough to cover the time interval of interest. In order to get a concise notation we introduce the following difference operators

$$\delta f_{j,k} = \frac{f_{j+1/2,k} - f_{j-1/2,k}}{\Delta s} , \quad \Delta f_{j,k} = 0.5 (\delta f_{j+1/2,k} - \delta f_{j-1/2,k}) . \quad (4.44)$$

If we use a weighted average of forward and backward approximation, equations (4.3) ... (4.8) become

$$V_j(u_{j,k+1} - u_{j,k})/\Delta t = \mu(\delta(T\delta x)_{j,k+1} + \delta(\delta M\delta y)_{j,k+1}) + (1 - \mu)(\delta(T\delta x)_{j,k} + \delta(\delta M\delta y)_{j,k}) , \quad j = 0(1)n_s , \quad (4.45)$$

$$V_j(v_{j,k+1} - v_{j,k})/\Delta t = \mu(\delta(T\delta y)_{j,k+1} + \delta(\delta M\delta x)_{j,k+1}) + (1 - \mu)(\delta(T\delta y)_{j,k} + \delta(\delta M\delta x)_{j,k}) , \quad j = 0(1)n_s , \quad (4.46)$$

$$(x_{j,k+1} - x_{j,k})/\Delta t = \mu u_{j,k+1} + (1 - \mu)u_{j,k} , \quad j = 0(1)n_s , \quad (4.47)$$

$$(y_{j,k+1} - y_{j,k})/\Delta t = \mu v_{j,k+1} + (1 - \mu)v_{j,k} , \quad j = 0(1)n_s , \quad (4.48)$$

$$1 = (\delta x_{j-1/2,k+1})^2 + (\delta y_{j-1/2,k+1})^2 , \quad j = 0(1)n_s + 1 , \quad (4.49)$$

$$M_{j,k+1} = W_j(\Delta x_{j,k+1}\delta^2 y_{j,k+1} - \Delta y_{j,k+1}\delta^2 x_{j,k+1} + \theta'_0(j\Delta s)) , \quad j = 0(1)n_s , \quad (4.50)$$

respectively. The boundary condition (4.9) at $s = L_0$ becomes for $0 < (k+1)\Delta t < t_p$

$$x_{0,k+1} = x_0(L_0), \quad y_{0,k+1} = y_0(L_0), \quad y'_0(L_0)\Delta x_{0,k+1} = x'_0(L_0)\Delta y_{0,k+1}. \quad (4.51)$$

For $t_p < (k+1)\Delta t$ and when the bow is shot open-handed, the first equation has to be replaced by the approximation of (4.11)

$$m_g(u_{0,k+1} - u_{0,k})/\Delta t = \mu(\Delta M_{0,k+1}y'_0(L_0) + 1/2(T_{1/2,k+1} + T_{-1/2,k+1})x'_0(L_0)) \\ (1 - \mu)(\Delta M_{0,k}y'_0(L_0) + 1/2(T_{1/2,k} + T_{-1/2,k})x'_0(L_0)). \quad (4.52)$$

To compute the recoil force $P(t)$ (4.10) we use the formula

$$P_{k+1} = 2(\Delta M_{0,k+1}y'_0(L_0) + 1/2(T_{1/2,k+1} + T_{-1/2,k+1})x'_0(L_0)). \quad (4.53)$$

When this force becomes zero we have $t = t_p$.

For $0 \leq (k+1)\Delta t \leq t_b$ the boundary conditions at $s = L_2$ (4.12) \cdots (4.14) are approximated by

$$m_e(u_{cg_{k+1}} - u_{cg_k})/\Delta t = \\ \mu(-1/2, (T_{n_s+1/2,k+1} + T_{n_s-1/2,k+1})\Delta x_{n_s,k+1} - \Delta M_{n_s,k+1}\Delta y_{n_s,k+1} + K_{\cdot,k+1}(b_{k+1} - x_{t_{k+1}})/l_{\cdot,k+1}) \\ (1 - \mu)[-1/2(T_{n_s+1/2,k} + T_{n_s-1/2,k})\Delta x_{n_s,k} - \Delta M_{n_s,k}\Delta y_{n_s,k} + K_{\cdot,k}(b_k - x_{t_k})/l_{\cdot,k}], \quad (4.54)$$

$$m_e(v_{cg_{k+1}} - v_{cg_k})/\Delta t = \\ \mu(-1/2(T_{n_s+1/2,k+1} + T_{n_s-1/2,k+1})\Delta y_{n_s,k+1} - \Delta M_{n_s,k+1}\Delta x_{n_s,k+1} + K_{\cdot,k+1}y_{t_{k+1}}/l_{\cdot,k+1}) \\ (1 - \mu)(-1/2(T_{n_s+1/2,k} + T_{n_s-1/2,k})\Delta y_{n_s,k} - \Delta M_{n_s,k}\Delta x_{n_s,k} + K_{\cdot,k}y_{t_k}/l_{\cdot,k}), \quad (4.55)$$

and

$$J_e((\mu\Delta y_{n_s,k+1} + (1 - \mu)\Delta y_{n_s,k})(\Delta u_{n_s,k+1} - \Delta u_{n_s,k})/\Delta t - \\ (\mu\Delta x_{n_s,k+1} + (1 - \mu)\Delta x_{n_s,k})(\Delta v_{n_s,k+1} - \Delta v_{n_s,k})/\Delta t) = \\ \mu(M_{n_s,k+1} - 1/2(T_{n_s+1/2,k+1} + T_{n_s-1/2,k+1})h_T + \Delta M_{n_s,k+1}h_Q + K_{\cdot,k+1}h_{K_{k+1}}) + \\ (1 - \mu)(M_{n_s,k} - 1/2(T_{n_s+1/2,k} + T_{n_s-1/2,k})h_T + \Delta M_{n_s,k}h_Q + K_{\cdot,k}h_{K_k}), \quad (4.56)$$

where h_T and h_Q are given by (4.17) and (4.18), respectively. The velocities of the centre of gravity of the ear in the x - and y -direction are approximated by

$$u_{cg_{k+1}} = u_{n_s,k+1} + (y_{cg_0} - y_0(L_2))\Delta u_{n_s,k+1} + (x_{cg_0} - x_0(L_2))\Delta v_{n_s,k+1}, \quad k = 0(1)n_t, \quad (4.57)$$

and

$$v_{cg_{k+1}} = v_{n_s,k+1} + (y_{cg_0} - y_0(L_2))\Delta v_{n_s,k+1} - (x_{cg_0} - x_0(L_2))\Delta u_{n_s,k+1}, \quad k = 0(1)n_t, \quad (4.58)$$

The distance h_K between the centre of gravity of the ear (x_{cg}, y_{cg}) and the string, equation (4.19) becomes, for $0 \leq (k+1)\Delta t \leq t_b$

$$h_{K_{k+1}} = \\ [(\Delta x_{n_s,k+1}y_{t_{k+1}} + \Delta y_{n_s,k+1}(b_{k+1} - x_{t_{k+1}}))((x_{t_0} - x_{cg_0})x'_0(L_2) + (y_{t_0} - y_{cg_0})y'_0(L_2)) + \\ (\Delta y_{n_s,k+1}y_{t_{k+1}} - \Delta x_{n_s,k+1}(b_{k+1} - x_{t_{k+1}}))((x_{t_0} - x_{cg_0})y'_0(L_2) + (y_{t_0} - y_{cg_0})x'_0(L_2))] / l_{\cdot,k+1}. \quad (4.59)$$

The x - and y -coordinates of the tip (4.20) and (4.21) become, for $k = -1(1)n_t$ and

$$x_{t_{k+1}} = x_{n_s, k+1} + (y_{t_0} - y_0(L_2))\Delta x_{n_s, k+1} + (x_{t_0} - x_0(L_2))\Delta y_{n_s, k+1}, \quad k = 0(1)n_t, \quad (4.60)$$

and

$$y_{t_{k+1}} = y_{n_s, k+1} + (y_{t_0} - y_0(L_2))\Delta y_{n_s, k+1} + (x_{t_0} - x_0(L_2))\Delta x_{n_s, k+1}, \quad k = 0(1)n_t, \quad (4.61)$$

while the x coordinate of the middle of the string is approximated

$$b_{k+1} = x_{t_{k+1}} + (l_{\cdot, k+1}^2 - y_{t_{k+1}}^2)^{1/2}, \quad (4.62)$$

for $0 \leq (k+1)\Delta t \leq t_b$. The time t_b is fixed by the moment that the approximation of the left-hand side of equation (4.23) becomes zero, or if

$$\begin{aligned} & (\Delta x_{n_s, k+1} y_{b_{k+1}} + \Delta y_{n_s, k+1} (b_{k+1} - x_{b_{k+1}})) ((x_{t_0} - x_0(L_2))x'_0(L_2) + (y_{t_0} - y_0(L_2))y'_0(L_2)) + \\ & (\Delta y_{n_s, k+1} - \Delta x_{n_s, k+1} (b_{k+1} - x_{b_{k+1}})) ((x_{t_0} - x_0(L_2))y'_0(L_2) - (y_{t_0} - y_0(L_2))x'_0(L_2)) = 0. \end{aligned} \quad (4.63)$$

For $t_b < (k+1)\Delta t$ the approximations of the boundary conditions are obtained in the same manner. Equation (4.29), which connects the force in the string to its elongation, is approximated by

$$K_{\cdot, k+1} = U_s \frac{l_{\cdot, k+1} - l_0}{l_0}, \quad k = -1(1)n_t. \quad (4.64)$$

The equations which apply to the motion of the arrow (4.30) \cdots (4.32) become

$$(b_{k+1} - b_k)/\Delta t = \mu c_{k+1} + (1 - \mu)c_k, \quad k = -1(1)n_t, \quad (4.65)$$

and for $0 \leq (k+1)\Delta t \leq t_b$, with $m_a(c_{k+1} - c_k)/\Delta t = E_{k+\mu}$

$$\begin{aligned} (m_a + 1/3 m_s)(c_{k+1} - c_k)/\Delta t = & \mu(-K_{\cdot, k+1}(b_{k+1} - x_{t_{k+1}})/l_{\cdot, k+1}) + \\ & (1 - \mu)(-K_{\cdot, k}(b_k - x_{t_k})/l_{\cdot, k}), \end{aligned} \quad (4.66)$$

while for $t_b < (k+1)\Delta t$,

$$\begin{aligned} (m_a + 1/3 m_s)(c_{k+1} - c_k)/\Delta t = & \mu(-K_{\cdot, k+1}(b_{k+1} - x_{b_{k+1}})/(l_{\cdot, k+1} - h_b)) + \\ & (1 - \mu)(-K_{\cdot, k}(b_k - x_{t_k})/(l_{\cdot, k} - h_b)), \end{aligned} \quad (4.67)$$

The time t_l is fixed by $E_{k+1} = 0$. For $(k+1)\Delta t > t_l$, hence when the arrow has left the string, the mass m_a has to be replaced by one sixth of the mass of the string $2m_s$, as we discussed.

We now turn to the finite-difference approximations for the equations (4.33) \cdots (4.43), the equations of motion and boundary conditions for the string. To that end we consider a grid in the r_0, t -plane; $0 \leq r_0 \leq l_0$, $t \geq 0$. The grid points are denoted by $(h\Delta r_0, k\Delta t)$,

where $h = -1(1)n_r + 1$, $n_r \Delta r_0 = l_0$. We attach for this grid to the difference operators δ and Δ the following meaning

$$\delta f_{h,k} = \frac{f_{h+1/2,k} - f_{h-1/2,k}}{\delta r_{h,k}}, \quad \Delta f_{h,k} = 0.5 (\delta f_{h+1/2,k} - \delta f_{h-1/2,k}). \quad (4.68)$$

Then (4.32) \cdots (4.36) can be approximated by

$$\Delta r_0 V_{s_0}(u_{s_{h,k+1}} - u_{s_{h,k}})/\Delta t = \mu \delta(K \delta x_s)_{h,k+1} + (1 - \mu) \delta(K \delta x_s)_{h,k}, \quad h = 0(1)n_r, \quad (4.69)$$

$$\Delta r_0 V_{s_0}(v_{s_{h,k+1}} - v_{s_{h,k}})/\Delta t = \mu \delta(K \delta y_s)_{h,k+1} + (1 - \mu) \delta(K \delta y_s)_{h,k}, \quad h = 0(1)n_r \quad (4.70)$$

$$(x_{s_{h,k+1}} - x_{s_{h,k}})/\Delta t = \mu u_{s_{h,k+1}} + (1 - \mu) u_{s_{h,k}}, \quad h = 0(1)n_r, \quad (4.71)$$

$$(y_{s_{h,k+1}} - y_{s_{h,k}})/\Delta t = \mu v_{s_{h,k+1}} + (1 - \mu) v_{s_{h,k}}, \quad h = 0(1)n_r, \quad (4.72)$$

Equations (4.37) and (4.38) give

$$K_{h-1/2,k+1} = U_s \left(\frac{\delta r_{h-1/2,k+1}}{\Delta r_0} - 1 \right), \quad h = 0(1)n_r + 1, \quad (4.73)$$

and

$$(\delta x_{s_{h-1/2,k+1}})^2 + (\delta y_{s_{h-1/2,k+1}})^2 = 1, \quad h = 0(1)n_r + 1, \quad (4.74)$$

respectively.

The approximations for the boundary conditions at $r_0 = 0$, equations (4.39) \cdots (4.41), resemble those given in (4.54) \cdots (4.56). They are approximated by

$$\begin{aligned} m_t(u_{n_s,k+1} - u_{n_s,k})/\Delta t = & \mu \left(-1/2 (T_{n_s+1/2,k+1} + T_{n_s-1/2,k+1}) \Delta x_{n_s,k+1} - \Delta M_{n_s,k+1} \Delta y_{n_s,k+1} + \right. \\ & \left. 1/2 (K_{1/2,k+1} \delta x_{s_{1/2,k+1}} + K_{-1/2,k+1} \delta x_{s_{-1/2,k+1}}) \right) + \\ & (1 - \mu) \left(-1/2 (T_{n_s+1/2,k} + T_{n_s-1/2,k}) \Delta x_{n_s,k} - \Delta M_{n_s,k} \Delta y_{n_s,k} + \right. \\ & \left. 1/2 (K_{1/2,k+1} \delta x_{s_{1/2,k+1}} + K_{-1/2,k} \delta x_{s_{-1/2,k}}) \right), \end{aligned} \quad (4.75)$$

$$\begin{aligned} m_t(v_{cg_{k+1}} - v_{cg_k})/\Delta t = & \mu \left(-1/2 (T_{n_s+1/2,k+1} + T_{n_s-1/2,k+1}) \Delta y_{n_s,k+1} - \Delta M_{n_s,k+1} \Delta x_{n_s,k+1} + \right. \\ & \left. 1/2 (K_{1/2,k+1} \delta y_{s_{1/2,k+1}} + K_{-1/2,k+1} \delta y_{s_{-1/2,k+1}}) \right) + \\ & (1 - \mu) \left(-1/2 (T_{n_s+1/2,k} + T_{n_s-1/2,k}) \Delta y_{n_s,k} - \Delta M_{n_s,k} \Delta x_{n_s,k} + \right. \\ & \left. 1/2 (K_{1/2,k+1} \delta y_{s_{1/2,k+1}} + K_{-1/2,k} \delta y_{s_{-1/2,k}}) \right), \end{aligned} \quad (4.76)$$

and

$$\begin{aligned} J_t \left((\mu \Delta y_{n_s,k+1} + (1 - \mu) \Delta y_{n_s,k}) (\Delta u_{n_s,k+1} - \Delta u_{n_s,k}) / \Delta t - \right. \\ \left. (\mu \Delta x_{n_s,k+1} + (1 - \mu) \Delta x_{n_s,k}) (\Delta v_{n_s,k+1} - \Delta v_{n_s,k}) / \Delta t \right) = \\ \mu M_{n_s,k+1} + (1 - \mu) M_{n_s,k}, \quad k = -1(1)n_t, \end{aligned} \quad (4.77)$$

In a similar way we get for equation (4.41)

$$\begin{aligned} E_{k+\mu} = & m_a(u_{s_{n_r,k+1}} - u_{s_{n_r,k}})/\Delta t = \\ & - \mu(1/2(K_{n_r+1/2,k+1}\delta x_{s_{n_r+1/2,k+1}} + K_{n_r-1/2,k+1}\delta x_{s_{n_r-1/2,k+1}})) \\ & - (1-\mu)(1/2(K_{n_r+1/2,k}\delta x_{s_{n_r+1/2,k}} + K_{n_r-1/2,k}\delta x_{s_{n_r-1/2,k}})) \end{aligned} \quad (4.78)$$

When $E_{k+1} = 0$, we have $t = t_l$. For $t_l < (k+1)\Delta t$, m_a in (4.78) equals 0.

We note that there are some differences between the finite-difference scheme given in this section and the scheme given in [8], even in those cases in which they could have been chosen the same. First, the last equation of (4.51) is the difference approximation of the last equation of (4.9) instead of the approximation of $y'(L_0, t) = y'_0(L_0)$, $t > 0$, as is done in [8]. Actually if $y'_0(L_0) = 1$, the method described in [8] is unsuited to the computations carried out there and in this paper. In all the computations of which the results were given in [8], we used already equation (4.51). Second, in (4.66), (4.67) and (4.78) the index of E is $k + \mu$ instead of $k + 1$. In this way we get a better convergence of the force E acting upon the arrow, with respect to Δt . Third, in the boundary conditions at $s = L_2$ (4.54) \cdots (4.56) and (4.75) \cdots (4.77) only central difference approximations with respect to s are used, so in (4.45) and (4.46) j has to range unto n_s . In [8] we used non-central difference approximations, but mainly because of (4.56) and (4.77) they are replaced here by central difference approximations.

We pay now some attention to (4.69) and (4.70), which are the approximations of (4.33) and (4.34), respectively. Like the length of the string, the mass per unit of length V_s occurring in (4.33) and (4.34) is a function of time. However, conservation of mass for the part of the string between $r_0 = (h - 1/2)\Delta r_0$ and $r_0 = (h + 1/2)\Delta r_0$, $h = 1(1)n_r - 1$ gives

$$\delta r_{h,k} V_{s_k} = \Delta r_0 V_{s_0}, \quad k \geq 0. \quad (4.79)$$

$$(V_s \dot{u}_s)_{h,k+1/2} = \delta(Kx')_{h,k+1/2}, \quad (4.80)$$

and multiply both terms by $\delta r_{h,k+1/2}$, we get using (4.79)

$$\Delta r_0 V_{s_0} \dot{u}_{s_{h,k+1/2}} = \delta r_{h,k+1/2} \delta(Kx')_{h,k+1/2}, \quad h = 1(1)n_r - 1. \quad (4.81)$$

The finite-difference approximation (4.69) is obtained from this equation in a straightforward manner. The same holds for equation (4.70). It is easy to show that (4.69) \cdots (4.74) are also the equations of motion for a lumped parameter model for the string. In that model we have mass points $\Delta r_0 V_{s_0}$ (thus $2m_s/n_r$), at equal distances Δr_0 , attached to each other by springs, with strain stiffness U_s and without mass. The finite-difference schemes given in this section form a set of non-linear equations for each time step. As in [8] we solve these equations with a Newtonian method, in the course of which we solve the occurring system of linear equations by means of a Gaussian elimination method with partial pivoting. The matrix is adopted only in the first iteration of each time step. As

starting values for the Newtonian method for the static calculations we use the results of a shooting method, developed in [9]. Because the string was assumed to be inextensible and the ear was reckoned with by putting the bending stiffness $W(s)$ for $L_2 \leq s \leq L$ very large with respect to the mean bending stiffness of the flexible part of the limb, we had to make some alterations in the procedure described in [9]. In order to get starting values for the next time steps we extrapolate the results of the preceding calculations. For reasons given in the Section 4.13 we use $\mu = 1$ for the first time step, from $t = 0$ to $t = \Delta t$, or for $k = 0$. The Δt used for this first step is taken small with respect to its magnitude used in the following steps. For the succeeding steps, $k > 0$, we use $\mu = 1/2$, thus a Crank-Nicolson scheme.

We adhere to that scheme until $t_{k+1} \geq t_b$ (string touches bridge again in the case of static-recurve bows) or $t_{k+1} \geq t_p$ (bow leaves bow hand) or $t_{k+1} \geq t_l$ (arrow leaves string). In these cases we iterate with respect to Δt until we find accurate approximations for t_b , t_p and t_l . During this iteration we have to avoid that Δt becomes too small, in order to ensure the convergence of the Newtonian method. After such an iteration the mesh-width in the time direction Δt is restored, except for the iteration for t_l . In that case we use $\mu = 1$ for $t > t_l$, thus a fully implicit backward time difference scheme. This is done to avoid instabilities in the numerical process. To obtain a sufficient accurate approximation we continue the process for $t > t_l$ with a Δt to a certain extend smaller than the one used for $t \leq t_l$.

During the computations of some bows it appears that the tensile force in the string becomes negative. In that situation the Newtonian method fails to converge and we are forced to stop the computations. Note that a string can only withstand tensile forces and for negative K equation (4.73), Hooke's law, is no longer valid.

In Section 4.13 we carry out a check on the numerical method described in this section. We compare the results obtained by means of the finite-difference method with the analytic solution in the case of a vibrating beam with small deflections.

The numerical results mentioned in Section 4.6...4.12 are obtained by using the numerical method given in this section.

4.5 The quality coefficients

In this section we discuss three coefficients, one static quality coefficient and two dynamic quality coefficients. These coefficients have been introduced in our previous papers [9] and [8], pertaining to an inextensible string. The static quality coefficient q is given by

$$q = \frac{\bar{A}}{|\overline{OD}| \overline{F(|\overline{OD}|)}}, \quad (4.82)$$

where \bar{A} is the energy stored in the bow by deforming it from the braced position into the fully drawn position. We can compute this amount of energy in two ways. First, if $\overline{F}(\bar{b})$ is

the static force-draw curve (SFD curve),

$$\bar{A} = \int_{\bar{b}=|\overline{OH}|}^{\bar{b}=|\overline{OD}|} \bar{F}(\bar{b}) d\bar{b} . \quad (4.83)$$

Second, it is the potential energy stored in the fully drawn bow, denoted by \bar{A}_D minus the potential energy stored in the bow in the braced situation, denoted by \bar{A}_H . In both cases the potential energy is the bending energy in the limbs plus the strain energy in the string. Thus

$$\bar{A} = \bar{A}_D - \bar{A}_H = \int_{\bar{L}_0}^{\bar{L}_2} \bar{W}(\bar{s}) (\theta'(\bar{s}) - \theta'_0(\bar{s}))^2 d\bar{s} + \bar{U}_s (\bar{l} - \bar{l}_0)^2 / \bar{l}_0 \Big|_{\bar{b}=|\overline{OH}|}^{\bar{b}=|\overline{OD}|} \quad (4.84)$$

Note that q is the dimensionless amount of energy put into the bow by drawing it from the braced situation into full draw.

One of the dynamic quality coefficients is the efficiency η defined by

$$\eta = \frac{\bar{m}_a \bar{c}_l^2}{\bar{A}} \quad (4.85)$$

where c_l is the muzzle velocity, the velocity of the arrow at the moment it leaves the string. Hence $\eta \bar{A}$ is the amount of energy imparted to the arrow. If $\bar{E}(\bar{b})$ is the dynamic-force-draw curve (DFD curve), then we have

$$\eta \bar{A} = \int_{\bar{b}=\bar{b}_l}^{\bar{b}=|\overline{OD}|} \bar{E}(\bar{b}) d\bar{b} . \quad (4.86)$$

where b_l is the x -coordinate of the middle of the string at $t = t_l$ the moment the arrow leaves the string.

The second dynamic quality coefficient is the dimensionless muzzle velocity ν ,

$$\nu = \left(\frac{q\eta}{m_a} \right)^{1/2} = c_l , \quad (4.87)$$

In the second part of this section we show that for common bows the maximum value of η is 1 or stated otherwise the maximum amount of energy that can be transferred to the arrow equals \bar{A} .

At arrow exit, the part of \bar{A}_D that is not transferred to the arrow is kinetic energy in limbs and string, denoted by \bar{A}_K , plus potential energy in limbs and string, denoted by \bar{A}_P . Conservation of energy implies that

$$\bar{A}_D = \eta \bar{A} + \bar{A}_K + \bar{A}_P . \quad (4.88)$$

Suppose now

$$\bar{A}_P \geq \bar{A}_H , \quad (4.89)$$

then, using (4.84), (4.88) this assumption yields

$$\eta \bar{A} + \bar{A}_K \leq \bar{A}, \quad (4.90)$$

and because $\bar{A}_K \geq 0$,

$$\eta \bar{A} \leq \bar{A} \text{ or } \eta \leq 1. \quad (4.91)$$

Hence it remains to show that under general conditions assumption (4.89) is valid. To that end we use the principle of stationary potential energy. It states: “Among the set of all admissible configurations the state of equilibriums characterized by the stationary property of the potential energy”. In our case the continuum we consider is the two limbs and the string together. The admissible configurations for symmetric bows are those by which the middle of the grip and the middle of the string are on the line of aim. There are no external forces in the braced situation, so the mentioned potential energy is the potential energy in the limbs and the string.

If we assume that the equilibrium in the braced situation is stable, then the principle yields that for all admissible configurations in the neighbourhood, of the braced situation, \bar{A}_H is a local minimum of the potential energy. If we assume further that there is only one state of equilibrium for the braced situation (and this is true for common bows), then \bar{A}_H is the global minimum of the potential energy. Because the configuration of the limbs and string at $\bar{t} = \bar{t}_l$ is an admissible configuration, we have (4.89) $\bar{A}_P \geq \bar{A}_H$.

In [9] we gave an example of the possibility of more than one braced situations of a not too realistic bow. In that case we had one unstable and two stable configurations. Then it is possible to start from one stable braced situation which does not possess the global minimum potential energy. If the bow terminates its motion after release of the arrow in the second stable braced situation with the global minimum of the potential energy, then (4.89) may be violated. Then it is possible that $\eta > 1$. For such a bow the archer has to bring the limbs from the second braced situation into the first one after each shot, by which he stores already some energy in the limbs and string, but this amount of energy stays out of sight in the definition of the efficiency given by (4.85).

In the case of the static-recurve bow (or working-recurve bow) the afore mentioned conclusions hold when the string can not slip past the limbs. When this happens, the bow does not return to its braced Situation, but it turns itself inside out and the results of this accident can be unpleasant both for bow and archer (see [page xxix][10]). We have in this case actually the same situation as we described just above. Note that (4.91) also holds when a string breaks.

In the following sections we use the quality coefficients when we compare the performance of different bow and arrow combinations.

4.6 Comparison of three mathematical models

In this section we compare a number of calculated results obtained by three different mathematical models of bows. One model was developed by Hickman in [6] (H model),

another in [12] by Marlow (M model). The third model is the one described in this paper (C model).

To that end we compare the results with respect to one realistic bow, the H bow. This H bow resembles a bow described by Hickman and has not to be confused with the H model of some bow. Using the notation of (4.2) the H bow is given by

$$\begin{aligned} &H(91.44, 10.16, \overline{W}, \overline{V}, \theta_0 \equiv 0, 0.0125, 0, 0, 0, 0, 0, \\ &91.44, 0, 91.44, 0, 91.44, \infty, 0, |\overline{OH}| = 15.24; 71.12, 15.53, 0.1625) . \end{aligned} \quad (4.92)$$

The bending stiffness $\overline{W}(\overline{s})$ and mass distribution $\overline{V}(\overline{s})$ along the limb are given by

$$\overline{W}(\overline{s}) = 1.30 \cdot 10^5 \left(\frac{\overline{L} - \overline{s}}{\overline{L}} \right) , \quad (4.93)$$

and

$$\overline{V}(\overline{s}) = 4.52 \cdot 10^{-3} \left(\frac{\overline{L} - \overline{s}}{\overline{L}} \right) . \quad (4.94)$$

In [8] we dealt already with this H bow, which possesses an inextensible string without mass. Because we drop in this paper the assumption the string to be without mass and inextensible, we have to specify these quantities. For the mass of the string we take the mass Hickman mentioned in [6], being 0.0068 kg. In [6], page 251, Taylor discusses the bow string. He measured the strain stiffness of a string made of one strand of linen. If we take a string with 12 strands, we get a strain stiffness (4.29) or (4.37)

$$\overline{U}_s = 2040 \text{ kgf} . \quad (4.95)$$

We call the H bow with an elastic string, $\overline{U}_s = 2040 \text{ kgf}$ and mass, $2\overline{m}_s = 0.0068 \text{ kg}$ the \tilde{H} bow, it is thus given by

$$\begin{aligned} &\tilde{H}(91.44, 10.16, \overline{W}, \overline{V}, \theta_0 \equiv 0, 0.0125, 0, 0, 0, 0, 0, \\ &91.44, 0, 91.44, 0, 91.44, 2040, 0.0068, |\overline{OH}| = 15.24; \\ &71.12, 15.59, 0.1625) . \end{aligned} \quad (4.96)$$

where \overline{W} and \overline{V} are given by (4.93) and (4.94).

Hickman invented his model for a bow with bending stiffness (4.93) (apart from a scalar factor), which is a linear function of the distance from the tip, being zero at the tip. As a result, the limb bends in a true arc of a circle for a small load at the tip, perpendicular to the limb. Then the flexible limb is replaced by a rigid one, connected to the grip by an elastic hinge S, see Figure 4.3. The place of this hinge is chosen so that the tip of the flexible limb and that of the rigid limb travel almost along the same path when the bow is drawn. In this way he finds the length of the rigid limb \overline{L}_1 to be 3/4 of the length of the flexible limb. Hence in the H model \overline{L}_0 is the length of the grip plus 1/4 of the lengths of

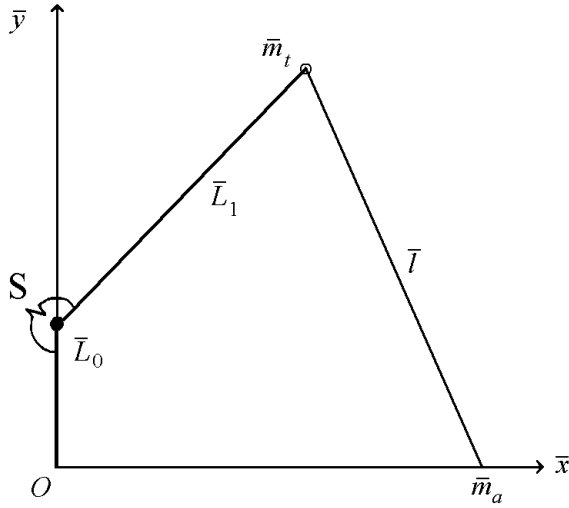


Figure 4.3: Bow with two elastic hinges and rigid limbs.

the flexible limb. In order to determine the strength \bar{k} of the elastic hinge, with neutral position the \bar{y} -axis, Hickman demands the deflection of the tip of the rigid limb to be equal to that of the flexible limb, both loaded with the same sufficiently small force at the tip, perpendicular to the limb.

Next he assumed the mass of the rigid limb to be concentrated at the tip, which is not essential because the dynamics of the limb is determined by its moment of inertia \bar{J} with respect to the hinge. This mass \bar{m}_t follows from the demand that the frequencies of free vibrations of the elastic limb and rigid limb are the same. The deflection during the oscillatory motion of the elastic limb is assumed to be the same as its deflection in the case of a static force acting upon the tip of the limb perpendicular to this limb, which causes the same deflection of the tip. The concentrated mass at the tip appears to be 1/15 of the mass of one flexible limb.

Hickman assumes the string to be inextensible and its mass $2\bar{m}_s$ is accounted for by adding 1/3 of it to the mass of the arrow $2\bar{m}_a$. In [12] Marlow replaces the flexible limb also by a rigid limb connected to the grip by an elastic hinge. However, the place of this hinge and its strength \bar{k} are determined differently. In this M model the hinge is placed at the point the grip meets the limb. So the length \bar{L}_1 of flexible and rigid limb are equal. For the evaluation of the strength of the elastic hinge, Marlow uses the second derivative of the function $\bar{A}(\bar{b})$ (4.83) at the point where \bar{b} equals the brace height $|\overline{OH}|$. We have using (4.83)

$$\left. \frac{d^2 \bar{A}}{d \bar{b}^2} \right|_{\bar{b}=|\overline{OH}|} = \left. \frac{d \bar{F}}{d \bar{b}} \right|_{\bar{b}=|\overline{OH}|}. \quad (4.97)$$

The inertia of the limb is, as in the previous H model, taken into account by placing a concentrated mass at the rigid limb. This mass possesses moment of inertia with respect to the place of the hinge equal to that of the undeflected flexible limb. If the concentrated mass is placed at the tip then it is in the case of the H bow 1/6 of the mass of one flexible limb.

The string is treated as a rod, rigid with respect to shear and bending, but elastic in its length direction as given by Hooke's law. Marlow assumes that the elongation of the string during the motion is the same as its elongation for a static tensile force which causes

Table 4.1: Characteristic constants of \tilde{H} bow in H and M model.

	\bar{L}_1	\bar{L}_0	$ \overline{OH} $	\bar{k}	$\frac{d\bar{F}}{d\bar{b}}$	$ \overline{OD} $	\bar{m}_t	$2\bar{m}_a$	$2\bar{m}_s$	\bar{U}_s
H model	60.96	30.48	15.24	15.92	—	71.12	0.0108	0.025	0.0068	-
M model	81.28	10.16	15.24	—	0.55	71.12	0.0271	0.025	0.0068	2040

the same elongation of the whole string.

The obtained equations of motion cannot be solved analytically. Marlow used a simple Newtonian integration method, but we apply a more accurate Runge-Kutta method.

The third model (C model) used in this paper is the one we discussed in Section 4.3. The limbs are considered as slender beams and they are represented by elastic lines which are endowed with bending stiffness $\bar{W}(\bar{s})$ and mass per unit of length $\bar{V}(\bar{s})$. In order to avoid difficulties in the calculations using the C model we take for the bending stiffness given in (4.93)

$$\bar{W}(\bar{s}) = 7.69 \quad \text{if} \quad 1.30 \cdot 10^5 \left(\frac{\bar{L} - \bar{s}}{\bar{L}} \right) \leq 7.69, \quad (4.98)$$

For the string we assume that neither internal nor external damping is present.

Before we compare the results obtained by using the three mathematical models H, M and C, we have to specify some characteristic constants for the M model. Instead of the brace height, Marlow took the half length of the string of the real bow in unloaded situation as a characteristic quantity. To facilitate comparison of the results of the M model with those of the H and C model correctly we adhere to the brace height as a physical constant of the M model. The derivative (4.97), also one of the characteristic constants in the M model, is obtained from computations with the C model with, according to Marlow, an inextensible string. We approximate this derivative by

$$\frac{d\bar{F}}{d\bar{b}} \Big|_{\bar{b}=|\overline{OH}|} \approx \frac{3\bar{F}(|\overline{OH}| + 2\Delta\bar{b}) - 4\bar{F}(|\overline{OH}| + \Delta\bar{b}) + \bar{F}(|\overline{OH}|)}{2\Delta\bar{b}} \quad (4.99)$$

In our calculations we took $\Delta\bar{b} = (|\overline{OD}| - |\overline{OH}|)/40$, yielding $\frac{d\bar{F}}{d\bar{b}} \Big|_{\bar{b}=|\overline{OH}|} = 0.55 \text{ kgf/cm}$.

However, if we had taken $\Delta\bar{b}$ two times as large, the approximation of the derivative differs more than 2 per cent from this value. It is clear that if one uses a measured SFD curve, this inaccuracy may be larger. In Table 4.1 we collect the characteristic constants belonging to the H and the M model, which both represent the \tilde{H} bow given in our C model by (4.96).

Figure 4.4 shows the SFD and DFD curves of the H bow. They reflect that the SFD curves for the H and the C model nearly coincide. The SFD curve calculated by means of the M model deviates clearly from these curves, while also the weight of the H bow predicted by the M model differs considerably from those predicted by the other two models. Further the jump at time $t = 0$ of the force acting upon the arrow ($\bar{F}(|\overline{OD}|) - \bar{E}(\bar{t} = 0)$) is for

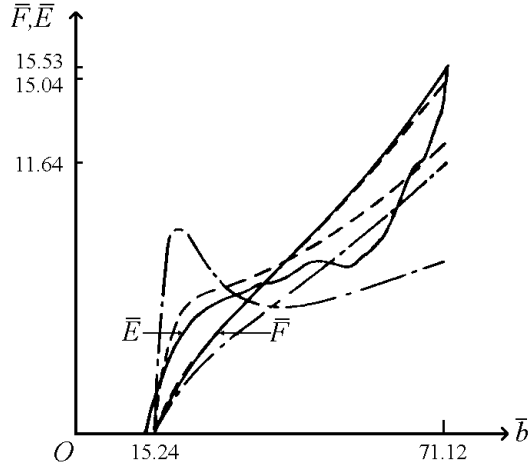


Figure 4.4: SFD and DFD curves of H bow: -- H model, - - - M model and — C model.

the M model larger than that computed by means of the H model. This effect is mainly produced by the difference in the magnitude of the mass \bar{m}_t at the tip. It is seen that with our C model there is no jump at all at the moment of release of the arrow. The DFD curves of all three models differ, although the curves belonging to the H and C model have some correspondence. The character of the one calculated by the M model is, however, strongly different from the other ones.

Figure 4.5 shows the SFD and DFD curves of the \tilde{H} bow computed by means of the M and C model. The SFD curves nearly differ from those of the H bow, and the same conclusions hold. The DFD curve in the M model shows that the acceleration force $\bar{E}(\bar{b})$ acting upon the arrow, for an elastic string oscillates strongly round this function for an inelastic string (compare Figure 4.4). The amplitude is nearly equal to the jump in the force on the arrow at time $\bar{t} = 0$ in the case of an inelastic string. The frequency with which the DFD curve of the M model oscillates depends also on the strain stiffness of the string. When this strain stiffness \bar{U}_s increases the same happens to the frequency. In fact in the it $\bar{U}_s \rightarrow \infty$ these DFD curves do not converge point-wise to the DFD curve of the H bow with an inelastic string. It seems that even for a bow with a conventional stiffness of the string, but certainly when the string is rather stiff, the M model yields unreliable results with respect to the DFD curve when no damping is introduced. This holds most probably for any model with rigid limbs.

As we remarked already, it follows from Figure 4.4 that the force on the arrow \bar{E} at $\bar{t} = 0$ equals the weight of the bow $\bar{F}(|\overline{OD}|)$ in the C model when, as is assumed here, no concentrated masses are present at the tips of the real bow. This elucidates why the DFD curve in Figure 4.5 computed by means of the C model does not oscillate and for $\bar{U}_s \rightarrow \infty$ the DFD curve does change gradually into the DFD curve of the H bow which has an inextensible string.

In Table 4.2 we give the static quality coefficient q , the efficiency η and the muzzle velocity ν of the H bow and of the \tilde{H} bow, which follow from the three different models. In order to investigate the influence of the mass and elasticity of the string purely we changed these two quantities also separately.

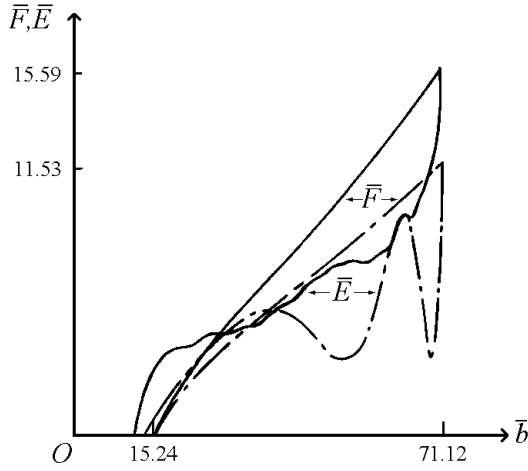


Figure 4.5: SFD and DFD curves of \tilde{H} bow: — M model and — C model.

The numbers show that the direction of the influence of the elasticity of the string with respect to the static quality coefficient predicted by both models M and C, is the same. However, the q 's predicted by the M model are much larger than those predicted by the C model.

In [9] we showed that the H and M model yield an efficiency $\eta = 1$, when the string is inextensible and without mass. This value differs a lot from that computed with the C model, being $\eta = 0.885$. If the string is inextensible and possesses a mass $2\overline{m}_s$, then the efficiency in the H model can be calculated analytically. It becomes

$$\eta = \frac{\overline{m}_a}{\overline{m}_a + 1/3\overline{m}_s} \quad (4.100)$$

This value is almost equal to the value predicted by the H and M model, namely 0.9167 and 0.9174, respectively. However, both efficiencies differ much from the efficiency computed by means of the C model, being 0.836. With respect to the influence of the elasticity of the string the results in Table 4.2 show that this influence on the efficiency is in the C model much smaller than that in the M model.

In [12] Marlow claims that his elastic string model gives an explanation for the long-standing discrepancy between theory (the H model yields an efficiency η over 91%) and experiment (Marlow measured an efficiency of 80% for more popular bows). However, the values of the efficiencies given in Table 4.2 reveal that the elasticity of the string accounts for this discrepancy only partly.

Even for the H bow with a string possessing mass, the C model predicts an efficiency of 83.6% instead of an efficiency more than 91% predicted by the H and M model. So, the discrepancy originates mainly because of the replacement of the flexible limb by a rigid limb connected to the grip by an elastic hinge.

In the case of the elastic string the muzzle velocities given by the M model differ not too much from those of the C model. For an inextensible string the H and M model yield both very large muzzle velocities whether the mass of the string is zero or not.

Summarizing this section, we have found that in comparison with our theory it seems that any rigid limb model combined with an elastic string can give inaccurate results with

Table 4.2: Quality coefficients of H bow and of \tilde{H} bow computed by means of the three models.

	H model			M model				C model			
	$2\overline{m}_s$	\overline{U}_s	∞	$2\overline{m}_s$	\overline{U}_s	∞	2400	$2\overline{m}_s$	\overline{U}_s	∞	2400
q	0		0.415	0		0.429	0.423	0		0.407	0.404
	0.0068		0.415	0.0068		0.429	0.423	0.0068		0.407	0.404
	$2\overline{m}_s$	\overline{U}_s	∞	$2\overline{m}_s$	\overline{U}_s	∞	2400	$2\overline{m}_s$	\overline{U}_s	∞	2400
η	0		1	0		1	0.806	0		0.885	0.868
	0.0068		0.9167	0.0068		0.9174	0.739	0.0068		0.836	0.807
	$2\overline{m}_s$	\overline{U}_s	∞	$2\overline{m}_s$	\overline{U}_s	∞	2400	$2\overline{m}_s$	\overline{U}_s	∞	2400
ν	0		2.32	0		2.36	2.11	0		2.16	2.14
	0.0068		2.23	0.0068		2.27	2.02	0.0068		2.11	2.06

respect to the three quality coefficients q , η and ν , and the shape of the DFD curve.

4.7 Influence of mass and stiffness of string on performance of H bow

The influence of mass and stiffness of the String on the performance of the H bow, hence on the quality numbers q , η and ν , is dealt with in this section. This completes the investigation, started in [8] of the influence of parameters on the performance of the H bow.

In Table 4.3 we change in a systematic way the strain stiffness \overline{U}_s and mass $2\overline{m}_s$ of the string, both separately and simultaneously. The third and fourth 5 row from above show the influence of the strain stiffness on the weight $\overline{F}(|\overline{OD}|)$ and on the static quality coefficient q . We recall that the brace height is the same in all the cases. Hence, the length $2\overline{l}_0$ of the string in unstrung condition is different for different values of \overline{U}_s . We find an increase of the weight $\overline{F}(|\overline{OD}|)$ and a decrease of the static quality coefficient q with decreasing stiffness. The influences are relatively small.

The lowest row gives the values of the efficiency η and muzzle velocity ν for several values of the stiffness of the string without mass. We conclude from this row: the stiffer the string the better the efficiency and the larger the muzzle velocity. The third and fourth column in Table 4.3 indicate for an inextensible string: the lighter the string the higher the efficiency and muzzle velocity. So, when we change the number of strands (mass is about directly and stiffness about inversely proportional to the number of strands) there are two effects which counteract each other, hence the influence of the number of strands is not dear beforehand.

In order to investigate this influence we change the strain stiffness and mass of the string simultaneously. On the diagonal in Table 4.3 these results are collected. It shows that the efficiency of the H bow decreases when we take more than 12 strands, the number

Table 4.3: Influence of mass $2\overline{m}_s$ and strain stiffness \overline{U}_s of string on H bow.

nos. strands		36	24	18	12	6	3
\overline{U}_s	∞	8160	4080	3060	2040	1020	510
$\overline{F}(OD)$	15.53	15.54	15.56	15.57	15.59	15.65	15.75
q	0.407	0.406	0.406	0.405	0.404	0.400	0.395

nos. strands			36		24		18		12		6		3	
\overline{U}_s	∞		8160		4080		3060		2040		1020		510	
$2\overline{m}_s$	η	ν	η	ν	η	ν	η	ν	η	ν	η	ν	η	ν
0.0272	.709	1.94	.698	1.92										
0.0136	.742	1.98			.728	1.96								
0.0102	.771	2.02					.754	1.99						
0.0068	.836	2.11							.807	2.06				
0.0034	.850	2.12									.809	2.05		
0.0017	.869	2.15											.807	2.04
0	.885	2.16	.881	2.16	.877	2.15	.874	2.15	.868	2.14	.853	2.11	.831	2.07

of strands corresponding to $2\overline{m}_s = 0.0068$ kg and $\overline{U}_s = 2040$ kgf. Apparently when the string has reached a certain stiffness, the disadvantage of becoming heavier has more effect than the advantage of becoming stiffer. For the H bow with number of strands between 3 and 12 the efficiency and muzzle velocity hardly depend on the number of strands. Here the two effects neutralize each other.

In Figure 4.6 we give the DFD curves of the H bow with changing number of strands. For heavy strings we see that the inertia of the string makes the force $\overline{E}(\overline{b})$ go down sharply after the loose of the arrow. During the second part of the shooting process, the force $\overline{E}(\overline{b})$ increases more than in case of a light string and the kinetic energy of the string is transferred into the arrow. This phenomenon resembles the energy absorption and restitution by concentrated mass at the tip of a bow with elastic limbs, as will be discussed in Section 4.9. The rather small oscillation with a high frequency occurring with the heavy strings may be physically unrealistic because of damping, which has been ignored in our theory. For light strings the DFD curves, but also the recoil force $\overline{P}(\overline{t})$ and tensile force in string $\overline{K}(\overline{t})$ are rather smooth because of the elasticity of the string. Note that for a string made of 12 strands, the \overline{x} -coordinate of the middle of the string ($\overline{b} = 11.04$ cm) is rather small at the moment the arrow leaves the string, in comparison with the brace height ($|\overline{OH}| = 15.24$ cm.)

Hickman investigated experimentally in [6], page 45, the effect of the mass of the string on the efficiency and muzzle velocity. He measured the muzzle velocities of four different arrows, each shot from bows made of three different kinds of wood. Because Hickman changed the number of strands he changed the strain stiffness as well as the mass of the string. He came to the conclusion that the velocity of the arrow is reduced about the same

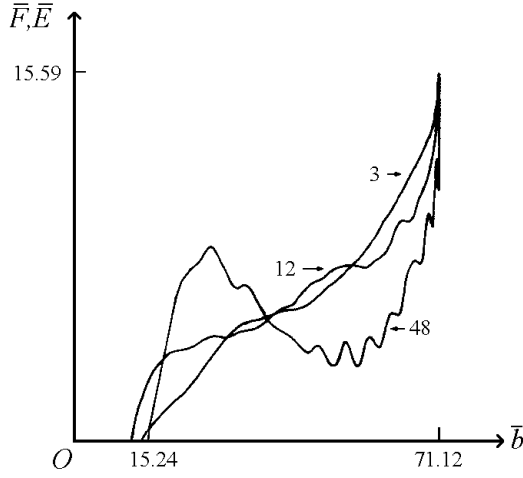


Figure 4.6: DFD curves of H bow, different numbers of strands, Table 4.3.

Table 4.4: Comparison Hickman's rule with C model.

nos. strands	36		24		18		12		6	
	η	ν	η	ν	η	ν	η	ν	η	ν
C model	0.698	1.92	0.728	1.96	0.754	1.99	0.807	2.06	0.809	2.05
Hickman's rule	0.679	1.89	0.762	2.00	0.785	2.03	0.807	2.06	0.830	2.09

amount as if the arrow were increased in mass by one third of the increase in mass of the string, while the string was kept the same. We have checked if this is in agreement with results from the C model.

To that end we start with the \tilde{H} bow and compute the efficiency η and muzzle velocity ν of the same bow with the same string, but shooting an arrow with an adapted mass according to Hickman's rule. We recall that we assumed as standard values a string with 12 strands and an arrow with $2\bar{m}_a = 0.025$ kg. For instance in the case of a string with 24 strands, the adapted mass of the arrow $2\bar{m}_a$ equals $0.0250 + 0.0022 = 0.0272$ kg. The obtained efficiencies and muzzle velocities are in Table 4.4 compared with those computed by means of the C model, which were given in Table 4.3. We conclude that there are some deviations. The results obtained with the C model (see also Figure 4.6) suggest that the occurring longitudinal and transverse vibrations, of which the frequencies depend on the number of strands, can affect the performance of a bow favourably or unfavourably. Further, we note that Hickman's rule does not reflect that mass and elasticity of the string are coupled and that the elasticity influences also the efficiency.

The flight shooters in Asia made their strings light. The mass of these strings of new and extremely strong wound silk, was half the mass of the strings used for other bows with the same ultimate drawing force or weight, see [10, page 20]. See also [1, page 101], where it is remarked that the strings used in flight shooting are always thin and that all archers agree on this specification. Also Ascham notes in *Toxophilus* that: "the great stringe is slower for the cast", see Hodgkin [7, page 74].

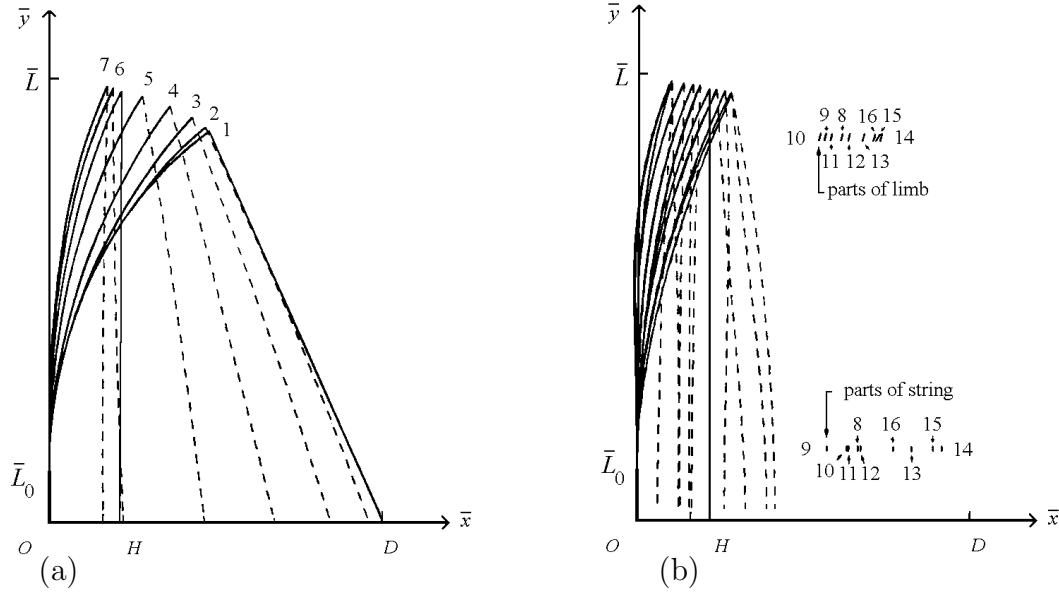


Figure 4.7: Vibratory motion of limb and string of the \tilde{H} bow: (a) $\bar{t} < \bar{t}_l$ and (b) $\bar{t} \geq \bar{t}_l$.

4.8 Fibratory motion of a bow before and after arrow exit

The vibratory motion of the limbs and string is the subject of this section. We pay attention to the bending moment $\bar{M}(\bar{s}, \bar{t})$, normal force $\bar{T}(\bar{s}, \bar{t})$ in the limb tensile force in string $\bar{K}(\bar{r}, \bar{t})$ and the recoil force $\bar{P}(\bar{t})$ on the bow hand. Finally we discuss the influence of the mass of the grip when a bow is shot open-handed.

Figure 4.7 shows the shape of limb and string of the \tilde{H} bow, defined in (4.96), for $\bar{t} < \bar{t}_l$ (Figure 4.7.a) and for $\bar{t} \geq \bar{t}_l$ (Figure 4.7.b). The configurations of the upper half of the bow are shown in unbraced situation ($i = 0$), braced situation ($i = 1/2$) and at times $\bar{t}_i, i = 1(1)16$, marked in Figure 4.8 on the \bar{t} -axis. We stopped the computations after about three quarters of an oscillation of limb and string after arrow exit. Because we neglect damping this vibratory motion holds on for $\bar{t} \geq \bar{t}_{16}$. For a real bow we have a damped free vibration and the bow returns quickly to its static braced situation. Hence, our calculations are only relevant for about one time period of vibration.

The amplitude of the vibration after arrow exit is rather large. The \bar{x} -coordinate of the middle of the string $\bar{x}_s(\bar{l}, \bar{t}) = \bar{b}(\bar{t})$ ranges between 4.0 cm and 24.7 cm, while the brace height is 15.24 cm. This means that there is not much space left for the bow hand; in Section 4.9 we return to this subject.

Note that in our model discussed in Section 4.3, the arrow leaves the string at the moment the acceleration force E on the arrow becomes negative. Doing this we assumed that the tension of the nock of the arrow on the string is zero. In [7, page 110], Hodgkin mentions that the width of the nock should be so that:

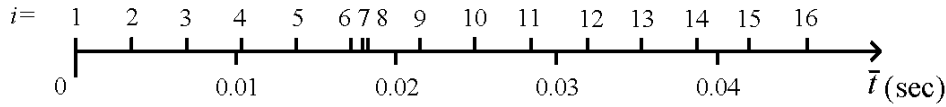


Figure 4.8: Times $\bar{t}_i, i = 1(1)16$, plotted on the \bar{t} -axis.

The whole arrow will just hang on your particular bow string without falling off.

For the \tilde{H} bow the weight of the arrow is 0.025 kgf and this is rather small with respect to the weight of the bow 15.59 kgf. Nevertheless a variation in this nock-tension may cause some variation in the moment of is rather small with respect to the weight of the bow 15.59 kgf. Nevertheless a variation in this nock-tension may cause some variation in the moment of separation of arrow from the string and the vibratory motion of the bow after arrow exit.

We proceed with a discussion in which way the energy stored in the limbs and string in fully drawn position is distributed between arrow, limbs and string as kinetic energy or potential energy. In the braced situation the bending energy in the limbs of the \tilde{H} bow is 107.21 kgfcm and the strain energy in the string is 28.62 kgfcm. In the fully drawn situation these amounts are 568.64 kgfcm and 14.95 kgfcm, respectively. So, $\bar{A} = 447.74$ kgfcm is stored in the bow by pulling it from the braced situation to full draw. The efficiency of the \tilde{H} bow is 0.807, thus 361.46 kgfcm is imparted to the arrow. This means that at the moment the arrow leaves the string at $\bar{t} = \bar{t}_l = 0.0181$ sec, 222.11 kgfcm remains behind in the limbs and string. This energy stored in limbs and string is, at $\bar{t} = \bar{t}_l$ the sum of the potential energy in the limbs 85.85 kgfcm, the potential energy in the string 65.90 kgfcm kinetic energy in the limbs 32.86 kgfcm and kinetic energy in the string 37.62 kgfcm. Hence, of the energy available, about 80.7% is put to good use, 7.3% is kinetic energy in limbs, 8.4% is kinetic energy in string and 3.6% is additional potential energy in limbs and string.

There is much more potential energy in the string at $\bar{t} = \bar{t}_l$ than in the braced situation (65.90; 28.62), the reverse holds for the limbs (85.85; 107.21), yielding that the total potential energy at $\bar{t} = \bar{t}_l$ differs not too much from its value it in the braced situation (151.75; 135.83). Note further that there is more kinetic energy in the string than in the limbs at $\bar{t} = \bar{t}_l$. In Table 4.5 we give the amounts of energy in the parts, limb, string and arrow of the \tilde{H} bow.

In Table 4.6 we collected these values in the case of the H bow (inextensible string without mass). In that case 107.21 kgfcm is stored in the limbs as bending energy in the braced situation. By pulling the bow from this situation into the fully drawn position an additional amount of energy $\bar{A} = 449.99$ kgfcm is stored, making the bending energy in the pulled bow 557.20 kgfcm. At $\bar{t} = \bar{t}_l = 0.017$ sec, 398.26 kgfcm has been imparted to the arrow, hence the efficiency is 85.5%. The potential energy in the limbs at that moment

Table 4.5: Energy in parts of \tilde{H} bow in a number of situations.

energy	limbs		string		total bow		arrow kin.
	pot.	kin.	pot.	kin.	pot.	kin.	
braced	107.21	0	28.62	0	135.83	0	0
fully drawn	568.64	0	14.95	0	583.59	0	0
arrow exit	85.85	32.86	65.90	37.62	151.75	70.48	361.64

Table 4.6: Energy in parts of H bow in a number of situations.

energy	limbs		string		total bow		arrow kin.
	pot.	kin.	pot.	kin.	pot.	kin.	
braced	107.21	0	0	0	107.21	0	0
fully drawn	557.20	0	0	0	557.20	0	0
arrow exit	151.72	7.26	0	0	151.72	7.26	398.26

is 151.73 kgfcm and the kinetic energy in the limbs 7.26 kgfcm. Thus, at $\bar{t} = \bar{t}_l$ of the original available energy, 1.6% is present as kinetic energy and 9.9% as additional potential energy in the limbs. The total energy which remains in the H bow is 158.99 kgfcm.

Comparing the numbers given in Table 4.6 for the H bow with those for the \tilde{H} bow given in Table 4.5, we conclude that the potential energy \bar{A}_D in fully drawn position is for both bows about the same amount higher than the potential energy \bar{A}_H in the braced situation. Hence, about the same amount of energy \bar{A} is available. With respect to dynamics, it appears that at the moment the arrow leaves the string, there is much more kinetic energy \bar{A}_K in limbs and string of the H bow than in the limbs of the \tilde{H} bow. However, less additional potential energy $\bar{A}_P - \bar{A}_H$ has remained in the \tilde{H} bow. Note that this amount $\bar{A}_P - \bar{A}_H$ is for a bow with one stable braced situation always positive, see Section 4.5, and that the energy in fully drawn situation stored in the limbs is for the \tilde{H} bow more than for the H bow.

These results show the action of a light and stiff string. Because of its lightness less kinetic energy is in the string and because of its stiffness it prohibits the limbs to move fast at the moment the arrow separates from the string. The amount of energy which remains in the bow after arrow exit equals

$$(1 - \eta)\bar{A}, \quad (4.101)$$

hence the efficiency is also an important quantity with respect to the vibratory motion of the bow after arrow exit.

We now turn to a discussion of the bending moment $\bar{M}(\bar{s}, \bar{t})$ and the normal force $\bar{T}(\bar{s}, \bar{t})$ in the limb, respectively. Both quantities are essential to the computations of the

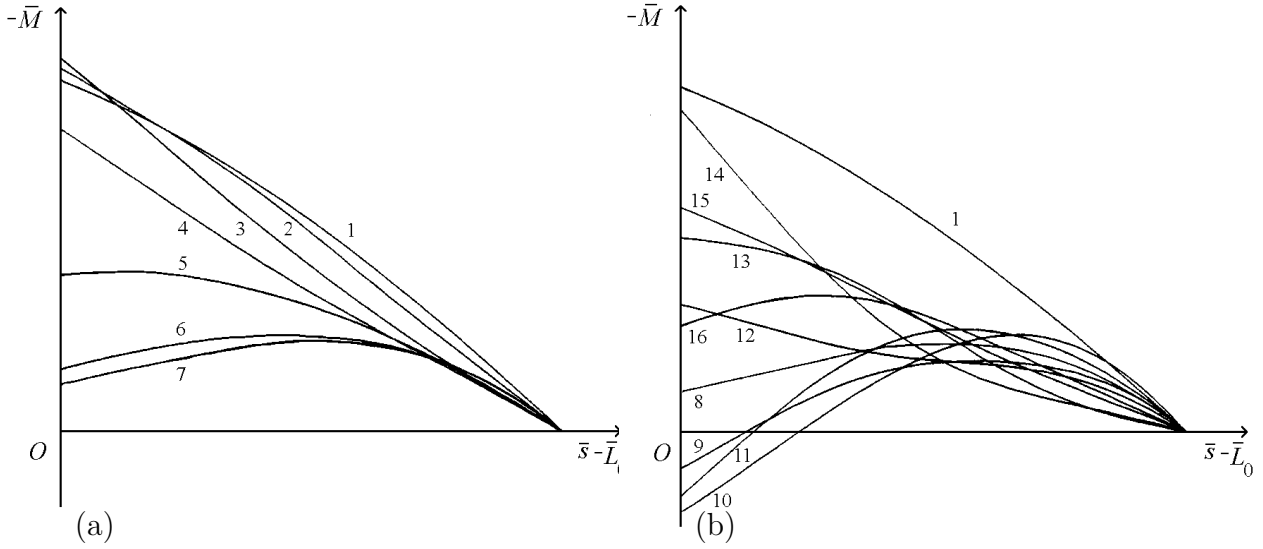


Figure 4.9: Bending moment $\bar{M}(\bar{s}, \bar{t}) \bar{t}_i < \bar{t}_l$: (a) $\bar{t} < \bar{t}_l$ and (b) $\bar{t} \geq \bar{t}_l$.

occurring stresses in the fibers of the limbs. In order to prevent the bow to be damaged this stress must not exceed the permissible stress.

Figure 4.9.a shows the bending moment as function of the length coordinate s for successive times $\bar{t}_i, i = 1(1)7$, thus before and at the moment the arrow leaves the string. The broken line is the distribution along the limb of the bending moment in the static braced situation. It follows that the bending moments during the shooting $0 < \bar{t} \leq \bar{t}_l$ are smaller than the bending moments in the fully drawn position of the bow, with the exception of the part of the limb near the grip. In Figure 4.9.b we show the curves for $i = 1$ and $i = 8(1)16$, thus in fully drawn position and after the arrow has left the string. These curves reflect that the bending moments for $\bar{t} > \bar{t}_l$ are smaller than those in the fully drawn position, but now with the exception of the outer part of the limb. However, in both parts the differences are rather small. So it seems to be allowed to use the function $\bar{M}_1(\bar{s}) = \bar{M}(\bar{s}, 0)$ for the evaluation of the maximum strain caused by bending.

The normal force is given in Figure 4.10.a for $\bar{t} < \bar{t}_l, i = 1(1)7$ and in Figure 4.10.b for $\bar{t} < \bar{t}_l, i = 8(1)16$. The broken line is the curve in the braced situation. In contrast with the bending moment the normal force is in the braced situation larger than in the fully drawn situation. Figure 4.10.a shows that this force increases sharply in a short period before the arrow separates from the string. At moment $\bar{t} = \bar{t}_l$ the normal force is already larger than in the braced situation. After arrow exit the force rises even further and obtains its maximum when the middle of the string is nearest to the grip, configuration $i = 9$. This maximum normal force is about 3 times the value in braced situation.

Note that at time t_9 the bending moment is rather small, see Figure 4.10. Besides the bending moment and normal force the shape of the cross-section has to be known to be able to compute the stresses caused by the bending moment and the normal force. In a

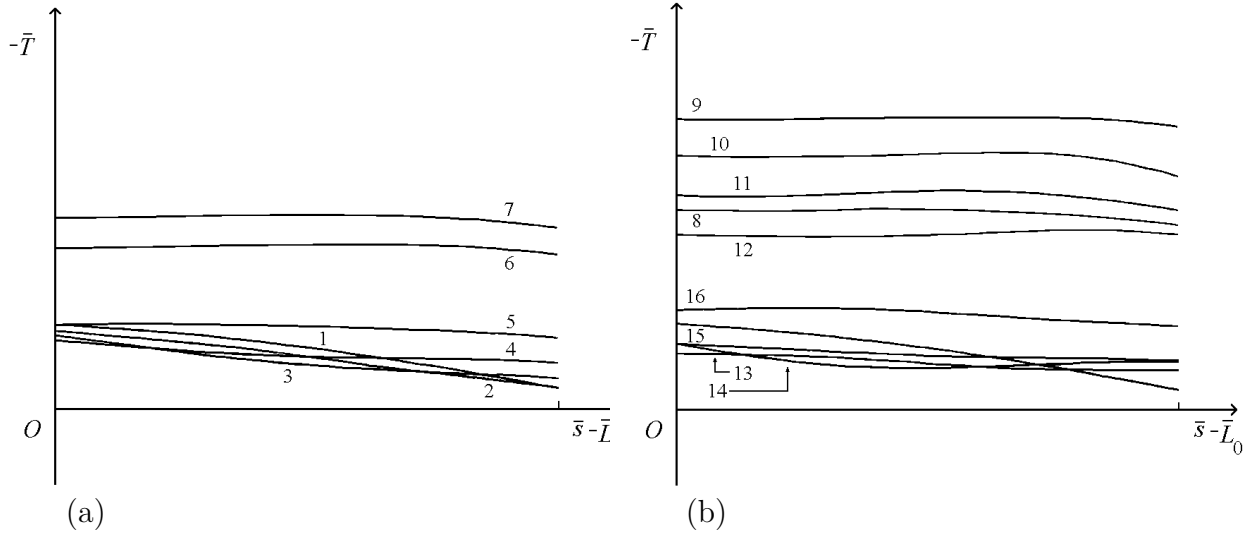


Figure 4.10: Normal force $\bar{T}(\bar{s}, \bar{t}_i)$: (a) $\bar{t} < \bar{t}_l$ and (b) $\bar{t} \geq \bar{t}_l$.

next paper we return to this subject, but we remark already that for common bows the stresses caused by the bending moment are much larger than those caused by the normal force.

In the previous section we changed the number of strands of the string in order to find its influence on the performance of one specific bow, the H bow defined in (4.92). But, of course, the tensile strength of the material of the string and the maximum tensile force in the string impose a condition on the number of strands one has to use to save it from breakage. The tensile strength of the string is a given physical constant. The tensile force \bar{K} is in the static case a function of \bar{b} alone and during the dynamics of shooting a function of \bar{b} or \bar{t} and of \bar{r} , which is the length coordinate along the string. It appears however that in the dynamic case \bar{K} changes only slight as function of \bar{r} , therefore only its value at the middle of the string $\bar{K}(\bar{l}, \bar{t})$ will be given.

In Figure 4.11 we plotted the tensile force \bar{K} in the static and dynamic case for the H bow as well as for the \tilde{H} bow, in the dynamic case for $0 \leq \bar{t} \leq \bar{t}_l$. First, we note that the elasticity and mass of the string have little influence on the force \bar{K} in the string in both cases. In the static case, starting from the braced position $\bar{b} = |\overline{OH}| = 15.24$ cm, \bar{K} decreases first, passes through a minimum and increases slightly up to a value in the fully drawn position, $\bar{b} = |\overline{OD}| = 71.12$ cm which is smaller than its value in the braced situation.

After the arrow is released \bar{K} decreases again after which it increases when the string becomes stretched. Its magnitude at $\bar{t} = \bar{t}_l$ is much larger than in the braced situation. However, this value appears not to be the maximum force which the string has to withstand.

In Figure 4.12 we give the acceleration force \bar{E} , the recoil force \bar{P} and the tensile force \bar{K} in the string as function of time \bar{t} in sec for the \tilde{H} bow. The moment \bar{E} becomes zero

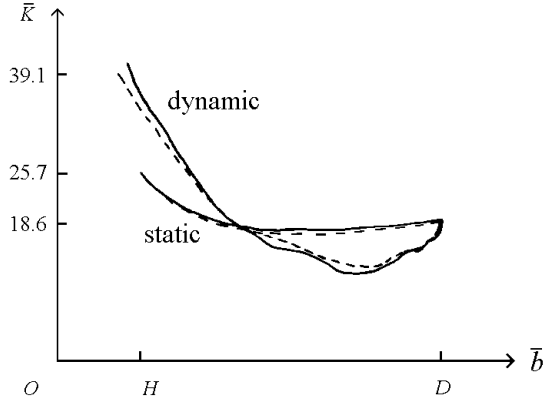


Figure 4.11: Tensile force \bar{K} in string in static and dynamic case: — H bow and -- \tilde{H} bow.

indicates the time the arrow leaves the string ($\bar{t} = \bar{t}_l$). It shows that for $\bar{t} \geq \bar{t}_l$ the tensile force \bar{K} oscillates between two values, of which the maximum is the value we are looking for. The maximum is for the \tilde{H} bow 57.7 kgf, about 2.2 times its magnitude in the braced situation, being 25.7 kgf.

In [6, page 252] Taylor decreased the strength of the string to the breaking point and found that the maximum dynamic force is usually about twice the maximum static force in the string. Taylor mentioned that \bar{K} reaches a maximum as the string becomes taut. From Figure 4.12 it follows that the peak is reached after arrow exit. In [3] Paterson states:

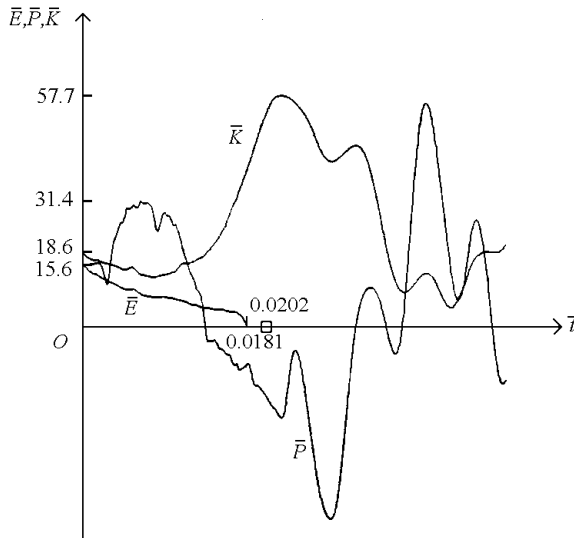


Figure 4.12: \bar{E} , \bar{P} and \bar{K} as function of \bar{t} in case of \tilde{H} bow; \square indicates moment the arrow passes grip.

‘That the maximum impact on the string is about five times the weight of the bow.’

The bow in question was a 40 Lb steel bow. For the \tilde{H} bow we find a peak tensile force of about 3.7 times the weight of the bow. Because we don’t know the physical constants

of the bows, arrows and strings used for the experiments, we are not able to compare our results with the quoted results, but they are certainly not contradictory.

That the peak force in the string occurs after arrow exit is in agreement with the experience of most archers that, although a bow string might break, the arrow finds its way to the target apparently unaffected. Indeed, if the breaking strength is larger than $\overline{K}(\bar{t} = \bar{t}_l)$ being 39.1 kgf, but smaller than the peak, 57.7 kgf, the string breaks at a moment the arrow is already on its way.

This knowledge is used by flight shooters. In [11] Learn describes the bow and string and arrow Drake used in shooting a mile. Drake built an footbow with a weight over three hundred pounds. Learn writes:

‘This tremendous strength of the bow made it impossible to make a string, that will shoot the arrow and not break. If you put turnes on the string in order to make it unbreakable you would not be able to put the nock on the string.’

However, in the previous section we found that the muzzle velocity for rather heavy strings decrease with increasing number of strands. This, together with the fact that breakage of the string after exit of the arrow does not affect its flight and that a flight shooter can afford to break the string every shot, shows that it is even not desirable to use an unbreakable, hence a heavy, string.

After the maximum the tensile force \overline{K} decreases and becomes fairly small at a minimum. In the case of the H bow, thus with an inextensible string without mass, \overline{K} becomes even zero.

Figure 4.12 shows also the recoil force \overline{P} , the force exerted by the \tilde{H} bow on the bow hand if this bow is clamped. For $\bar{t} \leq \bar{t}_l$ the maximum recoil force is about 31.4 kgf, about the same as in the case of the H bow. We observe that for $\bar{t} \geq \bar{t}_l$, $\overline{P}(\bar{t})$ oscillates round the \bar{t} -axis with a rather large amplitude of about 55 kgf, thus almost four times the weight of the bow! Note that these large fluctuations in \overline{P} occur after the nock of the arrow has passed the grip. The muzzle velocity is about 5330 cm/sec and the distance between the nock and the grip at $\bar{t} = \bar{t}_l$ equals, as already mentioned 11.04 cm, so the time the arrow needs to travel this distance is 0.0021 sec. This time is rather small compared with the shooting time, being 0.0181 sec. In Figure 4.12 the "□" on the \bar{t} -axis indicates the moment $\bar{t}_g = 0.0202$ sec the nock of the arrow passes the grip. Thus movements of the bow hand caused by a jerking recoil force after this moment \bar{t} do not affect the flight of the arrow. This means that if we want to judge the performance of a bow, the behaviour of the recoil force for $\bar{t} \leq \bar{t}_g$ is more important for the accuracy of the shooting and its behaviour for $\bar{t} \geq \bar{t}_g$ determines whether the bow is possible a pleasant how to shoot or not.

For a clamped real bow with internal and external damping in limbs and string, \overline{K} and \overline{P} will converge to their magnitude in the static braced situation, being 25.7 kgf and 0 kgf, respectively.

A subject close to the preceding one is the influence of the mass of the grip $2\overline{m}_g$ when a bow is shot open-handed. In that case the bow leaves the bow hand at the moment the recoil force \overline{P} becomes negative, $\bar{t} = \bar{t}_p$. It appears that the efficiency and the muzzle velocity of the arrow hardly depend on the mass of the grip, see Table 4.7. Further the

Table 4.7: Influence of mass of grip $2\overline{m}_g$ on performance of \tilde{H} bow shot open-handed, $q = 0.404$.

\overline{m}_g	0	0.0406	∞
η	0.807	0.807	0.807
ν	2.06	2.06	2.06

maximum force in the string is for the H bow shot open-handed with $\overline{m}_g = 0$, slightly smaller (about 53 kgf) than its value when the \tilde{H} bow is clamped (then 57.7 kgf). We conclude that, for efficiency η , muzzle velocity ν , maximum force in string and behaviour of the acceleration force \overline{E} , shooting a bow open-handed gives no disadvantages.

The Arab archers, see [10, page 43], used a very tight hold on the grip:

‘The pressure on the grip will give a hold as strong as a building, so that the bow will neither deviate no turn in the hand’

In [1, page 49], it is said that:

‘Although archers throughout the world have agreed that strong and accurate shooting depends upon a firm hold upon the grip, so that the finger tips all but bleed, the Persians maintained that the opposite, a loose hold upon the grip insured strength and accuracy.’

The modern target archer employs also a loose grip, to avoid twisting which can occur with a tight grip. This twisting tendency, either horizontally or vertically, throws the arrow off, see Nagler [6, page 194]. To prevent loss of the bow after shot the archer uses a wrist strap or a finger strap.

Modern bows possess stabilizers, a pair of extending metal arms attached to the handle section, the stiff part in the middle of the bow which we called the grip. These arms are provided with a heavy knob on the end, giving the stabilizers a large moment of inertia with respect to the \overline{y} -axis. One of the actions of stabilizers is to reduce bow "torque" or the twisting of the bow on the pivot of the hand round the \overline{y} -axis. Because we assume in our model (Section 4.3) that the limbs and arrow move in the $(\overline{x}, \overline{y})$ -plane, it is not possible to use this model to compute the influence of the magnitude of the mentioned moment of inertia. However, the action of the stabilizers is qualitatively dear.

Another effect of these stabilizers is that they add mass to the grip. Because the handle section of a modern take down bow is rather long, its mass is by itself already rather large. Hence, for modern bows $2\overline{m}_g$ the mass of the grip is much larger than for ancient bows. In this section we found that the performance of the bow shot open-handed hardly depends on this mass. However, a heavy grip gives a smaller recoil because the bowhand has some elasticity. Unfortunately our model developed in Section 4.3 is unsuited to deal with this phenomenon, because we assumed the bow to be fixed in the middle when the recoil force is positive.

Table 4.8: Energy in parts of KL bow in a number of situations.

energy	limbs		string		total bow		arrow kin.
	pot.	kin.	pot.	kin.	pot.	kin.	
braced	0.095	0	0.0276	0	0.1226	0	0
fully drawn	0.5155	0	0.0137	0	0.5292	0	0
arrow exit	0.0663	0.0491	0.0681	0.0344	0.1344	0.0835	0.3112

4.9 Systematic change of parameters of a straight-end bow

In [8] we changed, starting with the H bow, length of the grip, brace height, length of bow, bending stiffness and mass distribution along the limbs, shape of the unstrung bow, mass of the arrow and put concentrated masses at the tip. In Section 4.7 of this paper we completed this study of the H bow by varying the strain stiffness and mass of the string. We also compared if possible our calculated results with experimental ones given in [6]. In this section we change some of the parameters mentioned above one by one, but now starting from a more realistic bow and are able to give numerical results related to what happens after the arrow has left the string, for instance the peak tensile force in the string and the behaviour of the recoil force. At the end of this section we deal with an angular bow.

We start with a bow which we call the KL bow, given by

$$\begin{aligned} & \text{KL}(1.286, 0.1429, W, V, \theta_0 \equiv 0, 0.0769, 0, 0, 0, 0, 0, 0, \\ & 1.286, 0, 1.286, 0, 1.286, 1.286, 131, 0.0209, 0.214; 1, 1, 1) , \end{aligned} \quad (4.102)$$

with bending stiffness and mass distribution

$$W(s) = W(L_0) \left(\frac{L-s}{L-L_0} \right), \quad L_0 \leq s \leq \epsilon_3, \quad W(s) = 1/3 W(L_0), \quad \epsilon_3 \leq s \leq L, \quad (4.103)$$

and

$$V(s) = V(L_0) \left(\frac{L-s}{L-L_0} \right), \quad L_0 \leq s \leq \epsilon_3, \quad V(s) = 1/3 V(L_0), \quad \epsilon_3 \leq s \leq L, \quad (4.104)$$

where $W(L_0) = 1.409$ and $V(L_0) = 1.575$ and $\epsilon_3 = L_0 + 2/3 (L - L_0)$.

With respect to the $\tilde{\text{H}}$ bow the KL bow possesses more mass per unit of length near the tip to support the string. Apart from some minor details the KL bow is dealt with by Klopsteg in [6]. The computed values for q , η and ν are 0.407, 0.765 and 2.01, respectively. In Figure 4.13 we show the SFD curve and DFD curve of this KL bow and in Table 4.8 we give the amounts of energy in different parts of the KL bow in the braced and fully drawn situation and at the moment the arrow leaves the string. Comparing these results with

those of Table 4.5, after we made the latter ones dimensionless, shows that more kinetic energy is left behind in the limbs of the \tilde{H} bow. The maximum recoil force for $t \leq t_l$ is $P = 2.3$ and the maximum tensile force in the string is $K = 4.3$. For the \tilde{H} bow these values were 2.10 and 3.7, respectively. After the peak the force in the string becomes negative.

Before we discuss the consequences of the change of parameters, we describe the situations in which we stop the calculations. If nothing special happens we stop after one complete oscillation of limb and string. After one oscillation we know the information we are looking for; efficiency η , muzzle velocity ν , maximum recoil force for $t \leq t_l$, peak tensile force in string and behaviour of the recoil force for $t > t_l$.

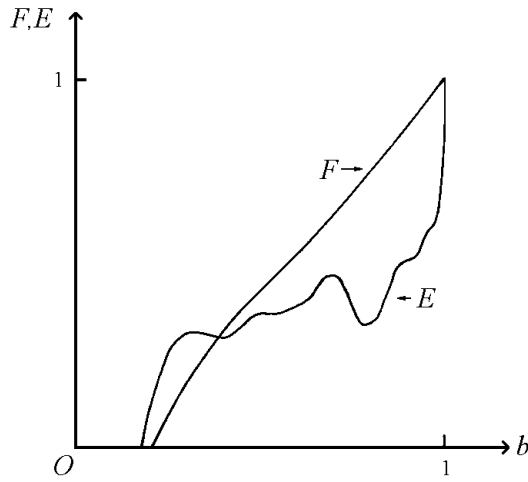


Figure 4.13: SFD and DFD curve of KL bow.

In the case of the KL bow and the H bow (Section 4.8) we mentioned already the possibility that the force in the string becomes negative. When this happens we are forced to stop the calculations because then the Newtonian method fails to converge. Figure 4.14.a shows the shape of the bow and string of the KL bow at that moment, which occurred after arrow exit. The distance between the tip of the limb and the x -axis approximates the length l_0 of the string in unloaded situation and the force in the string becomes zero. This phenomenon can happen also for $t \leq t_l$, if we take the mass of the arrow very small.

We also stop the computations when the x -coordinate of the middle of the string b becomes negative, then the string has passed the grip. Actually, because the bow is supported by the bow hand, we should stop the computations when b becomes smaller than some positive value in order to require some space for the bow hand. In Figure 4.14.b we depict the shape of the limb and string when b becomes negative for the KL bow with a concentrated mass at the tip with $m_t = 0.0769$.

Finally we stop when the string hits the limb near the tip, because then the string passes the limb. The shape of limb and string at the moment this occurs for the KL bow with $m_a = 0.0384$, are shown in Figure 4.14.c. It appears that the limb has passed the unstrung shape of the bow which coincides with a part of the y -axis. Obviously, because of a rather large dynamic force in the string it is stretched to such an extent that the length of the string exceeds the length of the bow.

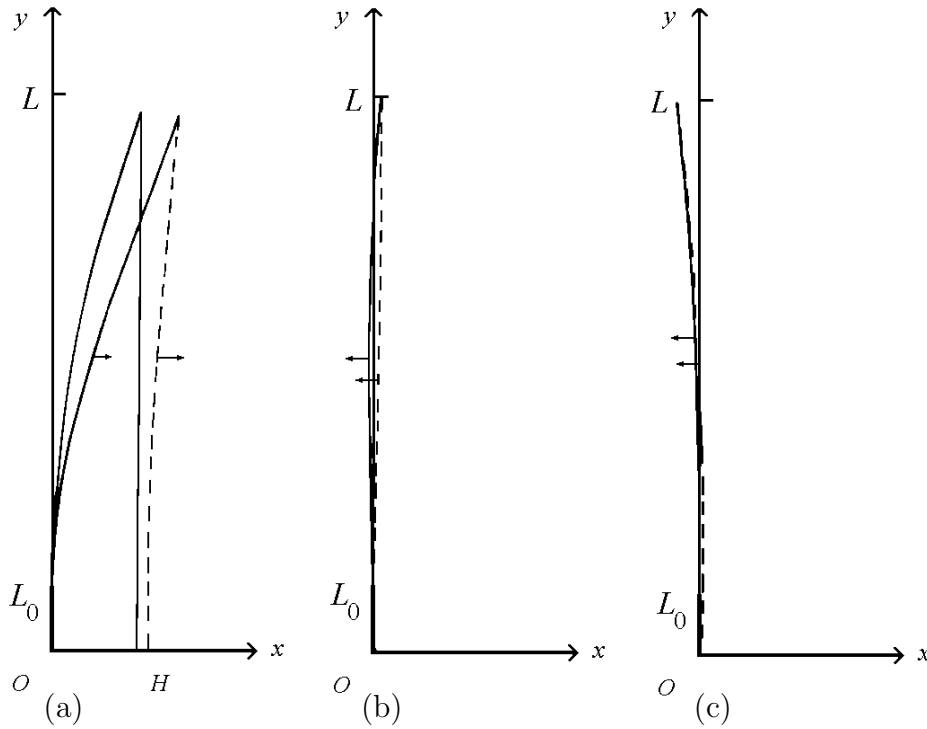


Figure 4.14: Calculated shapes of limb and string: (a) STOP=1, (b) STOP=2 and (c) STOP=3. Arrows indicate global direction of motion of limb and string.

For convenience we introduce the variable STOP, of which the domain is 0, 1, 2 and 3. If STOP=0; nothing special happens and we stop after one complete oscillation, STOP=1; then the force in the string becomes negative, STOP=2; the string hits the grip and STOP=3; the string hits the limb near the tip.

It is clear that situations occurring with STOP=2 and STOP=3 have to be avoided. Whether this is also the case with STOP=1 is not clear when this happens after arrow exit, but it does not seem to be a pleasant situation; perhaps it causes a so called "kick". We return to this in the discussion of Table 4.10.

We now change the parameters in (4.102) before the semicolon, one by one. Note that $W(L_0)$ is fixed by the requirement $\overline{F}(|\overline{OD}|) = 1$ and that $\overline{F}(|\overline{OD}|)$ is linearly dependent on λ when we replace $\overline{W}(\overline{s})$ and $\overline{U}(\overline{r}_0)$ by $\lambda\overline{W}(\overline{s})$ and $\lambda\overline{U}(\overline{r}_0)$. Hence, it is easy to adjust the weight of a described bow (1 in this case) to a desired value by multiplying $\overline{W}(\overline{s})$ and $\overline{U}(\overline{r}_0)$ by a suitable λ . $V(L_0)$ is fixed by the requirement $\overline{m}_b = 1$. Thus if we change one parameter then $W(L_0)$ and $V(L_0)$ may change. In equations (4.90) and (4.91) of [8] we suggest that $W(L_0)$ and $V(L_0)$ are the same for different bending stiffness and mass distributions along the limb, but that is wrong. In this section we give for the sake of completeness the values of $W(L_0)$ and $V(L_0)$ in all situations. With the discussion of the results we mention the behaviour of the tensile force K and recoil force P only when it differs strongly from the behaviour in the case of the \tilde{H} bow described in the former Section 4.8.

First we change the brace height $|OH|$ to investigate its influence on the performance of the KL bow. In Table 4.9 we collected the results. The efficiency η is nearly independent of the brace height. The static quality coefficient q and the muzzle velocity ν diminish

Table 4.9: Influence of the brace height on KL bow, $V(L_0) = 1.575$.

$ OH $	0.179	0.214	0.250	0.286
$W(L_0)$	1.419	1.409	1.397	1.385
q	0.418	0.407	0.393	0.378
η	0.763	0.765	0.766	0.765
ν	2.04	2.01	1.98	1.94
STOP	3	1	0	0
$\min b(t)$	≈ 0	0.02	0.10	0.14

with increasing brace height. For the smallest mentioned brace height $|OH| = 0.179$, we have STOP=3, the string hits the limb near the tip with a configuration which resembles the one of Figure 4.14.c. For the two largest brace heights mentioned in Table 4.9 we have STOP=0. It turns out that the minimum distance between the middle of the string and grip during the vibratory motion after arrow exit, denoted by $\min\{b(t)\}$ in Table 4.9, increases with increasing brace height as can be expected. Thus the requirement to have enough space for the bow hand yields a minimum brace height one has to use.

In [6, page 18], Hickman mentions that a bow which bends throughout its whole length, hence without rigid grip, is not a pleasant bow to shoot because it is likely to have an unpleasant "kick". Hence, it is interesting to change the Length of the grip $2L_0$ and by comparing the obtained results, to investigate if something special happens that indicates the possibility of a kick for $L_0 = 0$.

In Table 4.10 we give the results. We change the brace height as well as the length of the grip. The influence of the brace height on the three quality coefficients appears in the cases $L_0 = 0$ and $L_0 = 0.286$ to be the same as for $L_0 = 0.143$, the case we dealt with in Table 4.9. From Table 4.10 we conclude further that a longer grip gives a smaller static quality coefficient but also a larger efficiency, so leaving the muzzle velocity about the same

The behaviour of the recoil force for $t < t_l$ is for all bows referred to in Table 4.10, about the same. Thus, with respect to the dynamic behaviour for $t < t_l$ there is no indication for the occurrence of a kick for a bow without a grip. However, for $t > t_l$ the behaviour of the tensile force in the string K changes with varying L_0 and $|OH|$, what is reflected by the change of the variable STOP. If STOP=1, the tensile force in the string becomes negative and in reality the string will become slack. When the string is suddenly stretched again it is possible that a kick is felt by the bow hand of the archer. It is tempting to claim that this explains the occurrence of a kick. The results in Table 4.10 suggest that for smaller brace height the tensile force in the string becomes negative for a bow without or with a short grip. However, it indicates also that for a larger brace height the tensile force becomes negative just for bow with a long grip. To the knowledge of the author no book or paper mentions this latter phenomenon.

The third parameter we change, while we leave all the other ones given in (4.102) of the KL bow unperturbed, is the length $2L$ of the bow. Table 4.11 gives the quality coefficients.

Table 4.10: Influence of length of grip $2L_0$ on KL bow, also different values for $|OH|$.

L_0	0			0.143			0.286		
$ OH $	0.214	0.250	0.286	0.214	0.250	0.286	0.214	0.250	0.286
$W(L_0)$	1.945	1.934	1.922	1.409	1.397	1.385	0.972	0.960	0.948
$V(L_0)$	1.4	1.4	1.4	1.575	1.575	1.575	1.8	1.8	1.9
q	0.412	0.399	0.384	0.407	0.393	0.378	0.399	0.385	0.370
η	0.745	0.747	0.747	0.765	0.766	0.765	0.788	0.786	0.782
ν	2.00	1.97	1.93	2.01	1.98	1.94	2.02	1.99	1.94
STOP	2	1	0	1	0	0	0	1	1

Table 4.11: Influence of the length $2L$ on the KL bow.

L	1.429	1.286	1.143	1.0	0.8571	0.7857	0.7143
$W(L_0)$	2.095	1.409	0.881	0.491	0.221	0.1237	0.0495
$V(L_0)$	1.4	1.575	1.8	2.1	2.52	2.8	3.15
q	0.414	0.407	0.394	0.372	0.327	0.284	0.206
η	0.751	0.765	0.783	0.800	0.795	—	—
ν	2.01	2.01	2.01	1.97	1.84	—	—
STOP	2	1	1	1	1	1	1

We observe that the static quality coefficient q decreases when a bow is taken shorter. In Figure 4.15 we depicted the SFD curve for bows with different lengths of the limbs. It shows that the short bow has a tendency to stack. Stacking is the property of a bow to be drawn easily to the last few inches and to build up to full weight rapidly as the string comes to full draw. For the KL bow with $L = 1.286$, the force in the string is in the braced situation larger than in the fully drawn situation. For the short bow with $L = 0.7143$, it is the reverse. Further this static force K is for the whole range $|OH| \leq b \leq |OD|$ definitely smaller for the shortest bow than for the longer KL bow.

Figure 4.16 shows the DFD curves for different lengths $2L$. We conclude that the dynamic behaviour of the short bow is inferior to that of the long bow. For bows even shorter than the mentioned ones, for instance $L = 0.7143$, the acceleration force E becomes negative shortly after release (STOP=1, for $t < t_l$ by which the string becomes slacked. Hence, a minimum length for a straight end bow has to be used in order to get an effective bow.

We turn now to the influence of the distribution of the bending stiffness $W(s)$ and mass $V(s)$. In Table 4.12 we change W and V simultaneously, where we use the following

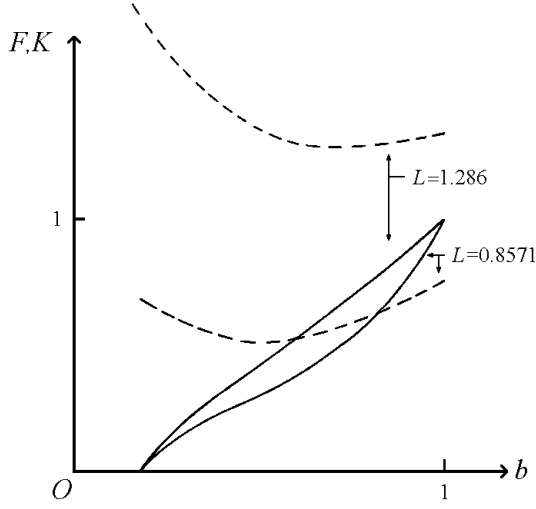


Figure 4.15: Influence of length $2L$ on KL bow: $F(b)$ and $K(b)$, Table 4.11.

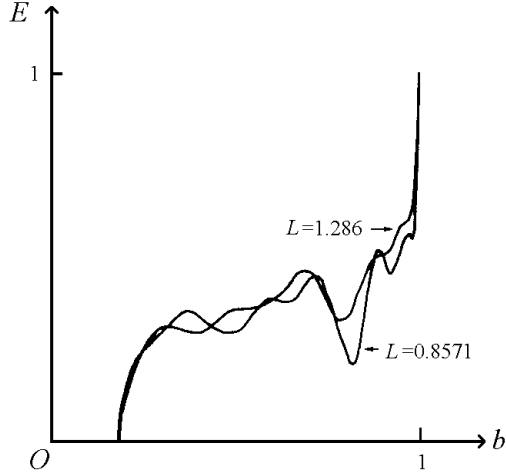


Figure 4.16: DFD curve of KL bow, different lengths, Table 4.11.

notation

$$W_n(s) = W_n(L_0) \left(\frac{L-s}{L-L_0} \right)^{\beta_n}, \quad L_0 \leq s \leq \epsilon_n, \quad W_n(s) = 1/3 W_n(L_0), \quad \epsilon_n \leq s \leq L, \quad (4.105)$$

and

$$V_n(s) = V_n(L_0) \left(\frac{L-s}{L-L_0} \right)^{\beta_n}, \quad L_0 \leq s \leq \epsilon_n, \quad V_n(s) = 1/3 V_n(L_0), \quad \epsilon_n \leq s \leq L, \quad (4.106)$$

where: $\epsilon_1 = L$, $\epsilon_n = L - (L - L_0) (1/3)^{1/\beta_n}$ for $n = 2, 3$; $\beta_1 = 0$, $\beta_2 = 1/2$, $\beta_3 = 1$.

For $n = 3$ these functions correspond to those defining the KL bow (4.102) ··· (4.104).

In [8] it appeared that for three bows $n = 1, 2, 3$ with an inextensible string without mass and ϵ_2 and ϵ_3 almost equal to L , the muzzle velocities are almost equal. From Table 4.12 we conclude that this is not the case for the bows given by (4.102) with (4.105) and (4.106). For the bow with a uniform bending stiffness and mass distribution (W_1, V_1)

Table 4.12: Influence of bending stiffness $W(s)$ and mass $V(s)$ on the KL bow.

W, V	W_1, V_1	W_2, V_2	W_3, V_3
$W(L_0)$	0.96	1.16	1.409
$V(L_0)$	0.875	1.289	1.575
q	0.412	0.409	0.407
η	0.704	0.744	0.765
ν	1.94	1.99	2.01
STOP	2	2	1

the muzzle velocity is smaller than for the other two bows. In Figure 4.17 we give the DFD curves for $n = 1, 2, 3$. It is seen that the DFD curve for a bow with (W_1, V_1) is less smooth than the DFD curve of a bow with (W_2, V_2) or (W_3, V_3) . This combined with the rather low efficiency makes this bow inferior to the other two bows, of which the one with (W_3, V_3) is the best. In the two cases $n = 1$ and $n = 2$ the string hits the grip (STOP=2). The shapes of limb and string when this happens resemble the one shown in Figure 4.14.b.

The next parameter we deal with is the mass of the arrow $2m_a$. Table 4.13 gives efficiencies and muzzle velocities for the KL bow shooting arrows with different masses. It is seen that although the efficiency of the KL bow shooting a light arrow is bad, its muzzle velocity will be high.

In [8] we discussed the concept of virtual mass, defined by Klopsteg in [6, page 167]. This virtual mass, denoted by K_h , is given by

$$K_h = m_a \left(\frac{1 - \eta}{\eta} \right). \quad (4.107)$$

Klopsteg found experimentally that this virtual mass is a constant for a large numbers of bows. For the H bow (inextensible string without mass), the virtual masses for the first three arrow masses given in Table 4.13 are 0.017, 0.010 and 0.003, respectively. When we compute these virtual masses, using the efficiencies given for the KL bow, we obtain 0.038, 0.024 and 0.017, respectively. Hence, for the more realistic KL bow, the virtual mass depends less on the mass of the arrow, but it is certainly not a constant. When the lightest arrow is shot, the string hits the limb near the tip after arrow exit, STOP=3. In Figure 4.14.c. we show the shape of limb and half of string at the moment this happens. Because the efficiency is small, a large amount of energy remains behind in the limbs and string, obviously large enough to stretch the string to a length longer than the length of the bow, permitting the limbs to pass the y -axis. As for the H bow (see [8]) the maximum recoil force P for $t < t_l$ increases for decreasing mass m_a . For the KL bow, these values are 3.1, 2.4, 1.8 and 1.4 for arrow masses 0.0384, 0.0769, 0.1538 and 0.3077, respectively.

For the heaviest two arrows we have STOP=0. Figure 4.18 shows the curves $E(t)$, $K(t)$ and $P(t)$ for both masses 0.1538 and 0.3077. For the heaviest ($m_a = 0.3077$) the oscillations of the recoil force are less intense, but the maximum force in the string is only

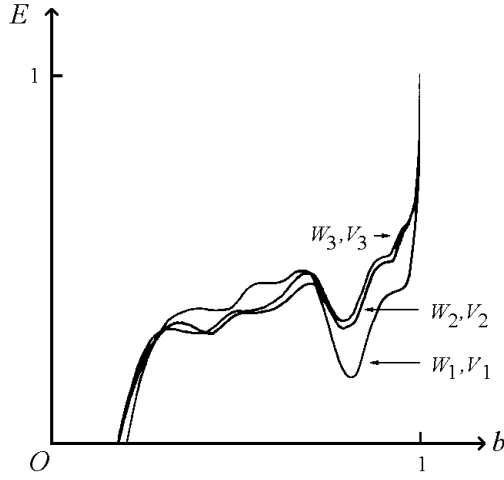


Figure 4.17: DFD curves for bows (W_1, V_1) , (W_2, V_2) and (W_3, V_3) , Table 4.12.

Table 4.13: Influence of mass of arrow $2m_a$ on the KL bow, $q = 0.407$, $W(L_0) = 1.409$, $V(L_0) = 1.575$.

m_a	0.0384	0.07169	0.1538	0.3077
η	0.505	0.765	0.898	0.931
ν	1.94	2.01	1.54	1.11
STOP	2	1	0	0

slightly smaller than in the case of the KL bow shooting an arrow with mass $m_a = 0.1538$. In the limit, when m_a tends to infinity, the efficiency tends to 1 and the energy in the limbs equals at arrow exit, the amount of potential energy in the limbs in braced situation. Hence, for $t \geq t_l$, the recoil force P tends to zero and the force K in the string tends to its value in the braced situation.

In [8] we found that the effect of concentrated masses at the tips of the H bow is rather small, in agreement with the findings of Hickman in [6, page 47]. From Table 4.14, however, we conclude that the performance of the KL bow depends on the mass of the tips more strongly. For the H bow the presence of mass at the tip with $m_t = 0.0769$ reduced the efficiency from 0.89 to 0.87 (see [8]), but for the KL bow from 0.765 to 0.695. In Figure 4.19 we draw the DFD curves for different values of m_t . These curves show clearly the influence of the mass at the tip in combination with the elasticity of the string. In [8] we showed that, when concentrated masses are present and an inextensible string without mass is used, there is a jump in the force on the arrow at time $t = 0$, just as in the case of the H model. The DFD curves for $m_t \neq 0$ in Figure 4.19 reflect a tendency to oscillate like the DFD curves in Figure 4.5, obtained by using the M model in the case of a bow with an elastic string with mass. As in the case of the M model the amplitude of this oscillation is larger for heavier tips. We remark that for very heavy tips or for moderately heavy tips combined with the use of a rather stiff string, the fluctuations of the force in the string become very large and that in those situations damping may become important. In both

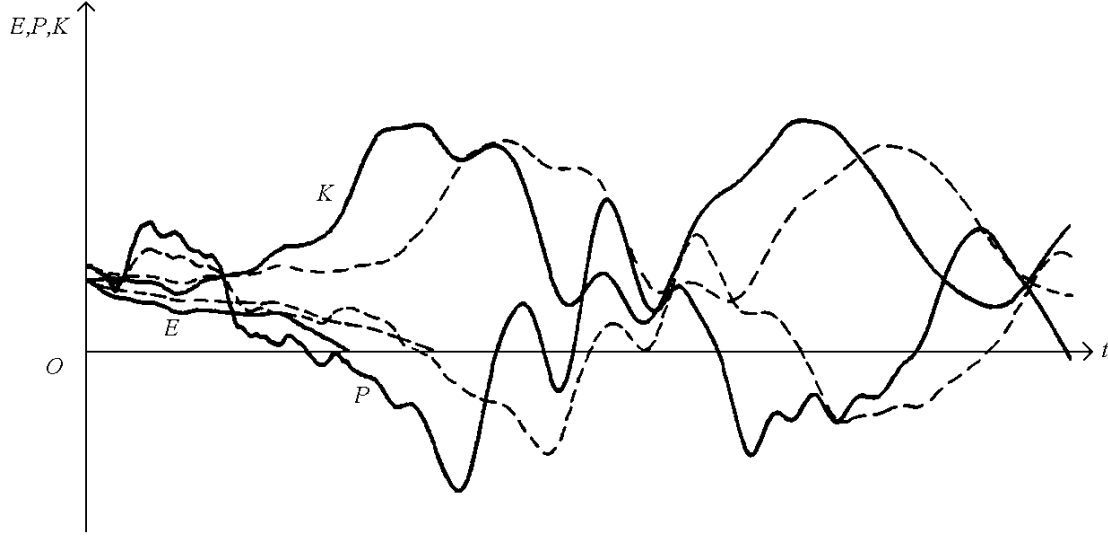


Figure 4.18: $E(t)$, $K(t)$ and $P(t)$ for KL bow with different arrow masses: $m_a = 0.1538$ and $m_a = 0.3077$, Table 4.13.

cases with masses $m_t = 0.0384$ and 0.0769 the string hits the grip at a certain moment $t \geq t_l$ (STOP=2).

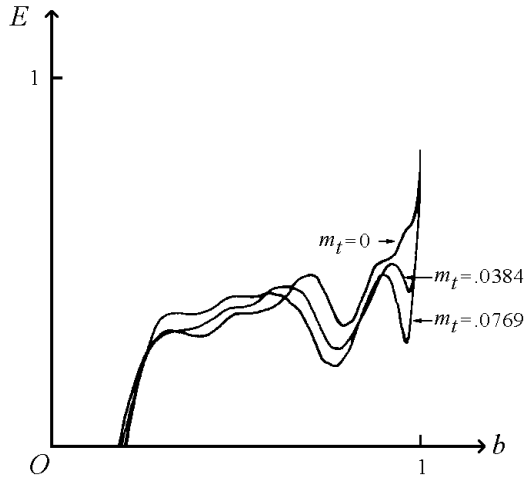


Figure 4.19: DFD curve for KL bow with masses m_t at the tips, Table 4.14.

Next we consider the influence of a rigid body possessing a moment of inertia J_t , but without mass, placed at the tip. In Table 4.15 we changed the moment of inertia of the rigid body, keeping all the other parameters the same as the ones given in (4.102) for the KL bow. A rigid body with $J_t = 9.8 \cdot 10^{-5}$ is for instance a rod of the length $1/14$ fixed in the middle of this rod at the tip with on both sides a mass equal to the half of the half mass of the arrow $m_a = 0.0769$. For $J_t = 1.56 \cdot 10^{-3}$ this rod is $4/14$ long.

In order to get the influence of the moment of inertia purely, we take the mass m_t zero, notwithstanding the fact that a actual rigid body with non-zero moment of inertia

Table 4.14: Influence of concentrated tip masses on the KL bow, $q = 0.407$, $W(L_0) = 1.409$, $V(L_0) = 1.575$.

m_t	0	0.0384	0.0769
η	0.765	0.721	0.695
ν	2.01	1.95	1.92
STOP	1	2	2

Table 4.15: Influence of moment of inertia J_t on the KL bow, $q = 0.407$, $W(L_0) = 1.409$, $V(L_0) = 1.575$.

J_t	0	$9.8 \cdot 10^{-5}$	$3.9 \cdot 10^{-4}$	$8.8 \cdot 10^{-4}$	$1.56 \cdot 10^{-3}$
η	0.765	0.765	0.765	0.761	0.785
ν	2.01	2.01	2.01	2.00	2.00
STOP	1	1	1	1	2

possesses some mass. It means that the just mentioned rods are very long, by which the masses tend to zero for a fixed moment of inertia Table 4.15 shows that the performance of the KL bow scarcely depends on J_t . This is in contrast with the influence of the point masses m_t , see Table 4.14.

We investigate now the influence of the stiffness and mass of the string in the case of the KL bow. We changed both quantities simultaneously in Table 4.16, this in order to simulate a change of the number of strands employed in making the string. For statics, the stiffest string yields the largest static quality coefficient q . With respect to the efficiency and muzzle velocity the stiffness and mass corresponding to that of the KL bow give best results. For the most elastic and lightest string mentioned in Table 4.16, the string hits the grip after the arrow has left the string (STOP=2), while for the other two strings the force in the string becomes negative (STOP=1).

Table 4.16: Influence of numbers of strands of the string on the KL bow, $V(L_0) = 1.575$.

U_s	66	131	197
m_s	0.0105	0.0309	0.0314
$W(L_0)$	1.404	1.409	1.410
q	0.403	0.407	0.408
η	0.750	0.765	0.744
ν	1.98	2.01	1.99
STOP	2	1	1

Table 4.17: Influence of shape of bow in unbraced situation on the KL bow, $V(L_0) = 1.575$.

$\theta_0(L_0)$	κ_0	$W(L_0)$	q	η	ν	STOP	$\min b(t)$
0	0	1.409	0.407	0.765	2.01	1	0.02
-0.12	0	1.097	0.425	0.710	1.98	2	0
0	-0.5	0.905	0.452	0.680	2.00	2	0
0.12	-1.0	0.770	0.464	0.673	2.02	3	—
0	0.1	1.590	0.389	0.795	2.01	1	0.06

Finally, we deal with the influence of the shape of the unstrung bow given by $\theta_0(s)$. We confine our attention to bows for which this function is given by

$$\theta_0(s) = \theta_0(L_0) + \kappa_0 \frac{s - L_0}{L - L_0}, \quad L_0 \leq s \leq L \quad (4.108)$$

where $\theta_0(L_0)$ and κ_0 are two parameters. $\theta_0(L_0)$ is the angle at which the limb is fixed to the grip (if this parameter is negative then the limb is said to be set back in the grip) and κ_0 is apart from the constant $1/(L - L_0)$ the curvature of a circle part of which coincides with the limb in unstrung situation. In Table 4.17 we changed these parameters; for $\theta_0(L_0) = 0$ and $\kappa_0 = 0$ we have the KL bow again. In [8] we dealt with bows for which $\theta_0(L_0) = -0.12$, $\kappa_0 = 0$ and $\theta_0(L_0) = 0$, $\kappa_0 = -0.5$ and $\theta_0(L_0) = 0.12$, $\kappa_0 = -1$, but in those cases the bending stiffness and mass distributions were different and the string was inextensible and without mass. The results show that the static performance is better for bows with more reflexed limbs, $\kappa_0 = -0.5$ and $\kappa_0 = -1$. Moreover the efficiency in these cases is worse, so that the dimensionless muzzle velocity is nearly independent of the shape of the bow in unstrung position (at least for the shapes we consider by which $\theta_0(L_0)$ and κ_0 change simultaneously)

Hickman in [6, page 22], notes that many bows take a permanent set after they have been used a great deal. In order to gain insight into this phenomenon we take the case $\kappa_0 = 0.1$. Hence, we consider a bow which "follows the string", of which the unstrung shape is a part of a circle with a rather small curvature. The static quality coefficient is smaller than that of the KL bow. However, the efficiency is larger so that the dimensionless muzzle velocity of both bows is again nearly unaltered. Note that the $\min b(t)$ is much larger in the case of the bow with some permanent set.

Besides bows with unstrung shape given by (4.108), we consider also angular bows (see Figure 4.1.b) which are also non-recurve bows, as we mentioned in the introduction. These bows were used in Egypt and Assyria. In [13] angular bows are depicted which have been found in the tomb of Tutankhamun. The bows do not possess a grip, $L_0 = 0$, and have a characteristic bend in the middle $\theta_0(L_0 = 0) > 0$. For the distribution of the bending stiffness and mass along the limb we take those given by (4.103) and (4.104) again. The values of the parameters m, J_t, m_a, U_s, m_s are equal to their values in (4.102). Using these data, the unstrung shape of the bow is fixed by the requirement that the limbs fall straight

back in braced situation. The equation of equilibrium of the bow in braced situation for the angular bow with $\theta'(s) \equiv 0$, reads

$$K_{1/2}(|OH| - x_{1/2}(s)) = W(s)\theta'_0(s), \quad 0 \leq s \leq L, \quad (4.109)$$

where $x_{1/2}(s)$ is the x -coordinate and $K_{1/2}$ the tensile force in the string. This formula yields the curvature as a function of the length coordinate s , apart from a constant which we call also κ_0 as in (4.108), which fixes the force $K_{1/2}$. We get

$$\theta_0(s) = \arcsin(|OH|/L) + \kappa_0 s/L, \quad 0 \leq s \leq 2/3 L, \quad (4.110)$$

and

$$\theta_0(s) = \arcsin(|OH|/L) + \kappa_0(s/L - 3/2(s/L - 2/3)^2), \quad 2/3 L \leq s \leq L, \quad (4.111)$$

Thus only for $0 \leq s \leq 2/3 L$ the unstrung shape of the limb is part of a circle. By means of (4.110) and (4.111) the constraint that the bow is an angular bow is satisfied for a bow with bending stiffness given by (4.103), as we have assumed. Next we have to choose the three parameters L , κ_0 and $|OH|$. For $L = 0.7857$, $\kappa_0 = -1$ and $|OH| = 0.214$ the unstrung bow resembles closely the bows shown in [13]. We call this bow the AN bow, it is determined by

$$\begin{aligned} &\text{AN}(0.7857, 0, W, V, \theta_0, 0.0769, 0, 0, 0, 0, \\ &-0.1551, 0.7427, -0.1551, 0.7427, -0.1551, 0.7427, 0.7857, 131, 0.0209, 0.214; 1, 1, 1), \end{aligned} \quad (4.112)$$

where W and V are given by (4.103) and (4.104) and θ_0 by (4.111). This bow is shown in various situations in Figure 4.20, note the angular form in braced situation.

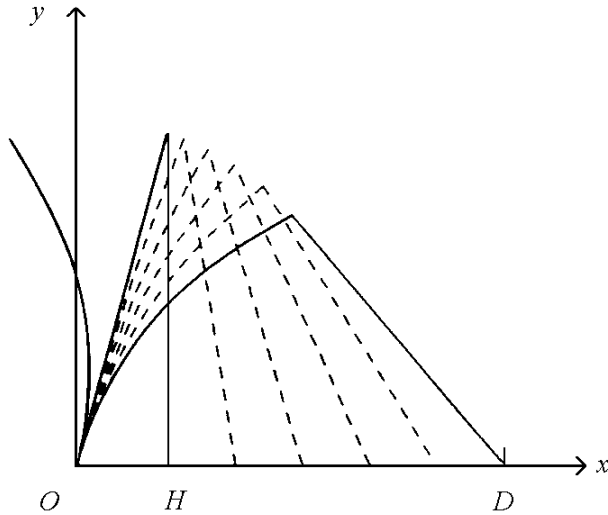


Figure 4.20: Angular bow AN in various situations. Note the angular form in braced situation, the limbs form the equal sides and the string the basis of an isosceles triangle.

In Figure 4.21 we have drawn the SFD and DFD curve of this bow. Its static quality coefficient $q = 0.395$, its efficiency $\eta = 0.716$ and its muzzle velocity $\nu = 1.92$ In Table 4.18

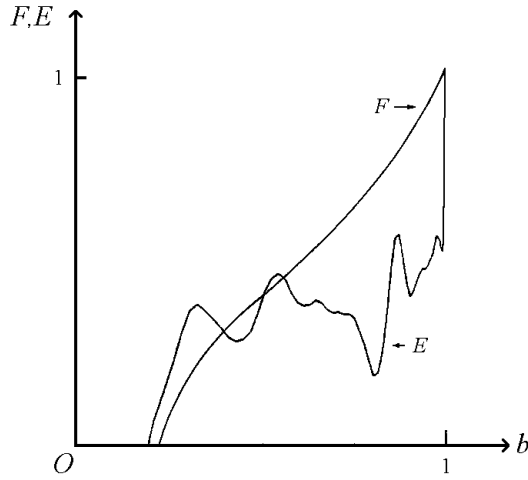


Figure 4.21: SFD and DFD curve of the AN bow.

Table 4.18: Energy in parts of angular bow AN in a number of situations.

energy	limbs		string		total bow		arrow kin.
	pot.	kin.	pot.	kin.	pot.	kin.	
braced	0.1461	0	0.0115	0	0.1576	0	0
fully drawn	0.5493	0	0.0033	0	0.5526	0	0
arrow exit	0.1380	0.0573	0.0385	0.0359	0.1765	0.0932	0.2961

we give the amounts of energy in the different parts of the AN bow for a number of situations. If we compare the quality coefficients of the AN bow with those of the KL bow, we find that less recoverable energy is available ($q = 0.395$; $q = 0.407$), its efficiency is smaller ($\eta = 0.716$; $\eta = 0.765$), hence its muzzle velocity is smaller ($\nu = 1.92$; $\nu = 2.0$). After arrow exit the force in the string K attains a maximum, being 5.0, which is larger than in the case of the KL bow, where it was 4.3. After this peak force it becomes zero, so we have STOP=1, just as with the KL bow. In Figure 4.22 we show the forces E , K and P as functions of time in the case of the AN bow.

The shape of the DFD curve resembles that of the KL bow with $L = 0.8571$ given in Figure 4.16, merely the oscillations are less intense. As a consequence, the acceleration force E acting upon the arrow remains positive during the shooting process, this in contradistinction to its behaviour in the case of the short KL bow with same length $L = 0.7857$. The amount of energy bound up in the pulled AN bow is slightly larger than in the case of the KL bow, see Table 4.18. ($A_D = 0.5526$; $A_D = 0.5292$). This holds also for the potential energies stored in different parts in the AN bow at corresponding times. The amounts of kinetic energy are about the same for both bows at arrow exit.

In Table 4.19 we change the length L of the AN bow, while the other parameters are kept the same as those given in (4.112). With increasing length the static quality coefficient q increases, but for $L = 1.000$ and $L = 1.286$ the difference is only small. In Figure 4.23 we show the SFD and DFD curves of the AN bow with $L = 1.286$ besides those of the

Table 4.19: Influence of length $2L$ on performance of the angular AN bow.

L	$W(L_0)$	$V(L_0)$	q	η	ν	STOP
1.286	1.409	1.4	0.453	0.652	1.96	3
1.000	1.097	1.8	0.450	0.689	2.01	3
0.8571	0.905	2.1	0.421	0.704	1.96	3
0.7857	0.770	2.3	0.395	0.716	1.92	1

AN bow with $L = 0.7857$. Note the path of the SFD curve for the first part of the draw. The force $F(b)$ is for a very small region negative, indicating that the braced situation with $|OH| = 0.214$ is an unstable one. For $|OH| = 0.232$ we have a stable configuration. Therefore we take this situation, in which the limb is not straight, as braced situation. The efficiency diminishes with increasing length. For $L = 1.000$ the muzzle velocity attains its largest value, being equal to that of the KL bow. Thus in contradiction with the results for the KL bow given in Table 4.11, the longest bow does not possess the largest muzzle velocity.

In this section we considered the performance of a bow as a function of the dimensionless parameters given before the semicolon in (4.2) which fix the characteristics of a non-recurve bow, namely the KL bow. In [8] and Section 4.7 of this paper the starting point was the H bow. Comparing the results obtained in [8] and in Section 4.7 with those given in this section, one can obtain insight into the influence of the elastic string with mass together with the stiffer and heavier part near the tip of the limb. Note that we changed in this section the bending stiffness and mass distribution along the limb simultaneously and also the strain stiffness and mass of the string. Because the bending stiffness of the limb of the H bow at the tip nearly vanishes, the finite-difference procedure developed in Section 4.4 fails when we put a rigid body possessing a moment of inertia at the tip.

At the end of this section we changed besides the shape of the unstrung bow also some other parameters. This in order to consider angular bows. A change of the shape of the KL bow in unbraced situation ($\theta_0(s)$) is, to a certain extend, also the subject of Section 4.11, in which we consider the static-recurve bow. In Section 4.12 we deal with the influence of the three parameters with dimension $|\overline{OD}|$, $\overline{F}(|\overline{OD}|)$ and \overline{m}_b behind the semicolon in (4.2) for non-recurve bows as well as for static-recurve bows.

4.10 A simple mathematical model for the static-recurve bow

We consider again the very simple type of symmetric bow consisting of a grip, two rigid limbs, two elastic hinges and an inextensible string without mass. This bow has by its symmetry only one degree of freedom. The aim of this section is to gain insight into the principles of the action of a static-recurve bow before we consider in section 4.11 a more

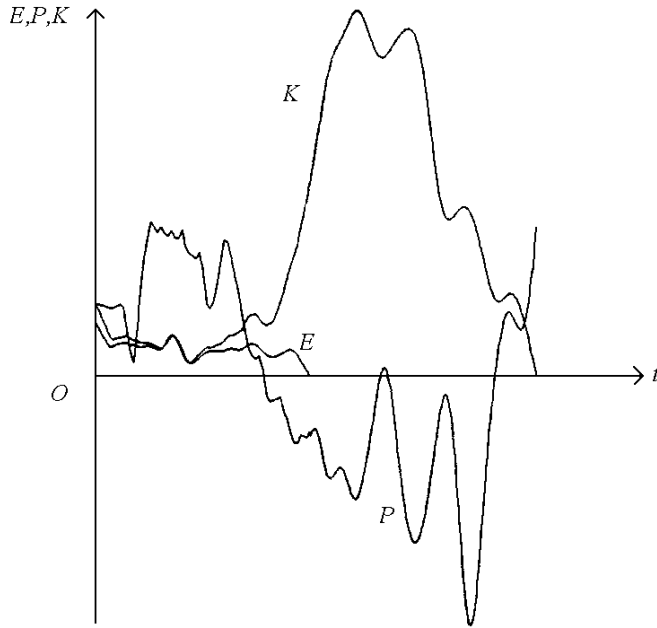


Figure 4.22: Calculated acceleration force E , string force K and recoil force P as function of time t for the AN bow. The calculation is stopped when the force in the string K becomes zero.

realistic model of it.

In Figure 4.24 we show a bow with a straight rigid limb ST_1 , referred to as a SB bow (Figure 4.24.a) and a static-recurve bow with a rigid limb ST_2 possessing a sharp bend at T_1 , called a CB bow (Figure 4.24.b)

The half length of the grip is denoted by \bar{L}_0 . The rigid limb is connected to this grip by means of the elastic hinge S of strength $\bar{k} > 0$. The moment of inertia of the limb with respect to S is in both cases \bar{J} . The length of the limb is denoted by L_1 , measured in the case of a CB bow along the limb ST_{12} . The string of half length \bar{l} is inextensible and without mass.

The angle φ denotes for both types of bows the angle between ST_1 and the \bar{y} -axis and α is the angle between the string and this \bar{y} -axis, both angles positive as indicated in Figure 4.24. For $\varphi = \varphi_0$ we have the unbraced situation, hence φ_0 is the angle of zero moment of the elastic hinge. In the braced situation $\bar{b} = |\overline{OH}|$ the angle φ is denoted by $\varphi_{1/2}$ and in the fully drawn situation $\bar{b} = |\overline{OD}|$ we have $\varphi = \varphi_1$ and $\alpha = \alpha_1$.

In the case of a CB bow, because of the sufficiently strong bend in the limb, the string lies along T_1T_2 in the braced situation. If such a bow is drawn, at a certain moment the string leaves the bridge at T_1 and the string has contact with the bow only at T_2 . The angle φ in that situation is denoted by φ_b . The action of a CB bow can be described by the action of two SB bows, one for $\varphi < \varphi_b$ and the other for $\varphi > \varphi_b$. These two SB bows are referred to as the SB_1 bow and SB_2 bow, respectively. The length of the grip, strength of the hinge and moment of inertia of the limb are for both bows the same as those of the CB bow. The length of the limb of the SB_1 bow equals the distance ST_1 in the case of the CB bow, the half length of the string is $\bar{l} - |\overline{T_1T_2}|$ and the angles φ_0 , $\varphi_{1/2}$ and φ_1 are equal

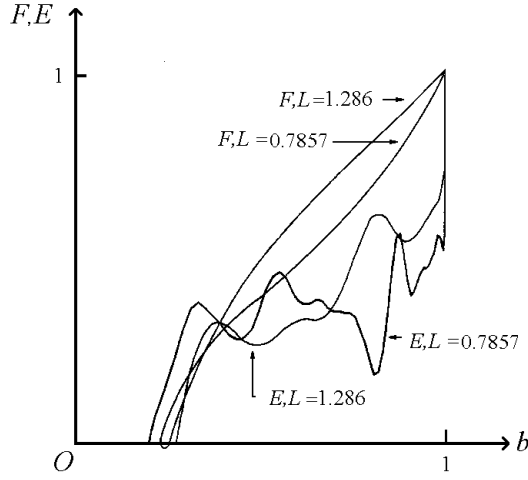


Figure 4.23: SFD and DFD curves of AN bow, different lengths, Table 4.19.

to the corresponding ones of the CE bow. For the SE bow, the length of the limb equals $|\overline{ST}_2|$, the half length of the string \bar{l} , φ_0 is the angle between the \bar{y} -axis and the line ST_2 of the CE bow in unbraced situation while \bar{b} in fully drawn position equals $|\overline{OD}|$ of the CB bow.

Note that it is not the intention to give a model for a bow, like the H model or M model dealt with in Section 4.6. In that case we should have to give rules to determine strength and place of the elastic hinge and moment of inertia of the limb from the dimensions of the bow and the distributions of the bending stiffness and mass along the elastic limbs.

Also in this section we introduce dimensionless quantities. As unit of mass we use $15\bar{J}/\bar{L}^2$ (this value corresponds with the mass of one flexible limb, with the use of the H model, see Section 4.6). The weight $\bar{F}(|\overline{OD}|)$ and draw $|\overline{OD}|$ are used as unit of force and length, respectively. Again we drop the bar in the case of dimensionless quantities, for instance $\bar{L}_1 = L_1 |\overline{OD}|$.

The static quality coefficient q (4.82) for a SB bow can be calculated as

$$q = \frac{(\varphi_1 - \varphi_0)^2 - (\varphi_{1/2} - \varphi_0)^2}{\varphi_1 - \varphi_0} \frac{L_1 \sin(\varphi_1 + \alpha_1)}{2 \sin \alpha_1}. \quad (4.113)$$

The two factors at the right hand side of equation (4.113) have a simple physical meaning. The first factor is the energy put into the two elastic hinges by bringing the bow from the braced situation ($\varphi = \varphi_{1/2}$) into the fully drawn position ($\varphi = \varphi_1$) divided by the moment exerted on one hinge at full draw.

In Figure 4.25 we draw the moment action upon the hinge as a function of φ , divided by the final moment in the fully drawn situation for two SB bows only differing in their value φ_0 . The first factor in (4.113) equals the area below this line between $\varphi = \varphi_{1/2}$ and $\varphi = \varphi_1$, shaded in Figure 4.25. We conclude that the smaller the angle φ_0 the larger the first factor in (4.113), and therefore the q when all the other parameters are taken the same.

The numerator in the second factor is the distance between the string and hinge in fully drawn position. The $\sin \alpha$, in the denominator of the second factor enters in the formula

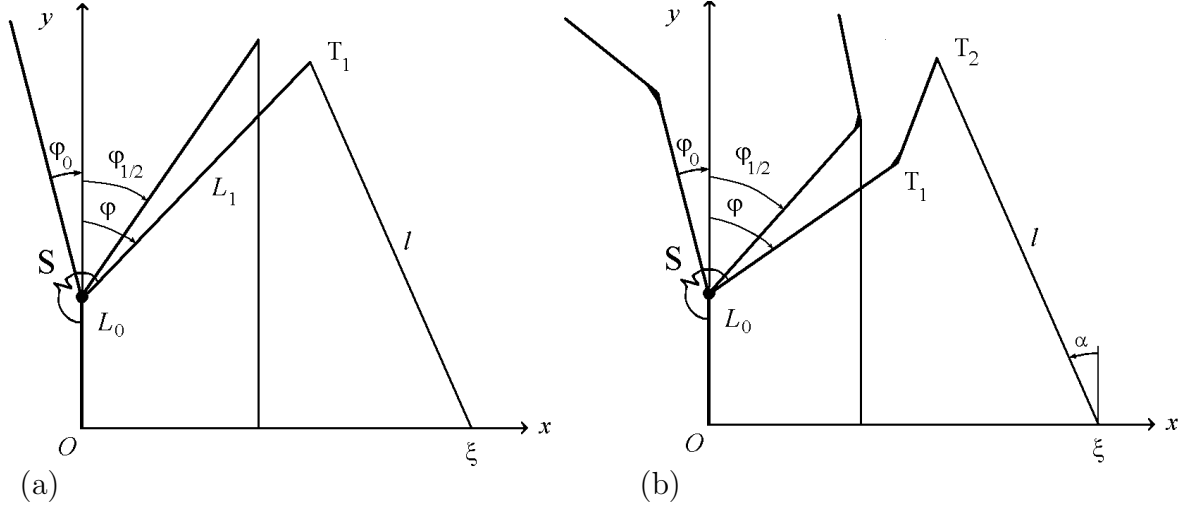


Figure 4.24: Bows with two elastic hinges and rigid limbs: (a) SB and (b) CB bow.

because we are interested in the amount of energy per weight and not per force in the string in fully drawn situation. The larger L_1 , the larger the second factor and it appears that q shows the same tendency. This is, however, not clear beforehand because also the first factor changes for different values of L_1 .

Equation (4.113) holds also for a CB bow. In that case the parameters occurring in (4.113) belong to the SB₂ bow except the parameter $\varphi_{1/2}$; its value is the $\varphi_{1/2}$ of the SB₁ bow minus the angle between the lines ST_2 and ST_1 .

In what follows we give the results for one specific SB bow and one CB bow referred to as the bow SB and the bow CB respectively. The characteristic constants of these bows are given in Table 4.20. In this table also those of the bow SB₁ and SB₂ belonging to the bow CB in the manner described above, are given. The other constants are the same for all the bows, they are: $L_0 = 0.4286$, $J = 0.0440$, $m_a = 0.0769$, where m_a is the half mass of the arrow.

In the last column of Table 4.20 we give the static quality coefficients q . Comparison of the bow SB with the bow CB shows a better static performance of the bow CB. Thus, because of the ears we are able to put more energy in the hinges by bringing it from the braced situation into the fully drawn situation. The static quality coefficient of the bow CB appears to be much larger than that of the bow SB₁. For the bow CB the second factor of the right-hand side is larger than that in the case of the bow SB₁, while the first factor is for both bows the same. Often the action of the ears of the static-recurve bow is explained by the leverage of its ears. This explanation fits mentioned effect.

However, we can also compare the static performance of the bow CB with that of a bow called CB₃. The characteristic constants of this bow are also given in Table 4.20. The length L_1 equals that of the bow SB₂ and its neutral position coincides with the y -axis.

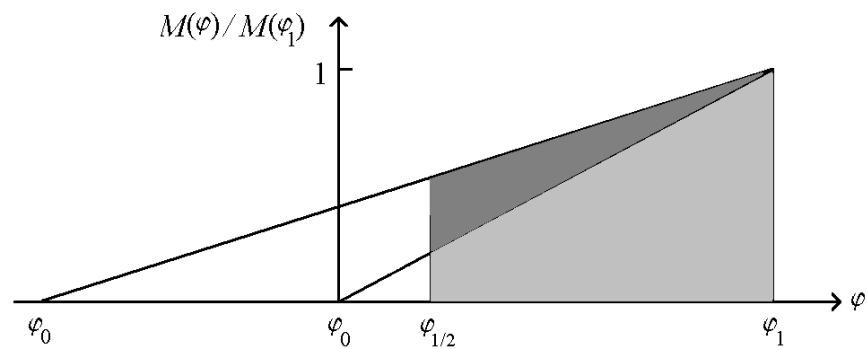
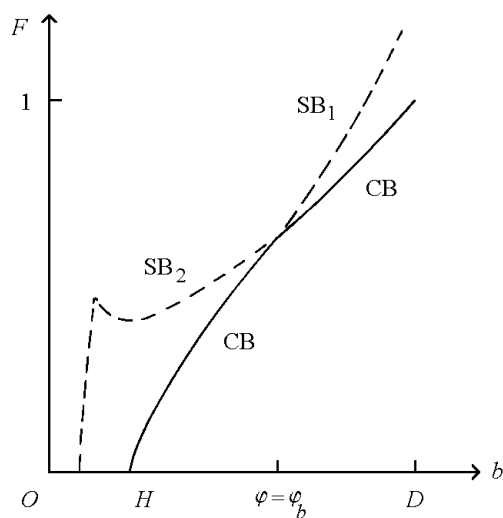
Figure 4.25: Moment M exerted an elastic hinge as function of angle of rotation φ .

Table 4.20: Comparison of different bows.

bow	L_1	$ OH $	$ OD $	l	φ_0	$\varphi_{1/2}$	φ_1	q
SB	0.8571	0.2143	1	—	0	0.2527	0.5852	0.415
CB	0.8571	0.2143	1	—	0	0.3272	0.7308	0.51
SB ₁	0.666	0.2143	0.9623	—	0	0.3272	0.7308	0.392
SB ₂	0.8126	—	1	1.2503	-0.1665	-0.1665	0.5643	0.564
SB ₃	0.8126	0.2143	1	—	0	0.2699	0.6181	0.411

Figure 4.26: SFD curve of CB bow, together with those of SB₁ and SB₂ bow, Table 4.20.

The static quality coefficient of the bow CB_3 is also larger than that of the bow SB_3 . In this case it is due to a larger first factor of the right-hand side of (4.113), while the second factor is now equal for both bows CB and SB_3 . In this way it is justified to state that the good static performance of the bow CB is due to the effective set back of the limbs in unstrung situation.

In Figure 4.26 we show the SFD curve of the bow CB . The dashed lines complete the SFD curves of the bows SB_1 and SB_2 . The SFD curve of the bow CB is more convex than that of the bow SB_1 indicating that its static coefficient is larger. The bow SB_2 possesses no braced situation because for this bow $l - L_0 < L_1$; thus $\varphi_{1/2} = \varphi_0 = -0.1665$. From Figure 4.26 we conclude that the static quality coefficient of this bow is extreme large, it appears to be 0.564. However, this SB_2 bow has a very bad dynamic performance as we will see.

In [9] we showed that the efficiency of the bows SB , CB , SB_1 and SB_3 equal 1. Thus for these bows all the energy put into the bow by the archer in bringing it from the braced situation into the fully drawn situation, is used to propel the arrow. For the SB_2 bow we have, as said before, $l - L_0 < L_1$, hence one of the requirements stated in [9] to ensure $E(b) \leq 0$ for $|OH| < b < |OD|$ is violated. In Figure 4.27 we draw the DFD curves of the bows CB , SB_1 and SB_2 and it appears that the acceleration force E acting upon the arrow becomes negative for some $b > |OH|$ in the case of the bow SB_2 . From Figure 4.27 we conclude that in the case of the SB_2 bow less energy is transferred to the arrow (the amount ηq imparted to the arrow equals the area below the DFD curve) than in the case of the CB bow. This despite the fact that more energy is available.

Figure 4.27 shows further a discontinuity at the time φ equals φ_b thus with the transition of SB_2 to SB_1 , of the acceleration force E . We recall that the velocity of the arrow \dot{b} is continuous during this transition (see [9]). So, at that time $t = t_b$ we have a situation which resembles the situation at $t = 0$; if we take an elastic string then the discontinuity disappears.

Because of the presence of the ears we expect that the DFD curve of a static-recurve bow with an elastic string and elastic limbs oscillates, at least for a model without damping. But if we replace the elastic limbs by rigid ones then, because of the added mass at the tip of the rigid limb in order to account for the mass of the limb, these oscillations will be too heavy as in the case of the M model. Therefore we do not elaborate this model further. However, these dynamic considerations show that we have to reckon with the possibility of a sharp alternation of the acceleration force E or even a discontinuity, when an inextensible or nearly inextensible string touches the string bridges of the static-recurve bow again.

In the next section we deal with these static-recurve bows with continuously distributed elasticity of the working part of the limbs. The ears remain rigid. Because the string is assumed to be elastic, the expected difficulties with respect to the use of a finite-difference method when the solution varies fast or even discontinuous as function of time, do not occur using the method described in Section 4.4.

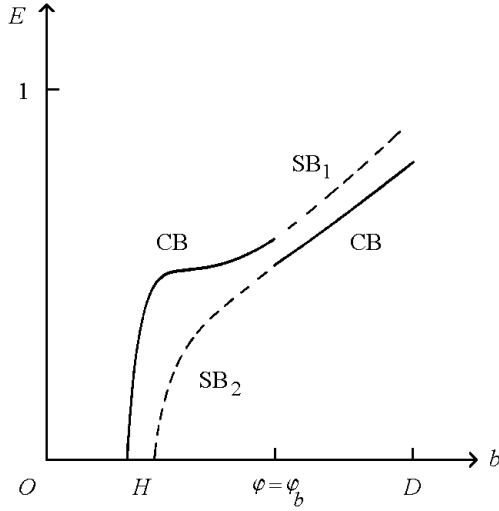


Figure 4.27: DFD curve of CB bow, together with those of SB_1 and SB_2 bow, Table 4.20.

4.11 Static-recurve bow

In this section we examine the influence of the rigid ears of static-recurve bows. To do this, we could change one by one the nine parameters (4.2) which determine the action of the ears. These parameters are: coordinates of centre of gravity (x_{cg0}, y_{cg0}) coordinates of the string bridge (x_{b0}, y_{b0}) coordinates of the tip where the string is attached to the bow (x_{t0}, y_{t0}) , mass m_e , moment of inertia J_e with respect to centre of gravity and the coordinates of this place at which the ear is attached to the elastic limb, which follows from L_2 . This would consume a tremendous amount of computing time and would yield an unsurveyable amount of information. Moreover, the other parameters mentioned in (4.2) affect the static and dynamic performance of the bow as well. Therefore we consider a static-recurve bow with features fixed by only a few parameters which remain to define. A change of these new parameters corresponds with a simultaneous change of some of the parameters and functions given in (4.2). We hope that the bows discussed here will reveal already the specific properties of the static-recurve bow. For the selection of the new parameters we were guided by figures and other data given in several books and papers [14, 10, 4, 1].

As we mentioned earlier in the introduction to this paper, the old static-recurve bow are mostly composite bows. Such a bow is formed by the union of staves of wood and horn combined with sinew. This makes it difficult to determine the bending stiffness along the elastic line which represents in our model the working part of the limb. Further, the place where the grip ends and the limb starts (L_0) and where the elastic working part ends and the ear starts (L_2) are not fixed unambiguously, because for real bows the transitions are gradual.

The results given in this section are obtained by using the model for the static-recurve bow given in Section 4.3, which adds parts of the mass of the string as concentrated masses to arrow and tip. In Section 4.7 we found that the use of such a model for the string causes some inaccuracy in the case of the straight-end bow and possibly this will also be the case

for the static-recurve bow.

In Figure 4.28 we show the unbraced, braced and fully drawn situation of the type of static-recurve bow which is the main theme of this section. The ear is made up of two straight, rigid pieces each of length $1/2L_e$, where L_e is the length of the ear; $L_e \stackrel{\text{def}}{=} L - L_2$. The angle between those two pieces is denoted by θ_t , reckoned positive in the indicated direction. The ear starts in a direct line with the end of the working part of the limb, of which the unbraced shape is given by

$$\theta_0(s) \equiv 0, \quad 0 \leq s \leq L_0, \quad \theta_0(s) = \theta_0(L_0) + \kappa_0 \frac{s - L_0}{L_2 - L_0}, \quad L_0 \leq s \leq L_2. \quad (4.114)$$

The limb is set back in the grip at an angle $-\theta_0(L_0)$ (the set back is positive as $\theta_0(L_0) < 0$) and the working part of the limb coincides with a part of a circle with curvature $\kappa_0/(L_2 - L_0)$.

The distributions of the bending stiffness and mass are

$$W(s) = W(L_0) \frac{L - s}{L - L_0}, \quad L_0 \leq s \leq L_2, \quad (4.115)$$

and

$$V(s) = V(L_0) \frac{L - s}{L - L_0}, \quad L_0 \leq s \leq L_2, \quad (4.116)$$

respectively. The mass distribution along the ear, $L_2 \leq s \leq L$, is chosen to be constant and equal to $V(L_2)$. The mass m_e and moment of inertia J_e of the ear with respect to its centre of gravity are given by

$$m_e = V(L_2)L_e, \quad (4.117)$$

and

$$J_e = m_e(1/12 + (1 + \cos \theta_t))(1/2L_e)^2, \quad (4.118)$$

respectively. Note that $V(L_0)$ is now fixed by the requirement

$$m_b = \int_{L_0}^{L_2} V(s)ds + m_e = 1. \quad (4.119)$$

This type of bow in unbraced position is entirely determined by the parameters L_e , θ_t , $\theta_0(L_0)$, κ_0 , L and the coordinates $x_0(L_0)$, $y_0(L_0)$ of the end points of the grip, being equal to 0 and L_0 , respectively. The coordinates of the point where the working part of the limb is connected without bend to the ear are

$$x_0(L_2) = \int_{L_0}^{L_2} \sin\{\theta_0(L_0) + \kappa_0 \frac{s - L_0}{L_2 - L_0}\} ds, \quad (4.120)$$

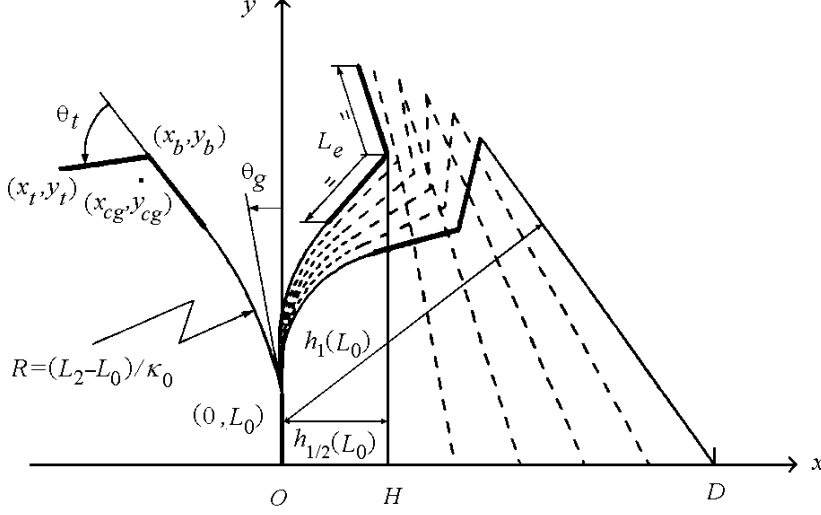


Figure 4.28: A static-recurve bow in various situations.

and

$$y_0(L_2) = L_0 + \int_{L_0}^{L_2} \cos\{\theta_0(L_0) + \kappa_0 \frac{s - L_0}{L_2 - L_0}\} ds, \quad (4.121)$$

For the other mentioned coordinates we find

$$x_{b_0} = x_0(L_2) + 1/2 L_e \sin(\theta_0(L_2) + \kappa_0), \quad (4.122)$$

$$y_{b_0} = y_0(L_2) + 1/2 L_e \cos(\theta_0(L_2) + \kappa_0), \quad (4.123)$$

$$x_{t_0} = x_0(L_2) + 1/2 L_e \{(1 + \cos \theta_t) \sin(\theta_0(L_2) + \kappa_0) - \sin \theta_t \cos(\theta_0(L_2) + \kappa_0)\}, \quad (4.124)$$

$$y_{t_0} = y_0(L_2) + 1/2 L_e \{(1 + \cos \theta_t) \cos(\theta_0(L_2) + \kappa_0) - \sin \theta_t \sin(\theta_0(L_2) + \kappa_0)\}, \quad (4.125)$$

$$x_{cg_0} = 1/4(x_{t_0} + 2x_{b_0} + x_0(L_2)), \quad (4.126)$$

$$y_{cg_0} = 1/4(y_{t_0} + 2y_{b_0} + y_0(L_2)). \quad (4.127)$$

We now introduce a bow, denoted by PE which, using the notation of (4.2) is defined by

$$\begin{aligned} & \text{PE}(1.000, 0.1429, W, V, \theta_0 \equiv 0, 0.0769, 0, 0, 0.4, 0.0025, 0, \\ & -0.0464, 0.7589, 0, 0.7857 - 0.1856, 0.8929, 0.5714, 131, 0.0209, 0.25; \\ & 1, 1, 1). \end{aligned} \quad (4.128)$$

The functions $W(s)$ and $V(s)$ are given by (4.115) and (4.116), respectively, with $W(L_0) = 0.2304$, and $V(L_0) = 1.867$. The parameters L_0 , m_a , U_s and m_s are equal to their values

Table 4.21: Energy in parts of PE bow in a number of situations.

energy	limbs		string		total bow		arrow kin.
	pot.	kin.	pot.	kin.	pot.	kin.	
braced	0.1515	0	0.0100	0	0.1625	0	0
fully drawn	0.5879	0	0.0053	0	0.5932	0	0
arrow exit	0.1271	0.0980	0.0506	0.0279	0.1777	0.1271	0.2884

in the case of the KL bow defined in (4.102), the brace height $|OH|$ is now 0.25 instead of 0.214, the length L is 1 instead of 1.286.

This bow will be used as a starting point for changing parameter values. The five parameters which can be calculated from (4.128) are: $L_e = 0.428$, $\theta_t = 60^\circ$, $\theta_0(L_0) = 0$, $\kappa_0 = 0$, $L = 1.000$. The unbraced, braced and fully drawn situation of the PE bow are shown in Figure 4.29. The computed quality coefficients of it are; $q = 0.432$, $\theta = 0.668$ and $\nu = 1.94$. In Figure 4.30 we give the SFD curve and the DFD curve and in Table 4.21 the amounts of energy in the different parts of the PE bow for a number of situations. In the following we still call a bow a PE bow when 'some' of its parameters have been altered, the not mentioned parameters are tacitly assumed to be equal to the original ones. A comparison of the performance of the PE bow with that of the KL bow dealt with in Section 4.9, shows that there is more energy available in the fully drawn PE bow ($q = 0.432; q = 0.407$). However, the efficiency of the PE bow is much lower ($\eta = 0.668; \eta = 0.765$) and this causes a smaller dimensionless muzzle velocity ($nu = 1.94; \nu = 2.01$). Further, the amount of energy in the braced PE bow is larger than that in the braced KL bow (see Table 4.8) ($A_H = 0.1575; A_H = 0.0950$). However, it is interesting to note that the energy in its string is smaller (0.010;0.0276). This is partly due to the difference in length of the strings but also to the force K in the string of the braced PE bow, being smaller than K in case of the KL bow (1.19;1.71). Thus in spite of the fact that there is more potential energy in the limbs in braced situation of the PE bow, the force in its string is smaller. We shall return to this subject later.

The SFD curve of the PE bow (Figure 4.30) possesses a bend at the moment the string leaves the string bridges, just as the SFD curve of the CB bow dealt with in the previous section (see Figure 4.26). The rate of increase of the force $F(b)$ is during the final part of the draw much smaller than during the first part, in which the string has contact with the bridge. This agrees with [10, page xxvii]:

'When the bow was about half drawn, the rigid end-pieces (or ears) began to act as levers so that the draw could be continued with less increase in the weight than would have been the case without them.'

For the PE bow the string leaves the bridge when $b \approx 0.5$.

The DFD curve of the PE bow oscillates. This oscillating behaviour of the acceleration force $E(b)$ resembles the behaviour shown in Figure 4.18 where we investigated the influence

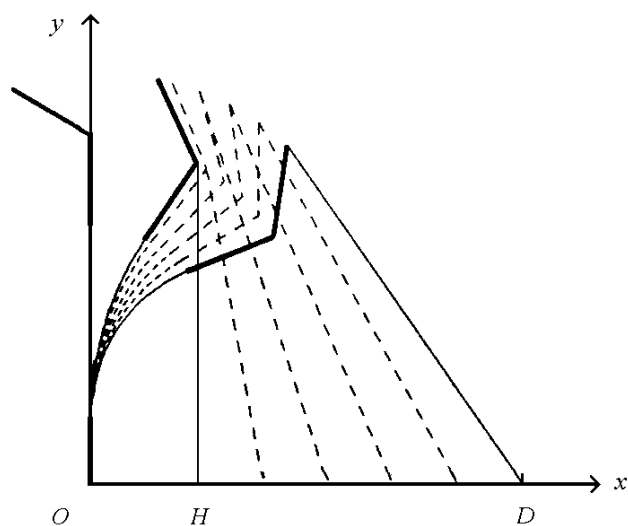


Figure 4.29: PE bow in various situations.

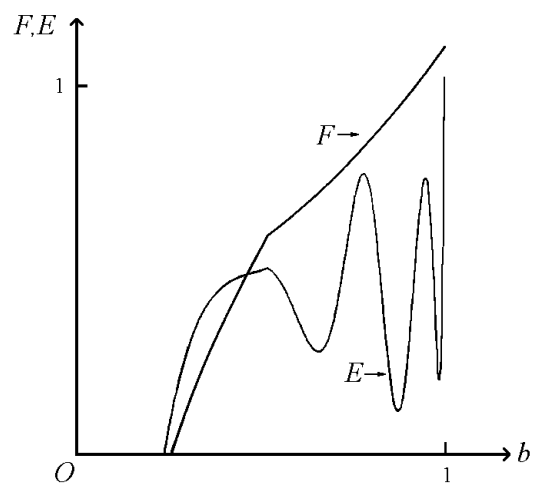


Figure 4.30: SFD and DFD curve of PE bow.

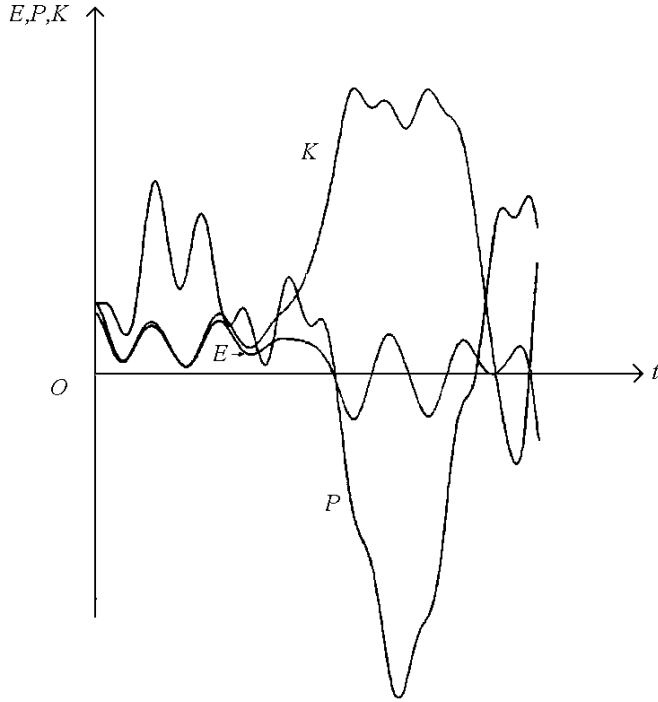


Figure 4.31: $E(t)$, $K(t)$ and $P(t)$ for PE bow.

of the presence of concentrated masses at the tip. The jump $F(|OD|) - E(0)$ is due to the model for the string we use in this section. To the mass $2m_a$ of the arrow we added $2/3m_s$ which gets the same acceleration as the arrow, hence the acceleration force at the arrow for $t = 0$, $E(0)$ equals $m_a/(m_a + 1/3m_s)$. From Figure 4.30 we conclude that the static-recurve bow PE imparts its energy less smooth to the arrow than the \tilde{H} and KL bow. The tensile force in the string K and the recoil force P have the same behaviour as can be seen in Figure 4.31 where we show the three function $E(t)$, $K(t)$ and $P(t)$. The maximum tensile force in the string equals 4.0; this is lower than in the case of the KL bow where it was 4.3. The maximum recoil force for $t \leq t_l$ is larger; 2.7 for the PE bow and 2.3 for the KL bow. After the arrow has left the string, the recoil force P reaches the value -4.5 . The force in the string becomes negative after the peak, so for our computing program we have STOP=1 (Section 4.9)

In what follows we change the parameters θ_t , L , $\theta_0(L_0)$ and κ_0 . Instead of L_e we consider as a parameter this length divided by the length of the limb, thus $L_e/(L - L_0)$ will be changed. The behaviour of the recoil force P and of the tensile force K will be discussed if it differs significantly from that in the case of the PE bow

First we change only the angle θ_t . Table 4.22 gives the static quality coefficients for the PE bow with varying θ_t . Starting with $\theta_t = 0$ the static quality coefficient q increases with increasing θ_t , it passes a maximum in the range $55^\circ \leq \theta_t \leq 65^\circ$ after which it diminishes again. In Figure 4.32 we show the SFD curves of PE bows with $\theta_t = 0^\circ$, $\theta_t = 30^\circ$ and $\theta_t = 60^\circ$. For $\theta_t = 0^\circ$ we have a straight bow and the string has no contact with the string bridge in all situations. This is also the case for the PE bow with $\theta_t = 30^\circ$ as can be seen in Figure 4.33, in which we show the shape of this bow in various situations. Therefore the

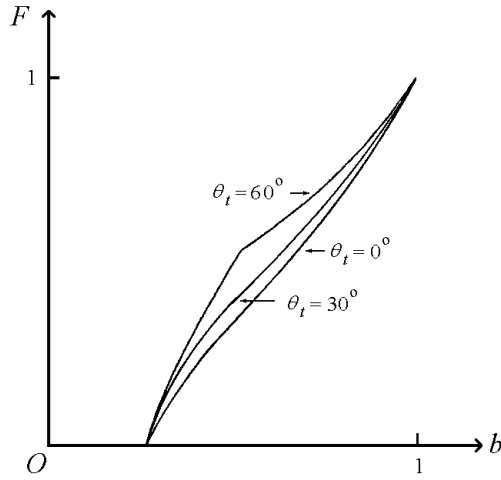


Figure 4.32: SFD curves for PE bow with $\theta_t = 0^\circ$, $\theta_t = 30^\circ$ and $\theta_t = 60^\circ$, Table 4.22.

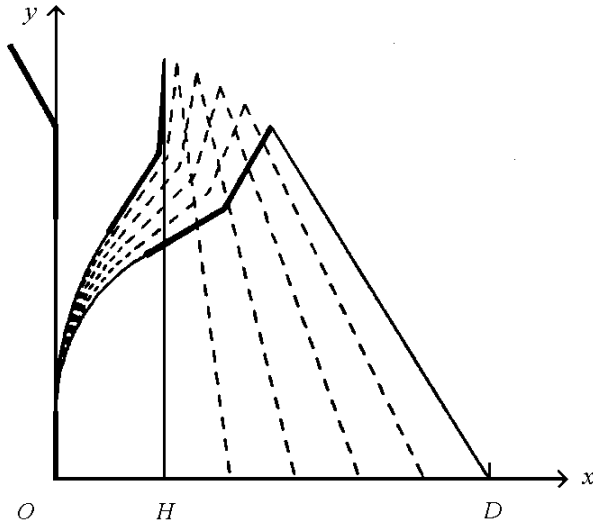


Figure 4.33: PE bow with $\theta_t = 30^\circ$ in various situations.

SFD curves in Figure 4.32 of these two bows with $\theta_t = 0^\circ$ and $\theta_t = 30^\circ$ increase without a bend.

The dynamic quality coefficients of the PE bow with $\theta_t = 0^\circ, 30^\circ, 45^\circ, 60^\circ$ and 75° are given in Table 4.23 ($L = 1.000$). In the range $30^\circ \leq \theta_t \leq 60^\circ$ the efficiency decreases with increasing angle θ_t . This negative influence is so large that it overshadows the positive influence of a larger θ_t on the static performance (Table 4.22). The maximum muzzle velocity and also the maximum amount of energy imparted to the arrow, of which the mass is given in (4.128), is obtained for $\theta_t = 30^\circ$.

In Figure 4.34 we give the DFD curves of the PE bows with $\theta_t = 0^\circ$, $\theta_t = 30^\circ$ and $\theta_t = 60^\circ$. The oscillations of the DFD curve for the bow with $\theta_t = 0^\circ$ are slightly less than those in the case of the bow with $\theta_t = 60^\circ$.

The second parameter we change is the length $2L$ of the bow. In Table 4.23 we give the results for $L = 1.286, 1.000$ and 0.7857 . We changed also the angle θ_t .

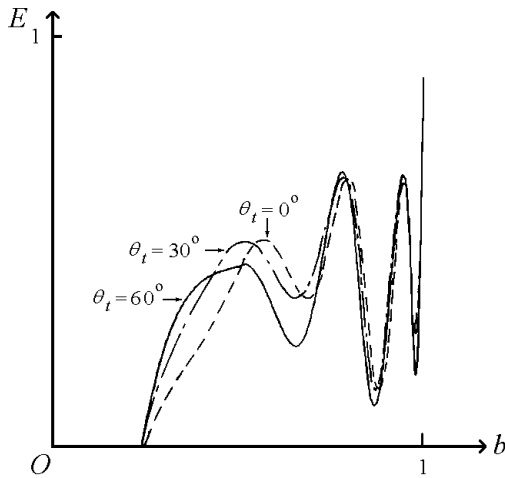
Table 4.22: Influence of angle θ_t on static quality coefficient q .

θ_t	0°	15°	30°	45°	55°	60°	65°	75°	90°
q	0.373	0.387	0.397	0.419	0.430	0.432	0.431	0.423	0.396

Table 4.23: Influence of length L and angle θ_t on PE bow.

L	1.286				1.000					0.7857			
θ_t	0°	30°	45°	60°	0°	30°	45°	60°	75°	0°	30°	45°	60°
$W(L_0)$	1.076	.7982	.6761	1.409	.3873	.3061	.2669	.2304	.1960	.1069	.0891	.0754	.0640
$V(L_0)$	1.4	1.4	1.4	1.575	1.867	1.867	1.867	1.867	1.867	2.489	2.489	2.489	2.489
q	0.400	0.441	0.470	0.407	0.373	0.397	0.419	0.432	0.423	0.301	0.314	0.310	0.314
η	0.770	0.740	0.652	0.765	0.782	0.788	0.730	0.668	0.693	0.796	0.809	0.789	0.723
ν	2.00	2.06	2.00	2.01	1.95	2.02	2.00	1.94	1.95	1.77	1.82	1.79	1.72

In the case of the longest bow, $L = 1.286$, q attains its maximum in the neighbourhood of $\theta_t = 45^\circ$ instead of 60° for the PE bow with $L = 1.000$. The difference for each length $L = 1.286$, $L = 1.000$ and $L = 0.7857$ between the value of q for $\theta_t = 0^\circ$ and the maximum q is 0.070, 0.059 and 0.013, respectively. It follows that for longer bows the influence of θ_t on q is larger. Possibly this decrease in the differences is caused not only by the change of length L , but also by the decrease of the length of the ears L_e when the bow becomes shorter; $L_e = 1/2(L - L_0)$ in all the cases. Further, this maximum value of q diminishes with decreasing length L , being 0.470, 0.432 and 0.314, respectively. In the case of the shortest bow the static quality coefficient as function of θ_t attains two maxima, one in the range $0^\circ \leq \theta_t \leq 45^\circ$ and another in $45^\circ \leq \theta_t \leq 75^\circ$. The SFD curves of the four bows with the greatest values of q for each length are shown in Figure 4.35. The configurations of

Figure 4.34: DFD curves for PE bow with $\theta_t = 0^\circ$, $\theta_t = 30^\circ$ and $\theta_t = 60^\circ$, Table 4.23. For SFD curves see Figure 4.32.

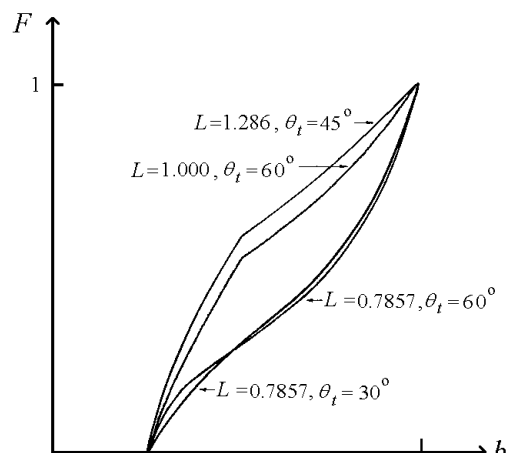


Figure 4.35: SFD curves for PE bow, different lengths and angle θ_t , Table 4.23.

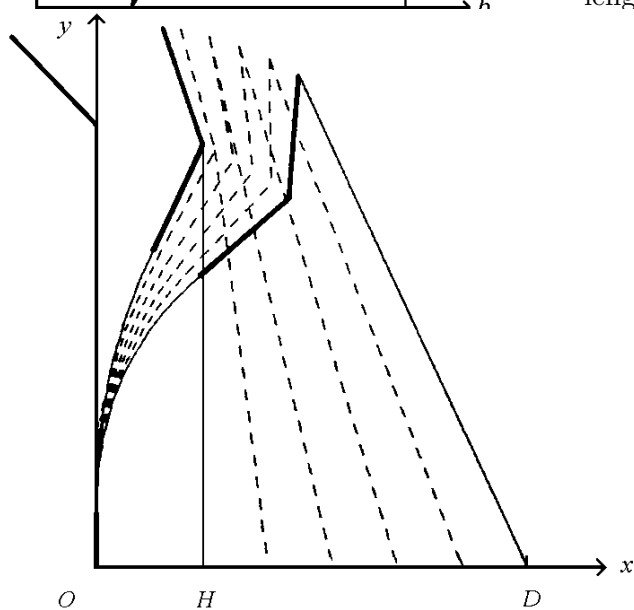


Figure 4.36: PE bow with $L = 1.286$, $\theta_t = 45^\circ$ in various situations.

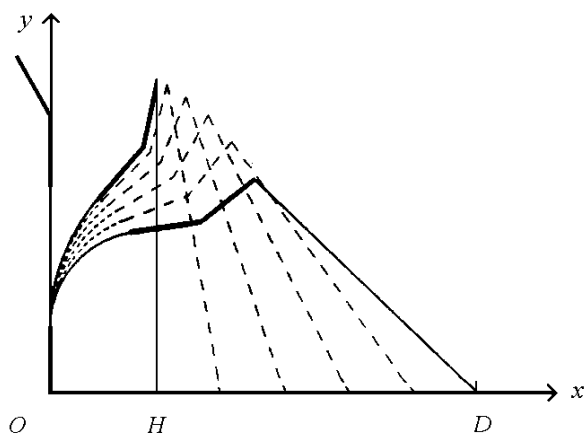


Figure 4.37: PE bow with $L = 0.7857$, $\theta_t = 30^\circ$ in various situations.

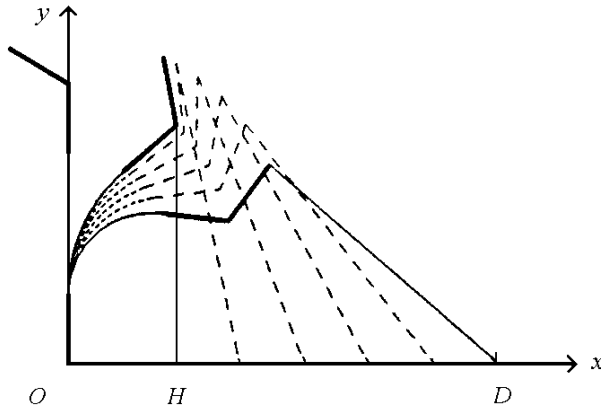


Figure 4.38: PE bow with $L = 0.7857$, $\theta_t = 60^\circ$ in various situations.

three of these bows, $L = 1.286$, $\theta_t = 45^\circ$ and $L = 0.7857$, $\theta_t = 30^\circ$ and $\theta_t = 60^\circ$ in various positions are shown in Figure 4.36, Figure 4.37 and Figure 4.38, respectively. The one with $L = 1.000$, $\theta_t = 60^\circ$ was already shown in Figure 4.29. Note that the angle between the string and the y-axis is rather large for the shortest bows $L = 0.7857$ (Figure 4.37 and Figure 4.38). This has a negative influence on the static performance of these bows.

For dynamics, changing θ_t has more influence on the efficiency in the case of longer bows, $L = 1.286$ and $L = 1.000$. In these cases the values of η for $\theta_t = 0^\circ$ are 0.118, 0.114, better than the values of η for which q is maximum. For the shortest bow $L = 0.7857$ with $\theta_t = 30^\circ$ the efficiency η is slightly better, while for $\theta_t = 60^\circ$, η is 0.073 smaller than η for $\theta_t = 0^\circ$. The DFD curves for the PE bow with $L = 1.286$, $\theta_t = 45^\circ$, $L = 1.000$, $\theta_t = 60^\circ$ and $L = 0.7857$, $\theta_t = 60^\circ$ are given in Figure 4.39. The oscillations of the DFD curve of the shortest bow are more intense than those of the PE bow. The acceleration force E becomes even negative for short intervals of time. In the simple mathematical model for the string (third paragraph of this section), which we use in this section, the string is able to withstand negative tensile forces. We did not apply STOP=1 for this calculation, but assumed that the arrow sticks to the string at those short intervals of time and leaves the string when it becomes stretched.

Just as for the bow of length $L = 1.000$ we find that also for bows of length $L = 1.286$ and $L = 0.7857$ the greatest muzzle velocity ν is obtained with $\theta = 30^\circ$. For $L = 1.286$ this is a bow where the string leaves the bridge almost immediately when it is drawn. For $L = 0.7857$ we have for $\theta_t = 30^\circ$ the same situation as for $L = 1.000$. The string has no contact with the string bridge in all situations, see Figure 4.37. In Figure 4.40 the DFD curves of the bows with $\theta_t = 30^\circ$ and different lengths are shown. The shapes of these curves resemble strongly those given in Figure 4.39 and the same remark has to be made with respect to the negative tensile force in the string.

We shorten now the relative length of the ear with respect to the length of the limb ($L - L_0$). In Table 4.24 we give the results. As expected, the static quality coefficients

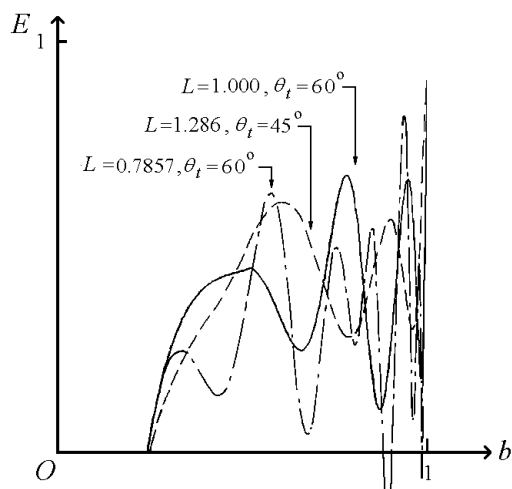


Figure 4.39: DFD curves of PE bow, different lengths and angle θ_t , Table 4.23.

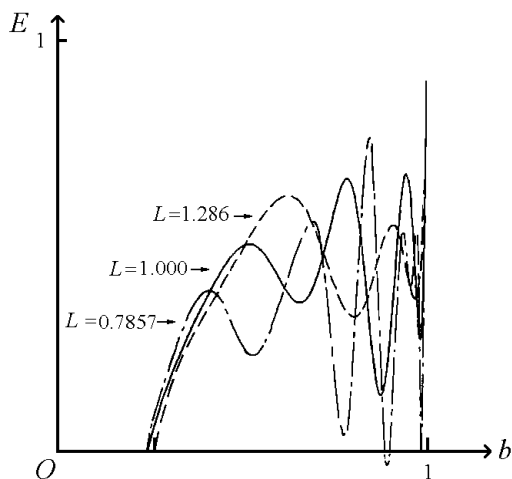


Figure 4.40: DFD curves of PE bow, $\theta_t = 30$ and different lengths, Table 4.23.

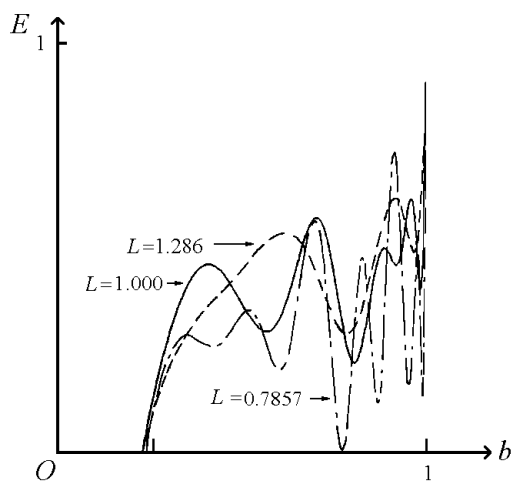


Figure 4.41: DFD curves of PE bow, short and light ears, $\frac{L_t}{L-L_0} = 1/3$, Table 4.24.

Table 4.24: Influence of the quotient $\frac{L_e}{L-L_0}$ on the performance of the PE bow.

L	1.286		1.000		0.7857	
θ_t	45°	45°	60°	60°	60°	60°
$L_e/(L - L_0)$	1/2	1/3	1/2	1/3	1/2	1/3
$W(L_0)$	0.6761	0.9222	0.2304	0.3140	0.0640	0.820
$V(L_0)$	1.4	1.575	1.867	2.100	2.489	2.800
q	0.470	0.445	0.432	0.408	0.314	0.296
η	0.652	0.719	0.668	0.753	0.723	0.784
ν	2.00	2.04	1.94	2.00	1.72	1.74

are smaller than those which belong to the corresponding bows with longer ears, for the three bow lengths. But the efficiencies are much better and this produces a somewhat higher muzzle velocity. In Figure 4.41 we show the DFD curves of the bows mentioned in Table 4.24 with $L_e = 1/3(L - L_0)$, those having relatively short ears. Comparison of these curves with those given in Figure 4.39 reveals that the amplitude of the oscillations is smaller for shorter and hence lighter ears. We conclude from these results that it is advantageous to use long but also light ears. Technical limitations determine of course what is realizable.

We now direct our attention to the influence of the two parameters $\theta_0(L_0)$ and κ_0 , which determine the set back and the curvature of the working part of the limb, see Equation (4.114). First we deal with PE bows with a straight working part of the limb, $\kappa_0 = 0$, set back in the grip at an angle $-\theta_0(L_0)$. The quality coefficients are given in Table 4.25. A negative angle $\theta_0(L_0)$, thus a positive set back, appears to be advantageous both for statics and dynamics. Second, we consider PE bows with $\kappa_0 = 0$, $\kappa_0 = -1$ and $\kappa_0 = -2$. In Table 4.26 we give the quality coefficients q , η and ν of these bows. Of these three bows the strongest curved one $\kappa_0 = -2$ possesses the largest static quality coefficient q . Notwithstanding its smallest efficiency, its muzzle velocity is the best $\nu = 2.01$. For $\kappa_0 = -1$ and $\kappa_0 = 0$ we find $\nu = 1.99$ and $\nu = 1.94$, respectively. In Table 4.26 we changed for $L = 1.000$ and $\kappa_0 = -1$ also the angle θ_t . The difference between the static quality coefficients for $\theta_t = 0^\circ$ and $\theta_t = 30^\circ$ is much smaller than in the case $\kappa_0 = 0$, see Table 4.23.

The muzzle velocity ν for $\theta_0 = 30^\circ$ is the best, just as in the case of a straight working part of the limb, $\kappa_0 = 0$. However, now the range of ν with changing θ_t is smaller. Thus the shape of the ear as a function of θ_t is less important for a bow with a curved flexible part.

Further, we changed for $\kappa_0 = -1$ the length of the bow. The static quality coefficients of the bows with $\kappa_0 = -1$ are unquestionably better than those of bows with $\kappa_0 = 0$ with same length L and angle θ_t , see Table 4.23. The characteristic behaviour with respect to sharp bends of the SFD curves given in Figure 4.42 resembles that of the bows given in

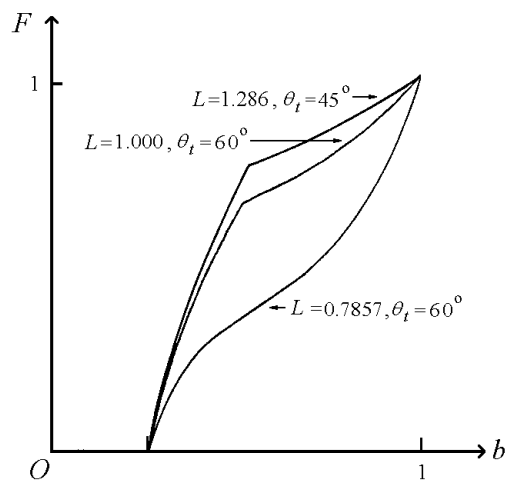


Figure 4.42: SFD curves of PE bow with $\kappa_0 = -1$ different lengths and angle θ_t , Table 4.26.

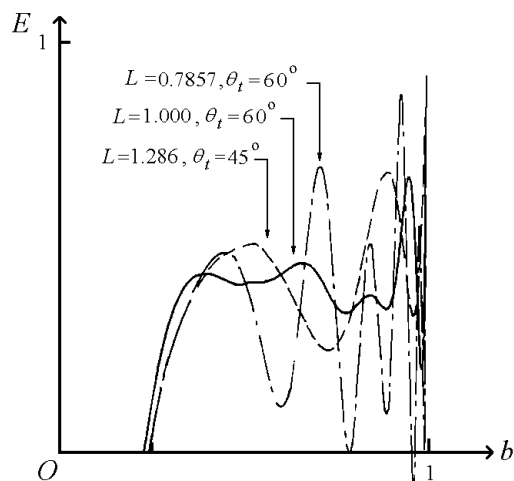


Figure 4.43: DFD curves of PE bow with $\kappa_0 = -1$ different lengths and angle θ_t , Table 4.26. For SFD curves see Figure 4.42.

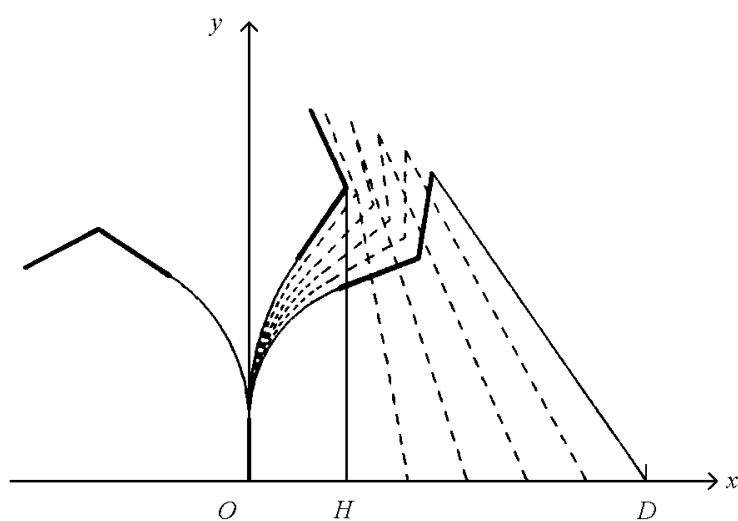


Figure 4.44: PE bow with $\kappa_0 = -1$ in various situation. Note that the braced and the fully drawn position are nearly the same as those given in Figure 4.29 for the PE bow.

Table 4.25: Influence of the angle $\theta_0(L_0)$ on the performance of the PE bow, $V(L_0) = 1.86$.

$\theta_0(L_0)$	-5°	0°	5°
$W(L_0)$	0.2077	0.2304	0.2576
q	0.437	0.432	0.421
η	0.684	0.668	0.648
ν	1.97	1.94	1.89

Figure 4.35. This holds also for the DFD curves given in Figure 4.43 ($\kappa_0 = -1$) compared with the corresponding ones of Figure 4.39 ($\kappa_0 = 0$). The amplitude of the oscillations for the bows with $\kappa_0 = -1$ tend to be slightly smaller. In spite of this, for the longest two bows, $L = 1.286$ and $L = 1.000$, the efficiency of the bow with $\kappa_0 = -1$ is smaller and by this the muzzle velocity is not that amount higher as we expected in connection with the static quality coefficient. For the two static-recurve bows with $L = 0.7857$, $\theta_t = 60^\circ$ the efficiencies are nearly the same, so in these cases a larger q yields a larger muzzle velocity.

The unbraced, braced and fully drawn position of the PE bow with $\kappa_0 = -1$ is shown in Figure 4.44. Note that the braced and the fully drawn position are nearly the same as those given in Figure 4.29 for the PE bow. This appears also to be true for the other two bows with length $L = 1.286$ and $L = 0.7857$. This feature is used in what follows.

We next want to gain insight into the static action of a bow with a strongly curved elastic part of the limb. To this end we compare two bows, the PE bow (4.128), $\kappa_0 = 0$, and a bow named PE^λ . The latter one differs from the PE bow only by its bending stiffness which is $\lambda W(s)$, where λ is some scalar $0 < \lambda \leq 1$, $W(s)$ is given by (4.115) with $W(L_0) = 0.2304$, and the unbraced shape of the flexible part of the limb. For the new bow PE^λ we adhere to the relevant quantities a superscript (λ). The question we will consider is the following; what is the shape of the flexible part of the unbraced PE^λ bow, for which at full draw ($|OD| = 1$) the PE^λ bow has nearly the same shape and weight ($F(|OD|) = 1$) as the PE bow. The strings of both bows are now assumed to be inextensible.

Equation (4.8) gives the relation between the bending moment and curvature along the limb of the PE bow in fully drawn situation.

$$M_1(s) = -W(s)\theta_1'(s), \quad L_0 \leq s \leq L_2. \quad (4.129)$$

For the PE^λ bow (4.8) reads, with $W^\lambda(s) = \lambda W(s)$

$$M_1^\lambda(s) = -\lambda W(s)\{(\theta_1^\lambda)'(s) - (\theta_0^\lambda)'(s)\}, \quad L_0 \leq s \leq L_2. \quad (4.130)$$

The bending moment and curvature in fully drawn situation are in both cases assumed to be the same, so

$$(\theta_0^\lambda)'(s) = \frac{\lambda - 1}{\lambda} \theta_1'(s), \quad L_0 \leq s \leq L_2. \quad (4.131)$$

Table 4.26: Influence of shape of unbraced working part of the limb, $\theta_0(L_0) = 0$.

L	1.286		1.000						0.7857	
θ_t	45°	60°	60°	0°	30°	45°	60°	60°	60°	60°
κ_0	0	-1	0	-1	-1	-1	-1	-2	0	-1
$W(L_0)$	0.6761	0.3173	0.2304	0.1769	0.1563	0.1418	0.1259	0.0867	0.0640	0.0400
$V(L_0)$	1.4	1.4	1.867	1.867	1.867	1.867	1.867	1.867	2.489	2.489
q	0.470	0.535	0.432	0.437	0.445	0.472	0.491	0.511	0.314	0.351
η	0.652	0.575	0.668	0.718	0.710	0.665	0.619	0.604	0.723	0.731
ν	2.00	2.00	1.94	2.02	2.03	2.02	1.99	2.01	1.72	1.63

The curvature of the working part of the limbs of the PE bow and the PE^λ bow appear to be almost constant in fully drawn as well as in braced situation. This means that we can use for the PE^λ bow an unbraced shape which is circular, hence characterized by a number κ_0^λ . In fully drawn situation the curvature is approximated by

$$\theta'_1(s) \approx K_1 h_1(L_0)/W(L_0) \stackrel{\text{def}}{=} \kappa_1/(L_2 - L_0), \quad (4.132)$$

and in the braced situation

$$\theta'_{1/2}(s) \approx K_{1/2} h_{1/2}(L_0)/W(L_0) \stackrel{\text{def}}{=} \kappa_{1/2}/(L_2 - L_0), \quad (4.133)$$

where $h_i(L_0)$ ($i = 1/2, 1$) is the distance between the end point of the grip $(0, L_0)$ and the string (see Figure 4.28), K_i ($i = 1/2, 1$) is as previously the force in the string and κ_i ($i = 1/2, 1$) is the curvature, apart from the factor $1/(L_2 - L_0)$.

The index $1/2$ indicates the braced situation and 1 indicates the fully drawn situation as before. For the values of the quantities on the right-hand side of (4.132) and (4.133) we take values computed by means of our model, in which the limb is considered as a slender elastic beam. These values can also be approximated in a straightforward manner without using our model, but we do not elaborate this. Using (4.132) the κ_0^λ of the PE^λ bow becomes

$$\kappa_0^\lambda = \frac{1 - \lambda}{\lambda} \kappa_1. \quad (4.134)$$

We now give an example. For the PE bow we have: $K_1 = 0.8684$, $h_1(L_0) = 0.725$, $W(L_0) = 0.2304$, $K_{1/2} = 1.188$ and $h_{1/2}(L_0) = |OH| = 0.25$. Then (4.132) and (4.133) yield $\kappa_1 = 1.17$ and $\kappa_{1/2} = 0.55$. For the PE^λ bow we take the one from Table 4.26 with $\theta_0 = 60^\circ$, $L = 1.000$, $\theta_0(L_0) = 0$, $\kappa_0 = -1$, $W(L_0) = 0.1259$. Hence we have to take $\lambda = 0.1259/0.2304 = 0.5464$. Substituting $\lambda = 0.5464$ and $\kappa_1 = 1.17$ in (4.134), we find $\kappa_0^\lambda = -0.97$, which is nearly equal to the correct value -1 given in Table 4.26.

Changing the parameter λ yields a class of bows $\{\text{PE}^\lambda\}$, of which the unbraced form of the flexible part of the limb is a part of a circle with a curvature characterized by

the coefficient κ_0^λ given by (4.134). For bows belonging to this class the static quality coefficient, expressed in κ_0^λ and in some parameters of the PE bow ($\kappa_0^\lambda = 0$), becomes

$$q = \int_{L_0}^{L_2} \frac{W(s)}{(L_2 - L_0)^2} (\kappa_1^2 - \kappa_{1/2}^2 - \frac{\kappa_0^\lambda}{\kappa_1 - \kappa_{1/2}^\lambda} (\kappa_1 - \kappa_{1/2})^2) ds \quad (4.135)$$

by which we assumed, as has been mentioned earlier, the string to be inextensible. For $\lambda = 1$ we have approximately the static quality coefficient of the PE bow again. Equation (4.135) yields $q = 0.430$, $q = 0.499$ and $q = 0.526$ for $\kappa_0 = 0$ ($\lambda = 1$), $\kappa_0 = -1$ ($\lambda = 0.5464$) and $\kappa_0 = -2$ ($\lambda = 0.3763$), respectively. The corresponding exact values from Table 4.26 are $q = 0.432$, $q = 0.491$ and $q = 0.511$, respectively. It follows that Equation (4.135) gives a rather good approximation for the static quality coefficient of a bow belonging to the class $\{\text{PE}^\lambda\}$, anyhow for the character of the dependency of q on κ_0 . From (4.135) we conclude that q increases for decreasing values of κ_0 . We now give an approximation for the force in the string in braced situation for the class of bows $\{\text{PE}^\lambda\}$. The equation of equilibrium of the PE bow in braced situation reads

$$M_{1/2} = K_{1/2} h_{1/2} = -W(s) \theta'_{1/2}, \quad L_0 \leq s \leq L_2, \quad (4.136)$$

and for the bow PE^λ

$$M_{1/2}^\lambda = K_{1/2}^\lambda h_{1/2}^\lambda = -\lambda W(s) ((\theta'_{1/2}^\lambda)'(s) - (\theta_0'^\lambda)'(s)), \quad L_0 \leq s \leq L_2, \quad (4.137)$$

The shape of both bows in braced situation is nearly the same, $(\theta'_{1/2})'(s) \approx (\theta'_{1/2}^\lambda)'(s)$, $L_0 \leq s \leq L_2$. Using (4.133) we get

$$K_{1/2}^\lambda \approx K_{1/2} \left(\frac{\theta'_1}{\theta'_{1/2}} + \lambda \left(1 - \frac{\theta'_1}{\theta'_{1/2}} \right) \right), \quad (4.138)$$

or by (4.132), (4.133) and (4.134)

$$K_{1/2}^\lambda \approx K_{1/2} \left(\frac{\kappa_1}{\kappa_{1/2}} + \frac{\kappa_1}{\kappa_1 - \kappa_0^\lambda} \left(1 - \frac{\kappa_1}{\kappa_{1/2}} \right) \right), \quad (4.139)$$

For $\kappa_0 = -1$ ($\lambda = 0.5464$) this formula yields $K_{1/2}^{(0.5464)} \approx 1.79$ and we computed, using the model developed in Section 4.3, 1.70, so there is a rather good agreement.

In [5, page 81], Gordon writes

‘...considerable force had to be applied to a bow which is initially bent in the opposite or ”wrong” direction, before it could be strung.’

This does not agree with our results; in the case of the straight-end KL bow dealt with in Section 4.9, the force in the string was 1.71 and in the PE bow with $\kappa_0 = -1$ it is 1.70. Equation (4.137) shows that $\kappa_{1/2}^\lambda$ increases with λ but a comparison of the unstrung shape of the PE bow with $\kappa_0 = -1$, given in Figure 4.44, with those depicted in many books

Table 4.27: Energy in parts of the PE bow with $\kappa_0 = -1$ in a number of situations, (Figure 4.44).

energy	limbs		string		total bow		arrow kin.
	pot.	kin.	pot.	kin.	pot.	kin.	
braced	0.5755	0	0.0204	0	0.5959	0	0
fully drawn	1.0817	0	0.0053	0	1.0867	0	0
arrow exit	0.5324	0.1346	0.0844	0.0312	0.6168	0.1658	0.3040

and papers indicates that its curvature is already on the large side. So with respect to the force in the string which one has to apply to a bow, it is not more difficult to brace a static-recurve bow than a straight-end bow. Although the bow is shorter and has an opposite curved unstrung shape, it will be more complicated to disentangle the unstrung situation and to transfer it into the braced one.

Gordon mentions that:

‘...the archer is no longer starting to draw the bow from an initial condition of zero stress and strain.’

This does agree with our finding that already in the braced situation a large amount of energy is stored in a static-recurve bow with curved elastic limbs. In Table 4.27 we give the amounts of energy in the parts of the PE bow with $\kappa_0 = -1$ in a number of situations. The energy in the braced bow, being 0.5959, is even larger than the energy put into the bow by drawing it from braced situation into fully drawn, being 0.491.

Balfour in [2] mentions:

‘...greater skill and dexterity are called for in stringing the strongly reflexed Asiatic bows, than are needed for any bow of simple or "single-stave" type. I can speak from experience and know how difficult and risky it is.’

Indeed, a static-recurve bow in braced situation has a tendency to capsize. In that situation we have static equilibrium, thus the potential energy, in limbs and string, is a minimum for this configuration among all the admissible configurations in the "neighbourhood" (see Section 4.5).

For bows whereby the string has contact with the bridge, those admissible configurations are configurations in which the string lies against the string bridges. However, if we permit the string to slip past these bridges then the braced situation does not need to be a configuration of a minimum potential energy and much energy (see Table 4.27) is disengaged when the bow is able to spring back into its unbraced form. In [14, page 6], Payne-Gallwey notes that separate loops are knotted to each end of the middle part of the string. These loops fit into the nocks of the bow and rest, when the bow is braced, upon small ivory bridges which are hollowed out to receive them and which, in this way, assist to retain the string in its place. Such a danger holds for ears with a sufficiently large θ_t for instance not

for the ones of Figure 4.33 or Figure 4.37, where the ear can even be taken straight, however with a bend at its connection with the working part of the limb.

We next show the influence of the remaining parameters given in (10.15) before the semicolon; the length of the grip L_0 , distribution of bending stiffness $W(s)$ and of mass $V(s)$ along the bow, mass of the arrow $2m_a$, strain stiffness and mass of the string U_s and $2m_s$ and the brace height $|OH|$. In Table 4.28 we collect the results obtained by changing one parameter at a time (L_0 , m_a and $|OH|$) or two parameters simultaneously ($W(s)$, $V(s)$ and U_s , m_s), where the not mentioned parameters are those of the PE bow given in (4.128). It follows that the influences of the parameters are roughly speaking the same as in the case of the KL bow, dealt with in Section 4.9. An exception has to be made for the influence of $|OH|$, which we will consider more closely.

We note that a larger brace height yields, as in the case of the KL bow, a smaller static quality coefficient but in the case of the PE bow a larger efficiency, so that the muzzle velocity ν remains nearly the same. In Table 4.28 we give with changing $|OH|$ also the values of $\min b(t)$, the smallest x -coordinate of the middle of the string for $t > t_l$. Comparing these values with those given in Table 4.9 for the KL bow, reveals that for $|OH| = 0.250$ both values are almost the same (0.09;0.10). However, for $|OH| = 0.286$ it is in the case of the PE bow larger (0.19;0.14). This property is favourable for the Turkish flight shooters who used a grooved horn in order to be able to shoot arrows shorter than the draw-length (see also Section 4.12).

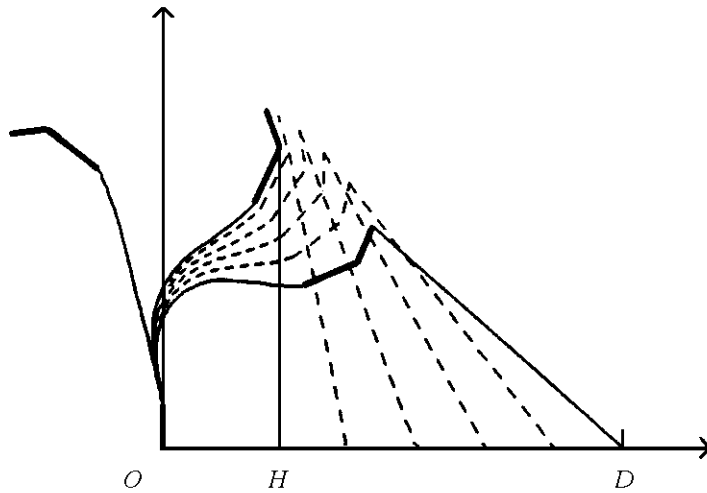


Figure 4.45: Dimensionless deformation curves of the "Asiatic bow". Compare Figure 2.10.a in [9].

In that situation the $\min b(t)$ has to be larger than the length of the grooved horn. From [4, page 175] we quote:

the groove is contrived to let the archer engender greater force by enabling the bow string to be drawn further than the length of the arrow would normally permit. However, it may not project more than about half a foot (6 inches)

Table 4.28: Influence of a number of parameters on the performance of the PE bow.

L_0	q	η	ν	$W(L_0)$	$V(L_0)$	$\min b(t)$
0	0.453	0.622	1.92	0.3469	1.6	—
0.1429	0.432	0.668	1.94	0.2304	1.867	—
W, V						
$W(s) \equiv W(L_0), V(s) \equiv V(L_0)$	0.433	0.594	1.83	0.1802	1.167	—
4.115, 4.116	0.432	0.668	1.94	0.2304	1.4	—
m_a						
0.0384	0.432	0.493	2.36	0.2304	1.867	—
0.0769	0.432	0.668	1.94	0.2304	1.867	—
0.1538	0.432	0.772	1.47	0.2304	1.867	—
m_s, U_s						
0.0105, 66	0.430	0.681	1.95	0.2300	1.867	—
0.0209, 131	0.432	0.668	1.94	0.2304	1.867	—
0.0418, 262	0.433	0.644	1.90	0.2307	1.867	—
$ OH $						
0.25	0.432	0.668	1.94	0.2304	1.867	0.09
0.25	0.432	0.668	1.94	0.2304	1.867	0.19
0.25	0.432	0.668	1.94	0.2304	1.867	0.23

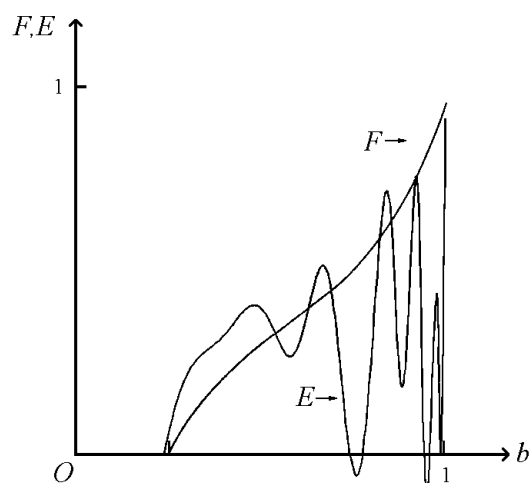


Figure 4.46: SFD and DFD curves of the "Asiatic bow". Compare SFD curve with the one given in Figure 2.10.b in [9].

from the belly without getting in the way of the string and, for that reason, it cannot reduce the length of an available arrow by more than that amount. For example, a thirty inch draw would require an arrow of about twenty-five and a half inches, which is, in fact the real length of many extant Turkish shafts.'

The dimensionless length of the groove is in this example $6/30 = 0.20$. The results given in Tables 4.9 and 4.28 show that the use of a groove with a straight-end bow would require a large brace height and this implies a bad performance, while in the case of a static-recurve bow the brace height can remain moderate and it has a less disadvantageous influence on its performance.

Finally we consider an Asiatic bow described in [10] by Latham and Paterson, where a reconstruction of it is shown in plate 18. In [9] we dealt with the statics of that bow. We showed earlier its configuration in unbraced, braced and fully drawn situation, its static quality coefficient and the SFD curve. In Figure 4.45 we show the bow in various situations again, but now computed with the model developed in Section 4.3 for the static-recurve bow. The bending stiffness as a function of \bar{s} for $6.24 \text{ cm} = \bar{L}_0 \leq \bar{s} \leq \bar{L}_2 = 46.8 \text{ cm}$ is the same as that chosen in [9]. There we tried to guess the bending stiffness 80 that the calculated braced and fully drawn shape of the bow resembled those of the reconstructed bow shown on the photographs in [10]. For $\bar{L}_2 \leq \bar{s} \leq \bar{L}$ we take now straight parts which connect the tip $(\bar{x}_{t_0}, \bar{y}_{t_0})$ and the end of the working part of the limb $(\bar{x}_0(\bar{L}_2), \bar{y}_0(\bar{L}_2))$ with the bridge $(\bar{x}_{b_0}, \bar{y}_{b_0})$. The length \bar{L} of this bow is 63.5 cm and the draw $|\overline{OD}| = 76.2 \text{ cm}$, so the dimensionless length L becomes 0.833. The brace height $|\overline{OH}| = 18.4 \text{ cm}$.

In [10] nothing is said about the distribution of the mass along the limb. We assumed this mass distribution to be uniform. The coordinates of the centre of gravity of ear, mass of ear and moment of inertia with respect to centre of gravity are computed using formulas which resemble the Equations (4.117), (4.118), (4.126). The dimensionless mass of the arrow and mass and strain stiffness of the string are taken the same as those in the case of the PE bow given in (4.128).

Under these assumptions the bow is given by

$$\begin{aligned} &B(0.833, 0.08, W, V = V_0 = 1.33, \theta_0, 0.0769, 0, 0, 0.2910, 0.00105, 0 \\ &, -0.2554, 0.6706, -0.2733, 0.6435 - 0.3358, 0.6603, 0.6125, 131, 0.0209, 0.2417; \\ &1, 1, 1) . \end{aligned} \quad (4.140)$$

The dimensionless quality coefficients are; $q = 0.332$, $\eta = 0.726$ and $\nu = 1.77$. The static quality coefficient q differs slightly from the value given in [9], there it was 0.339. In that article we assumed the bending stiffness $W(s)$ for $0 \leq s \leq L_0$ and $L_2 \leq s \leq L$ to be about 20 times the mean bending stiffness of the flexible part of the limb. However, if we take this factor equal to 200 instead of 20 we obtain $q = 0.331$ and this nearly equals the value of q calculated with the model of Section 4.3, when the string is chosen to be inextensible. This result shows that the assumption that grip and ears are rigid, introduces some extra inaccuracies because the first mentioned factor 20 seems to be realistic. That the static quality coefficient of the bow is 0.333 and not 0.331 is caused by the elasticity of the string.

As in the case of the short bows, Tables 4.23 and 4.26 the static quality coefficient q is poor, the efficiency is rather good and the muzzle velocity ν is bad. The SFD curve and DFD curve are shown in Figure 4.46. The DFD curve oscillates just as in the case of the short PE bow, see Figure 4.39, 4.40, 4.41 and 4.43. Thus also this Asiatic bow does not seem to be a pleasant bow to shoot with.

In [10, page 104] it is said:

If, in shooting, it is your wish to outdistance your competitors you should use a bow with short working part of the limb and choose a light arrow.'

In Section 2.6 we brought this already forward with the discussion of the simple H model (see Section 4.6). However, the results of this section indicate that long stiff ears are not advantageous if they are also heavy. The statement given in the last bit of the sentence quoted above, agrees with our results, see Tables 4.13 and 4.28.

Note that for a bow with a straight part of the limb and $L = 0.7857$ or $L = 1.000$, the bend in the ear, fixed by the angle θ_t yielding the maximum muzzle velocity ν is so small that the string is free from the string-bridges in all situations. Pictures of old Asiatic bows in many books and papers show braced bows at which the string touches the string-bridges. But, the angle between the vertical and the outer part of ear (between bridges and nock) in braced situation is generally small and in a few cases the string is even free from the "string-bridges".

We found in this section that a short static-recurve bow possesses no inherent better performance than a longer straight-end bow. Inherent properties of the bow are those fixed by dimensionless parameters given before the semicolon in (4.2). In Section 4.12, where we investigate the influence of the three parameters behind the semicolon in (4.2), the draw $|\overline{OD}|$, the weight $\overline{F}(|\overline{OD}|)$ and the mass of the limb \overline{m}_b , we return to this subject.

4.12 Influence of draw, weight and mass of limb

In Section 4.9 and 4.11 we studied the influence of the dimensionless parameters, given before the semicolon in (4.2), on the static and dynamic behaviour of a bow. This has been done in Section 4.9 for the non-recurve bow KL and in Section 4.11 for the static-recurve bow PE. In this section we continue with an investigation of the influence of the three parameters with dimension given behind the semicolon in (4.2), namely: the draw $|\overline{OD}|$, the weight $\overline{F}(|\overline{OD}|)$ and the mass \overline{m}_b of one limb, for both types of bows. To that end we consider a number of bows described in [14] and [15].

We recollect formulas for four important quantities. First, the amount of energy \overline{A} put into the bow by drawing it from the braced situation into the fully drawn situation is given by (4.82)

$$\overline{A} = q\overline{F}(|\overline{OD}|)|\overline{OD}|. \quad (4.141)$$

Second, the muzzle velocity \overline{c}_l , (3.81) in [8], by

$$\overline{c}_l = 31.32 \nu \{\overline{d}_{bv}^{1/2}\} \text{ cm/sec} \quad (4.142)$$

where

$$\bar{d}_{bv} \stackrel{\text{def}}{=} \frac{\bar{F}(|\overline{OD}|)|\overline{OD}|}{\bar{m}_b} . \quad (4.143)$$

The number 31.32 is caused by the choice of our units. Third, the amount of energy transferred to the arrow, using (4.87)

$$\bar{m}_a \bar{c}_l^2 = m_a \nu^2 \{ \bar{F}(|\overline{OD}|)|\overline{OD}| \} = \eta q \bar{F}(|\overline{OD}|)|\overline{OD}| . \quad (4.144)$$

Fourth, the linear momentum of the arrow at arrow exit

$$2\bar{m}_a \bar{c}_l = 62.64 m_a \nu \{ \bar{d}_{bp}^{1/2} \} = 62.64 \frac{\eta q}{\nu} \{ \bar{d}_{bp}^{1/2} \} \quad (4.145)$$

where

$$\bar{d}_{bp} \stackrel{\text{def}}{=} \bar{F}(|\overline{OD}|)|\overline{OD}|\bar{m}_b . \quad (4.146)$$

Of these four expressions, the first part contains only dimensionless quality coefficients which depend on the dimensionless parameters, the part between braces depends only on the parameters with dimension; $|\overline{OD}|$, $\bar{F}(|\overline{OD}|)$ and \bar{m}_b .

From (4.142) ··· (4.146) we conclude that for large values of \bar{c}_l , $\bar{m}_a \bar{c}_l^2$ and $2\bar{m}_a \bar{c}_l$ it is advantageous to have the draw and weight as large as possible. Equations (4.142) and (4.143) indicate that the mass of the bow \bar{m}_b has to be small to ensure a large muzzle velocity \bar{c}_l . But, on the other hand (4.145) and (4.146) show that \bar{m}_b has to be large in order to obtain a large linear momentum of the arrow. As already mentioned, for flight shooting a large initial velocity \bar{c}_l of the arrow is essential. For hunting or warfare both kinetic energy and linear momentum are important. A large initial velocity produces a flat trajectory of the arrow in which case it requires less space in a vertical direction.

The maximum weight and draw depend on the build of the archer. His strength determines the maximum weight and his span or the greatest distance between the bow hand and the ear, cheek or chin the maximum draw, so both have physical limitations. The minimum mass of the limb has technical limitations. Constants such as the admissible stress, Young's modulus, specific mass of the material of the bow enter into the problem. How this minimum mass \bar{m}_b depends on these various parameters is beyond the scope of this paper. Nevertheless, this dependence is of major importance for the construction of a good bow.

We now show how the results given in Section 4.9 and 4.11 can be used to approximate the quality coefficients of bows with values of dimensionless parameters different from those mentioned in these sections. One way to deal with the three functions $W(s)$, $V(s)$ and $\theta_0(s)$, $0 \leq s \leq L$, is to approximate them by functions in a finite dimensional space, for instance by polynomials or splines of some finite degree which has to be not too small in order to get reasonable approximations. In this way the three functions are fixed each by a number of parameters, which together with the other 18 parameters before the semicolon

in (4.2) represent a bow. In the Sections 4.9 and 4.11 we changed some parameters separately or simultaneously. For W and V we changed only one parameter, the exponent β_n see (4.105) and (4.106) and for $\theta_0(s)$ we had two parameters, namely $\theta_0(L_0)$ and κ_0 , see (4.108) and (4.114). Hence, the dimension of the parameter space we dealt with, was 23. Representations of different types of practical bows form clusters in the parameter space or stated otherwise, for some type of bow the range of the parameters is by definition limited. From this point of view, we approximated in Section 4.9 the partial derivatives with respect to the parameters in one point (representing the KL bow) in the cluster of the non-recurve bow C including the AN bow) and in Section 4.11 in one point (representing the PE bow) in the cluster of the static-recurve bows. The static quality coefficient q and the efficiency η of bows represented by points in the neighbourhood of the KL bow or PE bow can be approximated by using the first order terms of the Taylor expansion in mentioned points, in which the derivatives are replaced by their finite-difference approximations. Then the dimensionless muzzle velocity ν follows from these approximated values of q and η and the dimensionless mass ma of the arrow, see (4.87).

In order to elucidate this procedure we consider a KL bow. For the three parameters with dimension behind the semicolon we take, $|\overline{OD}| = 71.12$, $\overline{F}(|\overline{OD}|) = 28.1$ and $\overline{m}_b = 0.13$. Then this bow is given by

$$\begin{aligned} & \text{KL}(91.46, 10.16\overline{W}, \overline{V}, \theta_0 \equiv 0, 0.01, 0, 0, 0, 0, 0, 0 \\ & 91.46, 0, 91.46, 0, 91.46, 91.46, 3681, 0.0027, 15.24; \\ & 71.12, 28.1, 0.13) . \end{aligned} \quad (4.147)$$

The bending stiffness $\overline{W}(\overline{s})$ and mass per unit of length $\overline{V}(\overline{s})$ are given by

$$\begin{aligned} \overline{W}(\overline{s}) &= 200,263 \left(\frac{(\overline{L} - \overline{s})}{\overline{L} - \overline{L}_0} \right) , \quad \overline{L}_0 \leq \overline{s} \leq \overline{L}_0 + 2/3(\overline{L} - \overline{L}_0) , \\ \overline{W}(\overline{s}) &= 66,754 , \quad \overline{L}_0 + 2/3(\overline{L} - \overline{L}_0) \leq \overline{s} \leq \overline{L} , \end{aligned} \quad (4.148)$$

and

$$\begin{aligned} \overline{V}(\overline{s}) &= 0.0029 \left(\frac{(\overline{L} - \overline{s})}{\overline{L} - \overline{L}_0} \right) , \quad \overline{L}_0 \leq \overline{s} \leq \overline{L}_0 + 2/3(\overline{L} - \overline{L}_0) , \\ \overline{V}(\overline{s}) &= 0.001 , \quad \overline{L}_0 + 2/3(\overline{L} - \overline{L}_0) \leq \overline{s} \leq \overline{L} . \end{aligned} \quad (4.149)$$

Starting with this bow we will calculate the characteristic quantities of two neighbouring bows which differ from it by their lengths, which are chosen as $2\overline{L} = 194.95$ and $2\overline{L} = 172.72$. Hence we leave the cross section of the limb near the grip ($\overline{s} = \overline{L}_0$) unaltered as well as the number of strands of the string, the length of the grip $2L_0$ and the brace height $|\overline{OH}|$. In the functional dependency (4.148) and (4.149) we change the length \overline{L} , further we have also in the new situation $\theta_0(\overline{s}) \equiv 0$. In practice we could start with a stave of wood 194.95 cm long, shaped so that the distributions of the bending stiffness and mass become those given by (4.148) and (4.149) with $\overline{L} = 97.47$. The length of the string has to

be chosen so that the brace height becomes 15.24, see (4.147). We shorten this bow twice. After each shortening we have to taper the limbs so that the distributions of the bending stiffness and mass become those of (4.148) and (4.149) again with \bar{L} the actual half length of the bow. Further we have to shorten the string in order to keep the brace height 15.24.

For the calculation of the weight $\bar{F}(|\overline{OD}|)$ of the bows with length $2\bar{L} = 194.95$ and $2\bar{L} = 172.72$ we use the formula for the dimensionless bending stiffness $W(L_0)$ (see (3.26) in [8])

$$W(L_0) = \frac{\bar{W}(\bar{L}_0)}{\bar{F}(|\overline{OD}|)|\overline{OD}|^2} . \quad (4.150)$$

Since the cross-section of the limb near the grip is unaltered, $|\bar{W}(\bar{L}_0)|$ has the same numerical value as given in (4.148), $|\bar{W}(\bar{L}_0)| = 200, 263$. The dimensionless value $W(L_0)$ however will change (4.150), because $F(|OD|)$ will be different for the bows with different lengths. The two parameters which have changed by the process of lengthening or shortening the KL bow, are L and U_s , hence we can approximate $W(L_0)$ by

$$\begin{aligned} W(L_0) &= W(L_0)|_{\text{KL bow}} + \frac{\partial W(L_0)}{\partial L}|_{\text{KL bow}}(L - L|_{\text{KL bow}}) \\ &+ \frac{\partial W(L_0)}{\partial U_s}|_{\text{KL bow}}(U_s - U_s|_{\text{KL bow}}) . \end{aligned} \quad (4.151)$$

The dimensionless strain stiffness U_s can be written as

$$U_s = \frac{\bar{U}_s}{\bar{F}(|\overline{OD}|)} = W(L_0) \left\{ \frac{\bar{U}_s |\overline{OD}|^2}{\bar{W}(\bar{L}_0)} \right\} , \quad (4.152)$$

where the factor between braces at the right-hand side of (4.152) is the same for the three bows with different lengths, because of our assumptions. Substitution of (4.152) in (4.151) yields

$$\begin{aligned} &(W(L_0) - W(L_0)|_{\text{KL bow}}) \left(1 - \frac{\bar{U}_s |\overline{OD}|^2}{\bar{W}(\bar{L}_0)} \frac{\partial W(L_0)}{\partial U_s} \right)|_{\text{KL bow}} = \\ &\frac{\partial W(L_0)}{\partial L}|_{\text{KL bow}}(L - L|_{\text{KL bow}}) . \end{aligned} \quad (4.153)$$

From Table 4.16 (influence of U_s) we get

$$\frac{\partial W(L_0)}{\partial U_s}|_{\text{KL bow}} \approx \frac{W(L_0)|_{U_s=197} - W(L_0)|_{U_s=131}}{197 - 131} = \frac{1.410 - 1.409}{66} = 1.5 \cdot 10^{-5} . \quad (4.154)$$

This number shows that the influence of the strain stiffness on the weight of the bow is negligible. From Table 4.11 (influence of L).

$$\frac{\partial W(L_0)}{\partial L}|_{\text{KL bow}} \approx \frac{W(L_0)|_{L=1.429} - W(L_0)|_{L=1.286}}{1.429 - 1.286} = \frac{2.095 - 1.409}{0.1430} = 4.8 . \quad (4.155)$$

Substitution of (4.154) and (4.155) into (4.153) yields

$$(W(L_0) - 1.409)(1 - 0.0014) = 4.8(1.3706 - 1.286) \Rightarrow W(L_0) = 1.8155, \quad (4.156)$$

and with (4.150)

$$\overline{F}(|\overline{OD}|) = \frac{200,263}{1.8155 \cdot 71.12^2} = 21.8 \text{ kgf} ., \quad (4.157)$$

For $2\overline{L} = 172.72$ we obtain in the same way $\overline{F}(|\overline{OD}|) = 34.6 \text{ kgf}$.

The mass of one limb \overline{m}_b changes linearly with the length of the limb $(\overline{L} - \overline{L}_0)$. So, we have $\overline{m}_b = 0.1396$ for $2\overline{L} = 194.95$ and $\overline{m}_b = 0.1218$ for $2\overline{L} = 172.72$. When the same arrow with mass $\overline{m}_a = 0.010 \text{ kg}$ is shot from the three bows, then the dimensionless masses are $m_a = 0.0716$ for $2\overline{L} = 194.95$ and $m_a = 0.0821$ for $2\overline{L} = 172.72$. The mass of the string changes almost linearly with the length of the limb, so the dimensionless mass m_s remains almost unchanged.

As already remarked the parameter U_s changes according to (4.152). Meanwhile we see (4.154) that the influence of the strain stiffness of the string on the static performance is negligible and we assume that the same holds for the efficiency. Note that a change of both parameters m_s and U_s separately in Table 4.16 would have given more information.

Using the data given in Table 4.11 (influence of L) and Table 4.13 (influence of m_a) the static quality coefficients become $q = 0.411$ for $2\overline{L} = 194.95$ and $q = 0.401$ for $2\overline{L} = 172.72$ and the efficiencies become $\eta = 0.721$ and $\eta = 0.783$, respectively

In Table 4.29 we collect the results. In this table we give also the dimensionless muzzle velocity ν , the factors $\overline{d}_b \nu$ and the muzzle velocity \overline{v}_l in cm/sec, the kinetic energy and the linear momentum of the arrow in kg cm/sec. These results show that a shorter bow can deliver a larger muzzle velocity \overline{v}_l , although its dimensionless muzzle velocity ν is smaller. This can be understood by the following reasoning. First, shorter bows are stiffer. From Table 4.11 we conclude that $W(L_0)$ decreases sharply with decreasing length and (4.150) shows that the smaller $W(L_0)$ the larger the weight $\overline{F}(|\overline{OD}|)$ of the bow $|\overline{OD}|$ and $\overline{W}(\overline{L}_0)$ being the same in all cases. Second, shorter bows are lighter. For, $V(L_0)$ increases with decreasing length and a larger $V(L_0)$ implies a lighter limb. This follows from

$$V(L_0) = \frac{\overline{V}(\overline{L}_0)|\overline{OD}|}{\overline{m}_b} \quad (4.158)$$

where we have $\overline{V}(\overline{L}_0)$ and $|\overline{OD}|$ kept the same.

Both factors imply the $\overline{d}_b \nu$ to be larger for shorter bows. The effect of its stiffness is much larger than that of its lightness and this implies that $\overline{d}_b p$ is also larger for shorter bows. Further, the static quality coefficient q and the muzzle velocity ν increase with increasing length and the reverse holds for the efficiency η . This all combined shows an increase of the muzzle velocity, kinetic energy and linear momentum of the arrow with decreasing length in the way described above.

We now pay attention to the influence of a permanent set of a bow. We dealt already with this phenomenon in Section 4.9, see Table 4.17. Thus in this situation we have

Table 4.29: Influence of length $2L$ on performance of KL bow $|\overline{OD}| = 71.12$ cm, $m_a = 0.01$ kg.

$2\overline{L}$	$W(L_0)$	$\overline{F}(\overline{OD})$	$2\overline{m}_b$	q	η	ν	\overline{d}_{bv}	\overline{d}_{bp}	\overline{c}_l	$\overline{m}_a \overline{c}_l^2$	$\overline{m}_a \overline{c}_l$
194.95	1.812	21.9	0.278	0.411	0.721	2.03	11,205	216.5	6,730	462	135
182.88	1.409	28.1	0.260	0.407	0.765	2.01	15,373	259.8	7,805	622	156
172.72	1.144	34.6	0.246	0.401	0.783	1.96	20,006	302.7	8,695	772	174

computed values for various parameters at our disposal, this in contrast with the cases that just have been treated. The unbraced shape of the bow which "followed the string" was chosen to be a part of a circle with curvature fixed by $\kappa_0 = 0.1$, see (4.108). We compare the performance of the bow given by (4.147) with a bow, with the same dimensionless parameters, except the parameter κ_0 , namely $\kappa_0 = 0.1$ instead of $\kappa_0 = 0$. In Table 4.30 we give the results. The dimensionless parameters $W(L_0)$, $V(L_0)$, q , η and ν were already given in Table 4.17. Using (4.150), (4.158) and the fact that $\overline{W}(\overline{L}_0)$ and $\overline{V}(\overline{L}_0)$ are the same for both bows as well as $|\overline{OD}|$, we find for the bow with $\kappa_0 = 0.1$, $\overline{F}(|\overline{OD}|) = 24.9$ and $\overline{m}_m = 0.13$. Because the product of q and η is for both bows about the same, the smaller weight of the bow with permanent set implies a smaller \overline{d}_{av} , \overline{d}_{ap} , \overline{c}_l , $\overline{a}_a \overline{c}_l^2$ and $2\overline{a}_a \overline{c}_l$. In [6, page 22] Hickman studied also the influence of a permanent set and he found that it reduces the cast of the bow. This agrees with our results, although the conception "cast" has never been defined properly. Note that we assumed the bending stiffness $\overline{W}(\overline{L}_0)$ to be the same for both bows. In practice a decrease of the weight may be caused by a change of this entity when the bow has been used for some time.

In what follows we consider a number of bows described in [14] and [15]. Of these bows the draw, weight, the mass of the arrow and sometimes the mass of the limbs and part of the remaining parameters are given. When the mass m_b is not known we use instead of \overline{d}_{av} and \overline{d}_{ap} the quantities

$$\overline{d}_{av} = \frac{\overline{F}(|\overline{OD}|)|\overline{OD}|}{\overline{m}_a} \quad (4.159)$$

and

$$\overline{d}_{ap} = \overline{F}(|\overline{OD}|)|\overline{OD}|\overline{m}_a \quad (4.160)$$

for the estimation of the performance of the bow and arrow combinations.

Then, by (4.144) we have

$$\overline{c}_l = (q\eta)^{1/2} \overline{d}_{av}^{1/2} \quad (4.161)$$

and by (4.145)

$$2\overline{m}_a \overline{c}_l = 2(q\eta)^{1/2} \overline{d}_{ap}^{1/2} \quad (4.162)$$

Table 4.30: Influence of a permanent set of the KL bow, $|\overline{OD}| = 71.12$ cm, $m_b = 0.13$ kg.

κ_0	$W(L_0)$	$V(L_0)$	$\overline{F}(\overline{OD})$	q	η	ν	\overline{d}_{bv}	\overline{d}_{bp}	\overline{c}_l	$\overline{m}_a \overline{c}_l^2$	$\overline{m}_a \overline{c}_l$
0	1.409	1.575	28.1	0.407	0.765	2.01	15,373	259.8	7,805	622	156
0.1	1.590	1.575	24.9	0.389	0.795	2.01	13,623	230.0	7,350	548	146

Because only a few parameters of all those which determine completely the performance of a bow and arrow combination are given in [14] and [15], we are able to give only rough estimates for the quality coefficients q , η and ν . All bows mentioned by Pope in [15] were shot repeatedly at least six times and the greatest distance was recorded. The elevation at which each arrow was projected was approximately 45° from the horizontal.

We consider first a straight-end bow. In [15, page 31], Pope describes an experiment with a replica of an English longbow. He started with a bow 6 feet 4.75 inches (194.95 cm) long. When drawn 28 inches (71.12 cm) it weighed 53 pounds (23.6 kgf) and shot a flight arrow with mass 310 grains (0.020 kg), 185 yards (16916 cm). Then Pope cut down the bow to a length of 6 feet (182.88 cm), it weighed then 62 pounds (28.1 kgf), and shot the arrow 227 yards (20757 cm). This bow has been again cut down to a length of 5 feet 8 inches (172.72 cm) and the limbs were tapered a trifle. Its weight, when drawn 28 inches (71.12 cm) became 70 pounds (31.8 kgf) and shot the arrow 245 yards (22403 cm). Because Pope's information about the bow is not complete, we are not in a position to imitate his experiments theoretically. However, a comparison of his data with the results in Table 4.29 shows that the trends of the influence of shortening a bow, with respect to weight and muzzle velocity or range, are the same. In Table 4.31 we give the factors d_{av} in kgf cm/kg and d_{ap} in kgf cm kg for the three bows Pope mentioned.

Second, we consider a number of static-recurve bows. In what follows we have sometimes the situation in which the weight of the bow is given for a draw different from the draw used during shooting the arrow. In these cases we approximate the weight of the bow using the slope of the SFD curve of the static-recurve bows with different lengths, given in Figure 4.35, for $b = 1$ with

$$\overline{F}(|\overline{OD}| + \overline{\Delta}) = \overline{F}(|\overline{OD}|) + \frac{\partial \overline{F}}{\partial b} \Big|_{b=|\overline{OD}|} \overline{\Delta} = \overline{F}(|\overline{OD}|) + \frac{\partial F}{\partial b} \Big|_{b=|\overline{OD}|} \frac{\overline{F}(|\overline{OD}|)}{|\overline{OD}|} \overline{\Delta} \quad (4.163)$$

For $L = 1.286$ a finite difference approximation yields $\frac{\partial F}{\partial b} \Big|_{b=1} \approx 1$ and for $L = 0.7857$ we have $\frac{\partial F}{\partial b} \Big|_{b=1} \approx 2.5$

First, we consider two Tartar bows described by Pope in [15, page 23]. Both were 74 inches (187.96 cm) long. One weighed 1 1/2 pounds (.6804 kg) avoirdupois and pulled 30 pounds (13.6 kgf) when drawn 28 inches (71.12 cm). It shot a flight arrow 310 grains (0.020 kg) in weight 100 yards (9140 cm). Thus for this bow we have $L = 1.32$, $m_a = 0.0294$, $\overline{d}_{av} = 97,000$ kgfcm/kg and $\overline{d}_{ap} = 9.7$ kgfcm/kg. The other bow weighed 3 1/4 pounds

Table 4.31: Comparison of various bows described in [14] and [15].

type	ref.	$\overline{F}(\overline{OD})$	$ \overline{OD} $	$2\overline{m}_a$	$2\overline{m}_b$	$2\overline{L}$	$2\overline{m}_s$	range	\overline{d}_{av}	\overline{d}_{ap}
longbow	[15]	23.6	71.12	0.020	—	195	—	17,000	168,000	16.8
		28.1	71.12	0.020	—	188	—	21,000	200,000	20.0
		31.8	71.12	0.020	—	173	—	22,500	226,000	22.6
Tartar	[15]	13.6	71.12	0.020	0.680	188	—	9,140	97,000	9.7
Tartar	[15]	46	73.66	0.020	1.47	188	0.057	16,000	339,000	33.9
		46	73.66	0.020	1.47	188	0.170	8,230	339,000	33.9
		47.6	76.2	0.113	1.47	188	0.057	9,600	64,000	191.4
		47.6	76.2	0.113	1.47	188	0.170	9,140	64,000	191.4
Turkish	[15]	39	73.66	0.013	—	122	—	24,300	442,000	28.7
		39	73.66	0.020	—	122	—	22,860	287,000	28.7
Turkish	[14]	69	71.12	0.014	0.354	114	—	32,930	701,000	34.4.7

(1.5 kg) avoirdupois and when drawn 28 inches (71.12 cm) it pulled 98 pounds (44.45 kgf). The same flight arrow 310 grains (.020 kg) in weight drawn 29 inches (73.66 cm) shot only 90 yards (8230 cm) with a heavy string of 6 ounces (.17 kg) and 175 yards (16,000 cm) with a light string, 2 ounces (.0567 kg) in weight. If we approximate the weight of the bow when drawn 73.66 cm by 46 kgf then \overline{d}_{av} becomes 339,000 kgfcm/kg and $\overline{d}_{ap} = 33.9$ kgfcm/kg. Pope shot also a war arrow 4 ounces (0.1134 kg) ap in weight with this bow. Drawing that arrow 30 inches (76.22 cm), the weight is than 47.6 kgf approximately, it flew only 100 yards (9140 cm). In this case \overline{d}_{av} equals about 64,000 and \overline{d}_{ap} about 191.4 and the dimensionless mass of the m_a arrow m_a equals 0.0769. Using the light string again 2 ounces (0.0567 kg) in weight, the same arrow flew only 5 yards further, thus 105 yards (9600 cm).

Pope describes also a replica of a Turkish composite bow with which he hoped to exceed the American flight record of 290 yards (26,500 cm) made by Maxson in 1891. Unfortunately, Pope does not mention the mass of the bow. This bow weighed 85 pounds (38.56 kgf) when drawn 29 inches (73.66 cm) and its length was 48 inches (121.92 cm). It cast the arrow 310 grains (0.020 kg) in weight, 250 yards (22,860 cm). In that case \overline{d}_{av} equals 287,000 and $\overline{d}_{ap} = 28.7$. A 25-inch flight arrow, 200 grains (0.013 kg) in weight (shot with a groove) Pope was able to shoot 266 yards (24,300 cm). In this case we have $\overline{d}_{av} = 442,000$ and $\overline{d}_{ap} = 18.7$.

In [14, page 3], Payne-Gallwey describes also a Turkish bow. The length of this bow is 45 inches (114.3 cm), it weighed 12 1/2 ounces (0.354 kg) avoirdupois and pulled when drawn 25 2 inches (64.77 cm) 118 pounds (53.5 kgf). When drawn 28 inches (71.12 cm) the weight is approximated by 69 kgf. Then $\overline{d}_{av} = 701,000$ and $\overline{d}_{ap} = 34.4$. He shot 12 arrows, half an ounce (0.0142 kg) in weight each and the distance they travelled averaged 360 yards (32,900 cm). The dimensionless mass of the arrow $m_a = 0.04$ for this bow arrow

combination.

In Table 4.31 we collect the results. Besides \bar{d}_{av} and \bar{d}_{ap} , one has to know the two quality coefficients q and η to be able to estimate the performance of each bow-arrow combination, but as we mentioned earlier we can give only rough approximations for these coefficients because of lack of detailed information.

Comparison of the longbow with the weakest Tartar bow shows that the larger \bar{d}_{av} of the longbow is directly translated into a greater range. Obviously the product $q\eta$ is for both bows about the same when we assume the range to be about proportional to the square of the initial velocity of the arrow \bar{c}_l , see (4.161). The rather short range of the huge Tartar bow is partly caused by the heavy string, as Pope pointed out experimentally. For a heavy string gives a bad efficiency. In Section 4.7 we dealt with the influence of the mass of the string and we found that our results agree fairly well with the results obtained by using Hickman's rule. Hickman took the mass of the string into account by adding one third of this mass to the mass of the arrow. In that case an approximation of the maximum efficiency becomes (4.100)

$$\max \eta \approx \frac{\bar{m}_a}{\bar{m}_a + 1/3\bar{m}_s} \quad (4.164)$$

In the case of the static-recurve bow only the middle part of the string, thus not the loops which rest against the ears at the moment the arrow leaves the string, has to be taken into account. The mass of the middle part of the heavy string is about 0.7 times the total mass of the string, thus 0.040 kg. In this case (4.164) yields a maximum efficiency $\eta = 0.34$. For the lighter string this value becomes, using the same approximations 0.60. This explains why the range when the light string is used, is about double the range when the heavy string is used. The dimensionless mass of the arrow, being only 0.0136, is very small and the results given in Table 4.28 show that this causes a small efficiency too. This elucidates the relative short range, even in the case of the light string, despite the large \bar{d}_{av} . A war arrow is heavier, so in that case first the maximum efficiency according to (4.164) with the above made remarks with respect to the part of the string one has to account for, becomes larger, namely 0.74 and 0.89 for $2\bar{m}_a = .170$ and $2\bar{m}_s = 0.057$, respectively. Second, the dimensionless mass of the arrow is larger and this implies that the efficiency is not too much smaller than the mentioned maxima. However, the factor \bar{d}_{av} is small for such a bow-arrow combination. This implies the small muzzle velocity. Note that \bar{d}_{ap} is very large for this bow shooting the heavy arrow. Using the above mentioned facts with respect to static quality coefficient and efficiency, (4.161) indicates that the linear momentum of the war arrow is large.

For each bow there exists a minimum dimensionless mass of the arrow for which the arrow sticks to the string until the latter is stretched. Because short bows are light, the minimum is also small. Further, the mass of the string compared with the mass of the arrow is small and (11.23) indicates that the efficiency can be good. On the other hand, from Tables 4.23 and 4.26 we conclude that the static quality coefficient of such a short bow is rather bad in comparison with its value for longer bows. Despite this bad static

quality coefficient, the large factor \bar{d}_{av} makes the short static-recurve bow in combination with a light arrow well adapted to flight shooting.

In order to reduce the mass of the arrow and the drag of the arrow in the air, the Turk shot flight arrows shorter than the draw of the bow. This was made possible by using a horn groove siper”) which they wore on the thumb ([14, page 11]) or which was strapped to the wrist ([10, page 106]) of the bow hand. These grooves guided the arrow in safety past the side of the bow. In Section 4.11 we saw that after arrow exit the string remains free from such a groove when static-recurve bows with moderate brace heights are used. In [14] Payne-Gallwey mentions that flight arrows were shot from 600 to 800 yards (55,000 cm to 73,150 cm) by certain famous Turkish archers. In [10, page 109], Latham and Paterson write that the greatest recorded distance achieved with a hand bow is 972 yards (88,880 cm). It was shot by the Ottoman sultan Selim III in 1798. In June 1967 Harry Drake shot 851 yards 2 feet 9 inches (77,870 cm) and in September 1977 Don Brown shot 1,164 yards 2 feet 9 inches (106,520 cm).

For hunting and warfare the maximum range of the arrow is not a decisive quantity. Then the amount of kinetic energy (4.144) is more important and also the linear momentum (4.162). In that case, a heavier arrow gives a large efficiency and thus better performance, however, there is some bound. Very heavy arrows obtain a very small velocity and besides the increase of the kinetic energy with increasing mass of the arrow diminishes.

In [16] Rausing deals with the origin and development of the composite bow. He argues that the fact the static quality coefficient of the short static-recurve bow to be larger than that of the short straight bow disposes the statement of Pitt-Rivers, Balfour, Clark and also Beckhoff:

‘the composite bow has no inherent superiority over the wooden self-bow, so long as the latter was made from the most favourable kinds of timber and expertly used.’

In Section 4.11 we saw already that the short static-recurve bow has no inherent better performance than the long straight-end bow. On the other hand, much more energy per unit of mass of limb can be stored in the fully drawn composite bow than in the wooden bow. This must be the reason for the better performance of the static-recurve bow, if its performance was better. Further, a short static-recurve bow is easier in operation and is therefore suited for the use on horse back.

4.13 Another check on our numerical method

The finite-difference method used in [8] met four requirements. First, in the case of static deformations, agreement with the solution of the shooting method described in [9]. Second, the sum of the potential and kinetic energy has to be constant during the dynamic process of shooting. Third, convergence of the results when the grid used in the finite-difference method, was refined. Fourth, agreement with the solution obtained by using the finite-element method [8]. To be able to tackle the problems stated in Section 4.3 of this paper,

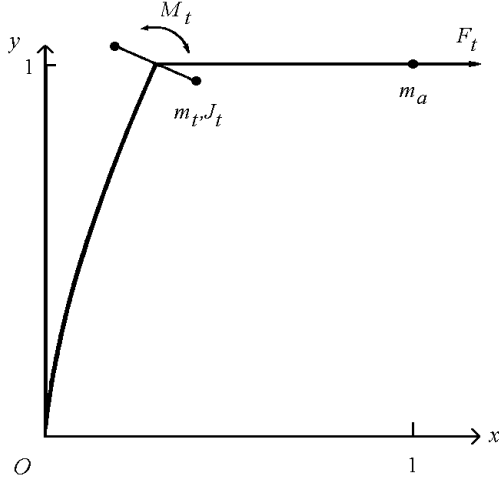


Figure 4.47: Cantilever beam, deflection of force F_t and moment M_t at the free end.

we had to introduce some changes in the finite-difference scheme of [8] and besides we made some improvements (See Section 4.4). After every change we checked the results and found that the method described in Section 4.4 of this paper meets the first three requirements mentioned above. Because of the improvements, the convergence we got was even better than the convergence described in Section 4.4 of [8]. In this section we carry out still another check.

At the end we consider a very simplified model of a bow, shown in Figure 4.47. In this case the bow is a straight beam of length 1 with constant bending stiffness $W = 1$ and constant mass distribution $V = 1$. In the undeformed situation it coincides with part of the y -axis and is clamped at the origin O . At the free end there is fixed a rigid body with mass m_t and moment of inertia J_t . Another mass m_a is connected to the free end of the beam by an inextensible string without mass as drawn in Figure 4.47. This mass m_a is allowed to move parallel to the x -axis. The length of this string is chosen so that in the deflected situation m_a is at place (1,1). This initial deflection is caused by a force F_t acting upon m_a and a bending moment M_t applied upon the free end (Figure 4.47). The external force actions F_t and M_t are removed at time $t = 0$.

We assume F_t and M_t to be sufficiently small, so that the elementary linearized beam theory can be applied. Then the equations of motion become

$$\ddot{x}(y, t) = -x''''(y, t), \quad 0 < y < 1, \quad t > 0. \quad (4.165)$$

The boundary conditions are for $t > 0$,

$$x(0, t) = x'(0, t) = 0, \quad (4.166)$$

$$J_t \ddot{x}'(1, t) = -x''(1, t), \quad (m_a + m_t) \ddot{x}(1, t) = x'''(1, t). \quad (4.167)$$

The initial conditions read

$$x(y, 0) = -1/6 F_t y^3 + 1/2 (F_t + M_t) y^2, \quad \dot{x}(y, 0) = 0, \quad 0 \leq y \leq 1. \quad (4.168)$$

Here the prime indicates partial differentiation with respect to y . We observe that these equations are the linearized versions of the equations of Section 4.3.

In order to obtain an analytic solution we use the Laplace transform technique with respect to the time variable t . The Laplace transform of the function $x(y, t)$, occurring in equations (4.165)–(4.168), denoted by $X(y, p)$ equals

$$X(y, p) = \int_0^\infty \exp\{-pt\} x(y, t) dt \stackrel{\text{def}}{=} X_1(y, p) + X_2(y, p), \quad (4.169)$$

where

$$X_1(y, p) = -(1/6 F_t y^3 + 1/2 (F_t + M_t) y^2)/p, \quad (4.170)$$

and

$$X_2(y, p) = [A(\sinh \sqrt{ip}y - \sin \sqrt{ip}y) + B(\cosh \sqrt{ip}y - \cos \sqrt{ip}y)]/pC \quad (4.171)$$

with

$$\begin{aligned} A(p) &= -F_t (\cos \sqrt{ip} + \cosh \sqrt{ip} - ip\sqrt{ip}J_t(\sinh \sqrt{ip} + \sin \sqrt{ip})) \\ &\quad - M_t (\sqrt{ip} \sinh \sqrt{ip} - \sin \sqrt{ip} + (m_a + m_t)ip(\cosh \sqrt{ip} - \cos \sqrt{ip})), \\ B(p) &= -F_t (\sin \sqrt{ip} + \sinh \sqrt{ip} - ip\sqrt{ip}J_t(\cosh \sqrt{ip} - \cos \sqrt{ip})) \\ &\quad + M_t (\sqrt{ip} \cosh \sqrt{ip} + \cos \sqrt{ip} - (m_a + m_t)ip(\sin \sqrt{ip} - \sinh \sqrt{ip})), \\ C(p) &= -2ip\sqrt{ip}[1 + \cos \sqrt{ip} \cosh \sqrt{ip} - (m_a + m_t)\sqrt{ip}(\sin \sqrt{ip} \cosh \sqrt{ip} - \sinh \sqrt{ip} \cos \sqrt{ip}) \\ &\quad - J_t ip\sqrt{ip}(\sinh \sqrt{ip} \cos \sqrt{ip} + \sin \sqrt{ip} \cosh \sqrt{ip}) \\ &\quad - (m_a + m_t)J_t p^2(1 - \cos \sqrt{ip} - \cosh \sqrt{ip})], \end{aligned} \quad (4.172)$$

where p is a complex variable. This complex-valued function $X(y, p)$ has simple poles, which are the zeros of the function $C(p)$ in (4.172), on the imaginary axis. It is easy to show that there is no singularity in the origin $p = 0$, this reflects the fact that the cantilever vibrates about its position of equilibrium $x = 0$. The inverse Laplace transform $x(y, t)$ of $X(y, p)$ is

$$x(y, t) = \frac{1}{2\pi i} \lim_{\beta \rightarrow \infty} \int_{\gamma - i\beta}^{\gamma + i\beta} \exp\{pt\} X(y, p) dp, \quad (4.173)$$

where $y > 0$. Because the poles of $X(y, p)$ are simple and $X_2(y, p)$ has a so called fractional form, $x(y, t)$ can be represented formally by an infinite series, infinite because there is an infinite number of poles.

The formal solution becomes

$$x(y, t) = 2 \sum_{n=1}^{\infty} \cos(q_n^2 t) x_n(y), \quad (4.174)$$

where

$$\begin{aligned}
x_n(y) = & [F_t \{-\sin q_n(1-y) + \sinh q_n(1-y) + \\
& \cosh q_n \sin q_n y - \cos q_n y \sinh q_n + \sin q_n \cosh q_n y - \cos q_n \sinh q_n y \\
& + q_n^3 J_t (-\cos q_n(1-y) - \cosh q_n(1-y) - \\
& \sinh q_n \sin q_n y + \cos q_n y \cosh q_n + \cos q_n \cosh q_n y + \sin q_n \sinh q_n y)\} \\
& + M_t \{q_n (-\cos q_n(1-y) + \cosh q_n(1-y) + \\
& \sinh q_n \sin q_n y - \cos q_n y \cosh q_n + \cos q_n \cosh q_n y + \sin q_n \sinh q_n y) \\
& + (m_a + m_t) q_n^2 (\sin q_n(1-y) + \sinh q_n(1-y) + \\
& \cosh q_n \sin q_n y - \cos q_n y \sinh q_n - \sin q_n \cosh q_n y + \cos q_n \sinh q_n y)\} \\
& / [q_n^4 \{(\sin q_n \cosh q_n - \sinh q_n \cos q_n)(m_a + m_t + 1) + 2(m_a + m_t) q_n \sin q_n \sinh q_n \\
& + 3J_t q_n^2 (\sinh q_n \cos q_n + \sin q_n \cosh q_n) \\
& q_n^3 (-2J - t \cosh q_n \cos q_n + 4(m_a + m_t) J_t (1 - \cosh q_n \cos q_n)) \\
& - (m_a + m_t) J_t q_n^4 (\sin q_n \cosh q_n - \sinh q_n \cos q_n)\}] .
\end{aligned} \tag{4.175}$$

The $q_n \in R$, $n = 1, 2 \dots$ occurring in (4.174) and (4.175) follow from

$$\begin{aligned}
& 1 + \cos q_n \cosh q_n - (m_a + m_t) q_n (\sin q_n \cosh q_n - \sinh q_n \cos q_n) \\
& - J_t q_n^3 (\sinh q_n \cos q_n + \sin q_n \cosh q_n) + (m_a + m_t) J_t q_n^4 (1 - \cos q_n - \cosh q_n) = 0 ,
\end{aligned} \tag{4.176}$$

To obtain an expression for the function $\ddot{x}(y, 0)$, $0 \leq y \leq 1$, we use the initial value theorem ([17, page 185, theorem 4]). This theorem states that, if the function $f(t)$ satisfies the inequality $|f(t)| < M \exp\{\alpha t\}$, for all $t > 0$, M being a positive constant, then

$$\lim_{p \rightarrow \infty} \int_0^\infty \exp\{-pt\} f(t) dt = \lim_{t \downarrow 0} f(t) . \tag{4.177}$$

We consider separately two different cases. First $F_t \neq 0$, $m_t \neq 0$, $m_a \neq 0$, $M_t = 0$ and $J_t = 0$, than we get

$$\ddot{x}(y, 0^+) = 0 , \quad 0 \leq y < 1 , \quad \ddot{x}(1, 0^+) = \frac{-F_t}{m_a + m_t} . \tag{4.178}$$

Second, $F_t \neq 0$, $m_t \neq 0$, $m_a \neq 0$, $M_t \neq 0$ and $J_t \neq 0$, then we have besides (4.178).

$$\ddot{x}'(1, 0^+) = \frac{-M_t}{J_t} . \tag{4.179}$$

In what follows we compare the analytic solution of the linearized version of the problem (in fact a numerical approximation) with the numerical approximation obtained by using the finite-difference method of Section 4.4.

As a matter of fact we can compare the analytic solution with the results of two finite-difference schemes. The first scheme is given in Section 4.4. The second scheme is the

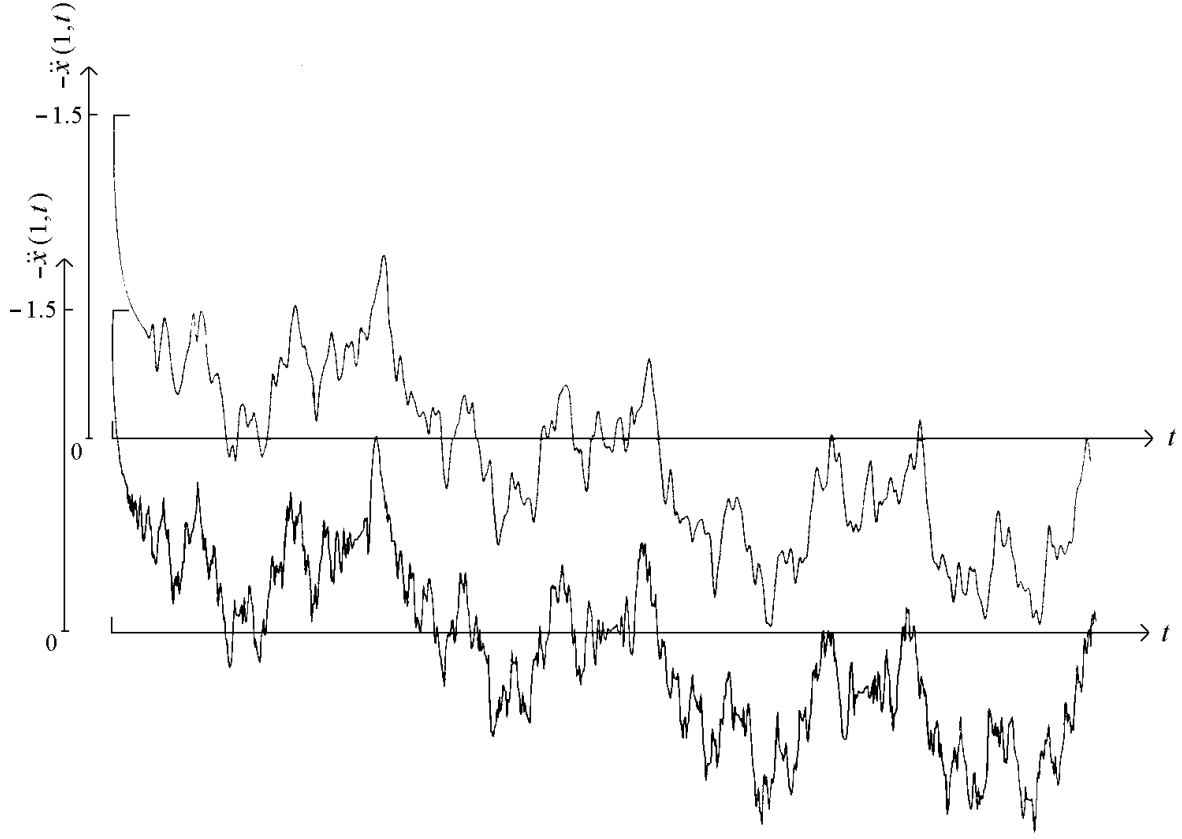


Figure 4.48: Acceleration $\ddot{x}(1,t)$ of the free end: (top) finite difference and (bottom) analytic situation, bow (4.180).

linearized version of the first one, it is a finite- difference scheme which belongs to the equations of motion (4.165)–(4.168). It turned out that for the cases we will consider, the results of both schemes are almost equal. So, in the following we mention only results obtained by the non-linear difference scheme.

First, we consider the bow

$$B(1, -1, 1, 1, 0.1, 0, 0, \infty, 0, 0.95; 1, 1, 1). \quad (4.180)$$

In Figure 4.48 we draw the analytic solution for the case $F_t = 0.15$, $m_t = 0$, $m_a = 0.1$, $M_t = 0$, $J_t = 0$ of the function $\ddot{x}(1,t)$ and the approximation of this function, or actually E/m_a , calculated by means of the finite-difference method. We conclude for this acceleration of the free end, that there is not a point wise agreement between the analytic solution and the approximation. Taking the highly fluctuating behaviour of the analytic solution into account, this is not surprising. For the finite-difference approximation neglects higher order terms in the Taylor expansion of the solution. However, there is good global resemblance. This is also expressed by the fact that the integral of these functions from $t = 0$, hence the velocities of the free end $\dot{x}(1,t)$ show a good correspondence, see Figure 4.49.

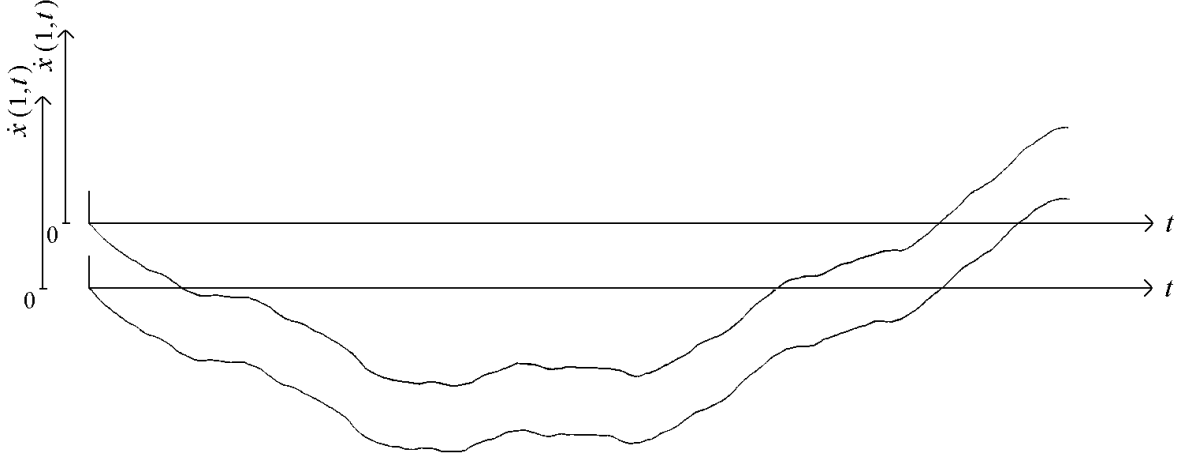


Figure 4.49: Velocity $\dot{x}(1,t)$ of the free end: (top) finite difference and (bottom) analytic situation, bow (4.180).

Further for $\lim t \downarrow 0$ the acceleration $\ddot{x}(1,t)$ converges to the value given by (4.178) for the analytic solution as well as for the approximation.

This notwithstanding the fact that there are large fluctuations of the solution near the free end shortly after removal of the external forces. These fluctuations are connected to the discontinuity as a function of y of $\lim_{t \downarrow 0} \ddot{x}(y,t)$ at the free end $y = 1$, given by equations in (A.14). It is also this discontinuity which causes some problems with the use of the crank-Nicolson scheme. In this scheme for $k = 0$, the second term on the right-hand side of equation (4.45) for $j = n_s$ is 0, according to the solution of the static equations, but it has to possess a value given by equation (4.178), $-F_t/(m_a + m_t)$. So, one way to solve the difficulties is to adjust the value of the mentioned term. However, for a real bow, thus solving the non-linear equations of motion, we have no analytic expression at our disposal. One can also drop equations (4.45) and (4.46) for $j = n_s$ and use in the boundary conditions at the tip non-symmetric finite-differences, as we did in [8]. But especially because of the presence of a rigid body possessing a moment of inertia (Equation (4.14) or (4.41)) we did not use this scheme in this paper. Another way to avoid the use of the acceleration at the free end for $t = 0$ is applied in this paper by taking $\mu = 1$, thus a fully implicit backward time difference-scheme for the first time step. In [8] we used already this method in order to avoid the use of the normal force T at $t = 0$ in the case of a bow with an inextensible string and concentrated masses at the tips.

Figure 4.50 shows the acceleration of the free end as function of time, both the analytic solution, in the case $F_t = 0.075$, $m_t = 0$, $m_a = 0.1$, $M_t = 0.05$, $J_t = 0.1$, and the numerical approximation in the case of the bow

$$B(1, -1, 1, 1, 0.1, 0, 0.1, \infty, 0, 0.95; 1, 0.1505, 1), \quad (4.181)$$

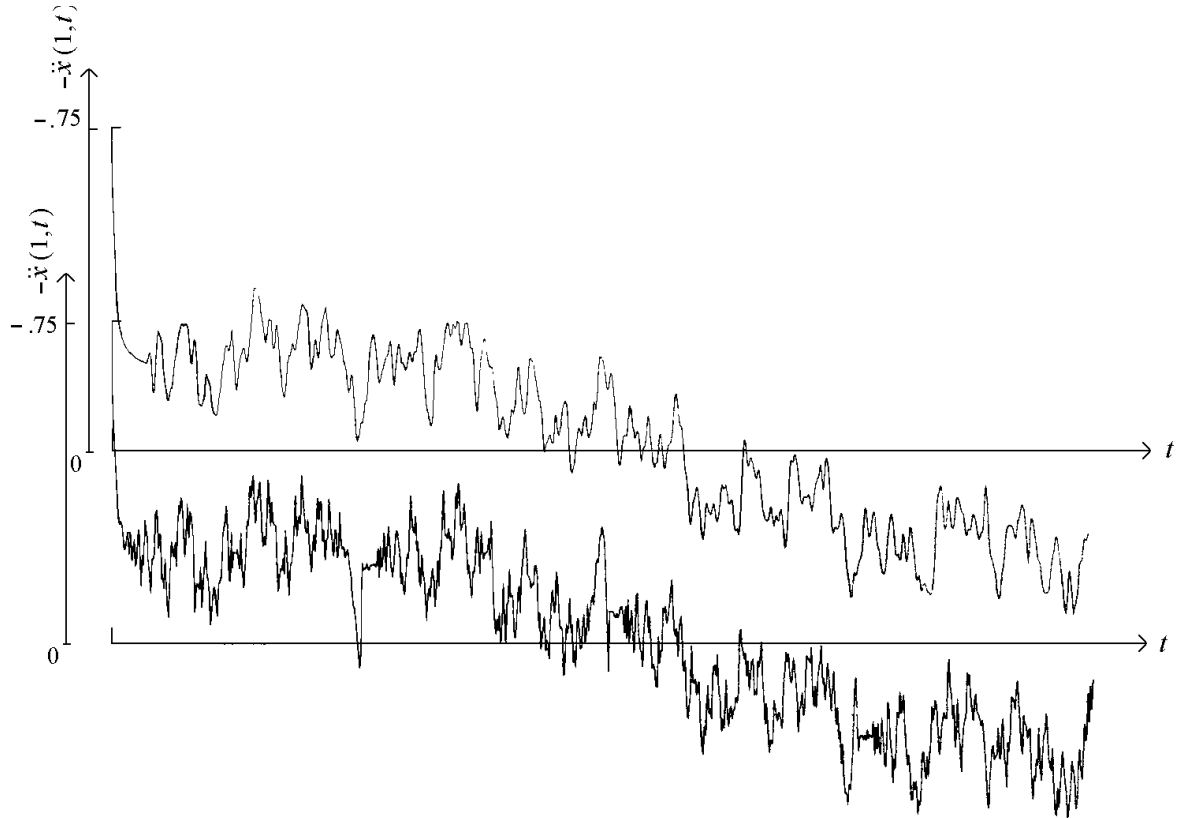


Figure 4.50: Acceleration $\ddot{x}(1,t)$ of the free end: (top) finite difference and (bottom) analytic situation, bow (4.181).

where we adapted the boundary conditions of the static finite-difference equations in an obvious way, in order to take the bending moment $M_t = 0.05$ exerted at the free end, into account. In Figure 4.51 we draw the velocity $\dot{x}(1,t)$, the analytic solution as well as the numerical approximation. From the Figures 4.50 and 4.51 the same conclusions can be drawn as those given above. Again the values of $\ddot{x}'(1,t)$ converge for $t \downarrow 0$ to the value given by (4.179).

The obtained results show the limitedness of the utility of the finite-difference method when the solution which is approximated is rather unsteady. However, for a real bow there are good reasons to presume the solutions to be smoother. First, the mass and stiffness distribution along most bows are not constant for the limbs are tapered to the tips. In [8] we compared already the performance of a bow with constant stiffness and mass distribution with that of a bow with limbs tapered off, and we found that the DFD curve of the last mentioned bow was much smoother. Second, for a real bow the string possesses elasticity and computations showed that this elasticity gives some smoothing effect.

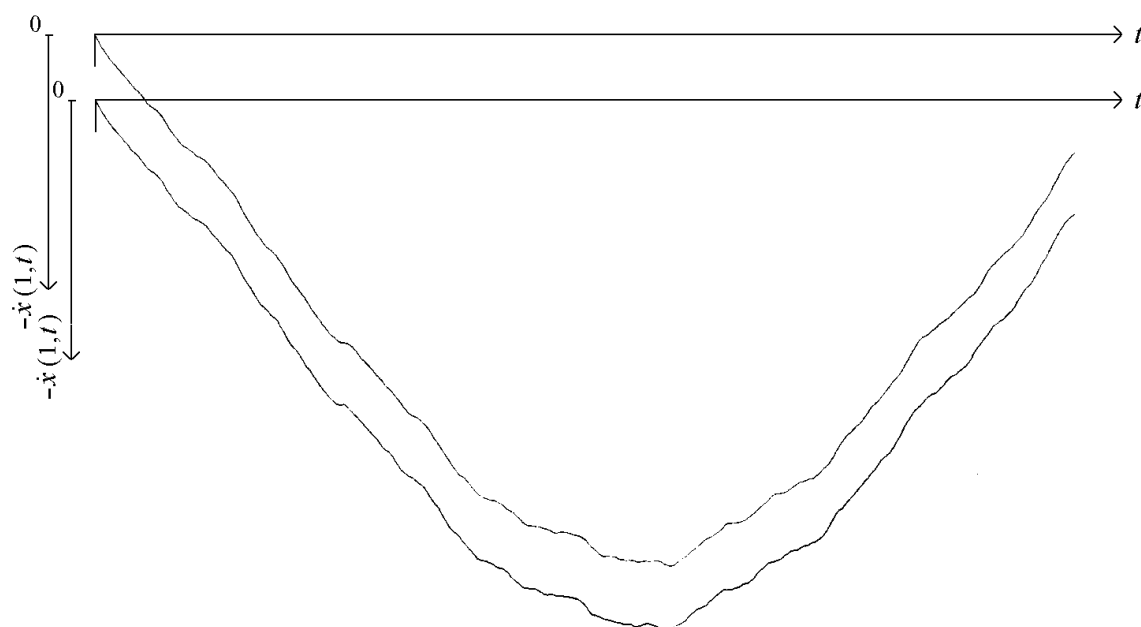


Figure 4.51: Velocity $\dot{x}(1, t)$ of the free end: (top) finite difference and (bottom) analytic situation, bow (4.181).

Bibliography

- [1] Balfour H. (1890). On the structures and affinities of the composite bow. *Journal of the Anthropological Institute of Great Britain and Ireland* XIX.
- [2] Balfour H. (1921). On the structures and affinities of the composite bow. *Journal of the Royal Anthropological Institute* LI:289–309.
- [3] Clover P. (1955). *Bowman's Handbook*. Porthmouth.
- [4] Faris NA, Elmer RP. (1945). *Arab Archery*. Princeton University Press, Princeton (NJ).
- [5] Gordon JE. (1978). *Structures or Why Things Don't Fall Down*. Pelican, Harmondsworth.
- [6] Hickman CN, Nagler F, Klopsteg PE. (1947). *Archery: the technical side*. National Field Archery Association, Redlands (Ca).
- [7] Hodgkin AE. (1974). *The Archer's Craft*. Faber and Faber Limited, London.
- [8] Kooi BW. (1981). On the mechanics of the bow and arrow. *Journal of Engineering Mathematics* 15:119–145.
- [9] Kooi BW, Sparenberg JA. (1980). On the static deformation of a bow. *Journal of Engineering Mathematics* 14:27–45.
- [10] Latham JD, Paterson WF. (1970). *Saracen Archery*. The Holland Press, London.
- [11] Lewis J. (1971). *Archer's Digest*. Chicago.
- [12] Marlow WC. (1981). Bow and arrow dynamics. *Am. J. Phys.* 49:320–333.
- [13] McLeod W. (1981). Tutankhamun's self bows. *Journal of the Society of Archer-Antiquaries* 24:37–41.
- [14] Payne-Gallwey SR. (1976). *The Crossbow*. Holland Press, London.
- [15] Pope ST. (1974). *Bows and Arrows*. University of California Press, Berkeley (CA).
- [16] Rausing G. (1967). *The Bow*. Acta Archaeologica Lundensia. CWK Gleerups Förlag, Lund, Sweden.
- [17] Sneddon IN. (1972). *The use of Integral Transforms*. New York.

Index

- aiming, 9
- archer, 53
- archers paradox, 15
- arrow, 53, 81
 - footed, 14
 - head, 7
 - nock, 7
 - point, 7
 - rest, 9
- back, 7
- backing, 12
 - close, 12
 - free, 12
- ballistics
 - exterior, 9
 - interior, 9, 53
- beam
 - inextensible, 53
- belly, 7
- bending stiffness, 33, 35
- bolt, 9
- boundary conditions, 94
- bow, 53
 - \tilde{H} , 102
 - Angular, 12, 81
 - Asiatic, 34
 - centre-shot, 53
 - composite, 11
 - compound, 9, 34
 - cross, 9
 - foot, 9
 - H, 99
 - hand, 9
 - laminated, 13
 - nock, 7
 - non-recurve, 5, 10, 81, 91
 - recurved, 81
 - reflexed, 81
 - self, 11
 - static-recurve, 5, 81, 83, 91
 - straight-end, 81
 - symmetric, 53
 - tip, 7, 35, 53, 81
 - working-recurve, 6, 81
- bow hand, 9, 53, 81
- brace height, 7, 55
- braced, 7
- centre shot, 13
- centre-shot, 83
- curve
 - Dynamic-Force-Draw, 9
 - Static-Force-Draw, 9
- damping, 83
- distribution
 - bending stiffness, 54, 83
 - mass, 54, 83
- drag constant, 20
- draw, 9, 55, 85
- drawing, 9, 33
- ear, 82
- ears, 10
- efficiency, 54
- elastic line, 33, 35, 54, 83
- energy
 - kinetic, 56
 - potential, 56
- equation
 - Euler, 57

- Euler-Bernoulli, 54
- facing, 12
- figure of merit, 18
- fistmele, 7, 35
- fletching, 7
- flight shooting, 54, 84
- fully drawn, 9
- grip, 7, 55, 86
 - pistol, 13
- handle, 7
- heart wood, 12
- heartwood, 83
- hinge, 51
- hunting, 54, 67
- hysteresis, 54
- kick, 70
- limb, 7, 53, 81
 - lower, 7
 - shooting, 13
 - upper, 7
- line of aim, 9
- longbow, 83
- loosing, 9
- mass distribution, 34, 46
- median plane, 13
- method
 - finite-difference, 53, 83, 85
 - finite-element, 54
 - Newtonian, 39
- model
 - C, 99
 - H, 98
 - lumped parameter, 83
 - M, 99
- multiplier
 - Lagrangian, 57
- muzzle velocity, 9, 54, 84
- nocking, 9
- height, 13
 - point, 9
 - tension, 17
- performance, 54
- permanent set, 7
- pile, 7
- pivot point, 9
- position
 - braced, 55, 82, 85
 - fully drawn, 55, 83, 85
 - unbraced, 55, 85
 - unstrung, 81
- principle
 - Hamilton, 53
- problem
 - initial-boundary-value, 53
- prod, 9
- quality coefficients, 83
- recoil, 67
- recurve, 53
- recurved, 10
- reflexed, 10
- release, 81
- sapwood, 12, 83
- scheme
 - Crank-Nicolson, 96
 - finite-difference, 91
- shaft hand, 9, 81
- shot
 - open-handed, 69
- spine, 15
- stabilizer, 13
- stave, 7
- stock, 9
- string, 7, 33, 81, 83
 - bridges, 82
 - elastic, 84
 - elasticity, 83
 - loop, 7
 - mass, 83, 84

- strain stiffness, 84
- string-bridges, 10
- strung, 7
- target, 7
- target shooting, 54
- unbraced, 10
- vanes, 7
- virtual mass, 18
- weight, 9, 55, 86